THE EFFECTS OF IMPACT LOADING ON REINFORCED CONCRETE PANELS

BY DEREK ALLEN MASON

A thesis submitted in partial fulfilment of the requirements
for a Master of Science (Civil) in Engineering

Department of Civil Engineering
University of Cape Town
November 1992

To my wife, Janet

DECLARATION

I, Derek Allen Mason, hereby declare that this thesis is my own work, except where otherwise indicated.

Signed by candidate

D A MASON

November 1992

SYNOPSIS

An investigation into the effects of impact loading on reinforced concrete panels (slabs) was conducted. The impact load was generated by means of a compound pendulum. The impact load was increased by increasing the height from which the pendulum was released as well as by the addition of weights (masses) to the pendulum. The duration of the impulse was varied by the addition of weights (masses). This meant that with low mass and high velocity a high initial intensity and short duration was achieved. The addition of weights (masses) gave low initial intensity and longer duration.

The reinforced panels tested were 2m x 2m in plan area and were 50mm thick. Two percentages of reinforcing mesh (0.2% and 0.5%) were used. The panels were impacted centrally with the pendulum which had a 100mm x 100mm 'hammer' fixed to it. It was this 'hammer' that made contact with the panel (slab) during impact.

The results showed that the panel with the lower reinforcement percentage (0.2%) was more efficient in absorbing the impact energy. This was shown by higher ductility and toughness indices. It was also shown that a slight change in the magnitude of the impulse dramatically changed the mode of failure of the reinforced panel. The failure mode changed from one of flexural failure to one of 'punching shear' failure. This meant that the shear failure became dominant. Dynamic Shear tests performed prior to the testing of the slabs showed a reduction in shear strength with increased strain-rate.

Damage criteria identified included residual strength, pendulum backswing, crack width and permanent deformation as well as 'punching' through of the panels. It was shown that residual strength was inadequate on its own to classify a specimen as failed, but had to be used in conjunction with one or more of the other damage criteria.

An Elasto-Plastic Design Method was developed and used in the analysis. The method is described in Chapter 8 and is given as a simplified method to design panels for impact loading.

ACKNOWLEDGEMENTS

The author wishes to thank the following:

Associate Professor Rolf Dietmar Kratz, Department of Civil Engineering, UCT, thesis supervisor for his excellent guidance and enthusiastic encouragement over the past two years. As well as for presenting two post-graduate courses that were invaluable for their contribution to the success of this thesis.

The following from the Civil Engineering Workshop:
Mr Eike von Guerard for his technical expertise and innovative ideas and solutions to experimental problems, as well as assistance in manufacturing the thesis apparatus. Mr Charles Nicholas for manufacturing thesis apparatus and Mr Noor Hassen for manufacturing parts of the thesis apparatus when required.

The following from the Civil Engineering Laboratory: Messrs D J Botha, J J Williams, J George and A Siko for their assistance in erecting thesis equipment, setting up slabs and related tasks. Mr J Lemmetjies for assistance in the concrete laboratory. Fellow UCT students who assisted at various times in the laboratory.

Mrs Eileen Mason for proof-reading parts of the thesis text.

To all those, too many to name, who assisted in various ways.

Finally, to my wife, Janet Mason, without whom this thesis would not have been possible: For her patience, enthusiasm and efficient typing of this thesis. Her continued encouragement, sacrifices and support that enabled this thesis to be completed.

TABLE OF CONTENTS

LIST OF FIGURES

LIST OF PHOTOGRAPHIC PLATES

LIST OF TABLES

CHAPTER 1

INTRODUCTION

Impact is a form of dynamic loading in which the load duration is very short. Loading is considered dynamic if the structural response involves inertia effects in addition to the structural stiffness. There is a need for a formalised approach to impact design, as some structures are more susceptible to impact loads. Since all impact effects have a dynamic action on structures this has to be reflected in the analytical method applied.

Concrete is a complex inelastic material consisting of many components. It behaves quite differently when compared to a relatively homogenous material such as steel. The matrix of concrete consists of a random distribution of particles which give it its heterogenous composition. This causes the non-linear behaviour of concrete under loading. It could be this composition and structure of concrete which make it strain-rate sensitive.

High strain rates occur in concrete when an impulse or impact load acts on it. An impact load is a load that is applied over a very short space of time. An impulse is the amount of energy which is equal to the area under the load-time curve. The strain-rate sensitivity of concrete makes it unrealistic to use its properties determined under low strain rates for statically determined properties under high strain-rate conditions or impact loading.

High strain-rate testing of concrete requires: (a) a testing apparatus capable of generating high strain-rates, (b) a method of acquiring the data and (c) a valid technique for analysing the test results.

A pendulum impactor was designed and constructed for this purpose, as described in Chapter 3. The mass of the pendulum was increased by the addition of additional weights (masses) to vary the duration of the impact. Measurements that were taken were the deflections relative to time. This was achieved by means of

deflection rods attached to the specimens and a falling board. Spring-loaded pencils drew on graph paper that was attached to the falling board. The starting position of the pendulum was recorded and the backswing of the pendulum after impact was also measured.

The samples tested consisted of steel beams, plain concrete as well as reinforced concrete beams and reinforced concrete slabs. The steel beams were used to 'calibrate' the measuring equipment as well as to gain experience with the equipment. The concrete beams were used to gather experience with concrete under impact loading that could be used for the reinforced concrete slabs. The duration of the impact was varied by means of the addition of extra weights (masses) to the pendulum. This meant that with low mass and high velocity a high initial intensity and short duration was achieved. The addition of weights (masses) gave low initial intensity and longer duration.

The type of equipment used for this thesis was limited by the funds available. For this reason appropriate electronic equipment was not used due to the very high cost of suitable equipment. Where necessary simplifications were made and appropriate assumptions and analytical techniques were used to analyse the data.

The thesis starts by describing the objectives and scope. It continues by describing the measuring equipment and then describes the calibration of the equipment. Various material properties required for the thesis were determined and are discussed next. The test procedures are given and the results and analysis follows. A suggested design method is given next. Finally conclusions are drawn and recommendations made.

C H A P T E R 2

OBJECTIVES AND SCOPE

The basic research involved an investigation into the effects of impact loading on reinforced concrete panels. Part of this thesis involved the design and construction of a pendulum impactor and recording apparatus. In order to establish the effective parameters for design purposes it was required to investigate:

a) the material behaviour of concrete and reinforcing steel when subjected to dynamic (high strain-rate) loading.

b) the physics of impact loading.

c) the structural response in dependence of percentage reinforcement, concrete strength and duration of impulse.

d) Establish dynamic failure criteria.

Part (c) required full-scale testing of reinforced concrete panels. The results of this investigation were to be compared to analysis and design procedures found in specialist literature. It was hoped that this research would lead to recommendations for simplified analysis and design procedures of impact-resistant reinforced concrete panels.

C H A P T E R 3

DESCRIPTION OF EQUIPMENT

3.1 INTRODUCTION

The equipment was designed and built, starting with a bare floor, as no existing equipment was available. Electronic measuring equipment was not used due to the very high cost of suitable equipment.

The equipment consisted of a pendulum impactor, support structures and deflection-measuring equipment. (See Figure 3.1. and Photographic Plate 3.1)

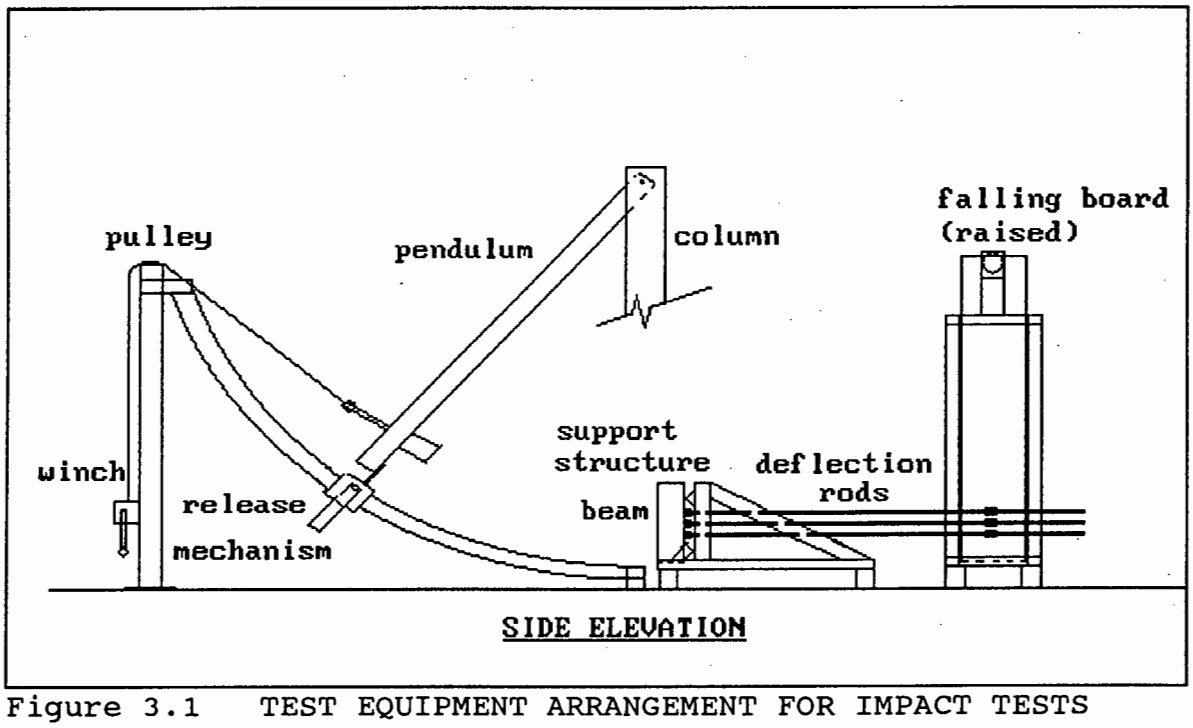

Figure 3.1 TEST EQUIPMENT ARRANGEMENT FOR IMPACT TESTS

3.2 PENDULUM IMPACTOR

3.2.1 Pendulum Arrangement

The pendulum consisted of a 4.15m length of 140mm x 60mm x 15.3kg/m parallel flange channel which was attached to a 750mm long 40mm diameter high yield steel hinge pin. This steel pin passed through two 40mm diameter self-lubricating pillar blocks which were mounted onto a 203mm x 133mm x 30kg/m cantilevered I-section. The cantilever was attached onto a 4.3m high column

consisting of a 203mm x 133mm x 30kg/m I-section. It was bolted to the floor by means of a 330mm x 330mm x 10mm base-plate. In order to reduce horizontal swaying of the cantilever section, it was braced between the roof and a nearby structure by means of 50mm x 50mm x 6mm and 125mm x 75mm x 8mm angle sections, respectively. The pendulum arrangement is shown in Figure 3.2.

The pendulum had a 200mm long "hammer", consisting of two 100mm x 50mm channel sections butt welded together, with a 100mm x 100mm x 5mm plate welded to their end. It was this "hammer" which struck the specimens.

The mass of the pendulum could be increased by bolting a number of 400N weights (masses) to it. This was achieved by means of a 25mm diameter bolt, 380mm long, which was welded to the channel section behind the "hammer".

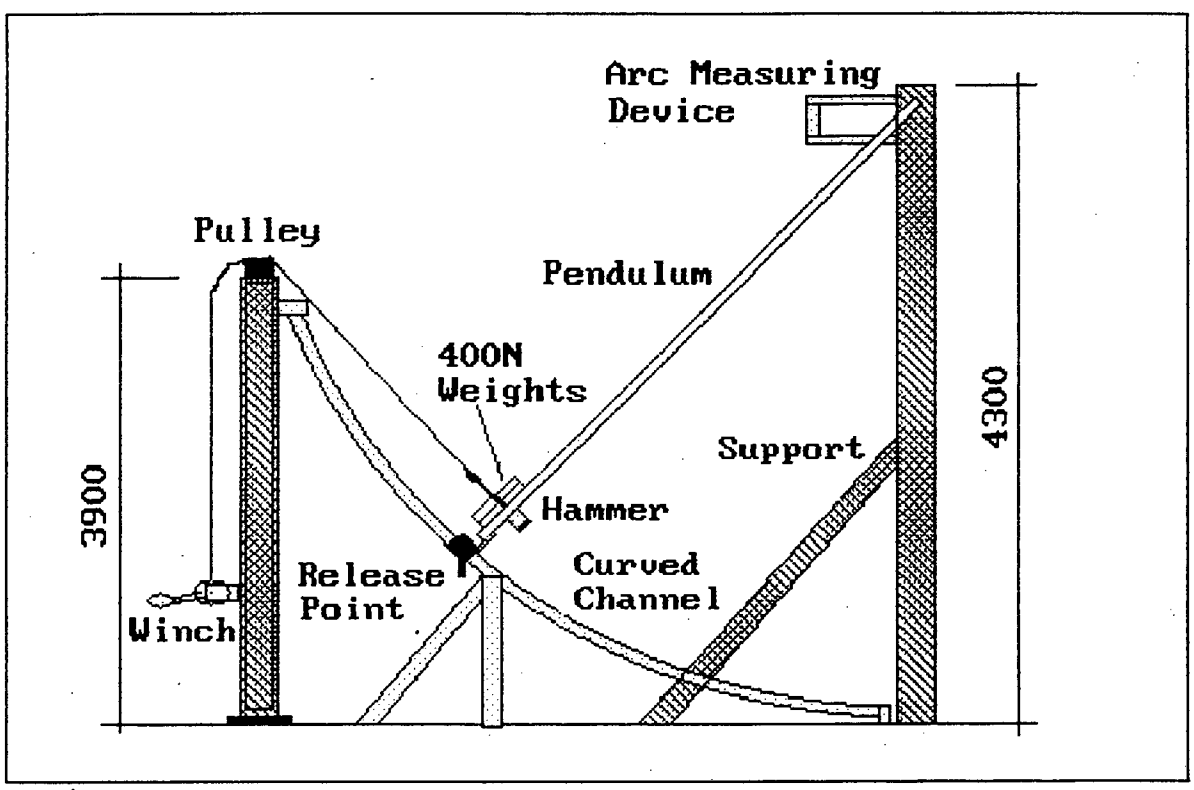

Figure 3.2 PENDULUM ARRANGEMENT

A curved 100mm x 50mm parallel flange channel section extended from below the pendulum to a 3.925m high column. The channel

section was notched at 250mm intervals and bent to a radius of 4.165m. The notches were fillet welded and ground flush. An adjustable support was positioned just off half way to ensure correct curvature when in place. This curved section supported the release mechanism for the pendulum. The column had a pulley on top and a winch which was used to raise the pendulum to the required height before securing it by the release mechanism. See Figure 3.2 for details of the pendulum arrangement.

The radius of the curved channel varied by a few millimeters over the whole length. This was overcome by means of an extension plate that was bolted to the lower end of the pendulum. The extension plate had four slotted holes which allowed the plate to be shifted along the axis of the pendulum to achieve the desired length.

3.2.2 Release Mechanism

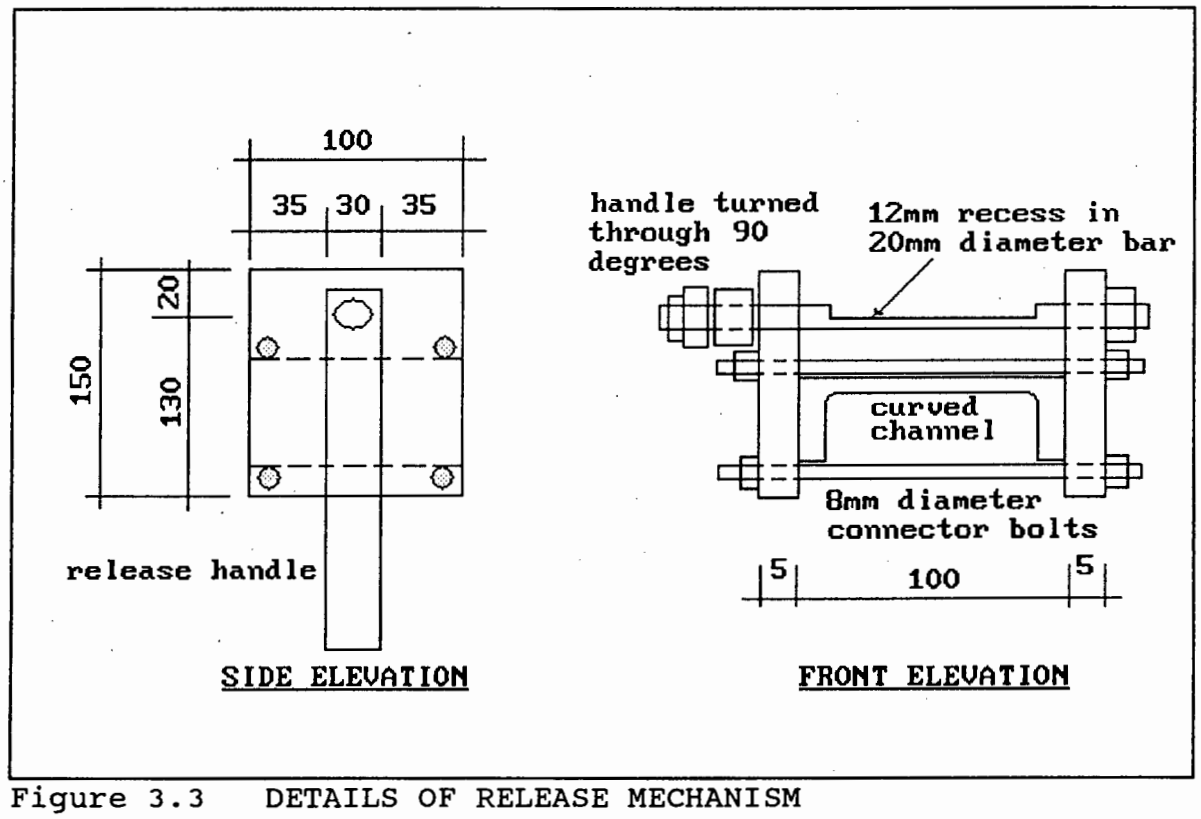

Figure 3.3 DETAILS OF RELEASE MECHANISM

The release mechanism consisted of two plates positioned on either side of the curved channel section. The plates were

connected by means of four 8mm diameter 150mm long bolts. A 20mm diameter shaft passed through the two plates. A 12mm deep by 70mm long recess was machined in the bar. The one end of the shaft was machined in the shape of a square. The turning handle had a square opening that fitted over the square end of the 20mm diameter bar. The arrangement was then bolted together. This method of attachment gave flexibility in the positioning of the handle relative to the position of the release mechanism on the curved channel.

Once the release mechanism had been positioned at the desired position, the winch was used to raise the pendulum to that position, so that the extension piece at the bottom of the pendulum was above the shaft. The shaft was turned so that the recess was perpendicular to the extension plate. A 1mm thick temporary spacer plate was placed onto the recess. The extension plate was then lowered until it touched the spacer plate, and was then bolted in position. The spacer plate was then removed. The pendulum was then raised to place the extension plate behind the recess in the shaft. The spacer plate ensured that the bottom of the extension plate was just above the recess when the handle was turned, so that it would just pass over the recess when the pendulum was released.

3.2.3 Light Trip

A light trip was used to trigger the falling board. This consisted of a photo-electric system transmitter and receiver that were mounted to a wooden board. An attachment system was connected to the board that enabled the whole arrangement to be attached to the curved channel section. This gave flexibility in that it could be positioned anywhere along the curved channel, according to the position of the release mechanism.

The light trip worked in the following way: When the light was on a light beam shone onto a photo-electic cell that kept a relay switch open. When the light beam was broken by the pendulum swinging through it, the relay switch was closed. A current was sent to the solenoid which pulled the shaft and released the

released the board.

3.3 SUPPORT STRUCTURES

Two types of support structures were designed and constructed to support the two sizes of samples tested. The small support structure could accommodate 500mm long concrete beams as well as 600mm long flat steel beams. The large support structure supported the 2m x 2m reinforced concrete slabs.

3.3.1 Support Structure for Small Beams

The support structure consisted of a frame made up of 45mm x 45mm x 6mm angles. The knife-edge supports were also made from the before-mentioned angles, spaced 450mm apart. The whole frame assembly was welded to two sections of 180mm x 70mm x 22kg/m channel sections, which were bolted to the laboratory floor. Wooden vertical spacer-blocks were inserted in front of the supports, according to the length of specimen to be tested, to ensure its correct vertical positioning relative to the knife-edges. The specimens were tied to the structure with cord, to keep the specimen against the knife-edges. The knife-edges acted as simple supports and allowed the specimen to rotate during flexure. A dimentioned sketch of the small support structure can be seen in Figure 3.4. The support strucure can also be seen in Photographic Plate 3.3. A reinforced concrete beam can be seen placed against the small beam support structure. It was tied against the knife-edge supports with cord and this can be seen clearly. The beam rested on wooden spacer blocks that can be seen at the bottom of the picture. The deflection rod attachment and connector can also be seen. The "hammer" can be seen touching the specimen.

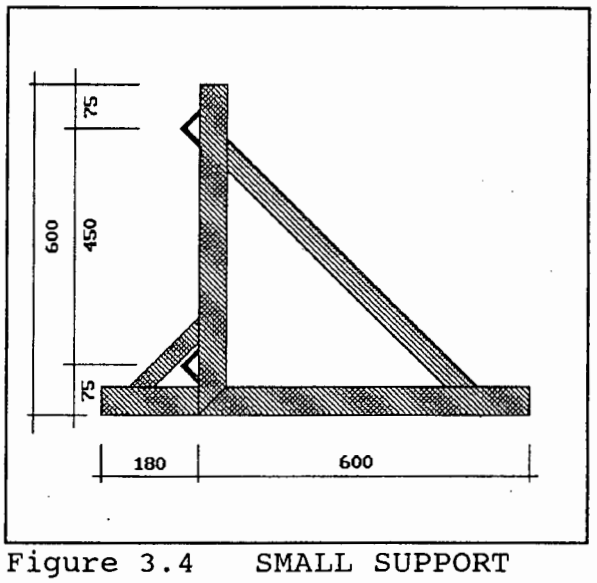

Figure 3.4 SMALL SUPPORT STRUCTURE

3.3.2 Support Structure for Slabs

The support structure consisted of a square 2m x 2m frame made up of 200mm x 75mm x 25kg/m channels sections. This was welded to 180mm x 70mm x 22kg/m channels to raise it to the correct height. The frame was supported from the back by bracing of 125mm x 75mm x 8mm angles. The front face of the channel section frame had 20mm diameter bars welded to it. This would allow the slab to rotate about its support during flexure. The bottom edge of the slab rested on a 25mm diameter bar to reduce friction and allow rotation.

It was not possible to use the over-head gantry crane to load the slabs into the support structure, as the crane could not pass over the pendulum due to it's height. The support structure was fitted with wheels to enable it to be moved. This was done in such a way that the 2m x 2m frame tilted back at an angle of 3.5° to the vertical to ensure stability during transport. Brackets were bolted in place at the top and bottom of the frame to ensure that the slab rested against the support frame.

The support structure was wheeled to a position where the crane could be used to load a slab into position. The safety brackets were bolted in place and wooden spacer blocks inserted. The slab remained connected to the crane by means of a sling, for as long as possible, as an additional safety measure. The support structure and slab was then moved into position on the test bed. The whole arrangement was lifted by means of a winch onto a spacer consisting of a 127mm x 102mm I-section and bolted in place. The supporting struts were then bolted into position. A sketch of the slab support structure can be seen in Figure 3.5.

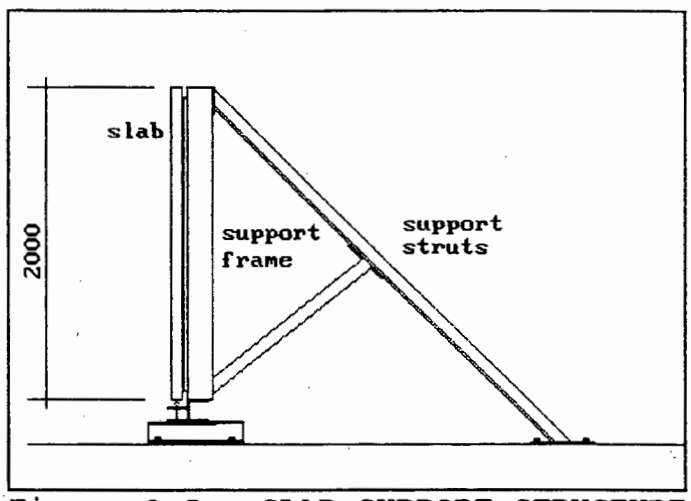

Figure 3.5 SLAB SUPPORT STRUCTURE

3.4 MEASURING EQUIPMENT

It was necessary to introduce a time element into the measuring equipment in order to obtain a deflection-time graph. This was achieved by means of a falling board. The rest of the measuring equipment consisted of a number of deflection rods that were attached to the specimen. The deflection rods had pencils attached to them that drew on graph paper that was attached to the falling board. The whole arrangement was supported in a frame that consisted of 40mm x 40mm x 6mm angle sections.

3.4.1 Falling Board

The time element for the deflection measurements was obtained by means of a falling board. The guillotine-like board consisted of a 300mm wide by 1800mm long galvanized steel plate, braced along the length by 30mm x 30mm x 3mm angles. Attached to these angles were three guides (two at the top and one at the bottom) of 12.5mm diameter. These ran along 12mm diameter stainless steel rods, all vertically aligned. The mass of the board was 18.2 kg and the maximum drop height was 320mm.

The release mechanism for the board consisted of a 12-Volt truck solenoid. When the board was in the raised position it clipped onto a spring-loaded shaft, that passed through a linear-bearing and was attached to the solenoid. (See Figure 3.6.) When the battery power was off the board would remain in the raised position. When the light-beam was broken, the relay switch closed and current was sent to the solenoid which pulled the shaft and released the board.

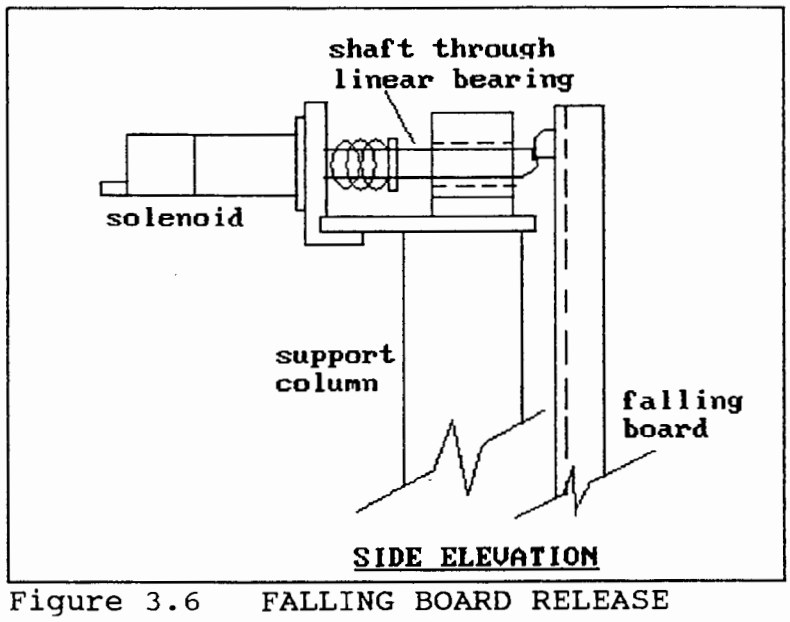

Figure 3.6 FALLING BOARD RELEASE MECHANISM

Graph paper was attached to the board by means of masking tape. When the board fell, before impact, the recording pencils (described in 3.4.2) drew vertical lines on the graph paper. During impact the deflection-time graph was drawn and the pencils followed the response of the specimen until the board reached the floor (ie had fallen through 320mm). The board took approximately 0.255 seconds to fall through the 320mm drop, with a maximum velocity of approximately 2.5 m/s.

3.4.2 Deflection Rods

The deflection rods consisted of 1m lengths of 12mm diameter grade 44 stainless steel. They passed through two 12.2mm diameter precision-engineered brass bushes spaced horizontally 300mm apart and set in the support frame. For the small beams, three rods were used. The one rod was positioned at the centre of the specimen, with the other two rods a distance of 55mm on either side. The one end of the rod was connected to an attachment that was secured to the specimen. The attachment was designed in such a way so as to allow for it to rotate without transverse pressure on the rods. (See Figure 3.7)

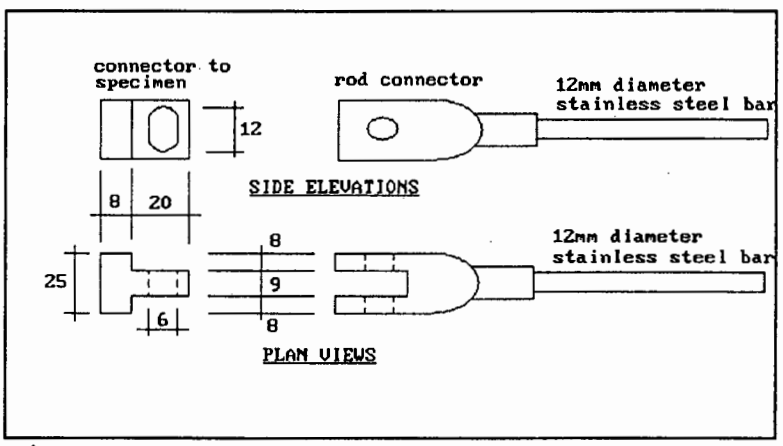

Figure 3.7 DETAILS OF ROD CONNECTORS

A pencil holder was attached to the rod between the two bushes. The pencil holder was completely adjustable. The pencil slid in a 8mm diameter aluminium sleeve. It had a spring at the end of the sleeve to make the pencil spring-loaded to ensure that it kept contact with the board. The pressure of the pencil on the graph paper could be adjusted by sliding the sleeve in or out of its adjuster hole and tightening the grub screw. Similarly the position of the pencil holder along the rod could be varied between the two bushes and secured in position by tightening the

grub screws. (See Figure 3.8 for sketch of pencil holders). The average mass of the deflection rod, attachments and pencil holder was 1.548kg. The rods and bushes were lubricated with teflon spray to reduce friction. The deflection rods, attachments and pencil holders can be seen in Photographic Plate 3.2. It shows the deflection rod attachments epoxied to a slab and the deflection rods disconnected. The pencil holders are attached to the deflection rods. The spring-loaded pencils are not touching the falling board.

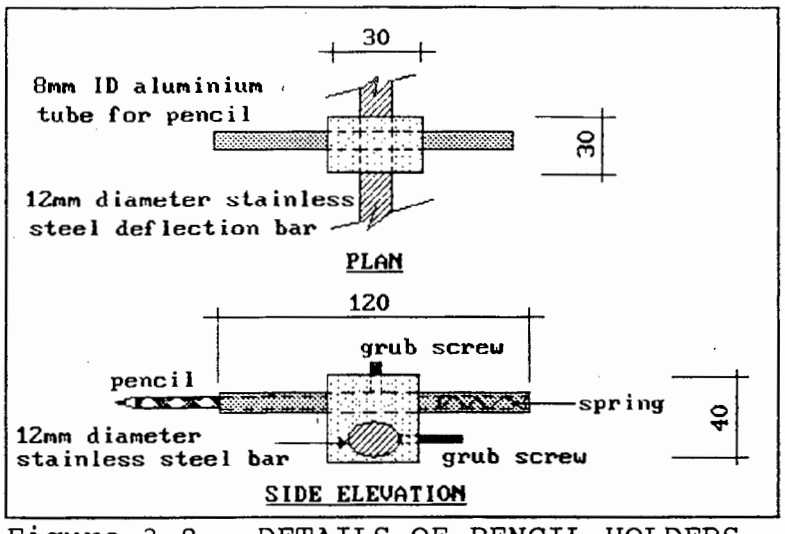

Figure 3.8 DETAILS OF PENCIL HOLDERS

When the specimen was impacted, it deflected and the rods followed the deflected shape as they were connected to the specimen. The pencils then drew lines on the graph paper representing the deflection.

3.4.3 Arc Measuring Device

An arc measuring device was designed and constructed to measure the backswing of the pendulum after impact.

This device was situated near the top of the pendulum. It consisted of a frame to which a movable board was attached. The board was hinged at the bottom and had two springs that pulled the top of the board against the frame. A pencil holder was attached to the pendulum. It was necessary to keep the board away from the pencil for the inswing of the pendulum, as it was desired to record the backswing. This was achieved by inserting a spacer-block between the top of the board and the frame. The spacer block had an adjustable cord attached to it that passed through a pulley and the other end of the cord was attached to

the pendulum. The length of the cord was adjusted so that the spacer block was pulled out just before impact.

The device worked in the following way: A piece of A4 graph paper was taped to the board. The board was initially kept in its closed position and the spring-loaded pencil was adjusted so that it made good contact with the graph paper. The board was tilted back by means of a temporary spacer block so that the pencil would not draw on the paper when the pendulum was moved and positioned in the release mechanism. Once the pendulum had been secured in the release mechanism, the spacer block, with the pull-out cord attached to it, was inserted in position, which kept the board tilted back.

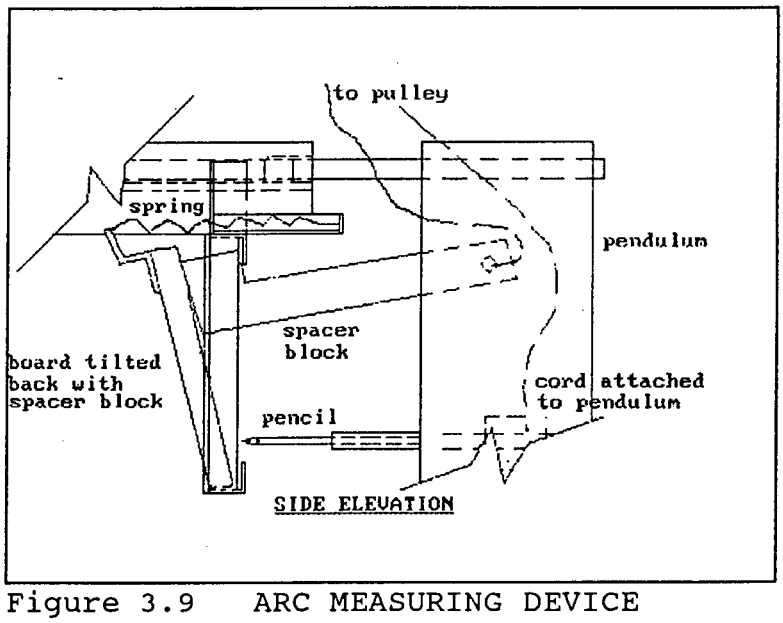

Figure 3.9 ARC MEASURING DEVICE

When the pendulum was released, the board remained tilted back until the spacer block was pulled out by means of the cord and pulley, just before impact. This ensured that the pencil did not draw on the inswing. Once the spacer block had been pulled out, the springs attached to the top of the board pulled the board against the frame, thus pushing it against the pencil point. The backswing arc was drawn on the graph paper as the pendulum rebounded. The end of this arc was marked 'B' for backswing. Before impact the pendulum was allowed to hang vertically with the hammer touching the specimen and the position of the pencil on the graph paper was marked and labelled 'O' for origin. The pendulum was then positioned in the release device and the position of the pencil on the graph paper was marked and labelled 'S' for start. These marked positions were used later

for analysis. A sketch of the arc measuring device can be seen in Figure 3.9. The arc measuring device can be seen in Photographic Plate 3.4. The pencil holder attached to the pendulum can be seen (The pencil had been removed.) The pull-out cord attached to the pendulum can be seen extending up to the pulley (not shown). The spacer block can be seen at the end of the cord. The board has been pulled against the frame by means of the springs. A portion of an arc can be seen on the white board. This occurred when the pendulum was moved with the pencil touching the board that had no graph paper attached.

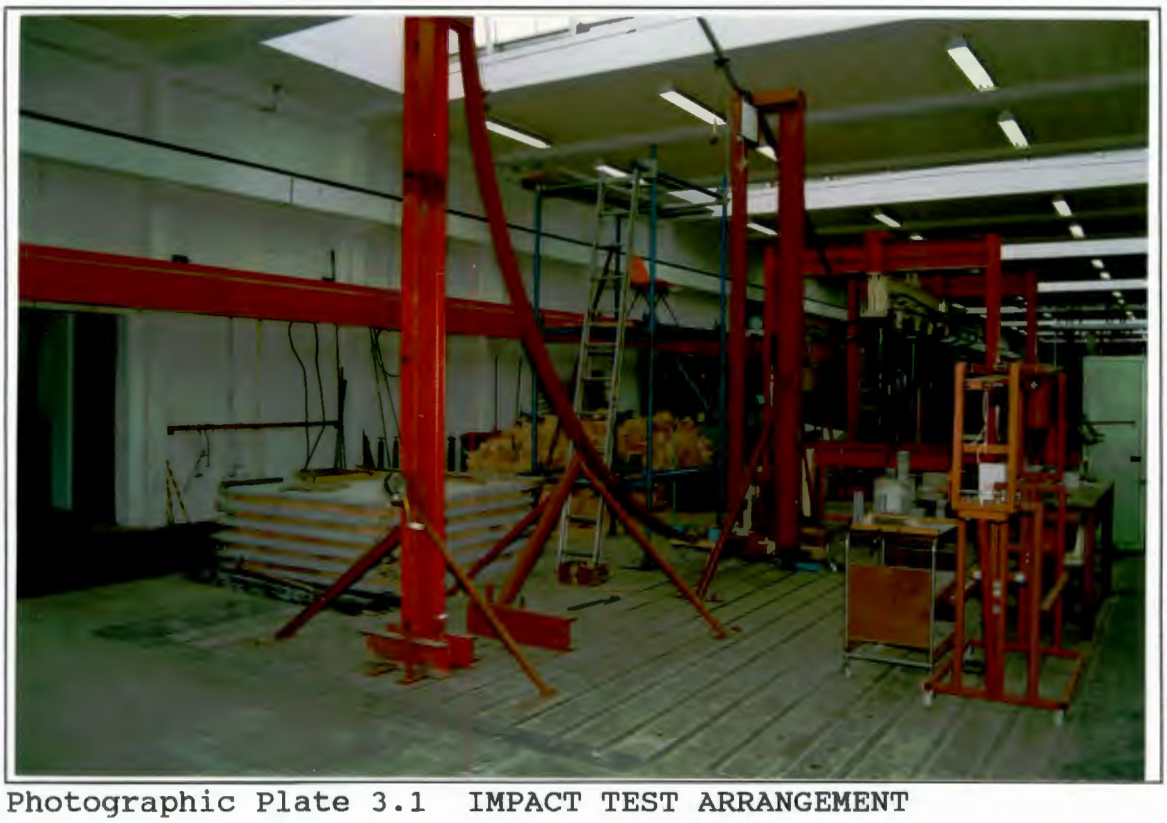

Photographic Plate 3.1 IMPACT TEST ARRANGEMENT

Photographic Plate 3.2 MEASURING EQUIPMENT ARRANGEMENT

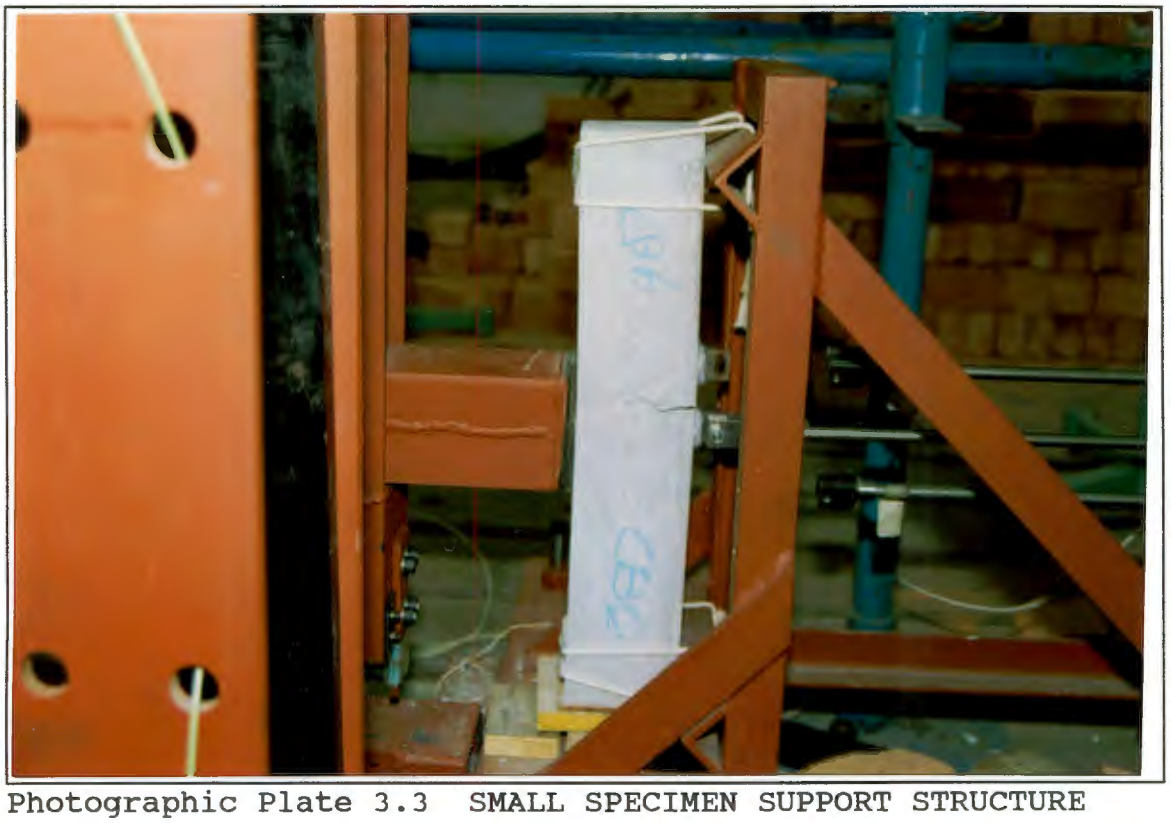

Photographic Plate 3.3 SMALL SPECIMEN SUPPORT STRUCTURE

Photographic Plate 3.4 ARC MEASURING DEVICE

C H A P T E R 4

CALIBRATION OF EQUIPMENT

4.1 CALIBRATION OF RELEASE POINT AND LIGTH TRIP

It was necessary to be able to position the light trip correctly so that it would release the falling board early enough before impact, for each position of the release mechanism.

The calibration was performed in the following manner:

1) A particular release point was chosen a certain distance from point of impact (POI).
2) A straight-edge was placed between the two knife-edge supports. The central rod was then positioned so that it touched the straight-edge. (This was to ensure consistant positioning of the deflection rod.)
3) A stopper board covered with styrofoam was positioned behind the other end of the rod, to prevent the pencil holder from damage by hitting the frame.
4) The falling board was raised and the pencil positioned.
5) A position for the light trip was chosen between the release point and the point of impact.
6) The electrical circuit was activated.
7) The pendulum was then released, which broke the light beam, the board was released and the rod was impacted.

This process was repeated several times for various positions of the light trip, with the release point being kept constant.

The release point was then changed and the process repeated as described before. This process was then repeated for a third release point.

For each release point, a graph of distance of light trip from POI versus distance of release from POI was plotted (See Figure 4.1 for an example.) Other graphs can be seen Appendix B).

The total drop height of the falling board was 320mm. It was decided to let the board fall 160mm before impact. This would allow the board to gain sufficient speed to allow the range of

the graph to be as large as possible, whilst still ensuring that the whole graph was obtained before the board hit the ground. The three calibrations described above were then used to draw a final graph to determine the position of the light trip for any position of the release for the board falling a distance of 160mm.

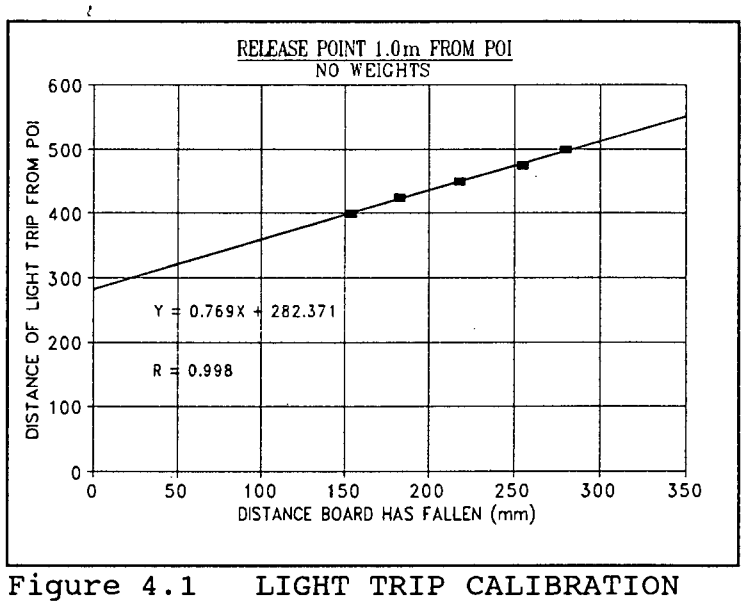

Figure 4.1 LIGHT TRIP CALIBRATION GRAPH

The calibration was performed for the pendulum on its own, with one 400N weight and for two 400N weights attached to the pendulum. (For an example of such a graph, see Figure 4.2) Other graphs may be seen in Appendix B.

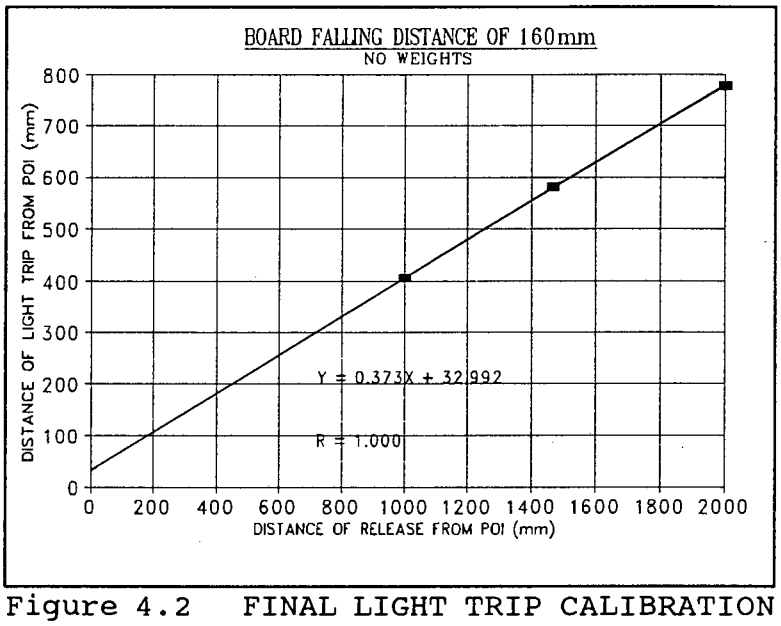

Figure 4.2 FINAL LIGHT TRIP CALIBRATION GRAPH

4.2 CALIBRATION OF DEFLECTION ROD FRICTION

Each deflection rod, to which the pencil holder was attached, passed through two brass bearings and was lubricated with teflon spray, to reduce friction. The friction force was required in order to make allowance for it in the impact tests.

The actual dynamic friction was obtained in the following manner:

1) A simple pendulum consisting of a cord and a lead weight

was made.

2) The simple pendulum was suspended from a stand so that in its vertical position the lead weight just touched the one end of the deflection rod. The distance that the deflection rod extended from the frame was set at 200mm (See Figure 4.3)

3) A second stand was positioned in line with the deflection rod and pendulum a distance of 500mm from the point where the pendulum touched the deflection rod. This was to serve as a reference point for raising the pendulum, to ensure consistency with the height to which the pendulum was raised.

4) The pendulum was released and allowed to impact the end of the rod. (This was repeated several times to ensure repeatability).

5) The distance between the original and final positions was calculated from measurements of original and final (after impact) positions of the rod.

6) The masses of the pendulum and deflection rod, as well as the pendulum geometry were known and elastic impact theory was used to calculate the dynamic friction force in the following way:

Referring to figure 4.3:

$$h = \sqrt{a^2-b^2} \tag{4.1}$$

The included angle, θ, could be related to h by means of the following formula:

$$h = R(1 - \cos\theta) \tag{4.2}$$

The velocity of the pendulum at point of impact was calculated using the principle of conservation of energy.

$$KE = PE$$

$$0.5mv^2 = mgh$$

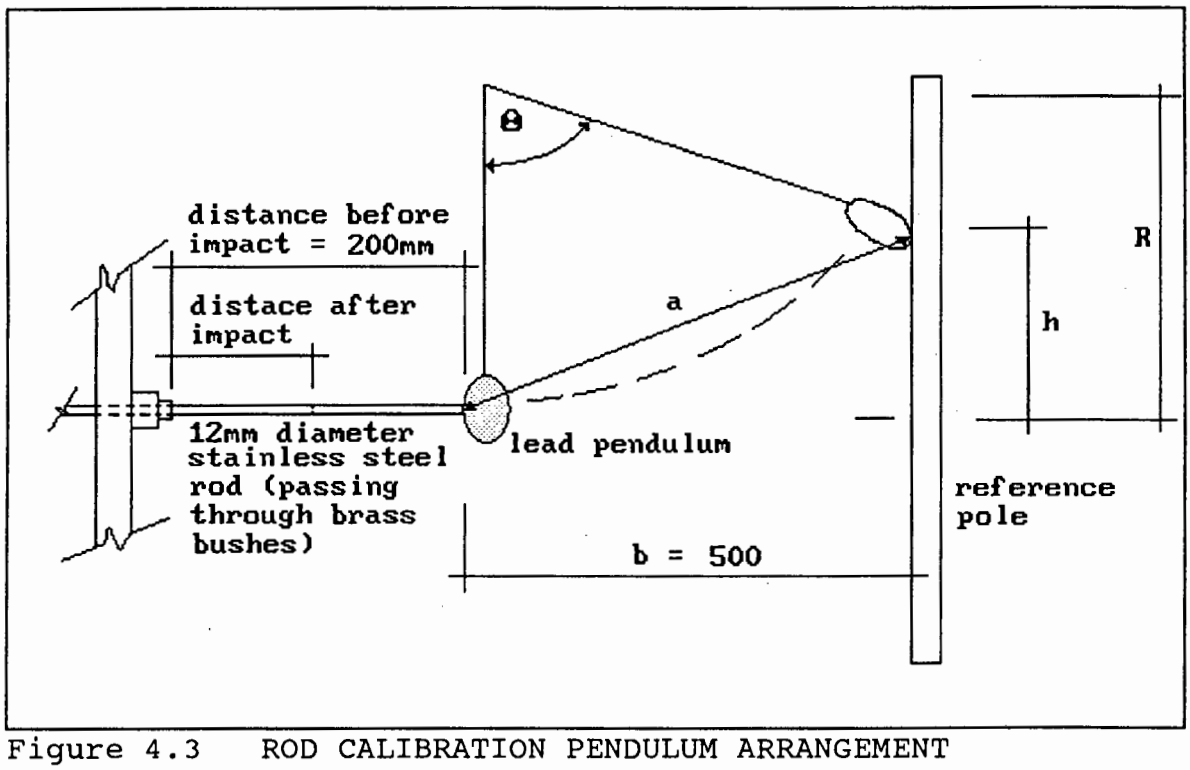

Figure 4.3 ROD CALIBRATION PENDULUM ARRANGEMENT

Solving for v:

$$v = \sqrt{2(gh)} \tag{4.3}$$

Considering simple idealized "elastic impact".[1] Referring to Figure 4.4 for conservation of momentum :

$$M_1V_1 + M_2V_2 = M_1V_1' + M_2V_2' \tag{4.4}$$

$$\therefore V_1 - V_1' = -\frac{M_2}{M_1}(V_2 - V_2') \tag{4.5}$$

It was observed that the pendulum came to rest immediately after impact. Therefore the final velocity of the pendulum (V_1') can effectively be taken as zero. The rod was initially at rest which meant that the initial velocity (V_2) was zero. Using these values and the masses of

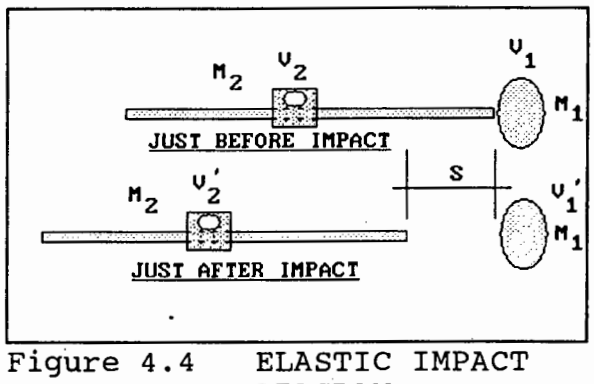

Figure 4.4 ELASTIC IMPACT DIAGRAM

the respective bodies, the velocity of the rod just after impact (V_2') was calculated using equation (4.5).

If it can be assumed that the deceleration of the rod was constant, due to a constant friction force, the deceleration can be calculated from the following formula:

$$v^2 = u^2 + 2a_R s \qquad (4.6)$$

where v = final velocity of rod = 0
u = initial velocity of rod(V_2')
a_R = deceleration of rod
s = average distance moved by rod due to impact.

The dynamic friction force (F_{df}) was calculated by means of the following formula:

$$F_{df} = m_R * a_r \qquad (4.7)$$

where F_{df} = Dynamic friction force acting on rod (N)
m_R = mass of rod including pencil holder and pencil, attachment etc. (kg)
a_R = deceleration of rod (m/s_2)

The results of the calibration tests and calculations for small beams can be seen in Table 4.1

TABLE 4.1 RESULTS OF DEFLECTION ROD FRICTION CALIBRATION (SMALL BEAMS)

Rod No.	2	3	4
Mass of Pendulum (kg)	0.339	0.339	0.339
Mass of rod etc (kg)	1.477	1.474	1.476
Average distance moved (m)	0.116	0.126	0.116
Height 'h' (mm)	175.8	175.8	175.8
V_1 (m/s)	1.857	1.857	1.857
V_2' (m/s)	0.426	0.427	0.427
a_R (m/s^2)	0.784	0.724	0.784
F_{df} (N)	1.157	1.067	1.157

The mean dynamic friction (F_{fd}) was found to be 1.127N and the coefficient of variation was 4.61%. The results of the calibration tests and calculations for the slabs can be seen in

Table 4.2

TABLE 4.2 RESULTS OF DEFLECTION ROD FRICTION CALIBRATION (SLABS)

Rod No.	1	2	3	4	5
Mass of Pendulum(kg)	0.339	0.339	0.339	0.339	0.339
Mass of rod etc (kg)	1.478	1.477	1.474	1.476	1.475
Average distance moved (m)	0.118	0.121	0.128	0.123	0.117
Height 'h' (mm)	175.8	175.8	175.8	175.8	175.8
V_1 (m/s)	1.856	1.856	1.856	1.856	1.856
V_2'(m/s)	0.426	0.426	0.427	0.426	0.427
a_R (m/s^2)	0.768	0.750	0.712	0.739	0.778
F_{df} (N)	1.135	1.108	1.049	1.090	1.147

The mean dynamic friction (F_{df}) was found to be 1.106N and the coefficient of variation was 3.51%.

This procedure was repeated for each rod in turn. The rods were numbered from 1 to 5 from the top to the bottom. For the small beams only the centre three rods were used (ie numbers 2, 3 and 4). For the slabs all five rods were used.

4.3 CALIBRATION OF THE FALLING BOARD

The falling board provided the time element in the deflection graph. In order to correct for the changing velocity during recording, it was necessary to measure the velocity the falling board gained over various distances. This would enable the equation of motion of the board to be calculated.

The equipment used was an electronic timer (measuring to 5 decimal places) which was connected to two light beams. A bracket and a piece of cardboard was attached to one side of the board, to break the light beams. A similar bracket was attached to the other side to ensure equal balance of the board. The one light beam was positioned just below the bracket when the board was in the raised position. The second light beam was positioned at various distances for the different tests. The distance between the light beams was measured with a calliper-vernia, accurate to 0.1mm.

Three sets of ten readings each were performed for various distances between the light beams. A summary of the results of the tests can be seen in Table 4.3.

TABLE 4.3 CALIBRATION OF FALLING BOARD

Test Number	1	2	3
Distance (mm)	86.98	213.5	315.1
Mean Time (sec)	0.1203	0.1960	0.2409
Std Deviation (sec)	0.0004	0.0005	0.0003
Maximum Time (sec)	0.1209	0.1966	0.2414
Minimum Time (sec)	0.1197	0.1953	0.2404
Coeff of Variation(%)	0.3	0.28	0.14
No. of Readings	10	10	10

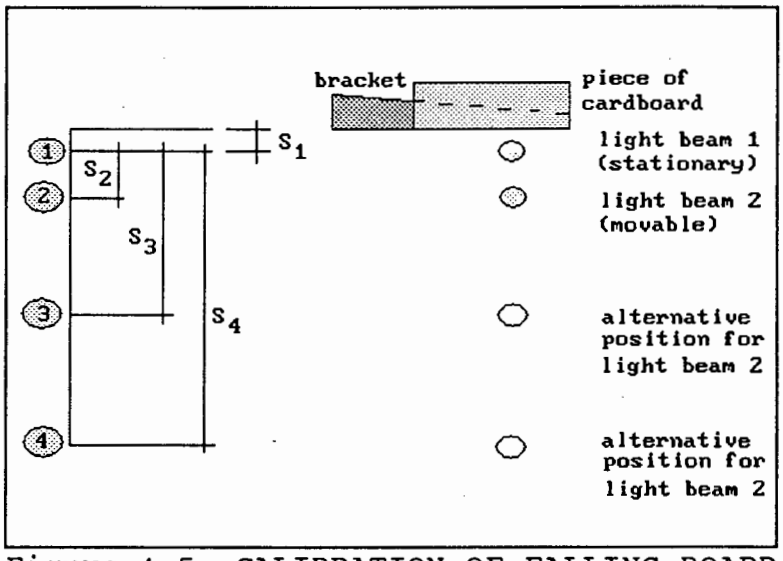

Figure 4.5 CALIBRATION OF FALLING BOARD

If it can be assumed that the downward acceleration (a_b) of the falling board was constant and if we know the time required to travel two adjacent segments of length s_2 and s_3 for example (see Figure 4.5). Then from the laws of motion, the acceleration of the falling board "a_b" can be obtained as follows:

Referring to Figure 4.5

s_1, u_1 and t_1 are unknown, however, u_1 can be calculated using measured times and distances.

$$s_2 = u_1 t_2 + 0.5 a_b (t_2)^2 \qquad (4.8)$$

$$s_3 = u_1 t_3 + 0.5 a_b (t_3)^2 \qquad (4.9)$$

$$s_4 = u_1 t_4 + 0.5 a_b (t_4)^2 \qquad (4.10)$$

By substituting the measured times and distances from Table 4.3 in the above equations and simplifying, three equations are obtained. By combining these three equations in the three possible combinations of two equations, three values for u_i and a_b can be obtained. The results of this analysis is given in Table 4.4

TABLE 4.4 CALCULATED VALUES FOR u_i AND a_b

Variable Type	u_i (m/s)	a_b (m/s^2)
Combination 1	0.142	9.66
Combination 2	0.14	9.70
Combination 3	0.13	9.779
Mean	0.138	9.72
Coeff of variation (%)	4.41	0.62

It should be noted that the value for the acceleration of the falling board was always less that g (9.80m/s^2 at UCT). The friction between the stainless steel guide rods and the board guides was thought to be the reason for this discrepancy. The guide rods were cleaned regularly to ensure that the amount of friction remained constant. The mean value for the acceleration of the falling board of a_b = 9.72m/s^2 was assumed in the analysis.

4.4 DETERMINING THE PERIOD OF OSCILLATION AND EFFECTIVE LENGTH OF THE PENDULUM

4.4.1 Determining Pendulum Period

The period of oscillation of the pendulum was determined by pulling it back, and timing the number of swings with a stopwatch accurate to one hundredth of a second. This was repeated five times. The procedure was performed for the pendulum with the impacting hammer in the positon for small specimens for three weight categories: with no additional weights, one 400N weight and two 400N weigths attached.

After all the small beams had been tested, the impacting "hammer" was removed and re-positioned in the correct position for the slab testing. The bar to which the weights were attached was also moved up and positioned centrally behind the impacting "hammer". The period was then determined as described above, for

two, three and five 400N weights attached.

The results of the period timing can be seen in Table 4.5 and Table 4.6.

TABLE 4.5 PENDULUM PERIOD OF OSCILLATION DETERMINATION FOR SMALL BEAMS

Weight Condition	No Weights	1 x 400N	2 x 400N
Timing 1	34.56	37.04	37.71
Timing 2	34.42	37.11	37.61
Timing 3	34.32	37.08	37.51
Timing 4	34.38	37.14	37.73
Timing 5	34.36	37.10	37.67
Mean	34.40	37.09	37.64
Coef of variation(%)	0.27	0.10	0.24
No. of Swings	10	10	10
Period	3.440	3.709	3.764

TABLE 4.6 PENDULUM PERIOD OF OSCILLATION DETERMINATION FOR SLABS

Weight Condition	2 x 400N	3 x 400N	5 x 400N
Timing 1	34.48	34.71	34.911
Timing 2	34.53	34.67	34.801
Timing 3	34.38	34.62	34.89
Timing 4	34.47	34.77	34.81
Timing 5	34.64	34.62	34.84
Mean	34.50	34.678	34.85
Coef of variation(%)	0.28	0.18	0.14
No. of Swings	10	10	10
Period	3.450	3.468	3.485

4.4.2 Determination of Effective Length of Pendulum

If the mass of the pendulum was concentrated at one point and was connected to the point of rotation by means of a cable, then this would represent a simple pendulum. The period of oscillation (T) of a simple pendulum is calculated from the following formula:

$$T = 2\pi \sqrt{\frac{L}{g}} \qquad (4.11)$$

where T = period of oscillation of the pendulum in seconds

L = length of cable between centre of mass and the point of rotation(m).

g = gravitational acceleration (9.80m/s^2 at UCT)

However, the pendulum used was a compound pendulum, as it consisted of a 4.15m length of 140mm x 60mm x 15.3kg/m parallel flange channel (described in the section on equipment). This meant that an equivalent length (L_e) and equivalent mass (M_e) had to be found for the pendulum.

By taking moments about the steel pin about which the pendulum rotated the length to the centre of mass (L_{cm}) was calculated. This length should have been equal to the length (L) from equation 4.11, obtained by using the measured period and solving for L. This was found not to be the case, which meant that the true point of rotation of the pendulum was some distance (x) from the steel pin. This was because the top of the pendulum column moved, despite having been braced. This meant that the point of rotation was not rigid and thus moved. This had the result that the true point of rotation was some distance (x) above the steel pin.

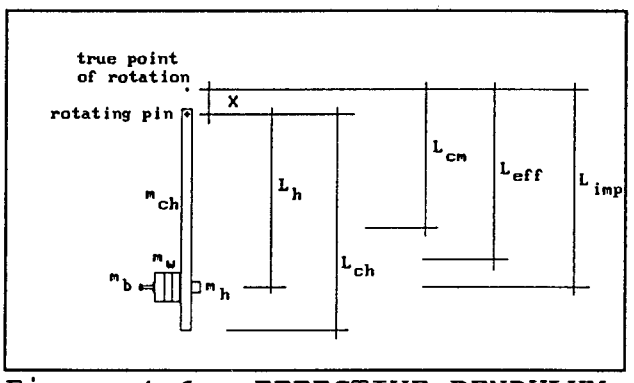

Figure 4.6 EFFECTIVE PENDULUM GEOMETRY

from Equation 4.11

$$L_e = g\left(\frac{T}{2\pi}\right)^2 \qquad (4.12)$$

where L_e = effective simple pendulum length (m)

g = gravitational acceleration (9.80m/s^2 at UCT)

T = timed period of oscillation in seconds

Referring to Figure 4.6, the distance 'x' was calculated as follows: for the compound pendulum the equivalent pendulum length is given by the following equation:.[2]

$$L_e = \frac{\int_o^L mx_2\delta x + \sum M_i L_i^2}{\int_o^L mx\delta x + \sum M_i L_i} \qquad (4.13)$$

For a continuous mass from L_1 to L_2 and a lump mass at L_3, Equation 4.13 is given as follows:

$$L_e = \frac{\frac{1}{3}m(L_2^3 - L_1^3) + ML_3^2}{\frac{1}{2}m(L_2^2 - L_1^2) + ML_3} \qquad (4.14)$$

where $L_1 = x$

$L_2 = L_{ch} + x$

$L_3 = L_h + x$

This amounts to the Centre of Momentum.

Equation 4.14 simplifies to:

$$x^2(M + L_{ch}m) + x[(2L_h - L_e)M + (L_{ch}^2 - L_{ch}L_e)m] + (L_h^2 - L_hL_e)M + (L_{ch}^3/3 - L_{ch}L_e/2)m = 0 \qquad (4.15)$$

By substituting the known values into Equation 4.15, the value of x was determined for each weight condition.

The distance from the centre of the hammer to the centre of the steel pin was defined as L_h. The impact length (L_{imp}) from the true point of rotation to the point of impact was defined as follows:

$$L_{imp} = L_h + x \qquad (4.16)$$

where L_{imp} = impact length of pendulum from true point of rotation to centre of the 'hammer'

L_h = distance from centre of hammer to centre of steel pin

x = distance from centre of steel pin to true point of rotation

In order to determine what proportion of the mass of the pendulum participated in the impact, an effective mass was calculated from the following equation:

$$M_{ep} = \left(\frac{L_e - x}{L_h}\right) M_T \qquad (4.17)$$

where M_T = total mass of pendulum

The effective length of the channel section is given by the following equation:

$$L_{(eff)ch} = \frac{2}{3} L_{ch} \qquad (4.18)$$

In order to deterimine what proportion of the mass of the channel section participated in the impact, an effective mass was calculated from the following equation:

$$M_{ech} = \left(\frac{L_{(eff)ch} - x}{L_h}\right) M_{ch} \qquad (4.19)$$

where M_{ch} = total mass of channel section

This analysis had to be repeated for a change in mass of the pendulum (due to the addition of weights). The analysis was also repeated when the "hammer" and weights' bolt was moved from the position for beam specimens to slab specimens. The results of this analysis can be seen in Table 4.7 and Table 4.8

TABLE 4.7 SUMMARY OF PENDULUM EFFECTIVE LENGTH & MASS ANALYSIS FOR SMALL BEAMS

Weight Condition	None	1 x 400N	2 x 400N
L_{cm} (m)	2.621	3.152	3.294
L_e (from period) (m)	2.941	3.418	3.513
Total Mass M_T (kg)	70.79	111.57	152.34
L_H (m)	3.87	3.87	3.87
Distance 'x' (m)	-0.0292	0.00674	-0.0600
L_{imp} (m)	3.841	3.877	3.810
M_{ep} (kg)	54.33	98.34	140.65
$L_{(eff)ch}$ (m)	2.767	2.767	2.767
M_{ech} (kg)	45.87	45.29	46.38

TABLE 4.8 SUMMARY OF PENDULUM EFFECTIVE LENGTH & MASS ANALYSIS FOR SLABS

Weight Condition	2 x 400N	3 x 400N	5 x 400N
L_{cm} (m)	2.797	2.858	2.924
L_e (from period) (m)	2.958	2.989	3.018
Total mass M_T (kg)	152.3	193.1	274.7
L_H (m)	3.067	3.062	3.068
Distance 'x' (m)	-0.00706	0.00236	0.00819
L_{imp} (m)	3.067	3.062	3.068
M_{ep} (kg)	147.6	188.5	270.2
$L_{(eff)ch}$ (m)	2.767	2.767	2.767
M_{ech} (kg)	57.56	57.37	57.25

4.5 REFERENCES

1. NORRIS, CHARLES, H. et al, Structural Design for Dynamic Loads, McGraw-Hill Book Company, Inc., New York, 1959.

C H A P T E R 5

EVALUATION OF MATERIAL PROPERTIES

5.1 INTRODUCTION

There were various material factors that had to be determined during the course of this thesis. These values included the Elastic Moduli for concrete and steel, concrete material properties as well as the dynamic shear strength of the concrete. The test methods and results are given in the following sections.

5.2 MATERIAL PROPERTIES OF CONCRETE

5.2.1 Conrete Mix Materials

5.2.1.1 Introduction

The concrete used for this thesis was made using cement, sand, stone and water available locally in the Western Cape. The materials chosen are those most commonly used in the Western Cape. Cape Flats Dune Sand was used as the fine aggregate, Greywacke (Peninsula), otherwise known as Malmesbury Shale was used as the coarse aggregate and the cement was De Hoek Ordinary Portland Cement.

5.2.1.2 Fine Aggregate

"Cape Flats Dune Sand is a wind-blown sediment characterised by a well-rounded particle shape. The sorting power of the wind results in a sand of uniform shape, size and relative density; ie it lacks both coarse and very fine particles."[1] (uniformly graded)

The grading of this sand is very poor and the particle size distribution falls outside the recommended limits laid down by SABS 1083 [1].

The fineness modulus (FM) of Cape Flats Dune Sand is dependent on its source and varies between 1.7 and 2.1. It may therefore be considered as a "fine" sand. However, "the well-rounded particles and the surface texture result in the relatively low water demand of the sand".[1] The relative density of the Cape Flats Dune Sand was found to be 2.64.

5.4.1.3 Coarse Aggregate

"Greywacke (Peninsula), otherwise know as Malmesbury shale is a Hornfels that developed by thermal metamorphism from argillaceous rocks. It is fine-grained and owing to its glassy nature, the Hornfels tends to produce a somewhat flaky aggregate when crushed."[1] However, recent improvements in crushing techniques have, to a large extent, helped to overcome this problem.[2]

A nominal 13.2mm Malmesbury Shale was used for the concrete in this thesis. A grading analysis was performed and the grading falls well within the recommended limits laid down by SABS 1083.

5.2.1.4 Cement

The cement used in this thesis was De Hoek OPC. "Portland cement consists of a mixture of calcium silicates, calcium aluminates and other molecular compounds which have hydraulic properties."[1] The proportions of the compounds present may vary from one plant to another and may even vary within a plant from day to day. These variations arise due to changes in the raw materials, production methods and production levels. The method of pre-blending the raw materials, regular testing and strict quality controls at the De Hoek plant does however, keep these variations to a minimum. The cement for each series of tests was from the same batch, so that it was the same for each specimen in the series.

5.2.2 Concrete Mix Design

5.2.2.1 Introduction

It was decided to use a normal strength concrete of 30MPa for this thesis, with a slump of 50mm. Locally available aggregates and cement were used and no additives were used.

Various trial mixes were made to obtain the desired 28-day compressive strength of 30MPa, for water-cured specimens.

5.2.2.2 Design Method

The design of the Ordinary Portland Cement (OPC) concrete mix was done according to the PCI method.[3] In this method cement/water

ratio (c/w ratio) is chosen from a graph according to the required 28-day compressive strength. The water requirement of the mix is determined by trial mixes, although an estimate can be made from the known properties of the aggregates. The cement content can thus be determined using the c/w ratio. The stone content is obtained from the published tables and the sand content is found from the remaining volume required to make up a concrete mix of one cubic meter.

The c/w ratio finally chosen was 1.5. The stone/sand ratio was also 1.5.

Final mix quantities for $1m^3$

Cement	=	333 Kg/m^3
Water	=	222 Kg/m^3
Stone	=	1085 Kg/m^3
Sand	=	723 Kg/m^3

5.2.2.3 Mixing Procedure

The materials were batched by mass. The mixing of the concrete was performed in either a 50 litre capacity pan mixer or a 100 litre capacity drum mixer, depending on the size of the batch.

All the dry materials were added to the mixer and thoroughly mixed in the dry state. The weighed water was then added in small quantities while the mixer was in motion. The concrete was then thoroughly mixed for approximately five minutes. A slump test was then performed to check if the desired slump of 50mm was achieved. If necessary the slump was reduced by adding additional stone and sand in the ratio 1.5:1, thus keeping the cement/water ratio constant at 1.5:1.

Once the concrete mix gave the correct slump, it was thoroughly mixed again and placed in the various moulds. The moulds were placed on a vibrating table for a set time (approximately 45 seconds) to achieve uniform compaction and to remove air bubbles. The slabs were compacted using a poker vibrator.

5.2.3 Elastic Modulus of Concrete

5.2.3.1 Introduction

"When a load is applied to a structural material it deforms. If on removal of the load the recovery is both complete and immediate the material is considered to be perfectly elastic. Concrete is not a perfectly elastic material in that all of the strain produced by an applied stress does not disappear on removal of the stress."[1]

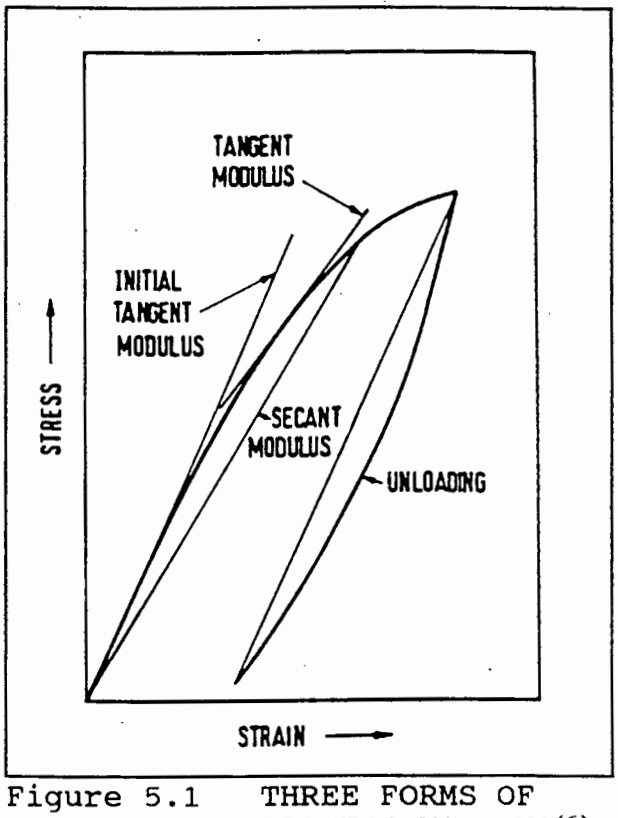

Figure 5.1 THREE FORMS OF ELASTIC MODULUS[6]

"If the ratio of the applied compressive (or tensile) stress to the longitudinal strain produced is constant, the constant is called the "modulus of elasticity" or Young's modulus. The stress-strain relationship for concrete is not constant or linear, ie it does not obey Hooke's law. The non-linearity of the stress-strain relationship for concrete is mainly due to creep or plastic deformation, particularly at slow rates of loading. A portion of the curve may however be regarded as effectively linear, and at stresses within this range the elastic modulus may be taken as the slope of this linear portion and it is referred to as the "initial tangent modulus". If the stress is above that at which the stress-strain relationship deviates from linearity, two further forms of elastic modulus may be considered, namely the "tangent modulus" as represented by the slope of the tangent to the curve at the particular stress, and the "secant modulus" represented by the slope of the line connecting the origin to the point of the curve corresponding to the stress selected."[1] The three forms of elastic modulus can be seen in Figure 5.1.

5.2.3.2 Static Elastic Modulus of Concrete

5.2.3.2.1 Making and curing of specimens

Three 300mm long by 150mm diameter test cylinders from the design mix were cast and cured in accordance with BS 1881 Part 3.[4] The moulds were filled in three layers and each layer was compacted using a vibrating table until all the air pockets had been removed. The specimens were cured under PVC sheeting for the first 24 hours.

Each specimen was then capped with a sand/cement mortar and a capping plate pressed down and left in place for a further 24 hours and cured under the same conditions as described above. The capping was performed to give the cylinders a smooth top surface.

The following day the specimens were demoulded and stored in a water bath, kept at a constant 22°C by means of a thermo-regulator. The specimens were cured in this way for 28 days.

5.2.3.2.2 Static Testing Method

The static modulus of elasticity was determined according to BS 1881: Part 121 : 1983.[5]

A wet specimen has a higher modulus of elasticity than a dry one, while strength varies in the opposite sense.[6] The beams would be tested in the dry state, therefore the cylinders should be in the same state when determining the Young's Modulus.

The cylinders were tested when air dried for at least one day. Three pairs of targets equally spaced around the perimeter of the cylinder, were attached to the specimens by means of epoxy. The targets consisted of brass discs with stainless steel balls set in the centre. Each pair of targets was positioned 100mm apart, placed symmetrically around the mid-length of the specimen.

The concrete cylinders were loaded in compression and the longitudinal strain measured with a Pfender precision strain gauge with a gauge length of 100mm.

In carrying out the test, the specimens were first loaded to about 40% of their ultimate compressive strength at a constant rate of 15MPa per minute. The load was maintained for one minute and then the stress was reduced to 1MPA. This process was repeated for a second time. This "exercising" of the test specimen reduces the creep and on the third or fourth loading the curvature of the stress-strain relationship is generally very small for compressive stresses which are less that half the ultimate stress.

The load was then applied again at the same rate and strain gauge readings taken at a lower and upper value not exceeding 40% of the ultimate compressive stress. When the strain observed at each pair of targets differed by more than 5% from the average strain, the specimen was unloaded and re-aligned on the platen. The procedure was then repeated until the difference was less than 5%.

The static modulus of elasticity is taken to be the slope of the straight line drawn through the plotted stress-strain points, expressed in GPA.

5.2.3.2.3 Discussion of Results of Static modulus of elasticity

The average value of the static modulus of elasticity was 31.2GPa. This falls within the range of 20GPa to 32GPa given in Table 7.5.[1]

The most important factor influencing E is the type of aggregate used. The stiffer the aggregate the higher will be the E of the concrete. For a given type of aggregate, the E of the concrete will increase with the strength of the concrete.[2]

The following formula has been developed [7] to estimate the static modulus of elasticity. It takes into consideration the aggregate properties as well as the strength of the concrete. This formula is not accurate for strengths less than 20MPa.

$$E_s(GPa) = K_o + \alpha f_{cu} \qquad (5.1)$$

where E_s = static modulus of elasticity for the particular age of concrete being considered

f_{cu} = cube strength in MPa (generally the characteristic strength) of concrete at age matching that required for E.

K_o = a constant related to the stiffness of the aggregate, and is expressed in units of GPa

α = a strength factor and is also related to the aggregate characteristics. It is expressed in units of GPa/MPa.

Using the corresponding values for Greywacke (Peninsula) as given in Table 4 [2] and substituting into the equation: (5.1)

$$E_s(GPa) = K_o + \alpha f_{cu}$$
$$= 24 + 0.25 * 30$$
$$= 24 + 7.5$$
$$= 31.5 \text{ GPa}$$

This compares well with the experimental value of 31.2GPa.

Table 6 [2] gives an E_s - value of 31GPa for 30MPa concrete made with Peninsula Greywacke. This corresponds well with the experimental value of 31.2GPa.

5.2.3.3 Dynamic Modulus of Elasticity

Unfortunately there was no equipment available to measure the dynamic modulus of elasticity. Due to limited funds such equipment could not be purchased for this thesis.

Some method had therefore to be found to obtain the dynamic modulus of elasticity. Various relationships between static and dynamic moduli have been suggested but the one proposed by SABS 0100 is probably the most suitable and is generally correct to within +/- 4GPa.[1]

The relationship is

$$E_c = 1.25E_{cq} - 19 \text{ (GPa)} \qquad (5.2)$$

where E_c = static modulus of elasticity
E_{cq} = dynamic modulus of elasticity.

Re-arranging equation 5.2

$$E_{cq} = \frac{(E_c + 19)}{1.25} \quad \text{GPa} \qquad (5.3)$$

Substituting the experimental value of 31.2GPa for E_c in equation 5.3 a value of 40.2GPa is obtained for E_{cq}.

However, Jones[8] has pointed out that the relationship between static and dynamic modulus vary when different types of aggregate are used.[1] For this reason, the results of Mukheibir[9] will be discussed.

Although the thesis dealt with fly ash, control mixes were made containing no fly ash. This mix used the same type of materials, Penisula Greywacke, Cape Flats dune sand, and OPC from the De Hoek Plant. The stone content has the largest influence on the elastic modulus[2], as mentioned earlier. For this reason it is important that the stone content is very similar if any comparison is to be made. A comparison of the static elastic modulus and mix proportions of Mukheibir's and the author's mixes are made in Table 5.1 for 30MPa mix.

TABLE 5.1 COMPARISON OF CONCRETE MIXES

Type	Mukheibir	Author
Static E (GPa)	31	31.2
Stone Content (kg/m^3)	1050	1085
Total Aggregate (kg/m^3)	1850	1808

From Table 5.1 it can be seen that the stone content is very similar, as is the total aggregate content. The static elastic moduli also compare well. For this reason it is felt that the value for the dynamic modulus of elasticity obtained experimentally by Mukheibir (with equipment no longer available)

could be accepted for the purpose of this thesis. The value for the dynamic modulus of elasticity determined by Mukheibir was 39GPa.

5.2.3.3.1 Discussion of Two Dynamic Elastic Moduli (E_d) Values

The two values of E_d are:

SABS 0100 40.2GPa

Mukheibir 39.0GPa

These differ by 2.9% which shows good agreement. It was decided however to accept the value of E_d = 39GPa (of Mukheibir), as this takes into account the additional fact that the aggregates used in the mix were very similar, as mentioned before. This would thus represent a truer value.

5.2.4 Dynamic Shear Strength of Concrete

5.2.4.1 Introduction

There was always the possibility that the specimen that was impacted could fail in shear instead of flexure. This was particularly possible with the slabs. It was for this reason that the effects of high loading rates on shear strength of concrete were investigated. A shear test method[10] was adapted for this purpose in this thesis. The tests were performed on samples made from the standard concrete mix used for all concrete specimens in this thesis.

5.2.4.2 Description of Test Apparatus

The test apparatus consisted of a test rig that clamped the sample and a plunger that was connected to the 'Denison' Universal Testing Machine.

5.2.4.2.1 Test Rig

The test rig consisted of two 40mm thick steel platens finished off with a flatness tolerance of 0.03mm as required by BS 308: part 3: 1972 (part 312) for compressive testing machines. The bottom platen was 200mm long and 180mm wide. The two platens were connected by means of four 20mm diameter bolts at 150mm centres. The bottom platen had two 15mm thick, 100mm by 60mm, plates welded to it to enable the whole arrangement to be bolted

to the 'Denison' Universal Testing Machine. (The test rig was later used in conjunction with the pendulum impactor). A photograph of the test rig and plunger can be seen in Photographic Plage 5.1.

5.2.4.2.2 Shear Test Plunger

The plunger that was attached to the 'Denison' Universal Testing Machine was 102mm wide, 320mm high and 20mm thick. The contact edge of the plunger had a radius of 10mm. The top of the plunger had a swivel point which permitted the plunger to align itself once it made contact with the concrete specimen.

5.2.4.2.3 'Denison' Universal Testing Machine

This machine was used to apply the load to the test specimen. The descent of the head was timed for various positions of the valve control wheel. This was to 'calibrate' the machine so as to have various rates of displacement that could be used to test the effect of rate of displacement on shear strength.

The timing of the speed of the head was performed as follows: A piece of 50mm wide by 5mm thick flat steel was clamped to the moving head so that the other end protruded past one of the uprights. A tape measure was secured to the upright. A reference mark was made on the wheel in its closed position by means of a piece of masking tape. The wheel was then opened so that the reference mark was in-line with previously-determined marks on the front face of the 'Denison'. The machine was switched on and when the steel marker passed a convenient number on the tape measure, the stopwatch was started. Depending on the speed, the head was allowed to travel for distances ranging from 50mm to 300mm at which point the stopwatch was stopped. Three sets of readings were taken to ensure repeatability. The results of the timing can be seen in Table 5.2.

TABLE 5.2 SPEED CALIBRATION OF 'DENISON'

Speed Category	A	B	C	D
Distance Travelled	50	300	300	300
Time 1 (Min:Sec)	8:15.05	4:45.28	1:57.22	1:14.54
Time 2 (Min:Sec)	8:15.46	4:44.66	1:56.98	1:14.39
Time 3 (Min:Sec)	8:14:54	4:45.09	1:57.01	1:14.54
Mean	8:15.02	4:45.01	1:57.81	1:14.54
Coeff of Variance(%)	0.09	0.11	0.18	0.23
Speed(mm/s)	0.101	1.053	2.564	4.025

The mean values for the respective speed categories were used in the analysis.

5.2.4.3 Dynamic Shear test using 'Denison'

5.2.4.3.1 Preparation for Testing

The two inner bearing surfaces of the testing rig had to be wiped clean. Loose material had to be removed from those surfaces of the test specimen which were to be in contact with the platens. The plunger was bolted to the 'Denison'.

5.2.4.3.2 Positioning of the test specimen

The rig was slotted into the 'Denison' but not bolted in position at first. A 500mm long, 100mm wide and 100mm deep unreinforced concrete beam was inserted in the test rig. The beam was placed on its side so that two moulded faces made contact with the platens. A clearance of 10mm between the bolts and either side of the specimen was allowed.

The rig was moved to the approximate position required for the test. The plunger was lowered until it almost touched the top surface of the specimen. A 20mm x 20mm box-section was used as a spacer between the inside surface of the plunger and the edge of the top platen. The specimen was aligned in the test rig so that a length of 60mm protruded in front of the top platen. (All specimens had been marked with a line across the top and dowm the sides of the specimens prior to being inserted into the rig.) The whole arrangement was then shifted forward until the spacer was against the plunger. The test rig was then bolted into

position. This position was then kept constant for all specimens from both series tested.

5.2.4.3.3 Clamping Stress

The clamping stress was obtained from a graph of torque versus stress.[10] "A load cell was used to calibrate the downward stress of the top plate. A graph of torque versus percentage load cell strain was obtained. The percentage load cell strain was further calibrated to obtain a downward force and by using the area of the clamped specimen, a stress versus torque graph was obtained."

The cube strength was required to determine the clamping stress. The compressive strength of the concrete used in the specimens was obtained by testing standard 100mm x 100mm x 100mm cubes in an "Amsler" Compression Machine of 3000kN load capacity. They were loaded in compression at a rate of 150kN/minute (ie 15MPa/min) until failure occurred. Reference [10] recommends that a clamping stress of 0.1 * compressive strength be used. The stress versus torque graph was then used to determine the torque for each bolt.

5.2.4.3.4 Method of clamping

The bolts were torqued down in stages as shown in Figure 5.2. A torque wrench was used to obtain the desired torque. Once the desired torque for each bolt had been applied, all bolts were checked in the same sequence as shown in Figure 5.2.

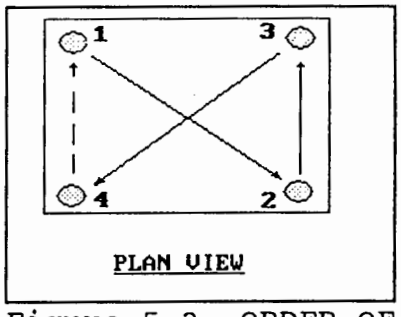

Figure 5.2 ORDER OF BOLT TIGHTENING

5.2.4.3.5 Loading of the specimen

The plunger was lowered slowly until it made firm contact with the top surface of the specimen. The spacer was removed to ensure that all the load was applied to the specimen. The 'Denison' was switched off. The valve handle was then turned to the position of the required displacement rate. This procedure applied the required displacement rate immediately when the

'Denison' was switched on. The load was removed immediately after the specimen was observed to fail. (ie cracking was observed) This was to prevent the sheared portion hitting the bolt that connected the rig to the 'Denison' and thus giving a higher reading on the dial.

The specimen was removed from the rig, turned around and inserted again, as described before. In this way two tests could be obtained from each sample. By using each end of the specimen, an undamaged end was used for each test. This eliminated 'damage' effects that would have influenced the results if sequential 'slices' were chopped off the specimen.

5.2.4.3.6 Results of 'Denison' Shear Tests

Earlier shear tests indicated a trend that needed to be investigated further. There were too few initial results and therefore two sets of ten 'rupture' beams were cast to be tested in the 'Denison' shear test. The test were performed as previously described. The results are listed in Tables 5.3 for Series A and in Table 5.4 for Series B.

TABLE 5.3 DYNAMIC SHEAR TEST RESULTS FOR SERIES A

Beam No.	Rate of Displace-ment (mm/sec)	Failure Load(kN)	Beam No.	Rate of Displace-ment (mm/sec)	Failure Load(kN)
SHA1(1)	0.101	21.0	SHA6(1)	1.053	20.9
SHA1(2)	4.025	14.7	SHA6(2)	2.564	14.4
SHA2(1)	1.053	28.9	SHA7(1)	4.025	25.2
SHA2(2)	2.564	28.6	SHA7(2)	0.101	19.8
SHA3(1)	4.025	18.5	SHA8(1)	1.053	23.6
SHA3(2)	0.101	26.7	SHA8(2)	2.564	30.0
SHA4(1)	1.053	19.5	SHA9(1)	4.025	15.0
SHA4(2)	2.564	16.7	SHA9(2)	4.025	15.5
SHA5(1)	4.025	14.75	SHA10(1)	2.564	27.4
SHA5(2)	0.101	13.8	SHA10(2)	0.101	30.2

TABLE 5.4 DYNAMIC SHEAR TEST RESULTS FOR SERIES B

Beam No.	Rate of Displace-ment (mm/sec)	Failure Load(kN)	Beam No.	Rate of Displace-ment (mm/sec)	Failure Load(kN)
SHB1(1)	4.025	20.1	SHB6(1)	2.564	25.4
SHB1(2)	0.101	22.2	SHB6(2)	1.053	25.7
SHB2(1)	2.564	24.6	SHB7(1)	4.025	7.2
SHB2(2)	1.053	17.1	SHB7(2)	0.101	17.0
SHB3(1)	4.025	16.0	SHB8(1)	2.564	13.7
SHB3(2)	0.101	25.7	SHB8(2)	1.053	17.4
SHB4(1)	2.564	24.1	SHB9(1)	4.025	18.2
SHB4(2)	1.053	26.8	SHB9(2)	0.101	16.5
SHB5(1)	4.025	8.5	SHB10(1)	2.564	11.1
SHB5(2)	0.101	20.8	SHB10(2)	1.053	21.3

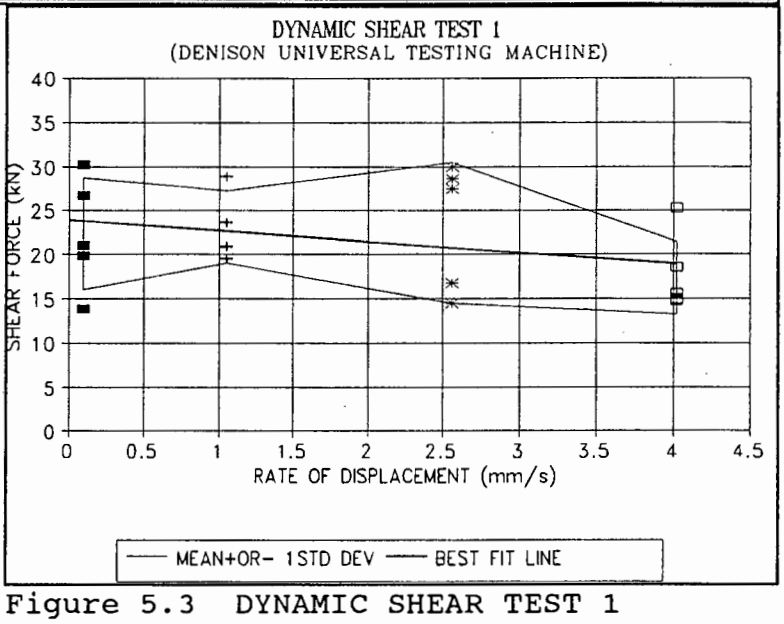

Figure 5.3 DYNAMIC SHEAR TEST 1 RESULTS (f_{cu} = 31.9MPa)

The results were plotted and are shown in Figures 5.3 and 5.4. The enclosed area in the graphs represent an envelope that has limits of one standard deviation above and below the mean of each set of readings, for a particular displacement rate. A least square regression line was then plotted, which fell within the envelope. This shows that there was a definite tendency for the shear strength to decrease with increasing rate of displacement. The dynamic shear tests gave different types of failure surface for flexural and shear failure. The tendency was for flexural failure to occur with higher rates of displacement. these modes of failure are shown in Photographic Plates 5.3 to 5.5. Photographic Plate 5.3 shows a set of three beams with flexural failure surfaces on the left and shear failures on the right. Photographic Plate 5.4 shows a close-up of the flexural failure and it can be seen that the cracks started at the edge of the

platen are almost vertical. Photographic Plate 5.5 shows a close up of the shear failure. The crack started under the load and continued down to the edge of the bottom platen.

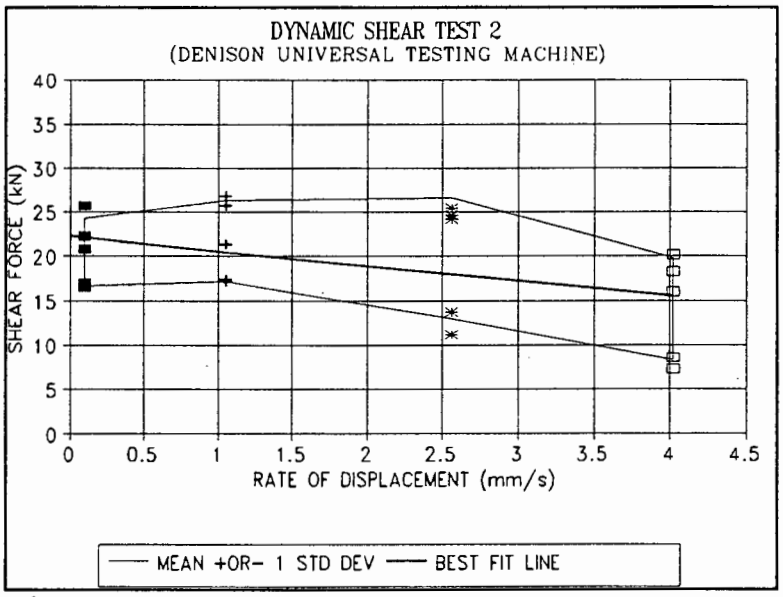

Figure 5.4 DYNAMIC SHEAR TEST 2 RESULTS (f_{cu} = 32.1MPa)

5.2.4.4 Dynamic Shear Tests using Pendulum Impactor

5.2.4.4.1 Introduction

The shear apparatus used in the 'Denison' was bolted to the small support structure. This was to perform dynamic shear tests at higher rates of displacement than that the maximum speed of the 'Denison'.

5.2.4.4.2 Positioning of the test specimen

The test specimens were the two halves of the beams that were tested with the pendulum impactor to obtain the dynamic modulus of rupture. The specimens were positioned in the rig with the cast end protruding 60mm above the top plate (as for the 'Denison Tests'). The bolts were torqued down as described in the section for the 'Denison'. The setup can be seen in Photographic Plate 5.1.

5.2.4.4.3 Positioning of Contact Point

The contact point between the rubber pad glued to the pendulum "hammer" and the test specimen was a 20mm diameter steel bar. It was not physically possible to allow the hammer to hit the specimen just above the top platen. To overcome this limitation the steel bar was supported on a 20mm high spacer. This meant that the point of contact of the bar with the specimen was 30mm

above the edge of the top platen. This was identical to the positioning that occurred with the 'Denison' shear tests, as the end of the plunger had a radius of 10mm (diameter of 20mm). This was identical to the positioning that occurred with the 'Denison' shear tests, as the end of the plunger had a radius of 10mm (diameter of 20mm). This was done so that some measure of comparison was possible between the 'Denison' tests and those from the impact test. The position of the specimen for the impact test can be seen in Photographic Plate 5.2. It shows the positioning of the 20mm diameter steel bar on the spacer.

5.2.4.4.4 Loading of Specimens

The release point was positioned at various distances from the specimen until the specimen failed. This was done for the first specimen to get an idea of the position of the release for failure to occur ('just failed'). A 'just failed' condition was defined as the condition at which the specimen had a crack right through, or when it had a crack length extending 90 percent or more of the beam depth. However, when the top portion was 'chopped' off so that it went 'flying, it was termed as excessive (ie too much energy was impacted to the specimen).

The loading was performed with the pendulum on its own (ie no 400N weights) for some samples. Other samples were tested with the pendulum and one 400N weight attached.

The results proved repeatable, as once the 'just failed' position had been determined, the other half of the same beam was used and impacted from the same release point and it too gave a 'just failed' result. The results for the 'just failed' results condition for both load conditions are summarized in Table 5.5.

TABLE 5.5 PENDULUM DYNAMIC SHEAR RESULTS

Load Condition	Dist POI(mm)	Velocity(m/s)	Force (kN)
No Weights	3050	4.412	8.76
1 x 400N weight	2300	3.360	7.62

5.3 MATERIAL PROPERTIES OF STEEL

5.3.1 Determination of Elastic Modulus of Steel Beams

5.3.1.1 Test Method

The Elastic Modulus was determined by means of a direct tension test performed using a 'Denison' Universal testing machine.

One steel beam from each series was cut down the centre, along the length to give two specimens, 600mm long and 50mm wide. The first specimen was used to get an idea of the yield load and fracture load of the steel beams.

The second specimen was tested, using an extensometer with a gauge-length of 101.6mm and a dial gauge accurate to 0.01mm. (The two values determined on the first specimen were required to prevent damage to the extensometer by premature fracture of the specimen with the extensometer still attached.) The dial gauge was read every 0.2kN of load applied, until well into the yield region, however, the extensometer was removed before final fracture. The specimen was then tested to fracture and the fracture load was recorded.

5.3.1.2 Results of Elastic Modulus Tests for Steel Beams

The readings were used to plot a stress-strain graph for each series of steel beams. The Young's Modulus was taken as the slope of the best fit line through the linear portion of the stress-strain graph. The stress-strain graphs for Series A and B can be seen in Figure 5.5 and Figure 5.6 respectively.

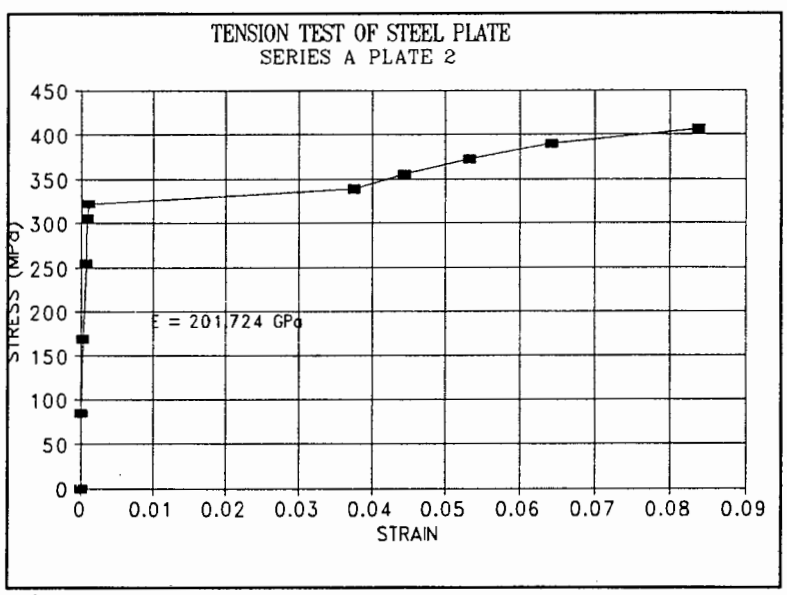

Figure 5.5 STRESS-STRAIN GRAPH FOR STEEL BEAM (SERIES A)

A summary of the results can be seen in Table 5.6
(The dimensions of the steel plates were measured with a calliper-vernia accurate to 0.02mm, before each test.)

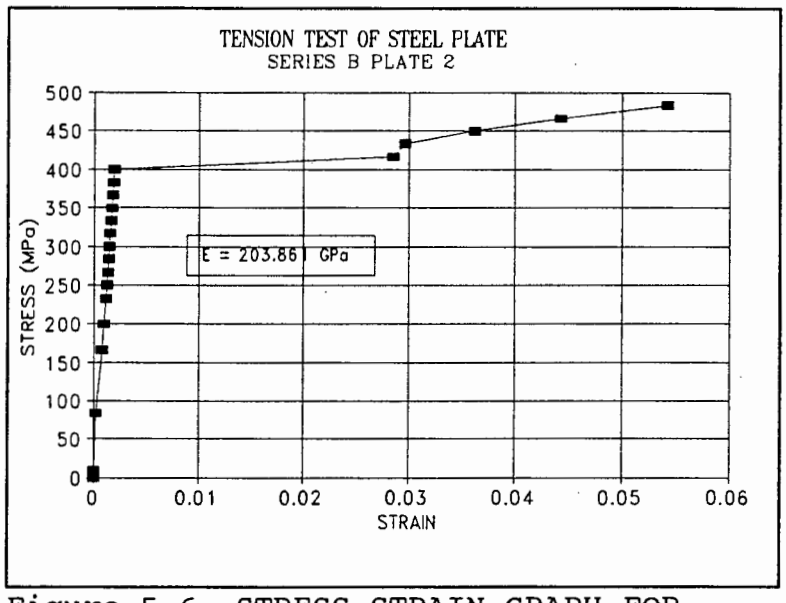

Figure 5.6 STRESS-STRAIN GRAPH FOR STEEL BEAM (SERIES B)

TABLE 5.6 SUMMARY OF TENSION TESTS

Series	A	B
Young's Modulus (GPa)	201.7	203.9
Yield Stress (MPa)	322.0	399.8
Fracture Load (KN)	135.0	157.58
Width of Plate (mm)	50.0	49.2
Thickness of Plate (mm)	5.9	6.1
Gauge Length (mm)	101.6	101.6

5.3.2 Determination of Elastic Modulus of Reinforcing Steel

5.3.2.1 Test Method

The Elastic Modulus was determined by means of a tension test performed using a 'Denison' Universal testing machine. This was for the 5.67mm reinforcing bars. A similar machine in the Department of Materials Engineering was used for the smaller reinforcing bars of 3.15mm and 3.55mm diameter.

The method used was the same as for the steel beams (see section 5.3.1.1).

5.3.2.2 Results of Elastic Modulus Tests for Reinforcing Steel

The average results of the tests for the various diameters are given in Table 5.7.

TABLE 5.7 ELASTIC MODULUS FOR REINFORCING STEEL

Bar diameter	3.15	3.55	5.67
Elastic Modulus (GPa)	208.9	207.8	203.5
Ultimate Yield Strength (MPa)	502.9	493.3	479.2

These values were used for both the beam and slab analysis, where applicable. For an example of a stress-stain graph see Figure 5.7.

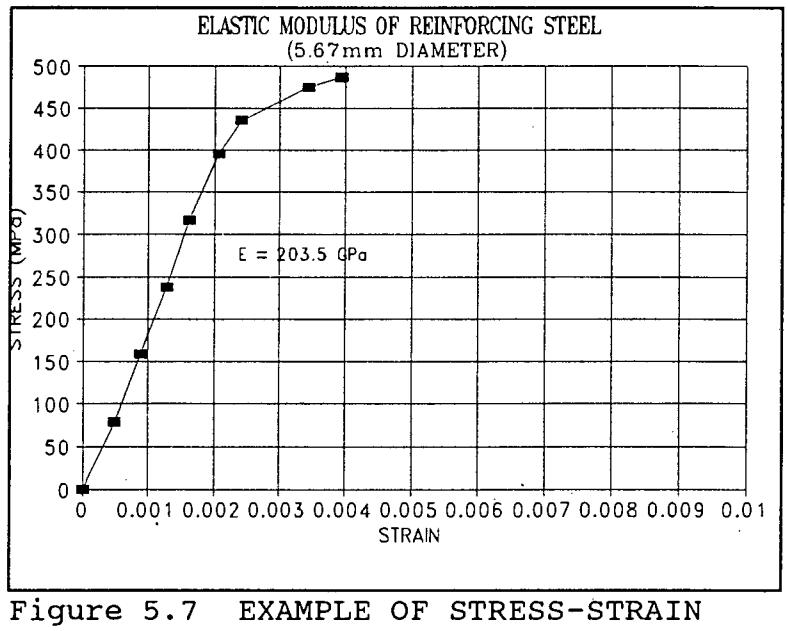

Figure 5.7 EXAMPLE OF STRESS-STRAIN GRAPH

5.4 REFERENCES

1. FULTON'S CONCRETE TECHNOLOGY, 6th revised edition, Midrand, Portland Cement Institute, 1986
2. HIPPO QUARRIES, Properties of Aggregates in Concrete, Part1, Technical Publication, Sandton 1992.
3. PORTLAND CEMENT INSTITUTE, Cement and Concrete, Halfway House, 1983
4. BRITISH STANDARD B.S 1881: "Methods of Testing Concrete", Part 3 - Methods of making and curing concrete.
5. BRITISH STANDARD B.S 1881: "Methods of Testing Concrete", Part 121 - Methods for determining the static modulus of elasticity in compression, 1983.
6. NEVILLE A.M., Properties of Concrete, London, Pitman Press, 1977.
7. HIPPO QUARRIES, Properties of aggregates in concrete, Part2, Technical Publication, Sandton, 1992.
8. JONES, R, Non-destructive testing of concrete, Cambridge, University Press, 1962.

9. MUKHEIBIR, P.V., The Deformation Properties of Concrete with Classified Lethabo Fly Ash, MSc Thesis University of Cape Town, 1990.
10. POSPORIS, C, Investigation of a "New" Shear Test Procedure, BSc Thesis, University of Cape Town, 1988.

Photographic Plate 5.1 SHEAR TEST RIG AND PLUNGER

Photographic Plate 5.2 PENDULUM DYNAMIC SHEAR ARRANGEMENT

Photo Plate 5.3
TESTED DYNAMIC SHEAR SPECIMENS

Photo Plate 5.4
CLOSE-UP OF DYNAMIC 'FLEXURAL' FAILURE FOR PLAIN CONCRETE SPECIMENS

Photo Plate 5.5
CLOSE-UP OF DYNAMIC 'SHEAR' FAILURE FOR PLAIN CONCRETE SPECIMENS

C H A P T E R 6

PREPARATION OF SPECIMENS AND TEST PROCEDURES

6.1 STEEL BEAMS

6.1.1 Introduction

It was decided to use flat steel beams as the first type of beam to be tested dynamically so as to check that all the equipment worked correctly. The steel beams could be tested elastically at first, giving reasonable deflections for analysis, before testing plastically.

6.1.2 Preparation of specimens

Each beam in a series was cut from a 6.0m length of 100mm wide, by 6mm thick flat steel plate. This was to ensure that all beams in a series were identical. Each beam was 600mm long, to allow enough overhang to ensure the beam was still supported during large deflections.

Initially it was intended to epoxy the deflection rod attachments to the steel beam. This, however, was not successful, as the attachments were dislodged after impact. The large curvature of the steel beam during deflection was thought to have caused the epoxy to peel off the steel beam and so dislodge the deflection rod attachments.

The problem was solved by tapping a 5mm diameter thread into the centre of the deflection rod attachment and drilling a 5.5mm diameter hole in the steel beam at the required position. The deflection rod attachment was then bolted to the steel beam by means of an allen key head bolt. Three deflection rods were attached to each steel beam for a test.

6.1.3 Static Deflection Tests

A static deflection test was performed on one steel beam from each series to obtain the failure load and the failure deflection.

The test was performed on the 'Denison' Universal testing machine. Two 50mm dial gauges were used in tandem, with sufficient overlap, to record the total deflection range.

Readings were taken every 0.1kN of load until the maximum load was reached, which was indicated by the load just starting to drop-off. The beam was then unloaded slowly and readings were taken.

6.1.4 Impact Testing of Steel Beams

Each steel beam was positioned in the small support structure and was held in place by means of tying the beam against the knife-edge supports with cord. This was to ensure that the beam was held firmly, yet was able to rotate during impact.

The three deflection rod connecters were bolted to the beam, ensuring that the slots to which the deflection rods were connected, were vertical and allowed free movement in a vertical direction. Graph paper was fastened to the falling board by means of masking tape. The pencils were positioned in a staggered manner so as to prevent the deflection diagrams from being drawn on top of each other. The board was raised with the pencils touching the graph paper, so as to draw a zero (base) line.

The position of the release mechanism was chosen and the light trip was positioned accordingly. The arc-measuring device was loaded with graph paper and the spacer block positioned, once the pendulum had been placed against the release mechanism.

The light beam of the light trip was switched on and the electric circuit was closed. After a final check that everything was in order, the release mechanism was activated. The pendulum then impacted the specimen and was caught after it had rebounded and started swinging towards the beam again. This was to allow the back-swing arc to be recorded, but to prevent the pendulum hitting the specimen a second time.

6.1.4.1 'Elastic' Impact Testing of Steel Beams

Each steel beam was first tested "elastically" to obtain data to check that the equipment worked correctly. This was usually performed twice for each beam to check repeatability of results.

6.1.4.2 'Plastic' Impact Testing of Steel Beams

Each beam was then tested "plastically" in an effort to achieve the permanent plastic deformation that was achieved during the static test. This permanent plastic deformation represented "failure" of the beam. If this permanent plastic deformation could be achieved by impacting the steel beam with the pendulum, the dynamic "failure" load could be calculated.

The "plastic" impact test consisted of two types of impact loads. The first type was impacting a number of steel beams with the pendulum on its own (ie no 400N weights attached - high initial intensity and short duration). The second type of impact load involved impacting a number of steel beams with the pendulum with one 400N weight bolted to the pendulum. (Low initial intensity and long duration.) This was done in an effort to vary the duration of the impact. The pendulum with one 400N weight bolted to it would give a larger duration of impact than the pendulum without a 400N weight bolted to it, due to its lower velocity.

6.2 CONCRETE BEAMS

6.2.1 Introduction

The concrete beams used in this thesis had the following dimensions: 500mm long, 100mm wide and 100mm deep. Both reinforced and unreinforced beams were made. The standard concrete mix was used for all beams.

6.2.2 Making and Development of Specimens

6.2.2.1 Initial Phase for Reinforced Concrete Beams

An initial phase was used to determine the arrangement and percentage reinforcement that was to be used for the impact tests.

It was decided to use three percentages of reinforcement, the details of which are listed in Table 6.1.

TABLE 6.1 REINFORCEMENT DETAILS OF BEAMS (Initial Phase)

Beam Type	1	2	3
Bar diameter(mm)	3.15	3.15	5.67
Number of Bars	2	4	2
Percentage Reinforcement	0.156	0.312	0.505

The arrangement of the reinforcement be seen in Figure 6.1 The above reinforcement was made using a bending machine and the appropriate bar size. The stirrups were made from 3.15mm diameter hard drawn wire. Cement-mortar spacer blocks of approximately 15mm in height were tied beneath the cages to ensure their correct positioning.

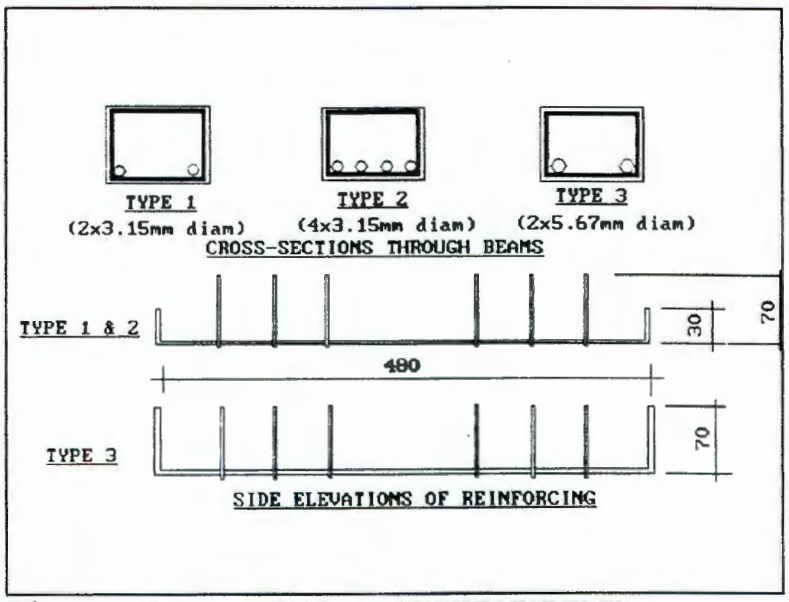

Figure 6.1 TYPE 1 REINFOREMENT ARRANGEMENT

The concrete beams were made by placing the reinforcing cages into the moulds and filling the moulds with the standard concrete mix in several layers. The moulds were placed on a vibrating table and the reinforcing cage was held in position while each mould was filled. The time of vibration was kept constant at approximately 45 seconds, to ensure good compaction and to remove air bubbles. Standard 100mm x 100mm x 100mm cubes were cast from the same mix to determine concrete strength.

The moulds were covered with PVC sheeting for one day. The specimens were then de-moulded, labelled and cured in a water bath at a constant temperature of 23°C ± 1°C for 28 days. The beams were tested in one-point loading, at various loading rates. The range of loading was from static loading to as fast as the 'Denison' Universal Testing Machine could go.

The results showed that for the Type 1 beams (0.156% Reinforcement) the percentage reinforcement was too low. This was shown when the load dropped off as soon as the concrete cracked. (ie the reinforcemnt was unable to sustain the load). The Type 2 beams showed insufficient anchorage of the reinforcement during loading. The Type 3 beams showed insufficient anchorage of the reinforcement, as well as bursting of the concrete at the corners. This bursting was thought to have occurred because of insufficient cover to the sides of the beams

The reinforcement for the next series of beams was modified to overcome the problems that occurred with the previous series. The percentages of the reinforcement was kept the same, but the arrangement was changed, as shown in Figure 6.2. The cover to the reinforcement on the sides of the beams was increased from 10mm to 15mm to prevent bursting. The reinforcing wire was thoroughly cleaned with paraffin to remove any traces of oil, to improve bond strength between the concrete and the steel. These beams were made in the standard way and were tested in the impactor, as series CB.

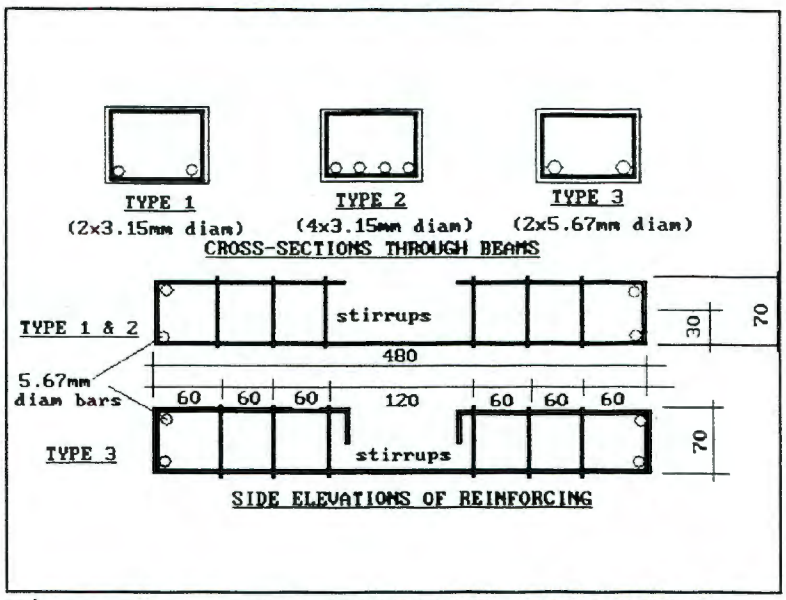

Figure 6.2 REINFORCEMENT ARRANGEMENT TYPE 2

A series of plain, unreinforced concrete beams were cast to be tested with the pendulum impactor, as series CA.

6.2.2.2 Final Series of Reinforced Concrete Beams

The final series of reinforced concrete beams made consisted of 9 beams. All were reinforced with the same reinforcement, namely

4 x 3.55mm diameter wire reinforcing. The reinforcing steel arrangement can be seen in Figure 6.3. The beams were made in the standard way, but were air-cured due to the unavailability of the water bath and thermo-regulators. This resulted in the beams having a final strength of less than the desired 28-day strength of 30MPa. These beams were tested as series CD.

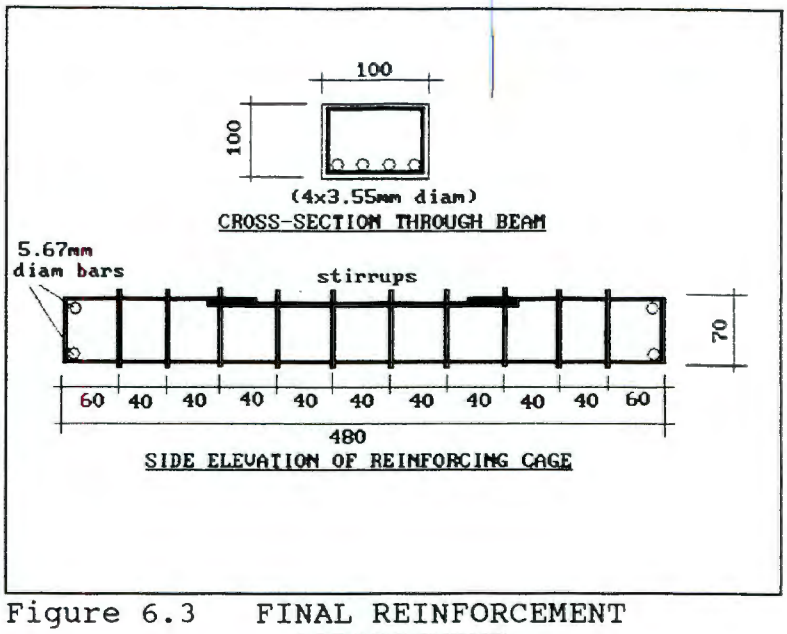

Figure 6.3 FINAL REINFORCEMENT ARRANGEMENT

6.2.3 Testing of Concrete Beams

6.2.3.1 Testing of Plain Concrete Beams

6.2.3.1.1 Static Testing of Concrete Beams

Twelve unreinforced beams (series CA) were tested. Two beams were tested statically in the 'Denison' Universal Testing Machine in single point loading, at a constant loading rate of 1kN/min. This was to determine the failure load from which the static modulus of rupture (MR) could be determined.

6.2.3.1.2 Impact Testing of Plain Concrete Beams

The remaining ten specimens were tested with the pendulum impactor. Each specimen was placed against the small support structure and was tied to the knife-edge supports by tying with cord. Only the central deflection rod was attached to each specimen, as it was felt that more rods would produce too much resistance. In addition, the deflections would have been so small that differences would not have showed.

It was found that the front face of the hammer was not exactly parallel to the front face of the concrete beams. This was

overcome by gluing a 8mm thick hard rubber pad to the front face of the hammer. This was to ensure that the load was spread evenly over the surface of the hammer during impact.

The release mechanism was positioned as close as possible to the beam, with enough room to place the light trip to allow the falling board to fall 160mm. The pendulum with no 400N weights was used. This was found to be insufficient, as there was no visible signs of damage or residual deflection on the graph paper. The release point was then moved higher in steps until the specimen failed. The point of the release at which the first beam failed was used as a guideline for the next release position. This was repeated for eight specimens in a effort to achieve a 'just failed' condition.

A 'just failed' condition for unreinforced concrete beams was defined as the condition at which the specimen had cracked right through or when it had a crack length extending 90 percent or more of the beam depth. However, when the specimen was 'chopped' in half, so that one half went 'flying' (ie left the support structure) it was termed as 'excessive' (ie too much energy was impacted to the specimen).

Ultra-sonic equipment was not available to test those specimens, that showed no cracks after impact for internal damage. In an effort to test this, one specimen (CA10) was impacted ten times from a release point that represented 40 percent of the height that represented a 'just failed' condition. After each impact, the specimen was inspected thoroughly for any sign of damage or cracking. Other than a small amount of local crushing of the concrete at the knife-edge supports there were no visible signs of damage to the specimen after impacting it ten times from the position that represented 40 percent of the 'just failed' height. (The 40 percent value was chosen in an effort to keep the impacts well within the 'elastic' range of the beam).

The release point was then moved to a position that represented 90 percent of the 'just failed' height and the beam was impacted.

The one specimen that failed at the same height as CA10 was specimen CA9. A specimen (CA9) was impacted three times from a height that represented 90 percent of the height of 'just failed'.

6.2.3.2 Testing of Reinforced Concrete Beams

6.2.3.2.1 Static Testing of Reinforced Concrete Beams

One beam from each type was tested statically. This was to determine the failure load of the beam. The test was performed in the 'Denison' Universal Testing Machine, as for the steel beams. Dial gauges were used to measure the deflection. The failure load was required as it was part of the failure criteria for the reinforced concrete beams. If a beam that had been impacted was tested in the 'Denison' and it could not reach a load equal to 95% of the static load, then the beam would have been classified as 'failed' due to the impact load. Crack widths at various loads were measured by means of a 'feeler' gauge and recorded. The 5% difference between the 'failure load' and the static test load was to allow for the 'scatter' in results. As only one specimen was tested statically, no standard deviation was available.

6.2.3.2.2 Impact Testing of Reinforced Concrete Beams

There were two series of reinforced concrete beams tested with the impactor. The first series (Series CB) consisted of three beams with three different percentages of reinforcements. (See Section 6.2.2.1) These were impacted with the pendulum without any additional weights added.

Three beams of 2 x 3.15mm diameter reinforcement: (CB2-CB4). The position at which the plain concrete beams failed was used as a starting position for the impact. Subsequently, each previous beam tested was used to determine the starting position for the next beam. Each beam was impacted from increasing distances from POI until it failed. Crack widths, if present, were measured by means of a 'feeler' gauge after each impact. (This was later found to be a bad approach and subsequent beams were impacted only once.)

Three beam of 4 x 3.15mm diameter reinforcement: (CB5-CB7) The results from the previous beams were used to determine the starting position for this set. The first beam was 'sacrificed' in that it was impacted from increasing distances from the POI until it failed. This position was then used in positioning the release for the other two beams. These were only impacted once and were then tested statically to determine their residual strength. Crack widths were also measured after impact.

Three beams of 2 x 5.67mm diameter reinforcement: (CB8-CB10) The procedure was the same as for the set described above (CB5-CB7) except that the first beam was only impacted once. The residual strengths and crack widths were also determined.

The second series (Series CD) consisted of eight beams and was divided in half (ie 4 beams for each set). One set of four beams was tested with no additional weights added to the pendulum. The other four were impacted with two 400N weights attached. Each beam was impacted once and the residual strengths were determined by means of the 'Denison', as with other beams. Crack widths were measured as described above.

6.3 REINFORCED CONCRETE SLABS

6.3.1 Introduction

Reinforced concrete slabs 2m x 2m x 50mm thick were cast using the standard concrete mix. Two sets of three slabs were cast. The first series (Series A) had 0.2% high yield reinforcing mesh both ways. Series B had 0.5% high yield reinforcing mesh both ways.

6.3.2 Casting Reinforced Concrete Slabs

Two sets of three reinforced concrete slabs, 2m x 2m x 50mm thick were cast. The formwork consisted of 75mm x 50mm x 6mm steel angles that were placed on the laboratory floor with the 50mm side vertical and bolted together. PVC sheeting of 150μm was then placed inside the formwork to make a water tight mould. The PVC sheeting was smoothed out and corner sections made from cement sacks were made and placed in the corners to prevent the

concrete from penetrating the folds at the corners and thus tearing the PVC sheeting during the stripping process.

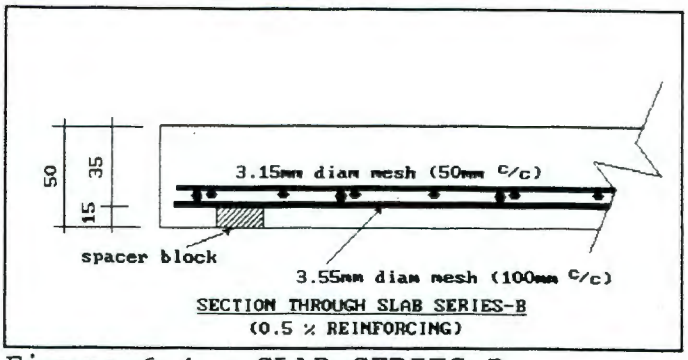

Figure 6.4 SLAB SERIES B REINFORCEMENT

Two percentages of reinforcement were used, 0.2% for series A and 0.5% for series B. Series A consisted of 3.55mm diameter mesh at 100mm centres both ways. Series B consisted of 3.55mm diameter mesh at 100mm centres together with a mesh of 3.15mm diameter at 50mm centres, to achieve the 0.5% reinforcement. The two meshes were tied together at 200mm centres, both ways, to ensure that they stayed together. The meshes were placed with the upper and lower bars of the two meshes parallel so as to minimize the distance between the two meshes. See Figure 6.4 for details of slab reinforcement. A lifting hook was tied to the reinforcing mesh at each corner of the slab, to enable the slab to be moved and placed in the desired position. Spacer blocks of approximately 15mm height were tied to the underside of the reinforcement at approximately 400mm centres to give sufficient cover and to ensure that the concrete enclosed the mesh. The mesh was weighed down by placing weights at regular intervals, which were removed as the mould was filled with concrete. The standard concrete mix was used and two batches were required to fill the mould. The concrete was compacted using a poker vibrator. A heavy wooden plank was used with its narrow edge across the formwork to further compact the concrete and to ensure equal thickness throughout.

The PVC sheeting was long enough so that it could be folded back to cover the whole slab. This was done on the same day as casting. The edges were folded a few times, to ensure the slab was completely sealed in the PVC sheeting. The folded edges were weighed down with weights to ensure that they remained closed. The concrete cubes made from the same mix as the slab, were also

sealed within the PVC sheeting, to ensure identical curing.

The PVC sheeting was opened once a day and the slabs and cubes were thoroughly watered. The PVC sheeting was then closed up, as before, to prevent loss of moisture. The slabs were cured in this way for seven days after which they were removed from their moulds and stored in a vertical position in a safe area, securely tied back. The corresponding cubes were labelled and stored nearby.

All slabs were cast and cured in the same manner. All three slabs from each series were cast within two days, to have similar ages for testing. The concrete cubes were tested in the standard way at seven, fourteen and twenty eight days to determine the concrete compressive strength curve.

6.3.3 Preparation of Reinforced Concrete Slabs for Testing

The slab support structure was adapted so that it could be wheeled into position. This was necessary as the overhead gantry crane was unable to pass over the pendulum column. The slab support structure was moved to a position where the crane could be used to load the slab into it. The slab was secured in position with 'safety brackets' and wooden wedges. Additional G-clamps were used during transport for added safety. The slab remained connected to the crane for as long as possible as an additional safety measure. The support structure and slab were moved into position. The whole arrangement was lifted by means of a winch onto a spacer consisting of a 127mm x 102mm I-section and bolted in position. The supporting struts were then bolted in position.

The slabs did not make proper contact over the entire length of the pivoting rods (20mm diameter rods). This was due to the fact that the floor on which the slabs were cast was later found to be slightly uneven. This was overcome by filling the gaps with an epoxy-grout. The pivoting rods were painted with mould oil prior to loading the slab to prevent the epoxy sticking to the pivoting rods. This was to ensure that the slabs could still

rotate under load. The epoxy-grout was squeezed into the gaps with a putty knife and a gloved finger. This was performed for all four sizes so that no daylight could be seen between the slab and the pivoting rods. This was necessary to ensure that the slab was completely supported all round.

The deflection-rod connectors were attached to the rear of the slabs with an epoxy glue. Five deflection-rods were attached to each slab. The gaps between the slots in the attachments and the rotating pin were temporarily filled with polystyrene to ensure that the attachments did not move while the epoxy set. The epoxy was spread onto the front face of the attachments which were then pushed against the slab. The deflection-rods were kept in position by tying the other ends of the rods to the deflection-rod frame.

The front face of the slab was thoroughly brushed to facilitate the identification of cracks after impact.

6.3.4 Testing of Reinforced Concrete Slabs

6.3.4.1 Introduction

Series A was impacted with three 400N weights attached to the pendulum, except for slab1 which had two 400N weights attached. Two slabs of Series B were impacted with five 400N weights attached to the pendulum. The final slab of series B was tested statically. The residual strength of the other two slabs of series B was also determined statically.

6.3.4.2 Impact Testing of Slabs

The impact testing was performed in the following manner: The graph paper was attached to the board of the arc-measuring device. The position of the pencil on the arc-measuring board was marked when the pendulum hung vertically and the 'hammer' touched the slab. This position was called the origin ('O'). Once the pendulum was secured in the release mechanism, the position of the pencil on the arc-measuring board was marked and designated 'S' for start. The previous method of releasing the board of the arc-measuring device could not be used due to the

high position of the pendulum required to impact the slabs. This was solved by using another spacer block that was pulled out at impact by an assistant. (Since the important part of the backswing was the end of the backswing arc, any loss of the first part of the backswing arc did not matter. This loss would be due to the spacer block having been pulled out a fraction of a second after impact.) The pieces of polystyrene were removed from the gaps in the deflection-rod attachments. The deflection-rods were cleaned and sprayed with teflon spray. This was to ensure that the dynamic friction was the same as that determined during the calibration phase, as described in the section on calibration of equipment.

Graph paper was attached to the falling board. The spring-loaded pencils were positioned in a staggered manner to prevent the deflection-time curves from being drawn on top of each other. The board was then raised and clipped into position. The pencils touched the graph paper and drew vertical lines. These lines were designated the base-lines that represented zero deflection.

The release mechanism was positioned. The end of the pendulum was positioned against the release mechanism. The electrical circuit was closed and the light beam was switched on. After a final check that everything was in order, the pendulum was released. The pendulum was allowed to rebound, but was caught before it impacted the slab a second time. This was to allow the backswing arc to be recorded but to prevent further damage to the slab due to a second impact.

The slab was pulled against the rotation rods by means of G-clamps after impact. This was necessary to record the true permanent deformation of the slabs. The slab had moved away from the pivoting rods due to the permanent deformation of the slab. The falling board was then raised again with the pencils still touching the graph paper. This was to record the permanent deformation of the slab.

The crack pattern was then drawn on the rear of the slab with

black felt-tip pen. This was so that the crack pattern could be photographed. The crack pattern on the front of the slab (impact side) was drawn with red chalk, as the felt-tip pen would not take on that surface. Photographs of the crack patterns were taken before the slab was removed from the test bed.

The supporting struts were removed and the whole arrangement was wheeled out. More photographs were taken of the crack patterns before the slab was removed. The slab was then removed from the support frame. The next slab was loaded into the support frame and the whole process was repeated.

6.3.4.3 Static Testing of Reinforced Concrete Slabs

One of the slabs from Series B was tested statically (ie only two of the three slabs in Series B were tested dynamically). This was to determine the static strength of the slab.

The slab was positioned horizontally on the same support frame that was used for the dynamic tests. The frame was supported on four concrete blocks below an 'Amsler' 2000kN hydraulic jack. A 140mm x 140mm x 8mm plate was positioned under the jack piston to transfer the load to the slab.

A 50mm dial gauge was positioned as close to the loading plate as possible. The end of the dial gauge rested on the concrete surface as it was felt that the steel loading plate could settle due to local crushing of 'high' spots on the slab surface. This would have given incorrect deflection readings. The load was applied at a constant rate of 4kN per minute until the load just started to drop off. The load was then immediately released. The deflections were recorded as the load was applied. The final reading on the dial gauge was recorded to obtain the permanent deformation of the slab.

The residual strength of the other two slabs in Series B were obtained by testing statically as described before. Slab number 5, which punched through in the dynamic test, had an additional steel plate (200mm x 200mm x 5mm) under the 8mm thick steel plate

to spread the load over the hole.

C H A P T E R 7

TEST RESULTS AND ANALYSES

7.1 STEEL BEAMS

7.1.1 Results of Static Deflection Tests

The readings from the load-deflection tests were plotted. The load-deflection graph for Series B can be seen in Figure 7.1. The unloading line AB is at the same slope as the linear portion of the graph during loading and extends from the point of maximum load to the point of permanent deflection. The point where the unloading line AB cuts the x-axis at B, was taken as representing the permanent deformation of the steel beam that represented failure. The results of the deflection tests are summarised in Table 7.1.

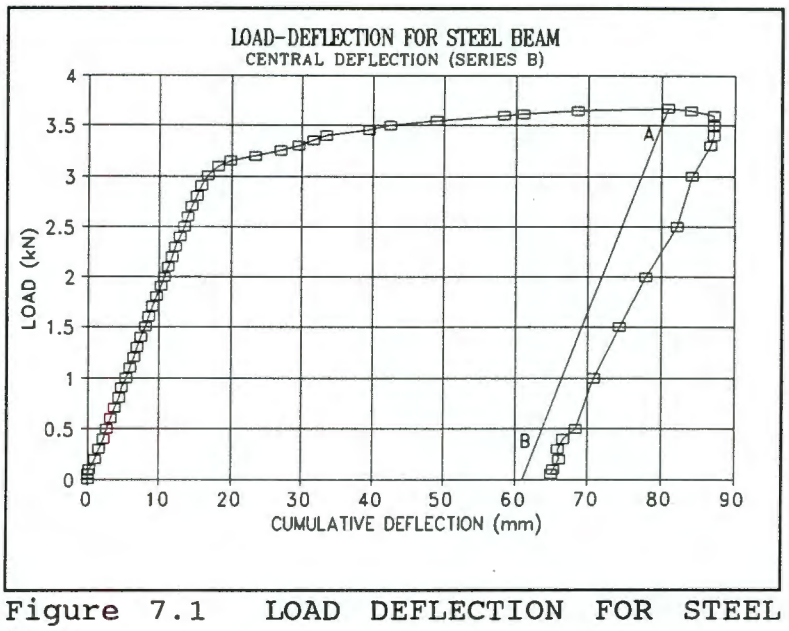

Figure 7.1 LOAD DEFLECTION FOR STEEL BEAM

TABLE 7.1 SUMMARY OF STATIC DEFLECTION TESTS

Series	A	B
Maximum Load (kN)	3.20	3.67
Permanent Deformation (mm)	55	61

7.1.1.1 Discussion of Results and Their Projected Effect on Impact Tests

The permanent deformation for each series of beams represented the failure permanent deformation. This was defined as a visual (and measurable) failure criterium for the steel beams. If the respective permanent deformation could be achieved due to an impact load then that would represent the impact load that caused failure of the beam.

7.1.2 Results of Impact Testing of Steel Beams

7.1.2.1 Results of 'Elastic' Impact Testing of Steel Beams

The results of the 'elastic' impact tests were identical for each beam from a particular series, provided they were impacted from the same position. This was achieved by releasing the pendulum a distance 1.0m from point of impact (POI). The distance was measured from the front face of the beam to the front edge of the release mechanism. This position was used for all 'elastic' tests on all beams for both Series A and Series B. When the pendulum hung vertically, the front face of the 'hammer' was a distance of 23mm from the head of the allen key bolt. The allen key bolt was used to connect the deflection rod attachment to the steel beam. The 'hammer' made contact with the head of this bolt during impact. This distance of 23mm therefore had to be taken into account in the analysis of the results. The front face of the pendulum channel section was taken as the reference-line for arc length calculations.

The results from each test consisted of a backswing arc graph and a deflection-time graph. Both were drawn on graph paper.

The end of the backswing arc was marked on the graph paper and labelled 'B' for backswing. The pendulum was then re-positioned in the release mechanism, with the pencil still in contact with the graph paper. This drew an arc representing the arc from the start position 'S'.

Typical examples of the deflection-time graphs and backswing arc graphs can be seen in Appendix C. On first inspection of the deflection-time graph it could be seen that it was not a smooth curve. It consisted of a number of small oscillations along the path of the deflected shape. These oscillations were due to the natural period of vibration of the channel section of the pendulum after impact. These vibrations were transferred to the beam through the 'hammer'. The vibrations were then transmitted by means of the deflection rods and the pencils to the graph paper. Never-the-less, the deflected shape could still be seen, since the vibrations only caused a secondary movement. The

results of a typical 'elastic' test for Series A and B are listed in Table 7.2.

TABLE 7.2 - SUMMARY OF 'ELASTIC' RESULTS FOR STEEL BEAMS

Series	A	B
Start Arc Length (mm)	865	865
Backswing Arc Length (mm)	49	50
Max. measured deflection (mm)	13.5	13.3

7.1.2.1.1 Analysis of 'Elastic' Impact Testing of Steel Beams

The deflection-time graph was analysed in the following way: A best-fit curve was drawn through the small oscillations representing the true deflection curve. The point of impact on the graph paper was defined as that position where the pencil line made an abrupt change of direction from the vertical line. The vertical line was drawn as the board fell, before impact. A photo-copy of the deflection-time graph was made. Marks every 5mm were made along the base-line from the point of impact until the deflection curve cut the base line. This represented the deflection of the beam from initial impact to where the pendulum left the beam again. The distances (deflections) from the base-line to the best-fit curve were measured perpendicularly to the base-line. These deflections were recorded together with their respective distance from the point of impact on the graph paper.

The fact that the board increased velocity as it fell, had to be taken into account in the analysis. This increased velocity gave a 'skewed' deflection-time graph. For this reason the vertical distances on the graph had to be corrected. The vertical distances represented distance travelled in a particular time. The time from the release of the board to any point on the graph could be calculated by the laws of motion:

$$s = ut + 0.5a_b t^2 \qquad (7.1)$$

where s= distance board has fallen(m)
u= initial velocity = 0
a_b = acceleration of board (a_b = 9.72m/s^2 from chapter 4)

t = time in seconds

By rearranging (7.1):

$$t = \sqrt{\frac{2*s}{a_b}} \qquad (7.2)$$

Equation (7.2) was used to calculate the time of the falling board at each deflection point. The velocity of the board was calculated using the following equation:

$$v^2 = u^2 + 2a_b s \qquad (7.3)$$

where v = velocity of falling board

u= initial velocity of falling board = 0

a_b = acceleration of board = 9.72m/s^2 (from chapter 4)

s = distance that falling board has fallen from time of release

If the velocity of the board had been constant, there would have been no need to correct the deflection-time graph. However, due to the increasing velocity this was necessary. The velocity of the board at each deflection point was used to calculate a scale-factor to correct the distances between the deflection points.

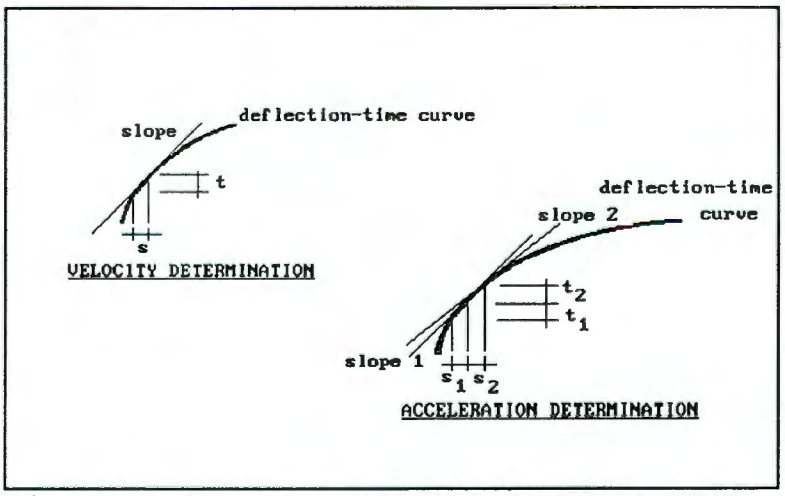

Figure 7.2 VELOCITY AND ACCELERATION DETERMINATION

It was assumed that the pendulum and beam stayed in contact with each other from the time of initial contact, to maximum deflection and until the beam had reached the vertical position again. Once the corrected deflection-time graph was obtained, it was used to obtain the velocities and deflections of the beam and pendulum at the various deflection positions. The velocity at any point was the slope of the deflection-time graph. The acceleration at any point was the change of slope of the

deflection-time graph. See Figure 7.2.

The maximum deflection was taken as that position at which point the velocity of the beam was zero. This analysis was performed on a spreadsheet and printouts can be found in Appendix C.

In order to check the validity of the results obtained from the tests and recording equipment, an analysis using the principle of conservation of energy was performed.

The specific positions shown in Figure 7.3 were investigated.

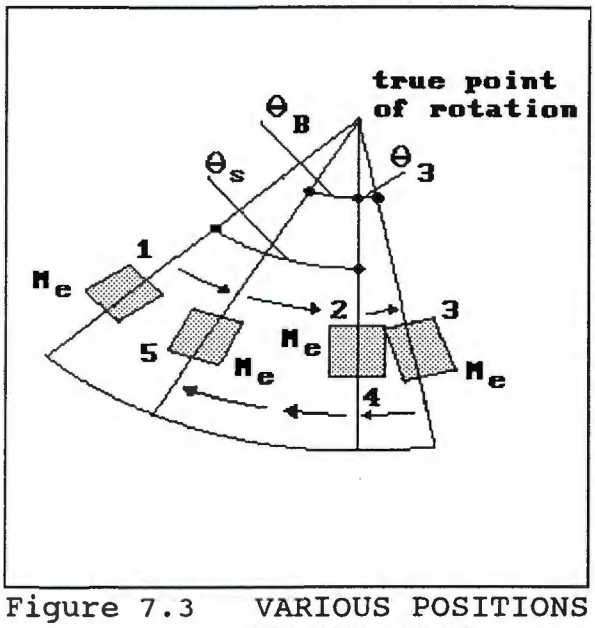

Figure 7.3 VARIOUS POSITIONS OF PENDULUM

Position 1 was the initial starting position (maximum potential energy (PE)). Position 2 was reached when the pendulum was vertical just before impact (maximum kinetic energy (KE)). Position 3 was at the point of maximum deflection (PE plus strain energy (SE)). Position 4 occurred when the pendulum was vertical again, just after parting from the beam (KE). Position 5 was the position to which the pendulum swung back (backswing height, as measured by arc-measuring device). (PE_5).

The starting arc was used to calculate the effective height to which the effective mass of the pendulum was raised. The included angle was calculated as follows:

$$\theta_s = \frac{S_1}{R} \qquad (7.4)$$

where θ_s = included angle due to starting position (radians)

S_1 = starting arc length (m)

R = Length from true point of rotation to top surface of curved channel

The effective height was calculated as follows:

$$h_e = L_e(1 - \cos\theta_s) \qquad (7.5)$$

where h_e = effective height to which the effective mass of the pendulum was raised

L_e = effective length of pendulum from true point of rotation to position of effective mass

Referring to Figure 7.3 and using the principle of conservation of energy:

$$PE_1 = KE_2$$
$$\therefore KE_2 = m_e g h_e \qquad (7.6)$$

where KE_2 = kinetic energy of pendulum at position 2

m_e = effective mass of pendulum

g = gravitational acceleration (9.80m/s^2 at UCT)

h_e = effective height to which the effective mass of the pendulum was raised

Most of the kinetic energy of the pendulum (KE_2) was transferred to the 'system' when the 'hammer' impacted the beam. The system was defined as the arrangement of beam, beam support structure and pendulum support arrangement. The mode of energy transfer was the impulsive load (B).

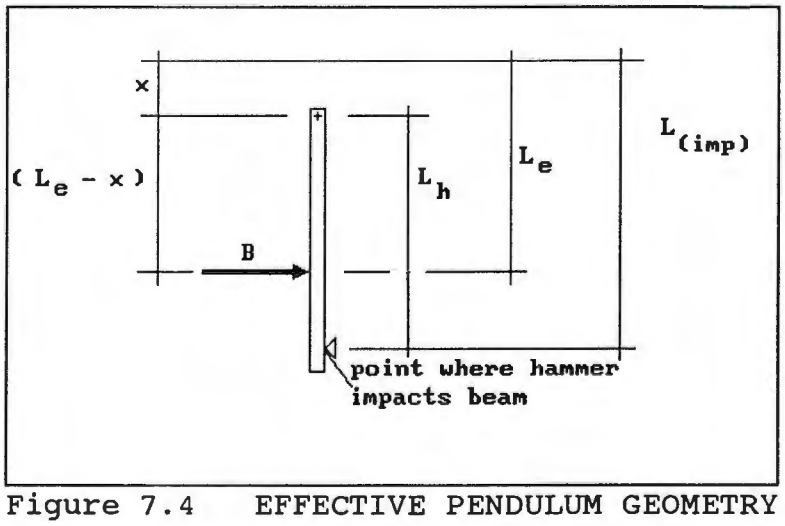

Figure 7.4 EFFECTIVE PENDULUM GEOMETRY

Referring to Figure 7.4 it can be seen that all of the impulsive load (B) was not transferred to the steel beam. The proportion

of the impulsive load that was imparted to the steel beam ($B_{(imp)}$) was obtained as follows:

$$B_{(imp)} = \frac{(L_e - x)}{(L_{imp} - x)} * B = f_p * B \qquad (7.7)$$

where $B_{(imp)}$ = impulsive load impacting on beam
L_e = effective length of pendulum from true point of rotation to the centre of the effective mass
L_{imp} = Length to point of impact from true point of rotation
x = distance from centre of rotating pin to true point of rotation
f_p = proportional factor as defined above

The same proportional factor (f_p) was used to determine the proportion of energy that was transmitted through the 'hammer'. The proportion of the KE_2 that was transmitted through the 'hammer' was obtained as follows:

$$E_{(imp)} = f_p * KE_2 \qquad (7.8)$$

where $E_{(imp)}$ = Energy imparted to the point of impact
f_p = proportional factor as described before
KE_2 = kinetic energy difference of the pendulum at position 2 before and after impact

The energy at impact ($E_{(imp)}$) consisted of the following components when the steel beam was at position 3 (position of maximum deflection).

$$E_{(imp)} = PE_3^P + SE_3^B + F_RE + SE_3^s + IL \qquad (7.9)$$

where $E_{(imp)}$ = Energy imparted to the point of impact
PE_3^P = potential energy of pendulum at position 3
SE_3^B = strain energy of beam at position 3
F_RE = friction energy due to friction of deflection rods in their bushes
SE_3^s = strain energy absorbed by the support system (assumed zero at this stage)

IL = Losses in energy during impact

The nett energy that was impacted to the beam, which was equal to the strain energy at point 3 (SE_3), is obtained by rearranging Equation (7.9):

$$SE_3^B = E_{(imp)} - PE_3^P - F_R E - SE_3^S - IL \qquad (7.10)$$

In order to use the calculated energies it was necessary to calculate the spring resistance of the beam. If only the fundamental mode of vibration of the beam is considered, this resistance may be expressed in terms of the displacement (x). The resistance in the elastic range is given by the following equation:[1]

$$R = kx \qquad (7.11)$$

where R = resistance of beam to deformation
k = elastic stiffness of beam
x = deflection of beam

The resistance function for the beam can be idealized as shown in Figure 7.5. This is an elasto-plastic resistance displacement relationship.

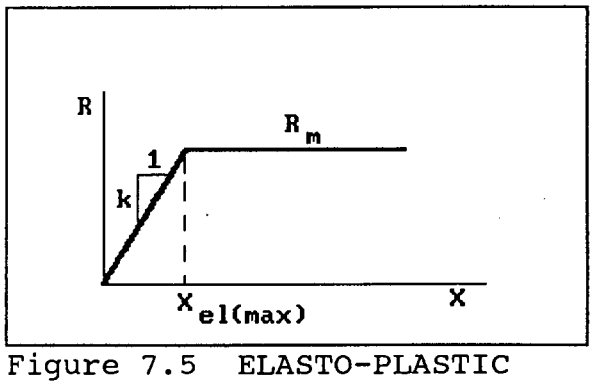

Figure 7.5 ELASTO-PLASTIC RESISTANCE CURVE

To enable the Energy method of analysis as given by Reference 1 to be used, the beam had to be converted to an idealized system. The idealized system consisted of a spring-mass system as shown in Figure 7.6. The deflection of the structure was of importance and therefore the deflections of the idealized system had to be equal to the real system(beam). The static deflection and the natural frequency of vibration of the equivalent system had to be the same as the real structure.

"The energy method of analysis is based upon the principle that at the time of maximum deflection and zero velocity the work done by the externally applied load must be equal to the internal strain energy in the structure. The method is applicable to both

elastic and plastic behaviour."[1]

The external work done by the impulsive load is given by the following formula from Reference 1:

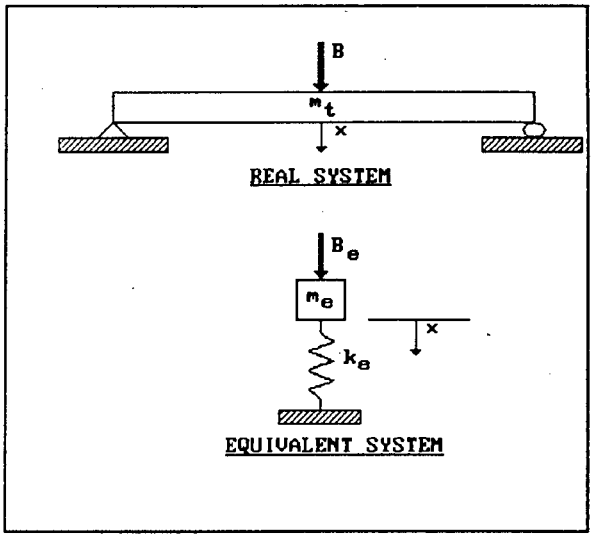

Figure 7.6 REAL & EQUIVALENT SYSTEMS

$$W_{Pe} = \frac{(H_{me})^2}{2M_e} \qquad (7.12)$$

where W_{Pe} = work done ignoring the contribution of the resistance *

H_{me} = the total impulse of the external load and is equal to the area under the load-time curve **

M_e = mass of spring/mass system without the inclusion of the effective pendulum mass

* ie. this is only applicable if the impulse duration (T) << T_n the natural period of vibration of the spring-mass system.

**"The external force in this case may be termed a pure impulsive load and during its application the resistance and internal strain energy of the system may be assumed to be zero."[1]

"After the application of the load the mass had acquired a kinetic energy equal to the work done." [1] This is given by the following equation from Reference 1.

$$\frac{(H_{me})^2}{2M_e} = 0.5M_eV^2 \qquad (7.13)$$

This initial velocity (V) is therefore given by the following

equation:

$$V = \frac{H_{me}}{M_e} \qquad (7.14)$$

where M_e = mass of spring/mass system without the inclusion of the effective pendulum mass

"At maximum deflection this kinetic energy is completely transferred into internal strain energy. In the case of a pure impulsive load the work done depends only upon the area under the load-time curve and is independent of the shape of that curve and the properties of the dynamic system."[1]

"In most cases the resistance ($R_e(x)$) cannot be neglected in the time between O and T. The internal resistance always acts to reduce the work done on the system. Therefore the work given by "[1] Equation (7.12)" may be considered to be the absolute maximum work which could be done by a given load on a dynamic system."[1]

"The energy method of analysis consists in part of a determination of the ratio W_{me} / W_{Pe}, which is the actual work done divided by the absolute maximum work. This ratio depends upon the shape of the load-time curve and the properties of the dynamic system and is called the work-done ratio, C_w."[1]

By using Equation (7.12) and rearranging, the impulse (H_{me}) can be obtained:

$$H_{me} = \sqrt{W_{Pe} * 2M_e} \qquad (7.15)$$

By substituting the value of SE_3^B for W_{Pe} in Equation (7.15) the value for the impulse was obtained.

The shape of the dynamic load was assumed as triangular with an initial peak value of B_e and a duration of T. (This is verified later.) This is shown in Figure 7.7 together with the idealized resistance function. The value of B_e was obtained by multiplying M_e by the acceleration of the beam. The total impulse of the external load (B_e) is equal to the area under the load-time

curve. The impulse can therefore be calculated by the following equation:

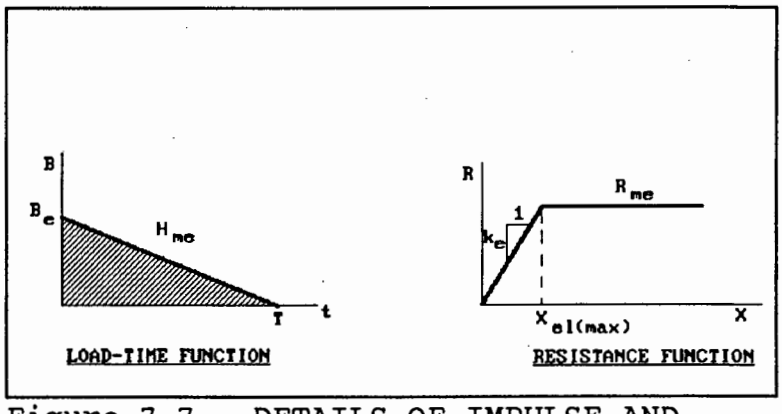

Figure 7.7 DETAILS OF IMPULSE AND RESISTANCE FUNCTION

$$H_{me} = 0.5B_eT \qquad (7.16)$$

Rearranging Equation (7.16), the duration of the load (T) can be calculated as follows:

$$T = \frac{2H_{me}}{B_e} \qquad (7.17)$$

Various factors necessary for further analysis had to be determined. The plastic moment capacity of the beam was determined as follows:

$$M_{pl} = Z_{pl} * f_{y(d)} \qquad (7.18)$$

where M_{pl} = plastic moment capacity of steel
Z_{pl} = plastic section modulus
$f_{y(d)}$ = dynamic yield stress of steel plate ($f_{y(static)}$ * DLF) DLF is the dynamic load factor (or increased strain rate factor)

The maximum resistance (R_m) could now be determined:

$$R_m = \frac{4M_{pl}}{L} \qquad (7.19)$$

where R_m = the maximum elastic (or plastic) spring resistance of the beam (See Figure 7.5)
M_{pl} = plastic moment capacity of steel beam
L = span of beam (length between supports)

For the equivalent system the maximum resistance (R_{me}) would be

equal to R_m described previously. (See Figure 7.7)

The equivalent spring stiffness (k_e) of the equivalent system was determined as follows:

$$k_e = \frac{48E_dI}{L^3} \qquad (7.20)$$

where k_e = equivalent elastic spring stiffness of equivalent system

E_d = Dynamic Young's Modulus of steel for beam. (Equal to Static E of steel)

I = second moment of area of steel beam

L = span of beam

The peak value of the external load ((B_e) (See Figure 7.7) was equal to the impact force $B_{(imp)}$ (ie $B_e = B_{(imp)}$).

The equivalent mass of the system was determined as follows: Reference 1 states: "If for the purpose of analysis the mass of the system is concentrated at certain points, the loads must be applied at the same points." Therefore, for a centrally applied load, the masses must be concentrated at the centre (ie lumped at the centre). Reference 1 states that the equivalent mass of the uniformly distributed mass of the beam is equal to 0.49 * total uniformly distributed mass of the beam. The total mass of any other loads at the centre of the beam must be included at the centre of the beam. This is for an idealization of lumping the equivalent mass at the centre of the beam. For the given case the equivalent mass had to include the masses of the deflection rods, rod connectors, pencil holders and pencils, as these were connected to the beam. The proportion of the effective mass of the pendulum that acted on the beam had to be included in the effective mass of the beam as well, as the pendulum was in contact with the beam during deflection. Therefore the equivalent mass of the beam (m_{eT}) was determined as follows:

$$m_{eT} = 0.49m_b + \sum m_r + f_p m_{ech} + m_{bh} + m_{add} \qquad (7.21)$$

where m_{eT} = equivalent mass of beam including the effective mass of the pendulum

m_b = mass of steel beam

$\sum m_r$ = sum of deflection rods and attachments etc.

$f_p m_{ech}$ = proportion of effective mass of channel acting on beam

m_{add} = additional masses

m_{bh} = mass of weights' bolt and 'hammer'

The first natural period of vibration of the beam (T_n) is given by the following equation:[1] [2]

$$T_n = 2\pi \sqrt{\frac{m_{eT}}{k_{eT}}} \qquad (7.22)$$

where m_{eT} = equivalent mass of beam (kg) including the effective mass of the pendulum

k_e = equivalent elastic stiffness of beam (N/m)

By using the data previously given, the Energy Method was applied in the following way:

In order to use the graphs of Reference 1, given in Appendix C, the resistance ratio and the time ratio had to be calculated first.

$$C_R = \frac{R_{me}}{B_e} \qquad (7.23)$$

where C_R = resistance ratio

R_{me} = equivalent maximum elastic (or the plastic) spring resistance of the beam. (See Figure 7.7)

B_e = peak value of the external load

$$C_T = \frac{T}{T_n} \qquad (7.24)$$

where C_T = time ratio
T = duration of impulse (seconds)
T_n = first natural period of vibration of the steel beam (seconds)

These values were used for the graph (Figure 7.6 of Reference 1) to determine the work-done ratio (C_w). "It may be observed in the figures that as the ratio T/T_n decreases, the load becomes more nearly a pure impulse and the work-done ratio approaches unity. It may also be observed that as C_R increases, the behaviour becomes more nearly elastic and the bottom curve applies to the completely elastic case."[1] It was found that the time ratio (C_T) was less than the smallest value on the graph (0.1). Therefore the work-done ratio was taken as unity. This meant that the actual work done was equal to the absolute maximum work.

The impulse was then calculated from Equation (7.16). The external work-done was then calculated from Equation (7.12).

The maximum elastic deflection (See Figure 7.7) was calculated from the following equation:

$$x_{el\,(max)} = \frac{R_{me}}{k_e} \qquad (7.25)$$

where $x_{el(max)}$ = maximum elastic deflection of beam

"The energy absorbed by the dynamic system may be determined as the area under the resistance-deflection curve shown in "[1] Figure 7.7. "If the behaviour is completely elastic, the absorbed energy is equal to the strain energy and is given by "[1] the following equation:

$$SE = 0.5k_e x_m^2 \qquad (7.26)$$

where SE = Strain energy of beam at maximum deflection

x_m = maximum deflection of beam

Rearranging Equation (7.26):

$$x_m = \sqrt{\frac{2SE}{k_e}} \qquad (7.27)$$

If the beam remained elastic (ie did not go into the plastic range) x_m would be less than $x_{el(max)}$.

It was not possible to use the graphs of Reference 1 for determining the time to maximum deflection (t_m). This was due to the fact that the test time ratio (C_T) was too small for the graphs.

However, Reference 2 gives an expression for determining t_m by means of the following equation:

$$t_m = \frac{T_n}{4} + \frac{T}{2} \qquad (7.28)$$

where t_m = time from impact to when maximum deflection occurs
T_n = first natural period of vibration of steel beam
T = duration of impulse

The analysis of the results was performed by using a spread sheet. Most materials exhibit an increase in capacity in most of their properties with increase in strain rate. To allow for this increase in stress capacity during dynamic loading, a strain rate factor (or dynamic load factor) is applied. Initially the dynamic load factor (DLF) was kept as unity and the spreadsheet analysis was performed. It was found that x_m was larger than $x_{el(max)}$, which could not have occurred if the beam remained elastic. Therefore the ratio of x_m over $x_{el(max)}$ was used as the DLF. The average DLF for the two series of beams was found to be 1.18. The value of x_m was found to be less then $x_{el(max)}$ when the DLF of 1.18 was used which showed the beam was still elastic. The DLF was used for further analysis. The spread sheet analysis was then repeated. Copies of the results can be seen in Appendix C.

A summary of the test results is given in Table 7.3.

TABLE 7.3 SUMMARY OF DYNAMIC 'ELASTIC' STEEL BEAM TEST RESULTS

Series	A	B
Plate Thickness (mm)	5.9	6.1
E Steel Plate (GPa)	201.7	203.9
Static Yield Stress (MPa)	322.0	399.8
Measured max defl (x_{max}) (mm)	13.5	13.3

A comparison of test and calculated values from the analysis is given in Table 7.4 and 7.5.

TABLE 7.4 COMPARISON OF MEASURED & CALCULATED VALUES FOR DYNAMIC 'ELASTIC' STEEL BEAM TESTS (SERIES A)

Source	Test	Calculated
x_m (mm)	13.5	13.7
T (sec)	-	0.00472
t_m (sec)	0.0191	0.0278

TABLE 7.5 COMPARISON OF MEASURED & CALCULATED VALUES FOR DYNAMIC 'ELASTIC' STEEL BEAM TESTS (SERIES B)

Source	Test	Calculated
x_m (mm)	13.3	13.4
T (sec)	-	0.00567
t_m (sec)	0.0205	0.0269

The times to maximum deflection (t_m) for Series A was 31.3% less than the calculated t_m. For Series B the test t_m was 23.8% less than the calculated t_m.

The test x_m for both Series A and B were less than the calculated values (1.5% and 0.7% less for Series A and B respectively).

If the maximum deflection (x_m) from the tests was used to calculate the SE absorbed by the beam, adjusted SE the SE was as given in Table 7.5. The adjusted strain energy ($SE_{(adj)}$) was then used to calculate the velocity of the pendulum as it left the beam (V_{adj}) (ie maximum kinetic energy of pendulum during

rebound).

TABLE 7.6 ADJUSTED ENERGIES & VELOCITIES FOR ELASTIC TESTS ON STEEL BEAMS

Series	A	B
Calculated SE (Joules)	26.1	26.1
Adjusted SE (Joules)	16.57	17.97
V_{adj} (m/s)	0.781	0.813
V_{bs} (m/s)	0.652	0.666
% Difference - velocities	16.5	18.1

The backswing arc-length was then used to calculate the maximum velocity of the pendulum as it left the beam (V_{bs}) and is also given in Table 7.6. Comparison of the two velocities shows that the backswing velocities is less than the adjusted velocity. This suggests that all the SE is not transferred to the pendulum. (ie beam retains some energy).

A method of analysis known as the Procedure of Successive Approximations [3][4] (see Appendix F) was used to evaluate the natural frequency and hence the period of the steel beam with all its attachments.

The equations given in Appendix F were used in a spread sheet to do the analysis. Printouts can be seen in Appendix C. The values for the period obtained by this method were compared with the period obtained from the test, as mentioned previously. These can be seen in Table 7.7. An additional fact derived from the method of successive approximations is the deflected mode shape. The values for the mode shape at rod 2, rod 3 and rod 4 are listed in Table 7.6, together with the test mode shape. The test mode shape was calculated by dividing the measured deflections at a particular point by the maximum measured deflection (ie that of rod 3).

TABLE 7.7 COMPARISON OF SUCCESSIVE APPROXIMATION AND TEST VALUES (SERIES B)

Source	Test	Succ Approx
Natural Period (sec)	0.0977	0.0989
Mode Shape Rod2 (mm)	0.96	0.92
Mode Shape Rod3 (mm)	1.0	1.0
Mode Shape Rod4 (mm)	0.96	0.92

From Table 7.7 it can be seen that all the values compare very well. This shows that the recorded deflections have the correct mode shape.

A plot of the mode shape obtained from successive approximation and test results can be seen in Figure 7.8.

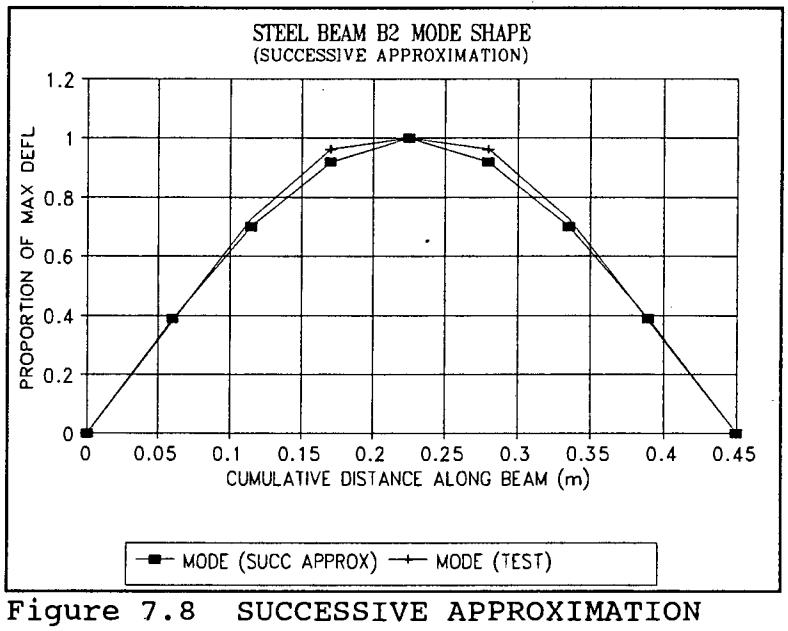

Figure 7.8 SUCCESSIVE APPROXIMATION MODE SHAPE

A method given by Reference 2 was used to calculate the maximum deflection of the beam. For a linearly decreasing impulse, the max deflection ($\delta_{(max)}$) is given by the following equation from Reference 2.

$$\delta_{(max)} = \delta_o \sin\left(\frac{2\pi}{T_n}\right)\frac{T}{2} = \delta_o \sin\left(\frac{\pi T}{T_n}\right) \qquad (7.29)$$

where δ_o = static displacement under a constant load
T = duration of impulse
T_n = natural period of vibration of steel beam

δ_o was calculated from the following equation:

$$\delta_o = \frac{B_e}{k} \qquad (7.30)$$

where B_e = magnitude of impulse force

k = elastic stiffness of steel beam

The values for B_e, k, T and T_n from previous calculations were used in the analysis and are listed in Table 7.8 together with the results of the analysis.

TABLE 7.8 RESULTS OF MAXIMUM DEFLECTION ANALYSIS FOR STEEL BEAMS

Series	A	B
B_e (kN)	21.142	17.588
k (kN/m)	181.838	203.156
T (sec)	0.00472	0.00567
T_n (sec)	0.0989	0.0961
δ_o (mm)	116.3	86.6
$\delta_{(max)}$ (mm)	17.4	16.0

The $\delta_{(max)}$-values from the above analysis is compared to the test x_m-values in Table 7.9.

TABLE 7.9 COMPARISON OF MAXIMUM DEFLECTION TEST VALUES AND CALCULATED FOR STEEL BEAMS

Series	A	B
Test x_m (mm)	13.5	13.3
$\delta_{(max)}$ (mm)	17.4	16.6
Percentage Difference	22.4	20.0

As can be seen from Table 7.9 the test values (x_m) are of the same order as the calculated maximum deflection ($\delta_{(max)}$)

7.1.2.1.2 Discussion of Results and Effects on Steel 'Plastic' Impact Tests

The fact that all the energy at impact was not transferred to the beam as strain energy might be important. (ie there were losses of energy). This meant that this would have to be kept in mind for further analysis. The agreement of the x_m-values and ($\delta_{(max)}$)-values with the test-values showed that the measuring equipment worked well and that measured deflections were representative of

actual deflections. The results of the backswing arc-measuring device showed that backswing measurements were reasonable as they took account of all but approximately ten percent of the SE of the beam. This ten percent could have caused the vibration of the beam after the pendulum had parted from the beam. These vibrations were shown on the time-displacement graph.

7.1.2.2 Results of 'Plastic Impact Tests of Steel Beams

A full set of results is given in Appendix C. Only those results that come closest to the permanent deformation that represented failure which was 55mm for Series A and for Series B it was 61mm. The results for the pendulum with no weights are listed in Table 7.10 and for one 400N weight in Table 7.11.

TABLE 7.10 SUMMARY OF RESULTS CLOSEST TO FAILURE (NO WEIGHTS)

Series	A	B
Beam Number	A3	B2
Dist Release POI (m)	3.0	3.5
Max Deflec (mm)	83.5	86.0
Perm Deformation (mm)	55.5	57.0
Original Arc *	283.0	334.0
Backswing Arc *	110.0	138.0

* Arc lengths from arc-measuring device.

TABLE 7.11 SUMMARY OF RESULTS CLOSEST TO FAILURE (ONE 400N WEIGHT)

Series	A	B
Beam Number	A7	B7
Dist Release POI (m)	1.90	2.22
Max Deflec (mm)	83.3	89.8
Perm Deformation (mm)	55.5	60.5
Original Arc *	173.0	210.0
Backswing Arc *	58.00	74.00

7.1.2.2.1 Analysis of Plastic Impact Test Results for Steel Beams

The deflection-time graphs were analysed in a similar manner to those for the elastic tests. The best-fit curve was drawn from the point of impact (shown on the graph by an abrupt change of direction of the pencil line), through the point of maximum deflection and continued until the curve crossed the permanent

deformation line. The deflections measured at various points and used in the spread sheets can be seen in Appendix C. An example of a corrected time-displacement curve for a plastic impact can be seen in Figure 7.9. Other graphs can be seen in Appendix C.

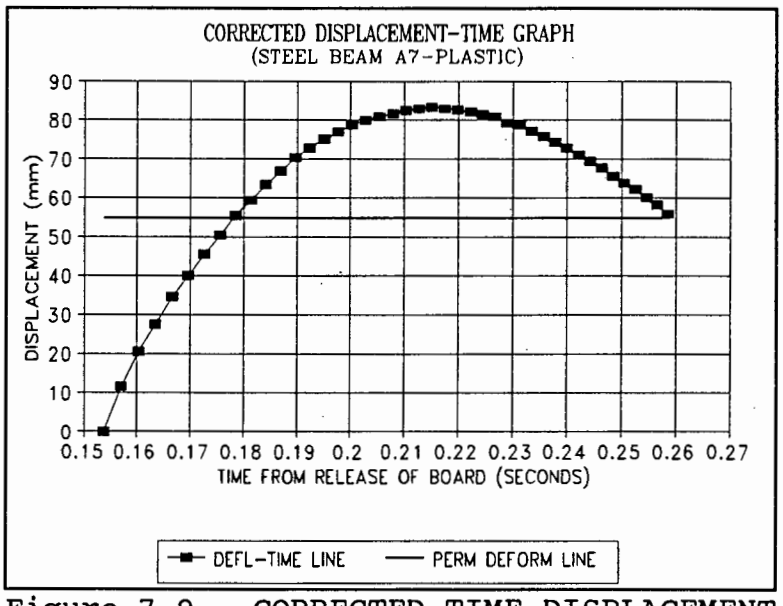

Figure 7.9 CORRECTED TIME-DISPLACEMENT CURVE(PLASTIC)

The energies at the various positions of the pendulum were calculated as for the elastic analysis. The Energy Method of Reference 1 was used again to obtain calculated values that could be compared with test values.

However, Equation (7.26) for the SE was replaced by the following equation, due to the beam having gone plastic.

$$SE = R_{me}\left(x_m - \frac{x_{el(max)}}{2}\right) \qquad (7.31)$$

where SE = Strain energy of beam at maximum deflection
R_{me} = equivalent maximum elastic (or the plastic) spring resistance of the beam
x_m = maximum deflection of beam
$x_{el(max)}$ = maximum elastic deflection of beam

Rearranging Equation (7.31):

$$x_m = \frac{SE}{R_{me}} + \frac{x_{el(max)}}{2} \qquad (7.32)$$

The rest of the equations as given in the section on elastic analysis still hold except for equations 7.22, 7.25, 7.26 and

7.28. It was found that x_m was larger than $x_{el(max)}$ as the beam had gone plastic.

The analysis was done by means of a spread sheet and printouts can be seen in Appendix C. A comparison of test and calculated values from the analysis is given in Tables 7.12 and 7.13 for Series A and B respectively for the weight condition of no additional weights added. The comparison for Series A and B with one 400N weight attached is given in Tables 7.14 and 7.15.

TABLE 7.12 COMPARISON OF MEASURED & CALCULATED VALUES FOR DYNAMIC 'PLASTIC' STEEL BEAM TESTS (A3 - NO WEIGHTS)

Source	Test	Calculated
$X_{el(max)}$ (mm)	15.6	19.7
x_m (mm)	83.5	86.9
T_n (sec)	0.129	0.104
Ductility Index	5.35	4.41
Toughness Index	9.71	7.82
t_m (sec)	0.0482	0.0467

TABLE 7.13 (B2 - NO WEIGHTS)

Source	Test	Calculated
$X_{el(max)}$ (mm)	18.3	23.5
x_m (mm)	83.5	90.4
T_n (sec)	0.122	0.0982
Ductility Index	4.56	3.85
Toughness Index	8.13	6.69
t_m (sec)	0.0465	0.0513

TABLE 7.14 (A7 - ONE 400N WEIGHT)

Source	Test	Calculated
$X_{el(max)}$ (mm)	15.6	17.8
x_m (mm)	83.3	87.6
T_n (sec)	0.174	0.146
Ductility Index	5.34	4.92
Toughness Index	9.68	8.84
t_m (sec)	0.0613	0.0667

TABLE 7.15 (B7 - ONE 400N WEIGHT)

Source	Test	Calculated
$X_{el(max)}$ (mm)	18.3	21.2
x_m (mm)	89.8	92.9
T_n (sec)	0.156	0.138
Ductility Index	4.91	4.38
Toughness Index	8.81	7.76
t_m (sec)	0.0589	0.0806

The natural period (T_n) from the test was derived in the following manner. Once the beam had reached maximum deflection and started to go back, it was acting elastically until it crossed the permanent deformation line. The time that it took was a quarter period. Therefore $T_n/4$ was obtained by taking the time at which the deflection-time graph crossed the permanent deformation line and subtracting the time from the point of impact to maximum deflection (t_m). The period was therefore four times this time interval. The time from the point of imp[act to maximum deflection could not be used to determine T_n as it had a plastic component in it when the beam went plastic.

The percentage difference between the calculated and the test values for the items listed in the previous four tables is given in Table 7.16.

TABLE 7.16 PERCENTAGES DIFFERENCE BETWEEN CALCULATED AND TEST VALUES FOR 'PLASTIC' STEEL TESTS

Beam No.	A3	B2	A7	B7
$x_{el(max)}$	20.8%	22.1%	12.4%	13.7%
x_m	3.9%	7.6%	4.9%	3.3%
T_n	24.0%	19.5%	19.2%	13.0%
t_m	3.1%	9.4%	8.1%	26.4%

From Table 7.16 it can be seen that the calculated $x_{el(max)}$ and x_m values compare well with the test values. All percentage differences for x_m are under ten percent which is within the accuracy expected from the test equipment. The calculated natural period of vibration (T_n) varied between thirteen and twenty four percent below the test T_n. The time to maximum deflection (t_m) compared well for all but one test (B7). The

percentage difference in this case was also below ten percent, except for B7, which was 26.4 percent.

The two different loading categories, namely one 400N weight attached to the pendulum and no weight attached, were used to vary the duration of impact (T). The impulse value (H_{me}) also differed for the different weight categories. This was also the case with the impulsive force at the point of impact (B_e). These values are given in Table 7.17 for the four beams given previously.

TABLE 7.17 SUMMARY OF IMPULSE VALUES FOR 'PLASTIC' STEEL TESTS

Weight Cat.	No weights		One 400N Weight	
Beam No.	A3	B2	A7	B7
T (sec)	0.0467	0.0513	0.0725	0.0806
H_{me} (Ns)	165.6	193.2	224.5	264.6
B_e (N)	7978.2	7216.8	6256.3	5758.7

The impulse values (H_{me}) were obtained from the energy analysis. The impulse force values (B_e) were obtained from the displacement-time graph analysis. The duration of the impulse (T) was calculated from the Elasto-Plastic Energy analysis. If the impulse force value (B_e) and the duration of the impulse (T) are used to calculate the impulse (H_{me}), using a triangular shaped impulse, an impulse value very close to that obtained from the Elasto-Plastic Energy analysis is obtained. This shows that the triangular shaped impulse was the correct one to use.

The "no weight" beams gave results requiring a higher impulsive load (B_e) than the beams impacted with one 400N weight. This was due to the higher velocity of the pendulum and resultant higher acceleration of the beam at impact. The duration of impact was shorter. This resulted in lower impulse values for beams A3 and B2 (no additional weights), compared to beams A7 and B7.

Another method of analysis called the Rigid-Plastic method [3] (see Appendix G) was used for the steel beams as well. It was found that it did no compare well at all with the test results. This is probably due to the fact that with this method the

material is taken to be rigid-perfectly plastic and all elastic strains are omitted.

7.1.2.2.2 Discussion of Results and Their Projected Effects on Concrete Impact Tests

The measured results compared well with the calculated values, particularly the x_m-values. The analysis of the impulse showed that the triangular shape was the correct one. This shape impulse was used for all further analysis. The results showed that the Rigid Plastic Method (to be explained later) was not applicable to the steel beams, due to the fact that all elastic strains are omitted in this method.

7.2 CONCRETE BEAMS

7.2.1 Results of Static Testing of Plain Concrete Beams

The two beams (CA11 and CA12) that were tested statically by single point loading in the 'Denison' Universal Testing Machine gave very similar results. The failure loads are given in Table 7.18.

TABLE 7.18 RESULT OF STATIC TESTS ON PLAIN CONCRETE BEAMS

Beam No.	Failure Load (kN)
CA11	9.60
CA12	9.65

7.2.1.1 Analysis of Static Testing of Plain Concrete Beams

The Failure Load (P) was used to determine the modulus of rupture (MR). The MR was the stress at failure ($f_{(t)}$) of the concrete and was determined from the following equation:

$$f_{(t)} = \frac{My}{I} \qquad (7.33)$$

where M = simply supported moment (M = PL / 4)
y = distance to outside fibre (y = h / 2)
I = second moment of area of beam (I = (bh^3) / 12)

By using these values (7.33) becomes

$$f_{(t)} = \frac{1.5PL}{bh^2} \qquad (7.34)$$

The results of the analysis are given in Table 7.19.

TABLE 7.19 RESULTS OF ANALYSIS OF STATIC TESTS ON PLAIN CONCRETE BEAMS

Beam No	CA11	CA12
Failure Load (kN)	9.60	9.65
MR (MPa)	6.48	6.51
Comp Cube Strength (MPa)	43.5	43.5

The beams were water cured for 28 days and were one year old when tested, hence the high cube strength. The average static MR was taken as 6.50MPa.

7.2.1.2 Discussion of Results and Their Projected Effects on Impact Tests

The results proved consistent and could therefore be used for further static analysis, when required.

7.2.2 Results of Impact Testing of Plain Concrete Beams

The plain concrete beam (CA20) that was impacted ten times from a height that represented 40% of the 'just failed' height showed no visible signs of damage. However, when it was subsequently impacted from a height that represented 90% of the 'just failed' height, it failed. This indicated that the previous impacts had caused internal micro-damage which weakened the beam. This result was supported by beam CA9 which failed after being impacted three times from a height that represented 90% of the 'just failed' height.

Two beams (CA7 and CA8) gave the 'just failed' condition after impact. This can be seen in Photographic Plate 7.1, at the end of this chapter. It shows beam CA7 with the crack extending the whole depth of the beam, yet is still connected at the top of the beam. A fine crack is visible on the top face of the beam. The distance of release was 950mm from POI in both cases. The pendulum had no weights attached for the impact. The backswing

arc for both beams was 1.5mm which is 1.9% of the starting arc length. (84mm)

7.2.2.1 Analysis of Impact Testing of Plain Concrete Beams

The backswing arc was ignored as it was so small (1.9% of starting arc) and was probably due to the pendulum 'swing through' during impact. The pendulum would thus have swung back the same amount.

The energy at the POI was calculated from the release position (as described in 7.1.2.1.1). This was the amount of strain energy (SE) absorbed by the beam which caused failure. This SE was used to calculate the value of the maximum resistance of the beam (R_{me}) by means of the following equation:

$$SE = 0.5R_{me}x_{el\,(max)} \qquad (7.35)$$

Since $x_{el(max)} = R_{me} / k$ Equation (7.35) can be written as follows:

$$SE = 0.5R_{me} * \frac{R_{me}}{k} \qquad (7.36)$$

where k = dynamic elastic spring stiffness of beam.

Rearranging.

$$R_{me} = \sqrt{2SEk} \qquad (7.37)$$

The analysis was done by means of a spread sheet and a printout can be seen in Appendix D. The impulse was found to be 54.6Ns and R_{me} was equal to 74.0. The energy required for fracture 'fracture energy' was equal to 23.3 Joules.

7.2.2.2 Discussion of Results and Their Projected Effects on Impact Tests of Reinforced Concrete Beams

The fact that two beams both gave the failure criteria when impacted from the same point indicated repeatability of results. The 'fracture energy' (23.3 Joules) would have to be taken into account for the analysis of reinforced concrete beams due to impact loads. (ie it would have to be deducted from the energy at POI). One series of plain concrete beams were tested in one-point loading at various displacement rates in the 'Denison'.

The results were not conclusive and did not show a significant increase in the failure load with increased displacement rate. However, more tests would have to be performed to confirm this, due to the 'scatter' of results. Unfortunately time did not allow for this to be done. In addition if a larger range of displacement rates were available, a trend may have become apparent.

7.2.3 Results of Static Testing on Reinforced Concrete Beams

The results for the static tests (performed on the 'Denison') of each type of beam are listed in Table 7.20.

TABLE 7.20 RESULTS OF STATIC TESTS ON REINFORCED CONCRETE BEAMS

Beam No.	CB1	CB11	CB12	CD1
No. and Bar Diameter	2 x 3.15mm	4 x 3.15mm	2 x 5.67mm	4 x 3.55mm
Percentage Reinf	0.156	0.311	0.505	0.40
Failure Load(kN)	10.9	12.28	18.15	14.75
Defl at max Load(mm)	0.020	3.44	4.76	11.09
Permanent Deformation(mm)	7.19	*	*	12.74

* = Beam broke in two halves before zero load was reached on unloading

7.2.3.1 Analysis of Static Testing of Reinforced Concrete Beams

The load-deflection readings were used to plot load-deflection graphs. An example of such a graph, (for beam CB12) can be seen in Figure 7.10. It can be seen from Figure 7.10 that the beam continued to deflect after the maximum load was reached and the beam broke in two before

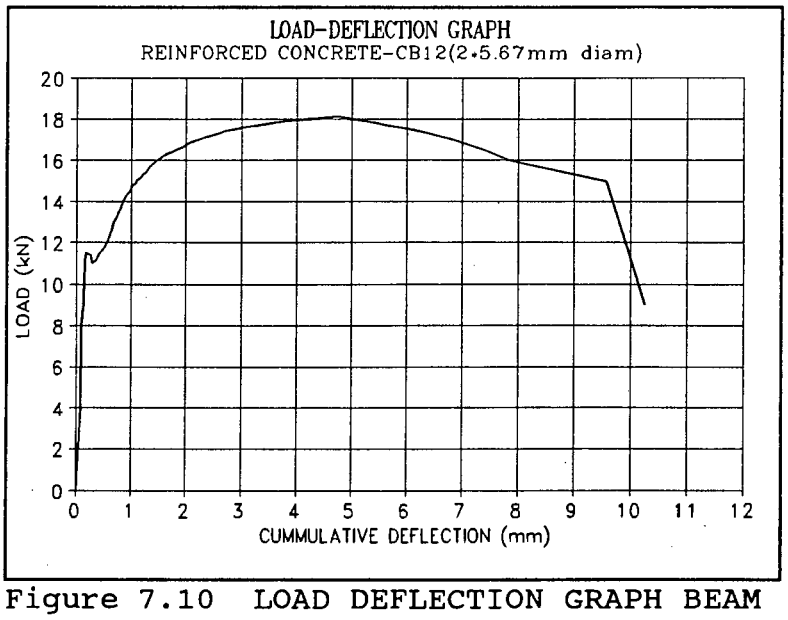

Figure 7.10 LOAD DEFLECTION GRAPH BEAM CB12

zero load was reached.

7.2.3.2 Discussion of Results and Their Projected Effects on Reinforced Concrete Beam Impact Tests

The failure loads determined in the static tests were used to determine the failure criteria for the reinforced concrete beams tested with impact loads. If an impacted beam was unable to reach the given load in Table 7.19 when it was subsequently tested statically, in the 'Denison', it was possible that it may have failed. This 'failure' was due to the impact load. The possibility that the beam had failed would depend on the difference between the residual strength of the impacted beam and the static failure load. If the difference was small, say less than 5% , then one could have said that the beam was naturally weaker due to the scatter. This scatter would be due to the variability of the concrete. If the difference between the residual strength and the static strength was less than 5% it was assumed that the beam had not failed.

Unfortunately only one beam of each type was tested statically, as there were only four beams of each type available. This meant that due to the variability of concrete, it was possible that the 'control' beam chosen for the static test could have been the weakest of the four. The choice of beam was entirely random which meant that the 'control beam had just as much chance of being the weakest in the set as the strongest. (It would have been preferable to have tested more beams statically and taken the mean, but this was not possible).

7.2.4 Results of Impact Testing of Reinforced Concrete Beams Series CB:

Beams CB2-CB5: At the start of this test series beams CB2 to DB5 were impacted from increasing distances from the POI until they failed. This was found to be a bad approach as the impact force that caused failure could not be determined. 'Failure' occurred when the beams were 'chopped' in half due to the low reinforcing percentage. (0.156%) Subsequently, once on estimate of the failure impact was obtained, the test beams were only impacted

once.

The results for the beams that were only impacted once are listed in Table 7.21. All arc lengths stated are those measured with the arc-measuring device, unless otherwise stated.

TABLE 7.21 RESULTS OF BEAMS IMPACTED ONCE ONLY

Beam No.	CB6	CB7	CB8	CB9	CB10
Dist from POI(m)	2.50	2.60	3.25	3.60	4.00
B/S Arc(m)	0.094	0.099	1.30*	0.141	0.152
Start Arc(mm)	0.239	0.246	3.25	0.345	0.384
Max Deflect(mm)	4.2	4.8	4.0	4.7	5.5
Perm Deform(mm)	1.0	2.5	0.85	1.1	1.3
Crack Width(mm)	2.1	2.2	1.7	3.1	3.8
Residual Strength(kN)	13.27	12.68	19.2	18.75	18.95

* Visual Backswing measurement as pencil on arc-measuring device broke. (A visual backswing measurement was always made to check results of the arc-measuring device. Results proved to be accurate.) A visual backswing was the point to which the end of the pendulum channel section swung back relative to the curved channel. The starting arc was the arc length as measured along the curved channel from POI to pendulum release mechanism.

Series CD:

Unfortunately, the deflection rod for each beam, except for one (CD6), came loose during impact. The deflection-rod attachment came loose by tearing a chunk of concrete from the beam. (ie the concrete failed in tension.) This meant that there were no deflection-time measurements for the beams except for CD6.

In an effort to determine the permanent deformation of the beams, the following method was employed: A line was drawn on the side of the beam from the position where the knife edge supports had touched the beam to the top of the beam. This was done for each end of the beam. A straight-edge was then placed so that its edge just touched the points where the drawn line reached the top of the beam. The amount of light that could be seen between the

edge of the straight-edge and the top of the beam represented the permanent deformation. The permanent deformation at the centre of the beam was measured with a feeler gauge. These values were recorded. The method was checked with beams from Series CB and gave excellent correlation. The same method was also used to check the steel beams except that a tape-measure was used instead of the feeler gauge, due to the larger permanent deformation. Once again the results gave excellent correlation with the permanent deformation shown on the deflection-time graphs.

The results for Series CD for impacting with no weights attached are given in Table 7.22 and those for two 400N weights attached are given in Table 7.23.

TABLE 7.22 RESULTS OF IMPACT TESTS ON REINFORCED CONCRETE BEAMS CD2 TO CD5 (NO WEIGHTS)

Beam No.	CD2*	CD3	CD4	CD5
Dist from POI(m)	3.13	3.13	4.00	5.00
B/S Arc(m)	0.125	0.127	0.160	2.00**
Start Arc(mm)	0.298	0.298	0.386	5.00
Perm Deform(mm)	2.10	2.76	3.24	6.41
Crack Width(mm)	2.26	2.26	4.39	6.20
Residual Strength (kN)	16.15	15.30	15.20	13.90

* Beam CD2 had 3 rods attached, all of which were dislodged by the impact. The rest of the beams were tested with only one deflection rod attached. All deflection rods in this set (CD2 to CD5) were dislodged, hence no maximum deflection readings were available.

** It was physically impossible to measure the backswing with the arc-measuring device, due to the large starting arc. A visual backswing measurement was taken, as discussed previously.

TABLE 7.23 RESULTS OF IMPACT TESTS ON REINFORCED CONCRETE BEAMS CD6 TO CD9 (TWO 400N WEIGHTS)

Beam No.	CD6	CD7	CD8	CD9
Dist from POI(m)	1.50	2.00	1.75	1.90
B/S Arc(mm)	40	20	33	39
Start Arc(mm)	139	187	163	177
Perm Deform(mm)	5.58	20*	8.30	11.00*
Crack Width(mm)	5.25	18.0*	8.26	3.67 & 5.15 **
Residual Strength (kN)	14.2	2.5	11.9	15.1

* measured with tape measure

** Beam CD9 developed two cracks 25mm either side of the centre line (ie either side of the deflection rod attachment.)

The small backswing value for beam CD7 showed that there was very little residual elastic energy in the beam. This meant that the specimen had failed as it had past its maximum resistance. This was supported by the large permanent deformation and very low residual strength of beam CD7. The deflection rod for beam CD6 remained attached and therefore a maximum deflection was obtained. This was found to be 12.3mm.

7.2.4.1 Analysis of Impact Tests of Reinforced Concrete Beams

7.2.4.1.1 Analysis of Series CB

The residual strengths were compared to the static failure load for each type of beam. The two beams chosen for further analysis from Series CB were CB6 for the beams with 4 x 3.15mm diameter reinforcement(0.31%) and CB9 for 2 x 5.67mm diameter reinforcement.(0.50%)

A comparison of the static failure load and residual strengths for these two beams is given in Table 7.24.

TABLE 7.24 COMPARISON OF STATIC FAILURE LOAD & RESIDUAL STRENGTH AFTER IMPACT (CB6 & CB9)

Beam No.	CB7	CB9
Weight Condition	No Weights	1 x 400N
Reinforcement	4x3.15mm diam (0.31%)	2x5.67mm diam (0.50%)
Static Failure Load(kN)	12.28	18.15
Residual Strength(kN)	12.68	18.75
Percentage Diff	3.3	3.3

Although both the residual strengths are slightly higher than the static failure loads, (ie they had not failed) they were chosen for further analysis.

The deflection-time graphs were analysed as before and the corrected displacement graphs were plotted. (See Appendix D)

The elasto-plastic energy method was used again for the analysis. The results for beams CB7 and CB9 are given in Table 7.25.

TABLE 7.25 RESULTS OF ELASTO-PLASTIC ENERGY METHOD FOR R.C. BEAMS (CB7 & CB9)

Beam No.	CB7	CB9
Weight Condition	No Weights	1 x 400N
Dist Release POI	2.660	3.60
Percentage Reinforcement	0.31	0.50
x_m (mm)	18.7	59.2
$x_{el(mm)}$	0.1	0.1
Ductility Index (DI)	187	592
Toughness (TI)	373	1183
t_m (sec)	0.0123	0.00405

The calculated values of x_m and t_m are compared with the test values in Table 7.26.

TABLE 7.26 COMPARISON OF TEST VALUES & ELASTO-PLASTIC ENERGY METHOD (EPEM) RESULTS FOR CB7 & CB9

Beam No.	CB7		CB9	
Source	Test	EPEM	Test	EPEM
x_m (mm)	4.8	18.7	4.7	59.2
t_m (sec)	0.0057	0.023	0.0057	0.00405

It can be seen from Table 7.26 that x_m results do not compare

very well. The EPEM values are 3.9 and 12.6 times the test values for beams CB7 and CB9 respectively. This suggested that not all the energy at impact went into the beam as SE. (ie there were losses.)

It was decided to use another method of analysis called the Rigid Plastic Analysis Method (RPM). This method is explained in Appendix G. The RPM requires the impulsive force (F_o) and the duration of the impulse (T). A Force Balance Method (FBM) was used to determine these values and a description of the procedure is described in 7.2.4.1.1.1.

7.2.4.1.1.1 Force Balance Method

Before the Rigid Plastic Method of analysis (see Appendix G) could be applied, the impulsive force (F_o) and duration of the impulse (T) had to be determined. This was achieved by means of a balance of forces.

The action of the impulsive force of the pendulum (F_o^P) had to be equal to the reaction force of the beam. (F_o^P) is equal to the effective mass of the pendulum at the POI multiplied by the deceleration of the pendulum due to the impact. If the interval of time during which this deceleration occurs is called Δt and the velocity of the pendulum at this time is called $v_{\Delta t}$, then the deceleration of the pendulum (a_{pend}) is given by the following equation: (see Figure 7.11)

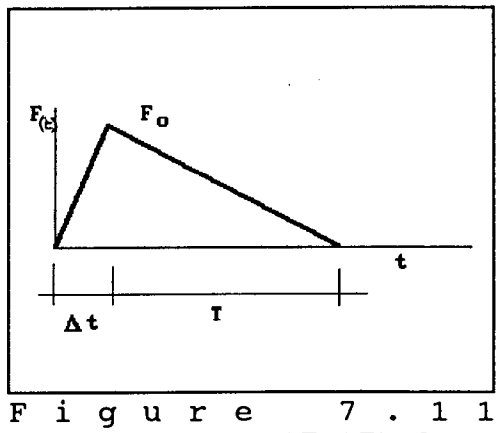

Figure 7.11
DETERMINATION OF DELTA T

$$a_{pend} = -\frac{V_{POI} - V_{\Delta t}}{\Delta t} \qquad (7.38)$$

where V_{POI} = velocity of effective pendulum mass at POI ($M_{ep(POI)}$) just before impact

The acceleration of the beam is given by the following equation:

$$a_{bm} = \frac{v_{\Delta t} - 0}{\Delta t} \qquad (7.39)$$

where 0 = initial velocity of beam (zero)

The impulse force for pendulum (F_o^P) is given as follows:

$$\begin{aligned} F_o^P &= M_{ep(POI)} * a_{pend} \\ &= [(M_{ep} - M_{ech}) + f_p M_{ech}] * (\frac{v_{POI} - v_{\Delta t}}{\Delta t}) \end{aligned} \qquad (7.40)$$

where M_{ep} = effective mass of pendulum
M_{ech} = effective mass of channel
f_p = proportional factor (See 7.1.2.1.1)

The impulse force for the beam (F_o^B) is given as follows:

$$\begin{aligned} F_o^B &= M_{ebm} * bm \\ &= [0.49m_b + \sum M_r] * (\frac{v_{\Delta t}}{\Delta t}) \end{aligned} \qquad (7.41)$$

where M_{ebm} = effective mass of beam
m_b = distributed mass of beam
$\sum M_r$ = sum of deflection rod and attachment

However, these two forces must be equal. The velocity at the time Δt ($v_{\Delta t}$) can be found by equating equations 7.40 and 7.41, as the time Δt is common to both and cancels out. This leaves only one unknown which can be determined. The velocity ($v_{\Delta t}$) is therefore given by the following equation:

$$\begin{aligned} \Delta t &= \frac{[(m_{ep} - M_{ech}) + f_p M_{ech}] * v_{POI}}{[(M_{ep} - M_{ech}) + f_{pM_{ech}}] + [0.49m_b + \sum M_r]} \\ &= \frac{M_{ep(POI)} * V_{POI}}{(M_{ep(POI)} + M_{ebm})} \end{aligned} \qquad (7.42)$$

The time Δt at which this velocity ($v_{\Delta t}$) occurred was still unknown. This was determined from the displacement-time graph as follows: The velocity of the beam was plotted against time, using data from the displacement-time graph spread sheet. A best-fit curve was plotted and the equation for the curve was derived. The velocity ($v_{\Delta t}$) was substituted into the equation and

the time (Δt) was determined.

The accelerations and F_0-forces were then determined from the previously given equations. A check was done to see that the two F_o-forces were equal.

The amount of kinetic energy lost by the pendulum and gained by the beam (KE^B) is given by the following equation:

$$KE^B = \frac{1}{2} M_{ebm} * v_{\Delta t}^2 \qquad (7.43)$$

The impulse (H_{me}) was calculated from the following equation:

$$H_{me} = \sqrt{KE^B * 2M_{ebm}} \qquad (7.44)$$

The shape of the impulse (H_{me}) was assumed as triangular, as validated before. The duration of the impulse (T) was calculated from the following equation:

$$T = \frac{2H_{me}}{F_o} \qquad (7.45)$$

The above analysis was performed by means of a spread sheet and print outs can be seen in Appendix D.

The results of the analysis for beams CB7 and CB9 are given in Table 7.27.

TABLE 7.27 RESULTS OF FORCE BALANCE METHOD FOR DETERMINING IMPULSE LOAD FOR CB7 &CB9

Beam No.	CB7	CB9
Weight Condition	No weights	1X400N
Percentage Reinforcement	0.31	0.50
Dist Release POI (m)	2.60	3.60
v_{POI} (m/s)	4.158	5.297
$v_{\Delta t}$ (m/s)	3.551	4.901
Δt (sec)	0.000280	0.000113
M_{emb} (kg)	7.521	7.525
$M_{ep(POI)}$ (kg)	43.66	92.97
a_{bm} (m/s^2)	12566.6	43406.7
a_{pend} (m/s^2)	-2164.6	-3513.4
F_o^B (kN)	94.513	326.635
F_o^P (kN)	94.513	326.635
KE^B (Joules)	46.392	90.360
Imp Duration 'T' (sec)	0.000559	0.000226
Impulse 'H_{me}' (Ns)	26.416	36.877

The information in Table 7.27 was used in a Rigid-Plastic analysis (RPA). The gain in KE of the beam was used to determine the duration of the impulse. (As given in Table 7.28). The results of this analysis are given in Table 7.28.

TABLE 7.28 RIGID PLASTIC ANALYSIS OF R.C. BEAMS CB7 AND CB9

Beam No.	CB7	CB9
Weight Condition	No Weights	1 x 400N
Percentage Reinforcement	0.31	0.50
Dist of Release POI (m)	2.60	3.60
Impulse H_{me} (Ns)	26.416	36.877
Impulse duration	0.000559	0.000226
F_o (kN)	94.513	326.635
x_m	1.9	1.3
t_m	0.0024	0.0023

The values for x_m and t_m obtained in this way are compared to the test-values in Table 7.29.

TABLE 7.29 COMPARISON OF RIGID PLASTIC ANALYSIS & TEST VALUES FOR R.C. BEAMS (CB7 & CB9)

Beam No.	CB7		CB9	
Source	Test	RPA	Test	RPA
x_m (mm)	4.8	1.9	4.7	1.3
t_m (sec)	0.0057	0.0024	0.0057	0.0023

From Table 7.29 it can be seen that the x_m-values do not compare well. The t_m-values do not compare well either, as the RPA-values are approximately 41% of the test values.

However, the RPA method seems to confirm the earlier assumption that not all the energy at POI (E_{POI}) was going into the specimen. This is shown by the KE of the beam, which is less than the total energy at POI. This means that a large proportion of the energy is unaccounted for. The amounts of energy are listed in Table 7.30.

TABLE 7.30 PROPORTIONS OF ENERGY FOR REINFORCED CONCRETE IMPACT TESTS (CB7 & CB9)

Beam No.	CB7	CB9
Weight Condition	No Weights	1 x 400N
Percentage Reinforcement	0.31	0.50
Dist Release POI (m)	2.60	3.60
E_{POI} before impact (J)	246.7	1179.6
KE^B (J)	46.4	90.4
ΔKE^P (J)	100.8	188.0
Difference in E (J)	99.5	901.2
Percentage Difference	40.3	76.4

The difference in energy is large. This unaccounted for energy was dissipated to various areas of the test arrangement. It was assumed that most of this energy was absorbed by the support structure. However, this energy would have been elastic energy in that the support structure did not go plastic. The proportion of the unaccounted energy that went into the support structure could not be determined without appropriate instrumentation.

It was presumed that the rest of the unaccounted for energy was dissipated in the vibration of the pendulum, support column cantilever section and supports etc. Immediately after impact

these members were observed to vibrate. This vibration was worse when a more rigid specimen such as concrete was impacted, than for a more flexible specimen like the steel beam. This would tend to indicate that the more rigid the specimen that was impacted, the more energy was dissipated in vibration of the rest of the system (pendulum, column, cantilever section etc). Also the more rigid the specimen, the more energy was put in the system by means of the impact.

The stiffness of the concrete beam was 941 times that of the steel beam from Series A. This shows that the steel beams were much more flexible that the concrete beams and could thus absorb a larger proportion of the energy. This left less energy available to be dissipated by vibration of the rest of the system. Therefore the amount of energy that went into the support system was taken as the kinetic energy at the POI minus the KE of the beam due to impact and the kinetic energy of the pendulum after impact.

7.2.4.1.2 Analysis of Series CD

The deflection rods from all but one beam (CD6) came loose during impact. For this reason the deflection-time graph of beam CD6 was analysed. A comparison of the static failure load and residual strength for beams CD6 and CD7 is given in Table 7.31. Beam CD7 was chosen for further analysis, as the residual strength was so low that it had clearly failed especially when taken together with a permanent deformation of 20mm.

TABLE 7.31 COMPARISON OF STATIC FAILURE LOAD & RESIDUAL STRENGTH AFTER IMPACT (CD6 & CD7)

Beam No	CD6	CD7
Dist Release POI	1.50	2.00
Static Failure Load (kN)	14.75	14.75
Residual Strength (kN)	14.2	2.5
Percentage Difference	3.7	83.1

It should be noted that an increase of the distance of the release to POI of 0.5m had a big effect on the residual strengths. It went from a 'not quite failed' beam (CD6) to a completely failed beam, with virtually no residual strength (only

17% of the static value remaining). This meant that the 'true impact load' lay somewhere between these two points.

The Elasto-Plastic Energy Method (EPEM) was used for the analysis. Beams CD6 and CD7 were analysed with this method. The fact that beam CD7 did not have a deflection-time graph (as deflection rod was dislodged) meant that a maximum displacement (x_m) was not available. However the permanent deformation of the beam was used in the spread sheet for the friction of the rods. This did not affect the results much as the friction of the rods had been found to be negligible with other beams.

The acceleration of beam CD7 could not be determined as there was no displacement-time graph. This meant that the impulsive force (B_e) and time to maximum displacement (t_m) could also not be calculated. The duration of the impulse could also not be calculated. The results of the Elasto-Plastic Energy method are given in Table 7.32.

TABLE 7.32 RESULTS OF ELASTO-PLASTIC ENERGY METHOD OF ANALYSIS OF R.C. BEAMS CD6 & CD7

Beam No.	CD6	CD7
Weight Condition	2x400N	2x400N
Dist Release POI (MM)	1.50	2.0
Percentage Reinforcement	0.40	0.40
x_m (mm)	16.3	30.2
t_m (sec)	0.00395	-

The result of CD7 seems reasonable, especially compared to its permanent deformation of 20mm. The results of the Elasto-Plastic Energy Method (EPEM) analysis for beam CD6 are compared to test results in Table 7.33.

TABLE 7.33 COMPARISON OF EPEM RESULTS & TEST VALUES FOR R.C. BEAM CD6

Beam No.	CD6	
Source	Test	EPEM
x_m (mm)	13.3	16.3
t_m (sec)	0.0045	0.00395

The results are of the same order. Once again the calculated value for x_m exceeds the measured value (by 24.5% this time) which tends to support the assumption that there were energy losses to the support system.

The Force Balance Method (FBM) (as described before) was used to determine the impulse (F_o) and duration of the impulse (T) for beam CD6. The results of this analysis are given in Table 7.34.

TABLE 7.34 RESULTS OF FBM FOR DETERMINING IMPULSE LOAD FOR R.C. BEAM CD6

Beam No.	CD6
Weight Condition	2x400N
Percentage Reinforcement	0.40
Dist Release POI (m)	1.50
v_{POI} (m/s)	2.106
$v_{\Delta t}$ (m/s)	1.997
Δt (sec)	0.000686
M_{emb} (kg)	7.521
$M_{ep(POI)}$ (kg)	137.04
a_{bm} (m/s^2)	2910.7
a_{pend} (m/s^2)	159.7
F_o^B (kN)	21.891
F_o^P (kN)	21.891
KE^B (Joules)	14.993
Imp Duration 'T' (sec)	0.00137
Impulse 'H_{me}' (Ns)	15.017

The results of Table 7.34 were used in a Rigid Plastic Analysis (RPA), as for the other reinforced concrete beams. The results are given in Table 7.35.

TABLE 7.35 RIGID PLASTIC ANALYSIS OF R.C. BEAM CD6

Beam No.	CD6
Weight Condition	2 x 400N
Percentage Reinforcement	0.40
Dist of Release POI (m)	1.50
Impulse H_{me} (Ns)	14.993
Impulse duration	0.001376
F_o (kN)	21.891
x_m	0.3
t_m	0.0012

The results show firstly, that the time to maximum displacement (t_m) was less than the duration of the impulse (T). This meant that there was no second phase (ie $T_2 = 0$). The maximum deflection (x_m) was very small compared to the measured value of 12.3mm. The reason for this is not clear, as $F_o > 4M_{pl} / L$ criteria was met (although only just), so the beam should have gone plastic. The results of more beams would be required before the reasons for this behaviour could be determined.

7.2.4.1.3 Discussion of Results and Effects on Reinforced Concrete Slabs

The results showed that the Elasto-Plastic Energy Method was not accurate enough, as it gave deflections three to 10 times the measured value. This was due to the assumption that all the energy at point of impact (E_{POI}) was absorbed by the beam as SE. It was subsequently shown that this was not the case.

The Force Balance Method proved to be a useful method of determining the impulse load (F_o) and the duration of the impulse (T). These values were used in the Rigid Plastic Analysis (RPA). The results of the RPA were reasonable for beams CB7 and CB9, with x_m-values of the same order as the measured values. The RPA method did no work for beam CD6 and the fact that $t_m < T$ may have had something to do with it. Nevertheless, the RPA was considered applicable to reinforced concrete members and would be applied to the slab analysis.

The fact that all the energy at the POI did not go into the beam as SE would have to be taken into account for the slab analysis.

7.3 REINFORCED CONCRETE SLABS

7.3.1 Results of Static Testing of Reinforced Concrete Slabs

Only the three slabs of the last series of slabs (ie slabs 4, 5 and 6) were tested statically. Slabs 4 and 5 were impacted and their residual strength was determined statically. Slab 6 was not impacted and was used to determine the failure load as well as the load-defection graph. (see Figure 7.12) Unfortunately

only one dial gauge of 50mm length was available. During all three tests, the dial gauge ran out of travel. This meant that the maximum deflection (under maximum load) was not measured. However, as will be shown under the next section (analysis of results) a good approximation of the maximum deflection was obtained. The maximum deflection measured and its corresponding load is given in Table 7.36. The results for the three slabs mentioned above can be seen in Table 7.36.

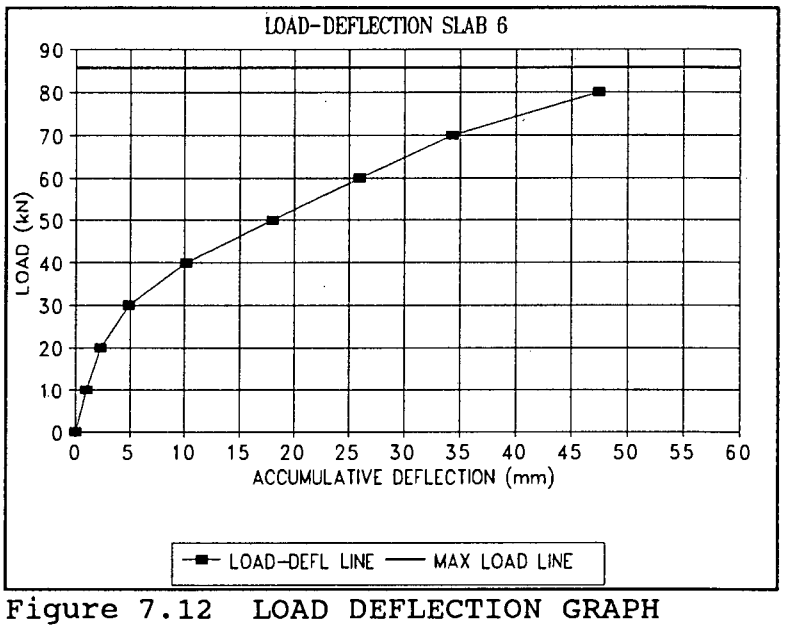

Figure 7.12 LOAD DEFLECTION GRAPH

TABLE 7.36 RESULTS OF STATIC TESTS OF REINFORCED CONCRETE SLABS

Slab No.	4*	5*	6
Failure Load (kN)	76.5	72.0	85.5
Max measured deflec (mm)	48.89	48.35	47.47
Corresp. Load to Max Defl (kN)	76.0	63	80
Permanent Deformation	47.86	34.4	34.61

* Results of Slabs that had been impacted prior to static test.

Comment: Slab 4 had a simultaneous flexural and shear failure at maximum load. A 'fan' failure occurred simultaneously with a punching through as maximum load was reached. The load then dropped off.

A photograph of failed slab 6 can be seen in Photographic plate 7.2. It shows the negative yield line (in red chalk) as well as the static test set-up.

7.3.1.1 Analysis of Static Testing of Reinforced Concrete Slabs

The load-deflection graph of slab 6 was converted to a

'simplified' trilinear graph. This was done in the following way: (Referring to Figure 7.12) A "best-fit" line was plotted through the first three points (ie from 0 to 20 kN). This line was extended past the 30kN mark.

A second "best-fit" line was plotted through the points five to eight (ie 40kN to 70kN). This line was extended both ways. The lower portion was extended until it intersected with the first line through the first three points. At this intersection point the load and corresponding deflection were read off. These denoted the cracking load and cracking deflection as it was at this point that the stiffness of the slab was reduced due to the cracking of the concrete.

The upper end of the second line was extended until it cut a horizontal line at the failure load (85.5kN). This gave the 'simplified' trilinear load-deflection graph. This process was done mathematically for greater accuracy. The values obtained from the analysis are given in Table 7.37.

TABLE 7.37 VALUES FOR SIMPLIFIED TRILINEAR LOAD-DEFLECTION GRAPH (SLAB 6)

Cracking Displacement (mm)	3.6
Cracking Force (kN)	32.9
Failure Displacement (mm)	46.7
Failure Load (kN)	85.5

The failure load given by slab 6 was equal to 85.5kN. A yield line analysis was performed on the two most probable modes of failure. Each will be dealt with separately here. (This work is based on work and notes of previous courses, including References 2 and 3).

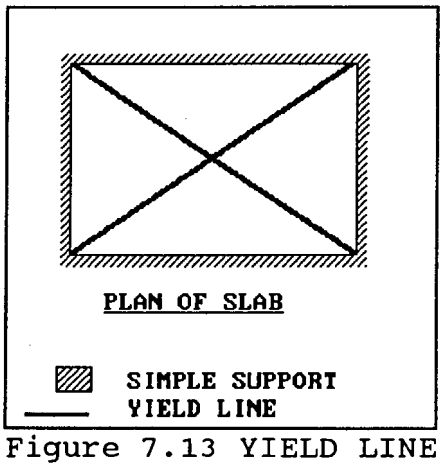

Figure 7.13 YIELD LINE FAILURE MODE 1

The first mode of failure (Mode 1) is shown in Figure 7.13. The yield line analysis is given in Appendix H. For

Mode 1, the force (F) that would cause failure is given by the following equation:

$$F = 8m \qquad (7.46)$$

where m = ultimate moment per unit length along the yield line

An alternative yield line pattern (Mode 2) is shown in Figure 7.14 and is more commonly known as a 'fan' failure and could occur due to a concentrated point load on the slab. The equation for the failure load (P) is given as follows:

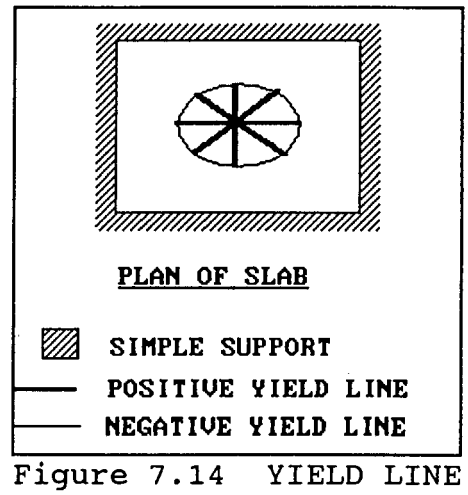

Figure 7.14 YIELD LINE FAILURE MODE 2

$$P = 2\pi(m + m_1) \qquad (7.47)$$

where m_1 = ultimate moment per unit length along the negative yield line

This means that the load P is independent of the radius of the fan.

The ultimate plastic moment capacity (M_{pl}) of the slab had to be calculated before P and F could be determined, This was calculated using no material or safety factors in order to get the true failure load. The results for the second set of slabs (slabs 4 to 6) are given in Table 7.38

TABLE 7.38 STATIC VALUES FOR SLABS 4 TO 6

Slab No	4	5	6
average f_{cu} (MPa)	37.5	36.3	38.2
A_s (mm^2/m)	255	255	255
d (mm)	29.3	29.3	29.3
$f_{y(first\ yield)}$ (MPA)	415.5	415.5	415.5
$f_{y(ult)}$ (MPa)	517.4	517.4	517.4
E_{steel} (GPa)	208.3	208.3	208.3
E_{conc} (GPa)	31.2	31.2	31.2
M_{pl} (kNm/m)	3.28	3.26	3.30

Using the value for M_{pl} given in Table 7.35 the failure Load for Mode 1 was found to be 26.4kN. Equation (7.47) gave the failure load for Mode 2 as 20.4kN. Both these calculated values are a lot less that the measured failure load of 85.5kN.

The static punching shear failure was calculated using reference 5: The shear stress (v_c) was calculated using the following formula:

$$v_c = \frac{0.79}{K_m} \left(\frac{f_{cu}}{25}\right)^{\frac{1}{3}} \left(\frac{100A_s}{ud}\right)^{\frac{1}{3}} \left(\frac{400}{d}\right)^{\frac{1}{4}} \qquad (7.48)$$

where K_m = material factor (taken = 1 here)

$\frac{(100A_s)}{ud}$ = effective steel area passing through shear area

$400/d \geq 1$

f_{cu} = compressive concrete strength (MPa)

The shear perimeter (u) was given by the following equation:

$$u = 4(1.5d + 2a) \qquad (7.49)$$

where a = length of loaded area = 140mm in this case

The value for v_c was found to be 1.66MPa. The static shear force (V_{st}) that would cause this shear failure, was calculated from the following equation:

$$V_{st} = v_c ud \qquad (7.50)$$

where d = effective depth of lowest reinforcing mesh

The static shear capacity (V_{st}) was found to be equal to 47.6kN. This value was higher than the other two capacities calculated from the yield-line analysis.

The Elasto-Plastic Method (EPM) was used to calculate the displacements and rotations up to yield and after yield. This would enable the maximum displacement to be determined, which could be compared to test results.

At the yield point of the slab, a parabolic stress-block was used,for the concrete in compression as the slab had not reached ultimate conditions (where a rectangular stress-block would be used).

The depth of the compression block at yield (x_y) was obtained from the following formula:

$$x_y = \frac{A_s f_y}{(\frac{2}{3})(0.6 f_{cu})b} \qquad (7.51)$$

where A_s = area of tension steel (m^2/m)
f_y = yield stress of reinforcing steel (MPa)
f_{cu} = compressive strength of concrete (MPa)

It was assumed that the steel had reached the full yield point. The strain at yield (ϵ_y) of the slab reinforcement was obtained from the tension tests on the reinforcement (See Chapter 5). The strain at yield was 0.00394. Standard curves for high yield reinforcement give the strain at yield (ϵ_y) as 0.00395. The test value of 0.00394 was used for further analysis.

The curvature at cracking (ϕ_{cr}) of the concrete was calculated from the following equation:

$$\phi_{cr} = \frac{M_{cr}}{EI} \qquad (7.52)$$

where M_{cr} = cracking moment of concrete(obtained from MR of concrete)
E = Static elastic modulus of concrete

I = second moment of area of slab

The curvature at the yield point of the reinforcement (ϕ_y) was obtained from the following equation:

$$\phi_y = \frac{\varepsilon_y}{(d - x_y)} \qquad (7.53)$$

where d = effective depth of the slab

The strain of the concrete was checked at this point by the following equation:

$$\varepsilon_{cy} = \phi_y * x_y \qquad (7.54)$$

The strain of the concrete was found to be much less that the ultimate strain of 0.0035.

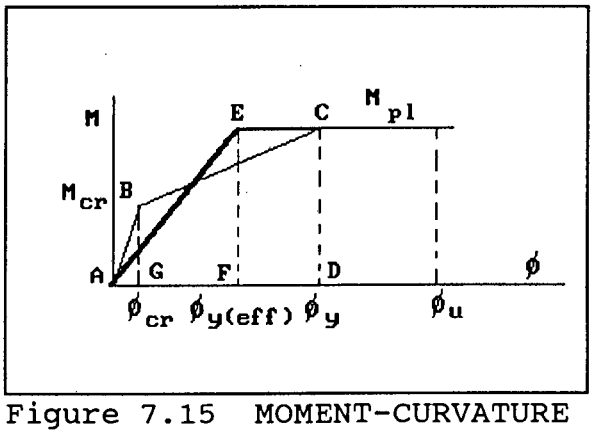

Figure 7.15 MOMENT-CURVATURE DIAGRAM

These curvatures can be seen in Figure 7.15. By referring to Figure 7.15, the effective curvature ($\phi_{y(eff)}$) was calculated in the following way: By equating the two areas ABCD and AECD, $\phi_{y(eff)}$) was calculated.
Area ABCD was calculated as follows:

$$\text{Area ABCD} = \frac{1}{2}(M_{cr} * \phi_{cr}) + 0.5(M_u + M_{cr})(\phi_y + \phi_{cr}) \qquad (7.55)$$

Area AECD was calculated as follows:

$$\text{Area AECD} = \frac{1}{2}(M_u * \phi_{y(eff)}) + (\phi_y - \phi_{y(eff)})M_u \qquad (7.56)$$

where M_u = Ultimate bending moment of Slab/m

By equating the two areas $\phi_{y(eff)}$ was obtained. However, $\phi_{y(eff)}$ was also given by the following equation:

$$\phi_{y(eff)} = \frac{M_U}{(EI)_{(eff)}} \qquad (7.57)$$

Thus $(EI)_{eff)}$, the effective stiffness could be evaluated.

The depth of the compression block at ultimate (x_u) was calculated as follows: A rectangular stress-block was used.

$$x_u = \frac{A_s f_y}{(0.6 f_{cu} b)} \qquad (7.58)$$

The curvature at ultimate (ϕ_u) was obtained from the following equation:

$$\phi_u = \frac{0.0035}{x_u} \qquad (7.59)$$

where 0.0035 = strain of concrete at ultimate
x_u = depth of compression block (m)
ϕ_u = curvature in radians

The plastic curvature (ϕ_p) was obtained as follows:

$$\phi_p = \phi_u - \phi_{y(eff)} \qquad (7.60)$$

These values were then used to calculated values for the idealized bilinear load-deflection curve (from the trilinear load-deflection curve, obtained from the static test (Slab 6).

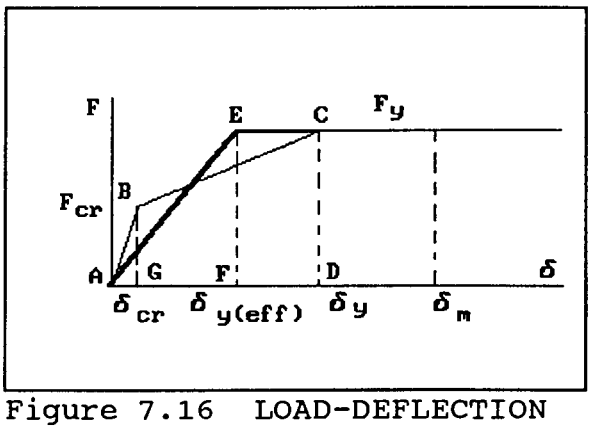

Figure 7.16 LOAD-DEFLECTION DIAGRAM

The deflections at the various stages were calculated as follows: Referring to Figure 7.16 the effective displacement at yield ($\delta_{y(eff)}$) was obtained by equating the two areas ABCD and AECD (the method as described previously).

The rotation of the slab in the plastic phase (θ_p) was obtained

from the following equation:

$$\theta_p = (\text{factor} * d)\ \phi_p \qquad (7.61)$$

where factor = plastic hinge factor 0.5 to 1.5 (average 1.0)
d = effective depth of slab

The displacement during the plastic phase (δ_p) was obtained as follows:

$$\delta_p = \frac{\theta}{2} * \frac{\sqrt{2L^2}}{2} \qquad (7.62)$$

where L = side length of slab

The maximum displacement $(\delta)_m$) was obtained as follows:

$$\delta_m = \delta_{y(eff)} + \delta_p \qquad (7.63)$$

where $\delta_{y(eff)}$ = the effective displacement at yield

By referring to Figure 7.16 for the effective bilinear graph:

$$\text{The ductility index} = \frac{\delta_m}{\delta_{y(eff)}} \qquad (7.64)$$

$$\text{The toughness index} = \frac{\text{Total Area}}{\text{Elastic Area}} = \frac{\text{Area AEFG}}{\text{Area AEH}} \qquad (7.65)$$

These two indices are a measure of how much energy the slab can absorb. The analysis described here was performed on a spread sheet and a printout can be seen in Appendix E. A summary of the results is given in Table 7.39.

TABLE 7.39 RESULTS OF MAXIMUM STATIC DEFLECTION ANALYSIS

Effective elastic displacement $\delta_{y(eff)}$ (mm)	33.3
Plastic displacement δ_p (mm)	13.4
Maximum displacement δ_m (mm)	46.7
Effective stiffness 'k' (kN/m)	2570.8
Ductility Index	1.40
Toughness Index	1.81

The maximum deflection of the slab was not measured due to the dial gauge running out of travel, as mentioned earlier. However, if the last portion of the graph (from 70kN to 80kN) is extended to cut the failure load line (85.5kN) a maximum displacement of 54.6mm is obtained. This is sixteen percent higher than the calculated maximum displacement.

However, if the simplified trilinear load-displacement curve (described earlier) of slab 6 is used, the maximum deflection is 46.7mm. This equals the calculated maximum deflection from the 'effective' bilinear load-displacement curve. For design purposes, an effective bilinear load-displacement curve is usually used, therefore it was decided to accept the 'effective' bilinear load-displacement curve for this analysis.

The test failure load (P_{Test} = 85.5kN) was much higher than the calculated values for either of the failure modes. The test failure load was 3.2 times that of the calculated failure load for Mode 1 failure and 4.2 times that of Mode Shape 2 'fan' failure. P_{TEST} was 1.8 times the punching shear failure load.

This was thought to be due to the 'plane stress action' or otherwise known as 'in plane arching action'.

7.3.1.2 Discussion of Results and Effects on Slab Impact Tests

The agreement of the maximum displacement-values between the test x_m and the 'equivalent' bilinear δ_m was excellent. This suggested that it was a good approximation to use and it would be used for further analysis. The test failure load and calculated failure loads did not agree well and the factors of 3.2 and 4.2 could be used for further analysis, to arrive at a better approximation of the failure load.

7.3.2 Results of Impact Testing of Reinforced Concrete Slabs

The results for the impact tests on the first set of slabs (0.2% reinforcement) are listed in Table 7.40.

TABLE 7.40 RESULTS OF IMPACT TESTS OF REINFORCED CONCRETE SLABS FOR SLABS 1 TO 3 (0.2% REINFORCEMENT)

Slab No.	1	2	3
Weight Condition	2x400N	3x400N	3x400N
Dist Release POI(m)	4.40	4.16	4.27
Backswing Arc (mm)	110	99	127
Starting Arc (mm)	425	400	410
Max Deflection Rod 1 (mm)	35.5	*	13.0
Max Deflection Rod 2 (mm)	41.0	46.5	17.3
Max Deflection Rod 4 (mm)	44	50	**
Max Deflection Rod 5 (mm)	31.0	29.0	12.5
Permanent Deformation Rod1	6.2	*	3.0
Permanent Deformation Rod2	6.9	8.2	2.2
Permanent Deformation Rod4	8.5	10.0	**
Permanent Deformation Rod5	6.5	8.0	2.5

* Pencil tore Graph Paper, hence no deflection was measured
** Rod 4 was dislodged as well as Rod 3.
Note: Centre Rod (Rod 3) was dislodged in each test
Slab 2 'failed' in flexure with open cracks easily visable.

Slab 3 failed in punching shear, as a hole (+/- 120mm x 115mm) was made by the 'hammer'. The flexural cracks were very fine, hardly visible. There were no 'open' cracks as with the previous two slabs. This was significant, as the difference between the release position of Slab 3 and Slab 2 was only 110mm, yet Slab 3 punched through and Slab 2 did not. Slab 2 failed in flexure and one would have expected Slab 3 to fail more in flexure, yet it did not. This meant that the shear failure was more vulnerable. Slabs 2 and 3 had the same mass attached to the pendulum (3 x 400N) and were released from approximately the same position which would give approximately the same impulse, yet it gave two completely different results. This seems to confirm the results of the dynamic shear tests (see Chapter 5) that the shear strength was strain-rate sensitive and shear strength reduces with increasing strain-rate.

The results of the second series of slabs (Slab 4 & 5) which were tested with five 400N weights attached, are given in Table 7.41.

TABLE 7.41 RESULTS OF IMPACT TESTS OF REINFORCED CONCRETE SLABS FOR SLABS 4 AND 5 (0.51% REINFORCEMENT)

Slab No.	4	5
weight Condition	5x400N	5x400N
Dist Release POI (m)	3.00	4.00
Backswing Arc (mm)	94	68
Starting Arc (mm)	284	378
Max Deflection Rod 1 (mm)	32	21.8
Max Deflection Rod 2 (mm)	40.5	29.8
Max Deflection Rod 3 (mm)	50.0	*
Max Deflection Rod 4 (mm)	40.3	28.5
Max Deflection Rod 5 (mm)	28.5	20.0
Permanent Deformation Rod1	5.0	3.8
Permanent Deformation Rod2	7.0	6.3
Permanent Deformation Rod3	9.2	*
Permanent Deformation Rod4	7.8	7.1
Permanent Deformation Rod5	5.5	6.0

* Rod 3 was dislodged during test.

Slab 4 had very fine flexural cracks after impact, none of which were open. There were very few negative flexural cracks on the front of the slab.

Slab 5 failed in punching, which made a hole approximately 115mm by 125mm in size. Most of the reinforcing mesh was broken in the hole area. At the back of the slab a spalled area of approximately 355mm in diameter was visible. The flexural cracks were very fine and not open.

7.3.2.1 Analysis of Impact Testing of Reinforced Concrete Slabs

The fact that all of the central rods (rod 3) except for one (Slab 4) were detached due to the impact, meant that the maximum deflection (x_m) was not measured. However, in most cases the other four rods had measured deflections. Since these rods were spaced at 250mm centres from the centre of the slab, they could be used to calculate approximately what the central defections should have been.

Slab 4 had recorded a deflection at Rod 3. This was used to

determine what ratio the deflection at the centre (Rod 3) was of the deflection at Rod 2 and Rod 4. The deflection at Rod 3 was divided by the average deflection of Rod 2 and 4. This gave the correction factor (CF) that had to be applied to the defections for other slabs to get an estimate of their central deflection. Therefore the maximum central defection (x_{mc}) for a particular slab was calculated by the following equation:

$$x_{mc} = CF * \left(\frac{x_{MR2} + x_{MR4}}{2}\right) \qquad (7.66)$$

where CF = correction Factor = 1.23

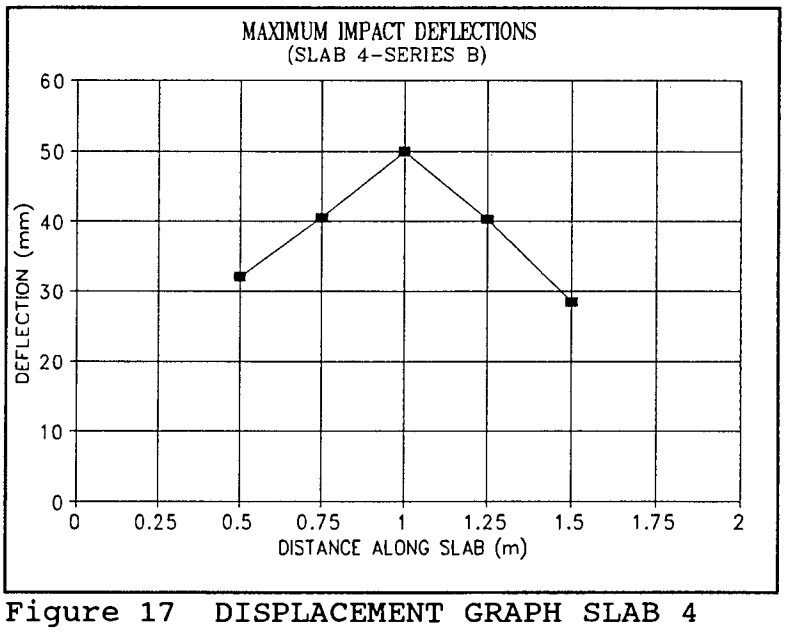

Figure 17 DISPLACEMENT GRAPH SLAB 4

The deflections for Slab 4 were very nearly linear (See Figure 7.17) (ie they fell on a straight line) from Rod 1 to 2 to 3. Similarly they were very nearly linear from Rod 3 to 4 to 5. This meant that a linear (or very nearly linear) relationship existed between the deflections and their distance along the slab. This confirms that a proper plastic hinge had formed along the yield lines. This relationship was used to determine the deflections at other points along the slab.

The calculated maximum central deflection at rod 3 (x_{mc}) was used together with the other two defections (Rod 1 and 2 or Rod 4 and 5) to determine the best-fit line through the points. The equation for this best-fit line was then used to calculate the deflections at other points along the slab. The linear relationship had to be used for some slabs, due to the fact that sometimes there were no measurements for a particular rod, for

example, Rod 4 of Slab 3 was also dislodged during impact, due to the punching through of the 'hammer'. This left only the measurement of Rod 5 for that half of the slab (the lower half of the slab). The two readings from the top half of the slab were then used to determine the central deflection. This calculated central defection was then used together with the deflection at Rod 5 to obtain the deflections at other points on the lower half of the slab. The average of the two calculated values for Rod 3 (from best-fit) lines was taken as the maximum deflection at Rod 3.

The results of this analysis are given in the following five tables, one for each slab. The measured and calculated values are given and the percentage difference (where applicable) is also given.

TABLE 7.42 MAXIMUM DEFLECTION ANALYSIS & ESTIMATION FOR SLAB 1 (SERIES A)

Dist along Slab(m)	Measured Displ (mm)	Calculated Disp (mm)	% Diff
0	-	18.7	-
0.5	35.5	34.7	2.3
0.75	41.0	42.6	3.8
1.0	*	51.5	-
1.25	44.0	42.1	4.3
1.50	31.0	31.9	2.8
2.0	-	11.5	-

* Rod 3 was dislodged during impact

TABLE 7.43 MAXIMUM DEFLECTION ANALYSIS & ESTIMATION FOR SLAB 2 (SERIES A)

Dist along Slab(m)	Measured Displ (mm)	Calculated Disp (mm)	% Diff
0	-	11.1	-
0.5	*	34.7	-
0.75	46.5	46.5	0.0
1.0	**	59.4	-
1.25	50.0	45.8	8.4
1.50	29.0	31.9	6.8
2.0	-	1.82	-

* Pencil tore graph paper, hence no deflection measured

** Rod 3 was dislodged during impact

TABLE 7.44 MAXIMUM DEFLECTION ANALYSIS & ESTIMATION FOR SLAB 3 (SERIES A)

Dist along Slab(m)	Measured Displ (mm)	Calculated Disp (mm)	% Diff
0	-	5.21	-
0.5	13.0	13.1	0.8
0.75	17.3	17.1	1.2
1.0	*	21.0	-
1.25	*	16.7	-
1.50	12.5	12.5	0
2.0	-	4.10	-

* Rod 3 and Rod 4 were dislodged during impact

TABLE 7.45 MAXIMUM DEFLECTION ANALYSIS & ESTIMATION FOR SLAB 4 (SERIES B)

Dist along Slab(m)	Measured Displ (mm)	Calculated Disp (mm)	% Diff
0	-	15.2	-
0.5	32.0	32.0	0
0.75	40.5	40.4	0.2
1.0	50.0	49.1	1.8
1.25	40.3	39.2	2.7
1.50	28.5	29.0	1.7
2.0	-	8.75	-

TABLE 7.46 MAXIMUM DEFLECTION ANALYSIS & ESTIMATION FOR SLAB 5 (SERIES B)

Dist along Slab(m)	Measured Displ (mm)	Calculated Disp (mm)	% Diff
0	-	8.7	-
0.5	21.8	22.2	1.8
0.75	29.8	29.0	2.7
1.0	*	35.7	-
1.25	28.5	27.9	2.1
1.50	20.0	20.3	1.5
2.0	-	5.0	-

* Rod 3 was dislodged during impact

The five tables (7.42 - 7.46), show that the linear distribution of the deflection was reasonable, as the percentage difference

between measured and calculated values was generally below five percent, with only two values exceeding five percent (8.4% and 6.8%). This meant that extrapolation to determine deflections at other point along the slab was permissable. Extrapolation was used to determine the cental deflection, as well as the deflections at the end of the slab. If the support structure was perfectly rigid, these deflections would have been zero. This was not the case , as can be seen for the above-mentioned five tables.

The deflections at the top of the slab were always larger than those at the bottom. This was to be expected as the support structure was less rigid at the top, as the bottom was bolted to the floor.

The bottom deflection of slab 1 was quite a bit larger than for the other slabs. This was due to the method of bolting the support structure to the laboratory floor. In this case it was bolted to the floor by means of long bolts that actually bent during impact. The method of bolting the bottom of the support structure to the laboratory floor was changed and extra bolts were used. The improvement can be seen in the reduced deflections for the other slabs. The deflection of the support structure, as given here was taken into account with further analysis. (ie the relevant deflection was subtracted from the measured deflections of the displacement-time curves).

The deflection-time curves were analysed in the same manner as for the reinforced concrete beams, with the addition of a few factors: For all slabs, except Slab 4, the displacement-time curve of Rod 4 or Rod 2 was analysed and deflections were multiplied by the correction factor (CF) mentioned previously. This was to achieve the best approximation of the deflections occurring at the centre of the slab.

The deflection of the support structure at the relevant position, was subtracted from the measured deflection on the deflection-time graph. This was done with the spread sheet before the

displacements were multiplied by the correction factor (CF), as described above. The analysis of the deflection-time graphs then proceeded as before.

Print outs of spreadsheets and graphs can be seen in Appendix E.

The natural period of vibration of the slab and the slab stiffness had to be calculated before any dynamic analysis could be performed. Calculation of the natural period of vibration of the slab (T_n) is based on notes of Reference 2.

The natural period of vibration of the slab (T_n) is given by the following equation:

$$T_n = 2\pi\sqrt{\frac{m_e}{k}} \qquad (7.67)$$

where m_e = equivalent mass of slab
k = elastic stiffness of slab

The elastic stiffness of the slab (k) was obtained from the static load-deflection test and calculated from the following equation:

$$k = \frac{P}{\delta} \qquad (7.68)$$

The equivalent mass of the slab (m_e) is given by Reference 1, by the following equation:

$$m_e = K_m * m_t \qquad (7.69)$$

where K_m = mass factor = 0.13 for simply supported square slab
m_t = total mass of slab

The masses of the rods (although small) were lumped at the centre, as they were all attached to the slab a distance of 0.5m or less from the centre. The equivalent mass of the slab was therefore given by the following equation:

$$m_e = 0.31m_t + \sum M_r \qquad (7.70)$$

where $\sum M_r$ = sum of the masses of all rods and attachments

However, during impact, the equivalent mass of the slab must include the equivalent mass of the pendulum, at POI. Therefore the equivalent mass of the slab 'system' (m_{es}) during impact is given by the following equation:

$$\begin{aligned} m_{es} &= m_e + f_p m_{ep} \\ &= 0.31m_t + \sum m_r + f_p m_{ep} \end{aligned} \qquad (7.71)$$

where m_e = equivalent mass of slab as given previously
f_p = proportional factor as defined by equation (7.7)
m_{ep} = effective mass of pendulum

Therefore the natural period of vibration of the slab (T_n) during impact is given by the following equation:

$$T_n = 2\Pi\sqrt{\frac{m_{es}}{k_{eff}}} \qquad (7.72)$$

where k_{eff} = effective stiffness of the slab (as calculated from equivalent bilinear load-deflection graph Section 7.3.1.1)

The results of these calculations are given in Table 7.47.

TABLE 7.47 PERIOD AND STIFFNESS OF REINFORCED CONCRETE SLABS

Equivalent mass M_e (kg)	159.2
Elastic Stiffness of Slab 'k' (kN/m)	8888.9
Natural Period 'T_n' of slab only (sec)	0.0266
Equivalent mass of slab system 'm_{es}' (kg)	159.2 + $f_p m_{ep}$
'Effective' stiffness of slab 'k_e' (kN/m)	2570.8

Note: The equivalent mass of the slab system (m_{es}) varies with the effective mass of the pendulum, as does the natural period of vibration (T_n) and will be different for each weight category. These are calculated as required and are therefore not given individually in

the table.

The energy of the pendulum at the various positions, as described previously, was calculated for each slab using the spread sheet. The Elasto-Plastic Energy method was then used, but with a 'modified' R_{me}-value. The yield line failure of mode 1 was used (ie yield lines from corner to corner, crossing at the centre) to calculate R_{me}. It was shown from the static test, that the failure load was 3.2 times the calculated value (due to plane stress action). This factor of 3.2 was used to increase the calculated R_{me}-value to give a more realistic maximum value. If a slab failed in punching shear, the factor applicable to the shear failure load (1.8) was used instead of 3.2. However, no dynamic factors were used for shear as it was found that the dynamic shear capacity was reduced under higher strain rates (see Chapter 5). Dynamic factors where applicable, were used in the calculations.

The following equations from Reference 3 give the dynamic factors for concrete and steel.

$$\text{for concrete: } K_{dyn(conc)} = 1 + 0.3\left(\frac{30}{f_{cu}}\right) < 1.3 \qquad (7.73)$$

where $K_{dyn(conc)}$ = dynamic factor for concrete

f_{cu} = compressive cube strength of concrete in MPa

$$\therefore f_{cu(dynamic)} = K_{dyn(conc)} * f_{cu(static)} \qquad (7.74)$$

For steel, diameter of bar less than 20mm

$$K_{dyn(steel)} = 1.2 \qquad (7.75)$$

$$\therefore f_{y(dynamic)} = K_{dyn(steel)} * f_{y(static)} \qquad (7.76)$$

The results of this analysis is given in Table 7.48.

TABLE 7.48 'MODIFIED' R_{me} DETERMINATION FOR REINFORCED CONCRETE SLABS

Series	A	B
Percentage Reinforcement	0.2	0.50
average $f_{cu(static)}$ (MPa)	33.5	36.9
$f_{y(static)}$ (MPa)	538.7	517.4
$E_{(dyn)}$ concrete (GPa)	39.0	39.0
E steel (GPa)	208.9	208.3
$K_{dyn(conc)}$	1.27	1.24
$K_{dyn(steel)}$	1.2	1.2
$M_{pl(dyn)}$ kNm/m	1.936	4.184
Mode 1 R_{me} (kN)	49.6	107.1
Mode 2 'fan' R_{me} (kN)	51.1	110.4
Shear Failure R_{me} (kN)	105.8	115.4

where R_{me} = equivalent maximum elastic (or plastic) spring resistance of the slab (See Figure 7.7)

The Elasto-Plastic Energy Method was used for all 5 slabs. Print outs can be seen in Appendix E. The results are summarized in Table 7.49 for Series A.

TABLE 7.49 ELASTO-PLASTIC ENERGY METHOD RESULTS FOR R.C. SLABS (SERIES A)

Slab No.	1	2	3
Weight Condition	2x400N	3x400N	3x400N
Dist Release POI	4.40	4.16	4.27
Percentage Reinforcement	0.2	0.2	0.2
x_m (mm)	49.7	56.5	58.9
t_m (sec)	0.0245	0.265	0.0317

The results of the Elasto-Plastic Energy Method (EPEM) are compared with the test values in Table 7.50.

TABLE 7.50 COMPARISON OF EPEM RESULTS & TEST VALUES FOR R.C. SLABS (SERIES A)

Slab No.	1		2		3	
Source	Test	EPEM	Test	EPEM	Test	EPEM
x_m (mm)	42.3	49.7	57.8	56.5	16.2	58.9
t_m (sec)	0.0321	0.0245	0.0359	0.0265	0.0163	0.0317

As can be seen from Table 7.50 the calculated values compare

well with the measured values, for slabs 1 and 2. For slab 3 however, the measured value is only 28% of the calculated value. This is due to the fact that slab 3 failed in punching, which meant there was less flexural cracking and defections. The calculated values of t_m for Slabs 1 and 2 have approximately 25% difference to the measured t_m values.

A summary of the Elasto-Plastic Energy method results for Slabs 4 and 5 (Series B) is given in Table 7.51.

TABLE 7.51 ELASTO-PLASTIC ENERGY METHOD RESULTS FOR R.C. SLABS (SERIES B)

Slab No.	4	5
Weight Condition	5x400N	5x400N
Dist Release POI	3.00	4.00
Percentage Reinforcement	0.50	0.50
x_m (mm)	37.4	50.1
t_m (sec)	0.0300	0.0415

The results of the Elasto-Plastic Energy Method (EPEM) are compared with the test values in Table 7.52.

TABLE 7.52 COMPARISON OF EPEM RESULTS & TEST VALUES FOR R.C. SLABS (SERIES B)

Slab No	4		5	
Source	Test	EPEM	Test	EPEM
x_m (mm)	38.1	37.4	29.0	50.1
t_m (sec)	0.0284	0.0300	0.0199	0.0415

From Table 7.52 it can be seen that the values for Slab 4 compare very well. There is 1.7% difference in the x_m values and 5.3% difference in the t_m values. The values for slab 5, however, differ by 42% for the x_m values and 52% for the t_m values. The reason being that Slab 5 also failed in 'punching'. This meant that there were smaller flexural cracks and hence smaller flexural deflections. Nevertheless, the Elasto-Plastic Method gave realistic values when the slabs failed in flexure.

The Elasto-Plastic Design Method as given in the static analysis was used to analyse the slabs. Dynamic factors were used where

appropriate. This was performed for Series A (0.2% reinforcement) and Series B (0.5% reinforcement). Print outs of the spread sheets can be seen in Appendix F. The results are summarized in Table 7.53.

TABLE 7.53 SUMMARY OF ELASTO-PLASTIC DESIGN METHOD (EPDM) ANALYSIS FOR REINFORCED CONCRETE SLABS

Series	A	B
Percentage Reinforcement	0.2	0.5
Eff Elastic Displ $\delta_{y(eff)}$ (mm)	20.9	36.7
Maximum displ δ_p (mm)	31.7	11.6
Maximum disp δ_n (mm)	52.6	48.3
Ductility Index	2.51	1.32
Toughness Index	4.03	1.63

From Table 7.53 it can be seen that Series B has the larger $\delta_{y(eff)}$, but Series A had the larger δ_p deflection. Series A had the largest deflection and higher ductility and toughness indices, which tend to indicate that it (Series A) had a higher energy absorbing capacity, as it was more ductile.

The results of the Elasto-Plastic Design Method(EPDM) are compared to the test values of one slab from each series in the following table. For Series A, Slab 2 was chosen as it took the largest impact without failing in punching shear. The same applied to slab 4 for Series B. The comparisons are given in Table 7.54.

TABLE 7.54 COMPARISON OF (EPDM) ANALYSIS & TEST RESULTS FOR SERIES A & B R.C. SLABS

Source	Test	EPDM
Series A δ_m (mm)	57.8	52.6
Series B δ_m (mm)	38.1	48.3

From Table 7.54, it can be seen that in both cases, the test values for the maximum deflection are larger that the EPDM values. This would tend to suggest that the test specimens had 'failed', as they had exceeded the maximum deflections as calculated with the Elasto-Plastic Design Method (EPDM).

If the residual strength was a reliable indicator of whether a specimen had failed or not, Slab 4 could have been classified as 'failed'. The residual strength for Slab 4 was 76.5kN, which was more than 10 percent below the static failure load. (The criteria set was that if the residual strength was five percent or more below the static strength, then the specimen had failed.) Unfortunately, as was shown with the reinforced concrete beams, this criteria was not good enough on its own to define 'failure'. It had to be used in conjunction with other factors such as crack pattern or permanent deformation.

Before the Rigid Plastic Method of analysis could be applied, the impulsive force (F_o) and duration of the impulse (T) had to be determined. The Force Balance Method (FBM), as described under reinforced concrete beams, was used. The results for Series A are listed in Table 7.55.

TABLE 7.55 RESULTS OF FORCE BALANCE METHOD FOR DETERMINING IMPULSE LOAD FOR SLABS (SERIES A)

Slab No.	1	2	3
Weight Condition	2X400N	3x400N	3x400N
Percentage Reinforcement	0.2	0.2	0.2
Dist Release POI (m)	4.40	4.16	4.27
v_{POI} (m/s)	5.478	5.149	5.278
$v_{\Delta t}$ (m/s)	2.617	2.782	2.852
Δt (sec)	0.00367	0.00374	0.00238
M_{esl} (kg)	159.2	159.2	159.2
$M_{ep(POi)}$ (kg)	145.6	187.1	187.1
a_{sl} (m/s^2)	712.9	743.9	1198.3
a_{pend} (m/s^2)	779.8	632.9	1019.5
F_{OB} (kN)	113.506	118.433	190.777
F_O^P (kN)	113.506	118.433	190.777
KE^B (Joules)	545.000	616.191	647.491
Imp Duration 'T' (sec)	0.00734	0.00748	0.00476
Impulse H_{me} (Ns)	416.567	442.9395	454.050

The results of the Force Balance Method for Series B are listed in Table 7.56.

TABLE 7.56 RESULTS OF FORCE BALANCE METHOD FOR DETERMINING IMPULSE LOAD FOR SLABS (SERIES B)

Slab No.	4	5
Weight Condition	5x400N	5x400N
Percentage Reinforcement	0.50	0.50
Dist Release POI (m)	3.00	4.00
v_{POI} (m/s)	3.721	4.939
$v_{\Delta t}$ (m/s)	2.339	3.104
Δt (sec)	0.01084	0.00382
M_{esl} (kg)	159.2	159.2
$M_{ep(POi)}$ (kg)	269.3	269.3
a_{sl} (m/s^2)	216.5	812.63
a_{pend} (m/s^2)	128.0	480.45
F_{OB} (kN)	34.4743	129.360
F_O^P (kN)	34.4743	129.360
KE^B (Joules)	435.358	766.926
Imp Duration 'T' (sec)	0.02168	0.00476
Impulse H_{me} (Ns)	372.3155	494.155

The impulse (H_{me}) was calculated from the KE of the slab due to impact of the pendulum. The impulse was then used to calculate the duration of the impulse (T), using F_O and a triangular shape impulse.

The information in the two tables was used in a Rigid-Plastic analysis. The details of the Rigid Plastic analysis are given in Appendix I. Print outs of the analysis spread sheets can be seen in Appendix E. A summary of the results for slabs of Series A (0.2% reinforcement) is given in Table 7.57.

TABLE 7.57 SUMMARY OF RESULTS OF RIGID PLASTIC ANALYSIS FOR R.C. SLABS (SERIES A)

Slab No.	1	2	3
Weight Condition	2x400N	3x400N	3x400N
Dist Release POI (m)	4.40	4.16	4.27
F_O (kN)	113.506	118.433	190.777
Imp Duration 'T' (sec)	0.00734	0.00748	0.000476
x_m (mm)	40.4	45.8	51.1
t_m (sec)	0.0269	0.0286	0.0293

From Table 7.57 it can be seen that the maximum deflection (x_m) increase with higher F_O-values, while the time to maximum

deflection (t_m) stayed relatively constant. The results of the Rigid Plastic Analysis(RPA) for Series A are compared with test values in Table 7.58.

TABLE 7.58 COMPARISON OF RPA RESULTS & TEST VALUES FOR R.C. SLABS (SERIES A)

Slab No.	1		2		3	
Source	Test	RPA	Test	RPA	Test	RPA
x_m (mm)	42.3	40.4	57.8	45.8	16.2	51.1
t_m (sec)	0.0321	0.269	0.0359	0.0286	0.0163	0.0293

From Table 7.58 it can be seen that the RPA values and test values compare well, except for Slab 3. As mentioned earlier, Slab 3 failed in 'punching'. If Slab 3 had not failed in 'punching', it may have had a deflection close to the RPA value due to the large impact. The RPA t_m values were approximately 80% of the test t_m values.

The results of the Rigid Plastic Analysis (RPA) for Series B slabs are given in Table 7.59.

TABLE 7.59 SUMMARY OF RESULTS OF RIGID PLASTIC ANALYSIS FOR R.C. SLABS (SERIES B)

Slab No.	4	5
Weight Condition	5x400N	5x400N
Dist Release POI (m)	3.00	4.00
F_O (kN)	34.474	129.360
Imp Duration 'T' (sec)	0.0216	0.00764
x_m (mm)	-11.2	43.9
t_m (sec)	0.0111	0.0148

From Table 7.52 it can be seen that the maximum deflection (x_m) for Slab 4 is a negative value. This means that the impulsive force (F_O) was too small to cause plastic failure. This does not seem logical, as the steel had yielded, as shown by the permanent deformation of the slab given earlier. However, the time t_m is less than the duration of the impulse (T) which meant there was no second phase and time (T_2) was equal to zero. This meant that displacement δ_2 was equal to zero as well.

The RPA x_m result for Slab 5 was larger than the test x_m (43.9 as opposed to 29.0mm). However, Slab 5 failed in punching and therefore never reached its maximum flexural displacement. Therefore the RPA value seem reasonable. The RPA t_m values were 75% of the test t_m.

7.3.2.2 Discussion of Results and Their Effects on the Simplified Design Method

The Elasto-Plastic Energy Method of analysis worked for all slabs. The Elasto Plastic Energy Method of analysis was therefore acceptable for analysis of the slabs, as it showed that all the energy did not go into the slab. This was confirmed by the calculated deflections, which showed that the support structure had moved. This would have absorbed the energy that was not converted into SE of the slab.

The Design Elasto-Plastic Method worked very well and gave excellent results. This method will be developed further in the next chapter.

The Rigid Plastic Method of analysis worked very well for the slabs except Slabs 3 and 5 which failed in punching and Slab 4. The reason for Slab 4 not complying are not clear, but it is felt that the agreement of the other slabs overrides this problem. The Rigid Plastic Method was therefore found to be an acceptable form of analysis for reinforced concrete slabs.

7.4 References

1 NORRIS, C H et al, Structural Design for Dynamic Loads, McGraw-Hill, 1959

2 The Analysis and Design of Blast-resistant Structures, Course Notes (CIV 561W), UNIVERSITY OF CAPE TOWN, 1991

3 Design of Concrete Structures for Impact Loading, Course Notes (CIV562F), University of Cape Town 1992

4 Blume, J A et al, Design of Multistorey Reinforced Concrete Buildings for Earthquake Motion

5 British Code of Practice, BS8110 Part 1 1985, Section 3

Photographic Plate 7.1 'JUST' FAILED IMPACTED PLAIN CONCRETE BEAM

Photographic Plate 7.2 STATIC SLAB TEST ARRANGEMENT

Photographic Plate 7.3 FAILED SLAB SHOWING YIELD LINES AND PUNCHING FAILURE

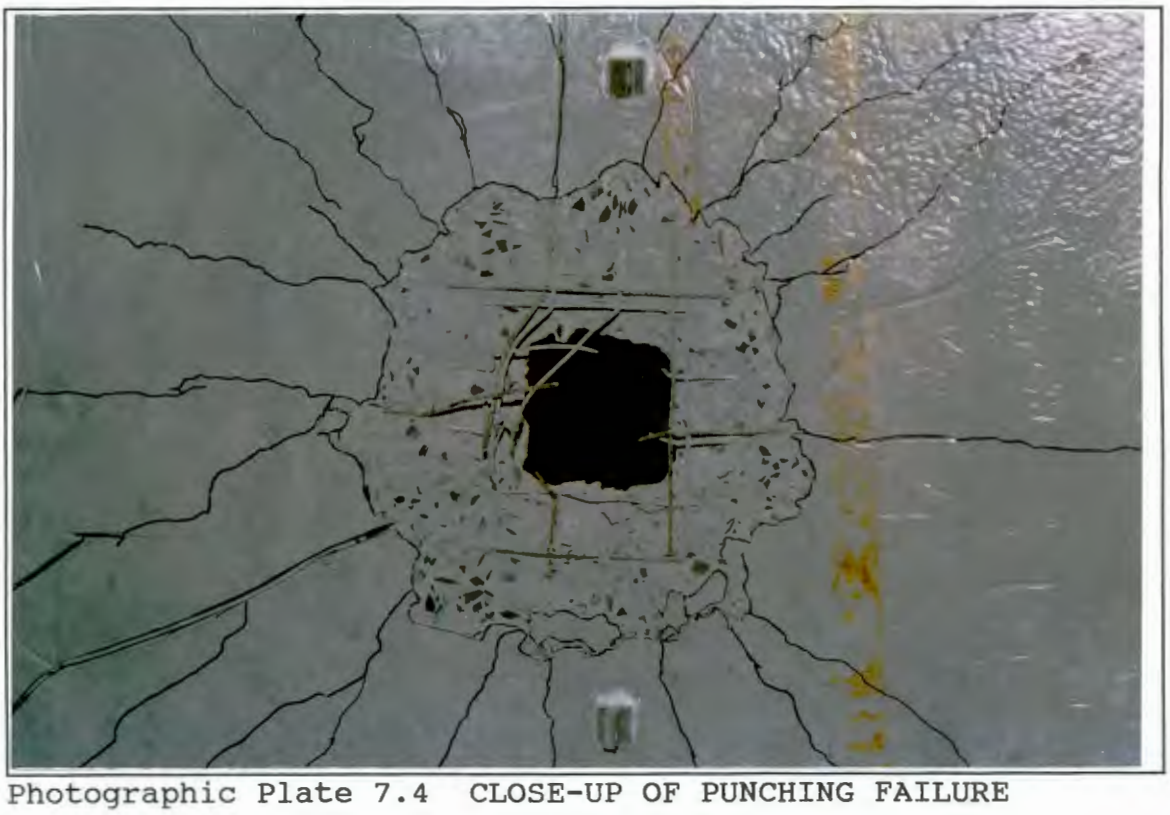

Photographic Plate 7.4 CLOSE-UP OF PUNCHING FAILURE

C H A P T E R 8

ELASTO-PLASTIC DESIGN METHOD

8.1 INTRODUCTION

An elasto-plastic design method is given to design slabs for impact loading. Elasto-plastic conditions are assumed. The capacity of the slab is calculated and maximum allowable rotations and deflections are determined. The response of the slab due to the design impulse is determined and deflections are calculated. These are then checked with the allowable deflections. If the allowable values are exceeded, the capacity of the slab is increased and the process is repeated.

The general design procedure is given first and details of each step are discussed separately.

8.2 GENERAL DESIGN PROCEDURE

1. Assume Elasto-Plastic conditions
2. Assume a failure mechanism (ie yield line pattern).
3. Evaluate the plastic moment capacities (M_{pl}) at the yield lines from reinforcement required for static load combinations or for the assumed reinforcement. Dynamic properties and yield-line analysis are used.
4. Determine the maximum resistance in the elastic range.
5. Determine the equivalent bilinear moment-curvature diagram and maximum allowable deflection for the assumed reinforcement.
6. Calculate the amount of energy imparted to the slab from the design impulse.
7. Check actual displacements with allowable values determined in Step 5. If actual values exceed allowable values, change the design by increasing plastic moment capacity of the plastic hinges or increase the hinge ductility. Restart from Step 2.

8.2.1 Steps 2 and 3

Steps 2 and 3 use standard design procedures and will not be dealt with here.

8.2.2 Step 4

The maximum resistance in the elastic range is determined from the results of the yield-line analysis. It is the maximum force that causes the full yield line pattern to develop.

8.2.3 Step 5

The equivalent bilinear moment-curvature diagram is derived as follows:

The curvature at cracking (ϕ_{cr}) of the concrete is calculated from the following equation:

$$\phi_{cr} = \frac{M_{cr}}{E_d I} \qquad (8.1)$$

where M_{cr} = cracking moment of concrete / m (obtained from Modulus of Rupture values).

E_d = Dynamic Elastic Modulus of concrete

I = second moment of area of slab / m

At the yield point of the slab reinforcement a parabolic stress-block should be used, as the slab has not reached ultimate conditions (where a rectangular stress-block would be used).

The depth of the compression block at yield (x_y) is obtained from the following formula:

$$x_y = \frac{0.87 f_{y(dyn)} A_s}{(\frac{2}{3})(0.4 f_{cu(dyn)})b} \qquad (8.2)$$

where A_s = area of tension reinforcement (m^2/m)

$f_{y(dyn)}$ = dynamic ultimate yield stress of reinforcing steel (MPa)

$f_{cu(dyn)}$ = dynamic compressive strength of concrete (MPa)

The strain at yield (ϵ_y) of the slab reinforcement is obtained from standard stress strain curves for the particular reinforcing steel used. (eg. high yield reinforcement $\epsilon_y = 0.00395$). The curvature at the yield point of the reinforcement (ϕ_y) is obtained from the following equation:

$$\phi_y = \frac{\varepsilon_y}{(d - x_y)} \qquad (8.3)$$

where d = effective depth of the slab

The strain of the concrete at yield (ϵ_{cy}) can be checked at this point by the following equation: ($\epsilon_{cy} < 0.0035$)

$$\varepsilon_{cy} = \phi_y * x_y \qquad (8.4)$$

The calculated moments and curvatures are then plotted on a moment-curvature (M - ϕ) diagram. (See Figure 8.1)

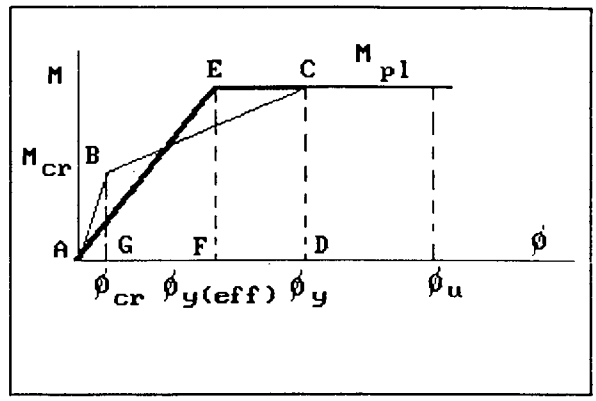

Figure 8.1 MOMENT CURVATURE DIAGRAM

By referring to Figure 8.1, the effective curvature at yield ($\phi_{y(eff)}$) is calculated as follows: By equating the two areas ABCD and AECD, $\phi_{(y(eff))}$ is calculated. Area ABCD is calculated as follows:

$$\text{Area ABCD} = \frac{1}{2}(M_{cr} * \phi_{cr}) + \left(\frac{M_{pl} + M_{cr}}{2}\right) * (\phi_y - \phi_{cr}) \qquad (8.5)$$

Area AECD is calculated as follows:

$$\text{Area AECD} = \frac{1}{2}(M_{pl} * \phi_{y(eff)}) + (\phi_y - \phi_{y(eff)})M_{pl} \qquad (8.6)$$

where M_{pl} = ultimate bending moment capacity of slab/m

By equating the two areas $\phi_{y(eff)}$ is obtained and is given by the following equation:

$$\phi_{y(eff)} = \phi_{cr} + \phi_y \left(1 - \frac{M_{cr}}{M_{pl}}\right) \qquad (8.7)$$

$\phi_{y(eff)}$ is also given by the following equation:

$$\phi_{y(eff)} = \frac{M_{pl}}{EI_{(eff)}} \qquad (8.8)$$

where $EI_{(eff)}$ = slope of line AE (See Figure 8.1)

By rearranging Equation (8.8), $EI_{(eff)}$ is given by the following equation:

$$EI_{(eff)} = \frac{M_{pl}}{\phi_{y(eff)}} \qquad (8.9)$$

The depth of the compression block at ultimate (x_u) is calculated from the following equation, assuming a rectangular stress-block.

$$x_u = \frac{0.87 f_{y(dyn)} A_s}{(0.4 f_{cu} b)} \qquad (8.10)$$

where $f_{y(dyn)}$ = dynamic yield stress of reinforcement

The curvature at ultimate (ϕ_u) is obtained from the following equation:

$$\phi_u = \frac{0.0035}{x_u} \qquad (8.11)$$

where 0.0035 = strain of concrete at ultimate

x_u = depth of compression block (m) at ultimate

The value for ϕ_u is then plotted on the moment-curvature diagram to complete the diagram.

The plastic curvature (ϕ_p) is obtained as follows:

$$\phi_p = \phi_u - \phi_{y(eff)} \qquad (8.12)$$

The curvatures are then used to calculate the various displacements for the equivalent bilinear load-displacement diagram.

Referring to Figure 8.1, the slope of line AE ($EI_{(eff)}$) is used to determine the effective stiffness of the slab. The effective stiffness ($k_{(eff)}$) of a simply supported slab is given by the

following equation:*

$$k_{(eff)} = 20 * EI_{(eff)} \qquad (8.13)$$

where $EI_{(eff)}$ = the effective slope of the moment-curvature diagram (See Figure 8.1 line AE)

* Note: The factor of '20' in Equation 8.13 was obtained from test data for a simply supported slab. It was found to give an accurate value for the effective displacement, when compared to that determined from converting a real trilinear load-displacement curve to an effective bilinear load-displacement curve.)

The effective displacement at yield ($\delta_{y(eff)}$) is obtained from the following equation:

$$\delta_{y(eff)} = \frac{F_u}{k_{(eff)}} \qquad (8.14)$$

where F_u = ultimate force to cause failure of the slab (obtained from yield-line analysis)

The rotation of the slab in the plastic phase (θ_p) is obtained from the following equation:

$$\theta_p = (\text{factor} * d)\phi_p \qquad (8.15)$$

where factor = plastic hinge factor 0.5 to 1.5 (average 1.0)
d = effective depth of slab

The displacement during the plastic phase (δ_p) is obtained as follows:

$$\delta_p = \frac{\theta_p}{2} * \frac{\sqrt{2L^2}}{2} \qquad (8.16)$$

where L = side length of slab (square root of $2L^2$ is the span for a yield line from corner to corner of a square slab)

The maximum displacement (δ_{max}) is obtained as follows:

$$\delta_{max} = \delta_{y(eff)} + \delta_p \qquad (8.17)$$

8.2.4 Step 6

The assumed or design impulse is used to calculate the amount of energy imparted to the slab. The impulse (H_{me}) is the area under the load-time curve. If the impulse was triangular, the maximum force (F_O) and the duration of the impulse was T, then the impulse is given by the following equation:

$$H_{me} = \frac{1}{2} F_O T \qquad (8.18)$$

where H_{me} = impulse (area under curve) (kNs)
F_O = maximum peak force (kN)
T = duration of impulse (sec)

The energy imparted to the slab (W_{pe}) is given by the following equation:

$$W_{pe} = \frac{H_{me}^2}{2m_e} \qquad (8.19)$$

where m_e = equivalent mass of slab (0.31 times total mass of slab for a simply supported square slab).

8.2.5 Step 7

The deflections of the slab are calculated as follows:

The maximum elastic deflection ($\delta_{el(max)}$) is calculated as follows:

$$\delta_{el(max)} = \frac{F_u}{k_{eff}} \qquad (8.20)$$

where F_u = ultimate force to cause failure of the slab (obtained from yield line analysis)

The maximum deflection (δ_m) is calculated as follows using the energy of the impulse (W_{pe}). It is assumed that all the energy of the impulse is converted to strain energy (SE) of the slab at

the point of maximum deflection (δ_m)

$$\delta_m = \frac{SE}{F_u} + \frac{\delta_{el(max)}}{2} \qquad (8.21)$$

8.2.6 Step 8

The maximum deflection of the slab is checked with the maximum allowable deflection, (δ_{max}).

If δ_m is not less than δ_{max} then the process must be repeated from Step 2. By increasing the plastic moment capacity of the plastic hinges, or increasing the hinge ductility the requirements should be met.

Once the above criteria have been met, the design and checks for the slab proceed as with the static case.

C H A P T E R 9

CONCLUSIONS AND RECOMMENDATIONS

9.1 CONCLUSIONS

Based on the findings of this investigation, the following conclusions may be drawn:

9.1.1 Test and Measuring Equipment

9.1.1.1 Test Equipment

The test equipment worked well as the magnitude of the impact could be varied with ease by placing the release mechanism at any position along the curved channel. The variation of the duration of the impulse by the addition of weights (masses) to the pendulum was successful as shown by the results of the load-displacement graphs. The support structures, however, did not perform as well, as they were not rigid enough. This was shown by the large amounts of energy that was not transferred to the specimens but was absorbed by the support structure.

The compound pendulum posed problems with the determination of the effective length of the pendulum. This was overcome by appropriate analysis techniques.

9.1.1.2 Measuring Equipment

The measured deflection-time graphs proved to be accurate, as proved by the elastic tests on the steel beams. The calibration of the falling board proved to be a satisfactory method of correcting for the increased velocity of the falling board.

The backswing arc measuring device proved to be an excellent method of determining the amount of energy that was converted from the strain energy of the specimen back into the kinetic energy of the pendulum.

9.1.2 Steel Beams

The steel beams proved to be a good method of checking the operation of the test equipment and the accuracy of the measured deflections by means of the elastic impact tests. The plastic impact tests showed that there was less loss of energy to the

support structure with a flexible specimen than for a more rigid specimen such as a concrete beam.

9.1.3 Reinforced Concrete Beams

The concrete beams proved to be a good method of determining the behaviour of concrete under impact loading of a simple structural system. The fact that residual strength was insufficient as a failure criteria on its own was significant. Other factors such as crack width, permanent deformation and backswing had to be taken into account as well. The fact that beams with higher percentages of reinforcement absorbed a lower percentage of the impact energy meant that from an impact point of view, they were less efficient. (ie higher strength does not necessary mean a higher impact absorbance capacity. It is the total area under the load displacement curve that is important, not the peak value.) If the tensile strength of the concrete is low, the deflection rods will be dislodged during impact.

9.1.4 Reinforced Concrete Slabs

The slabs confirmed the earlier results of the dynamic shear tests. The results showed that there was a reduction in shear strength with increased strain-rate. This was observed with the slabs when they failed in punching with an impact not much larger than a previous slab which failed in flexure. This meant that the shear failure was more vulnerable and became dominant with the increased impact load. The slab absorbed most of the energy in shear which meant that only a small amount of energy was available for flexure. This was shown by reduced deflection and reduced flexural cracking. The slab with the lower percentage reinforcement proved to be a more efficient slab from an impact point of view. This was shown by its larger ductility and toughness indices which are measures of the slab energy absorbtion capacity.

9.1.5 Methods of Analysis and design

The Elasto-Plastic Energy method proved to be accurate for the steel beams. It did not prove to be as accurate for the reinforced beams and slabs. This was due to the amount of energy

lost to the support structure, as the method assumes that all the energy at impact is converted to strain energy of the specimen. This was proved not to be the case. The reason the method worked relatively well for the steel beams was because only a small amount of energy was lost to the support structure, as the steel beam was more flexible.

The Elasto-Plastic Design Method was used for the analysis of the slabs and proved to be accurate.

The Rigid Plastic Analysis method was shown to be inaccurate for the steel beams, yet was satisfactory for the reinforced concrete beams and slabs. This was true provided the impulse force and impulse duration were correctly determined.

9.1.6 Damage Criteria

The damage criteria developed was a visual and mostly measurable way of determining whether a specimen had failed.

The permanent deformation of a steel beam that was tested to failure under static conditions was taken as the damage criteria representing failure. This proved accurate as the impact beams closest to the failure criteria had higher backswing arc / start arc ratios which meant that the maximum energy left in the beam was converted to kinetic energy of the pendulum, producing the larger relative backswing.

The damage criteria for the reinforced concrete beams and slabs was the residual strength, permanent deformation, crack widths and backswing. It was shown that residual strength on its own was insufficient to classify a specimen as failed, but had to be used in conjunction with at least one of the other criteria. For the slabs the crack pattern proved to be more informative than the crack width.

9.2 RECOMMENDATIONS

Based on the findings and conclusions the following recommendations may be made:

1) That the compound pendulum be replaced with a simple pendulum consisting of a cable and steel ball.

2) The support structure be made more rigid.

3) A method be devised to measure the deflection of the support structure due to impact.

4) A better solution be found to prevent detachment of deflection rods during impact.

5) At least three specimens be tested statically and the mean taken as the failure load for failure criteria, to reduce the scatter of results.

6) An "electronic" assessment of the impulse would be a great improvement and would add to the credibility of results. This is due to the short impact duration relative to the capacity of present recording equipment.

7) The findings and conclusions contained in this thesis were based on a limited number of tests and it is recommended that more tests be performed to confirm results.

A P P E N D I X A

COURSES TAKEN AS PART FULFILMENT FOR MSc DEGREE

Course No.	Description	Credits	%
CIV561Z	Loading Analysis & Design of Blast Resistant Structures	4	77
CIV528F	Road Pavements	3	73
CIV591S	Rehabilitation of Road Pavements	3	80
CIV562F	Design of Concrete Structures for Impact Loading	3	74
CIV525S	Contract Law	3	83
SEM522F	Engineering Economy & Optimisation	5	*
		21	
Thesis		20	
	Total	41	

Total Credits Required = 40

* Final Result not available at time of printing

A P P E N D I X B

LIGHT TRIP CALIBRATION GRAPHS

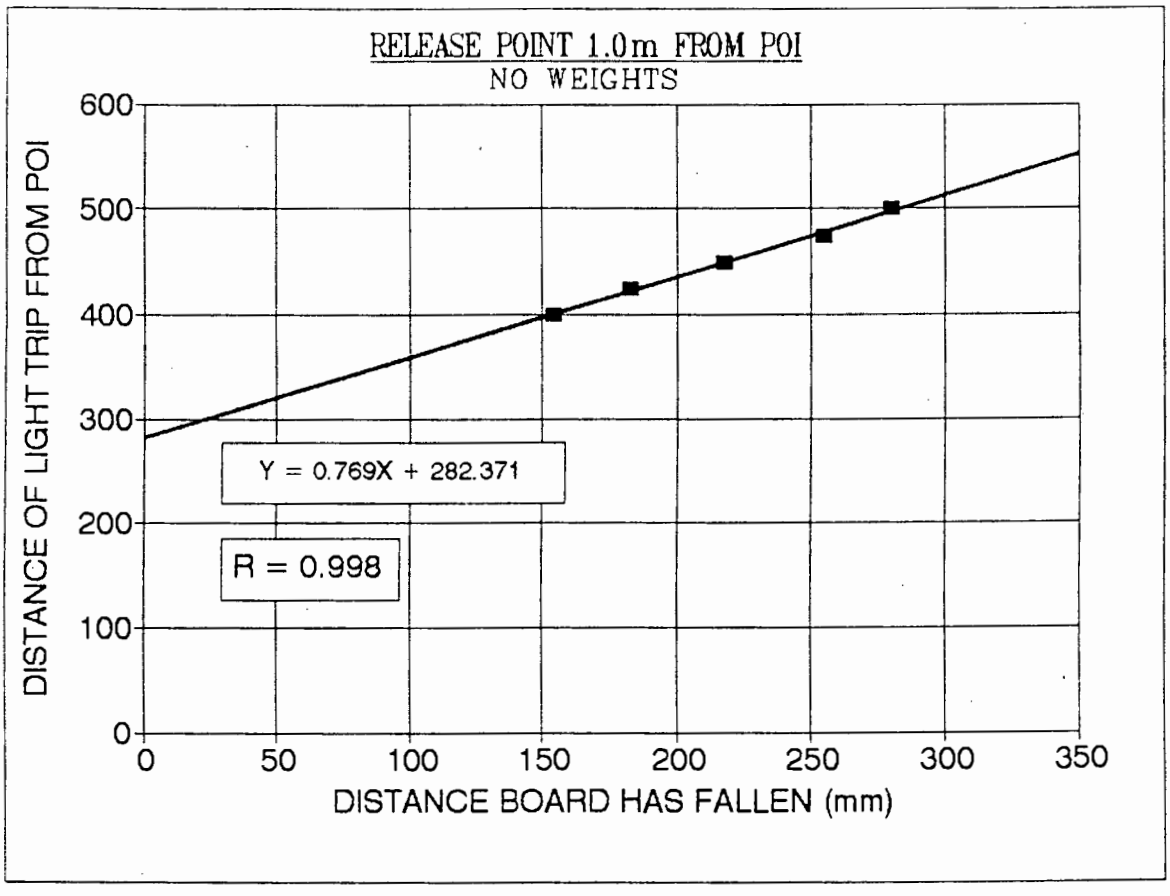
RELEASE POINT 1.0m FROM POI
NO WEIGHTS
DISTANCE OF LIGHT TRIP FROM POI
600
500
400
300
200
100
0
Y = 0.769X + 282.371
R = 0.998
0
50
100
150
200
250
300
350
DISTANCE BOARD HAS FALLEN (mm)

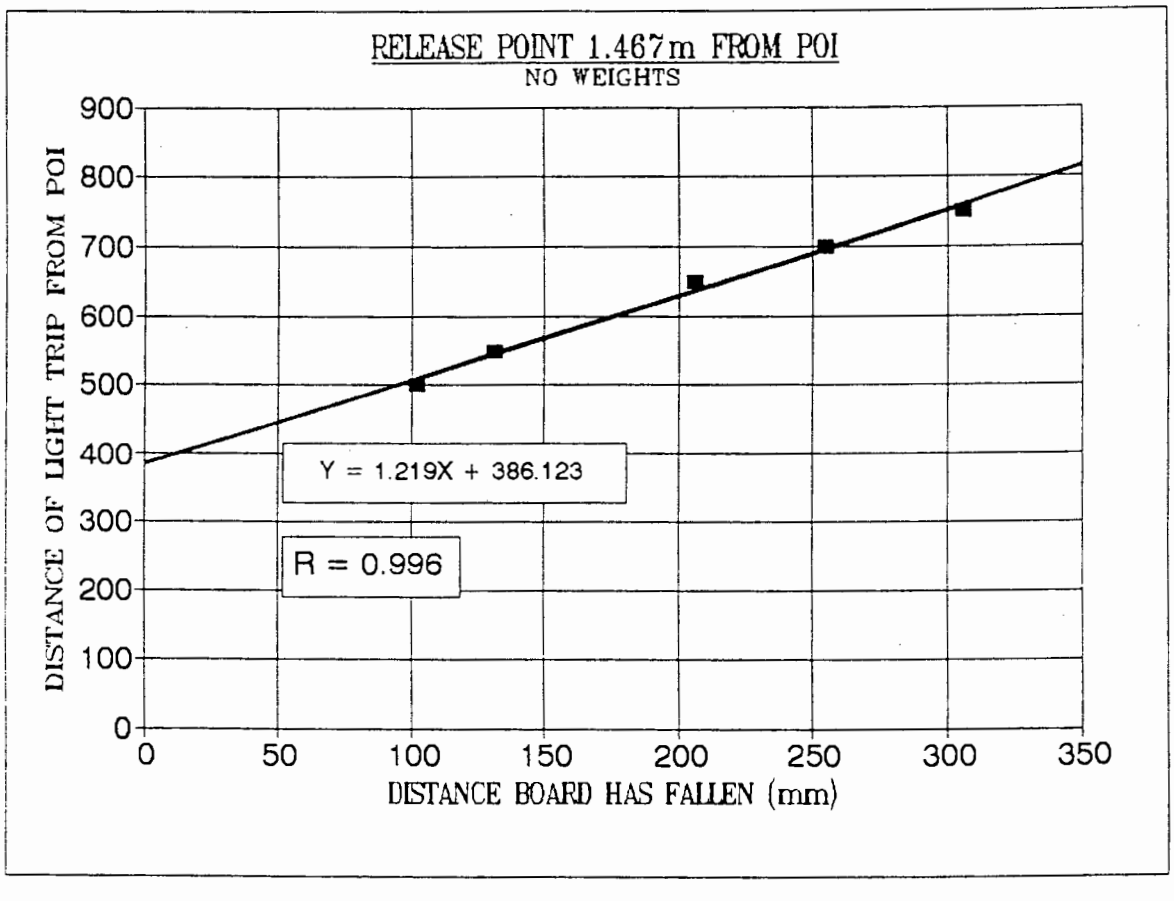
RELEASE POINT 1.467m FROM POI
NO WEIGHTS
DISTANCE OF LIGHT TRIP FROM POI
900
800
700
600
500
400
300
200
100
0
Y = 1.219X + 386.123
R = 0.996
0
50
100
150
200
250
300
350
DISTANCE BOARD HAS FALLEN (mm)

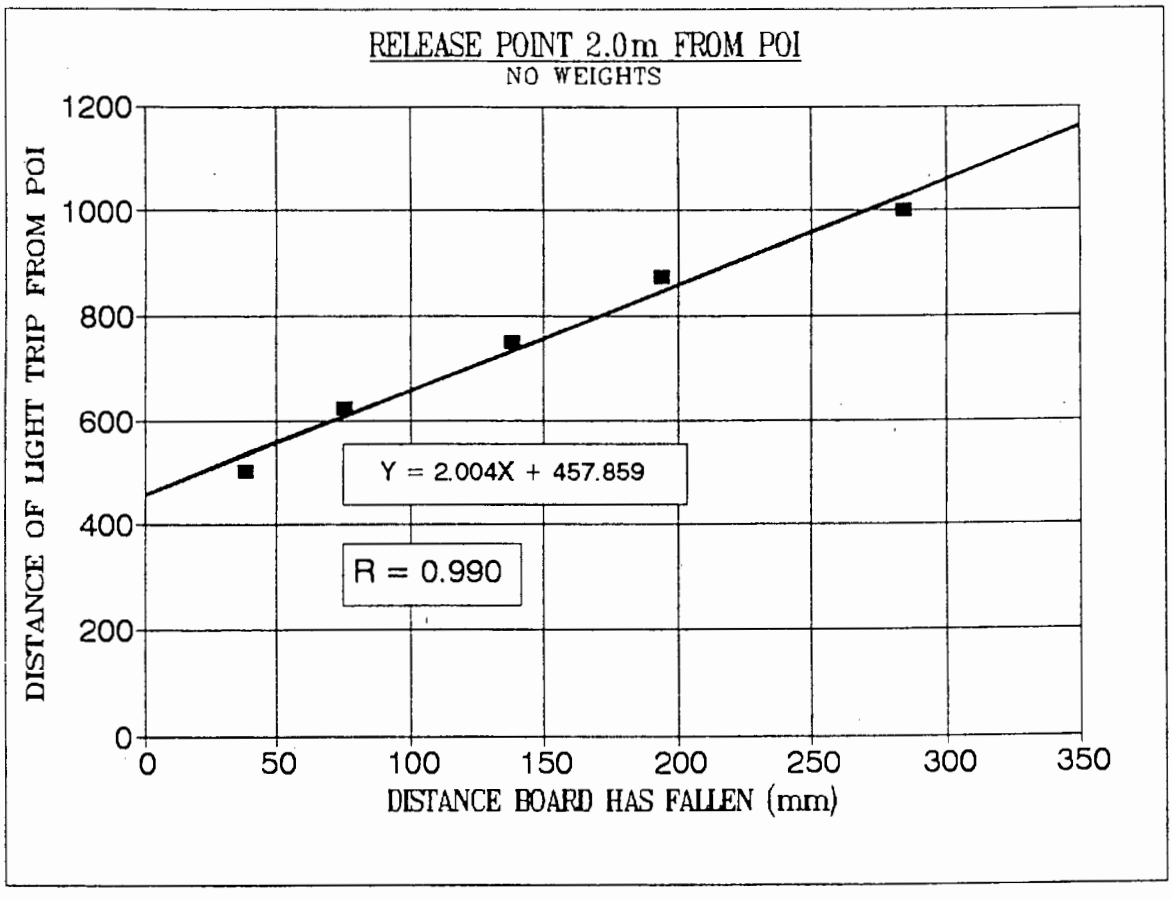
RELEASE POINT 2.0m FROM POI
NO WEIGHTS
DISTANCE OF LIGHT TRIP FROM POI
1200
1000
800
600
400
200
0
0
50
100
150
200
250
300
350
DISTANCE BOARD HAS FALLEN (mm)
Y = 2.004X + 457.859
R = 0.990

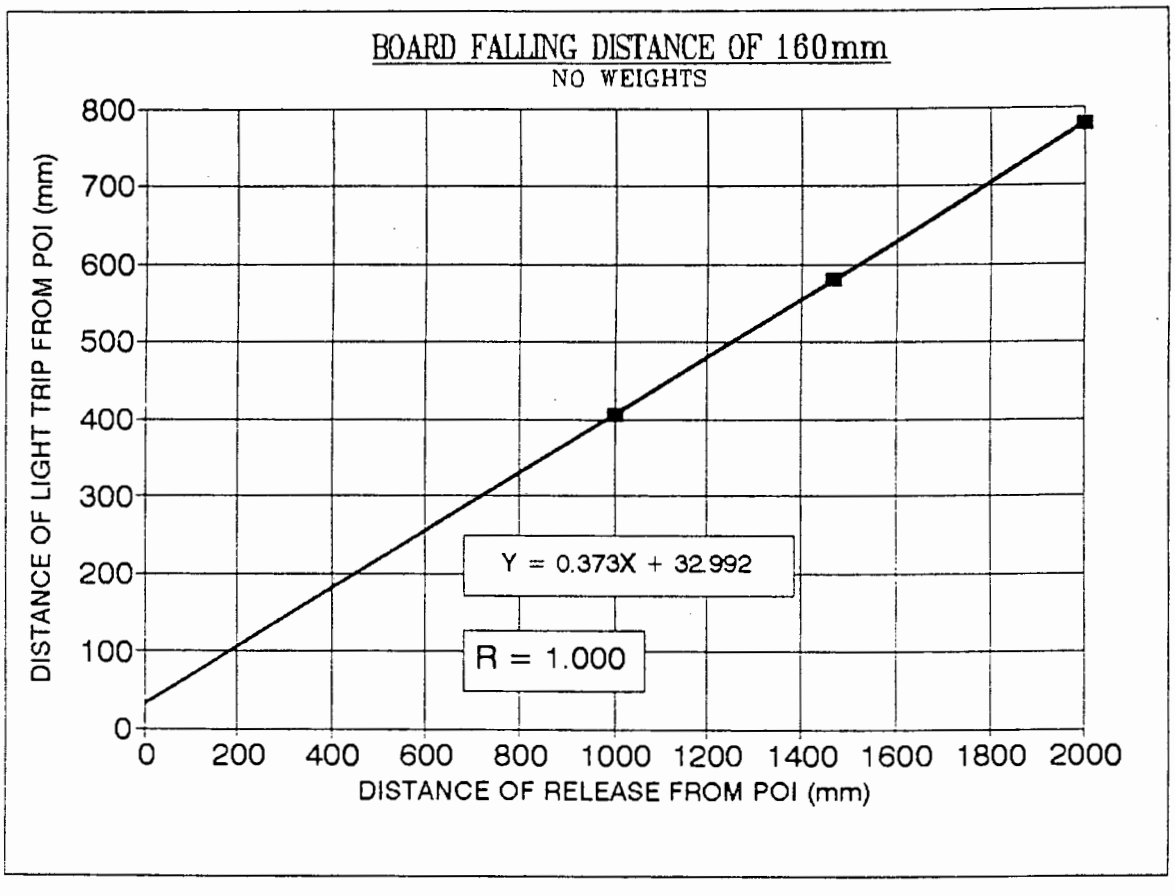
BOARD FALLING DISTANCE OF 160mm
NO WEIGHTS
DISTANCE OF LIGHT TRIP FROM POI (mm)
800
700
600
500
400
300
200
100
0
0
200
400
600
800
1000
1200
1400
1600
1800
2000
DISTANCE OF RELEASE FROM POI (mm)
Y = 0.373X + 32.992
R = 1.000

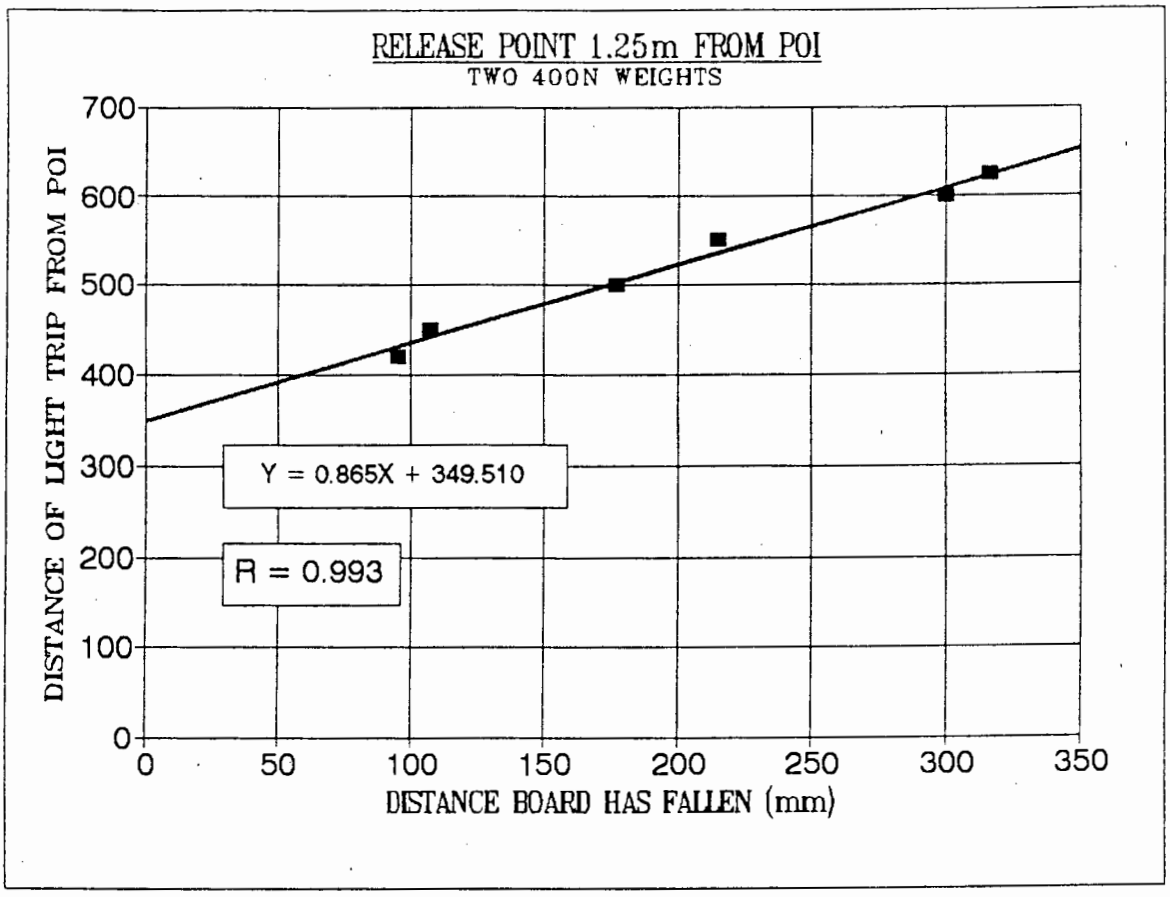
RELEASE POINT 1.25m FROM POI
TWO 400N WEIGHTS
DISTANCE OF LIGHT TRIP FROM POI
700
600
500
400
300
200
100
0
Y = 0.865X + 349.510
R = 0.993
0
50
100
150
200
250
300
350
DISTANCE BOARD HAS FALLEN (mm)

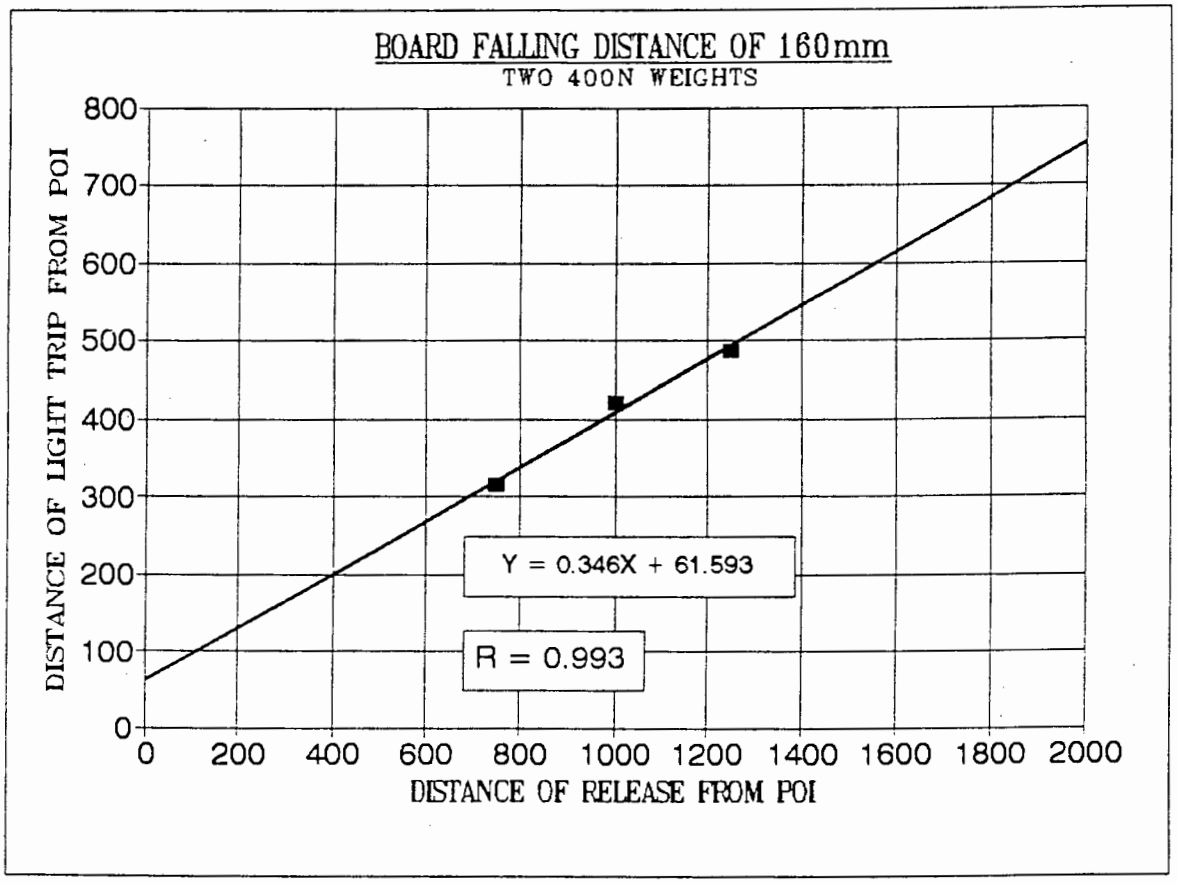
BOARD FALLING DISTANCE OF 160mm
TWO 400N WEIGHTS
DISTANCE OF LIGHT TRIP FROM POI
800
700
600
500
400
300
200
100
0
Y = 0.346X + 61.593
R = 0.993
0
200
400
600
800
1000
1200
1400
1600
1800
2000
DISTANCE OF RELEASE FROM POI

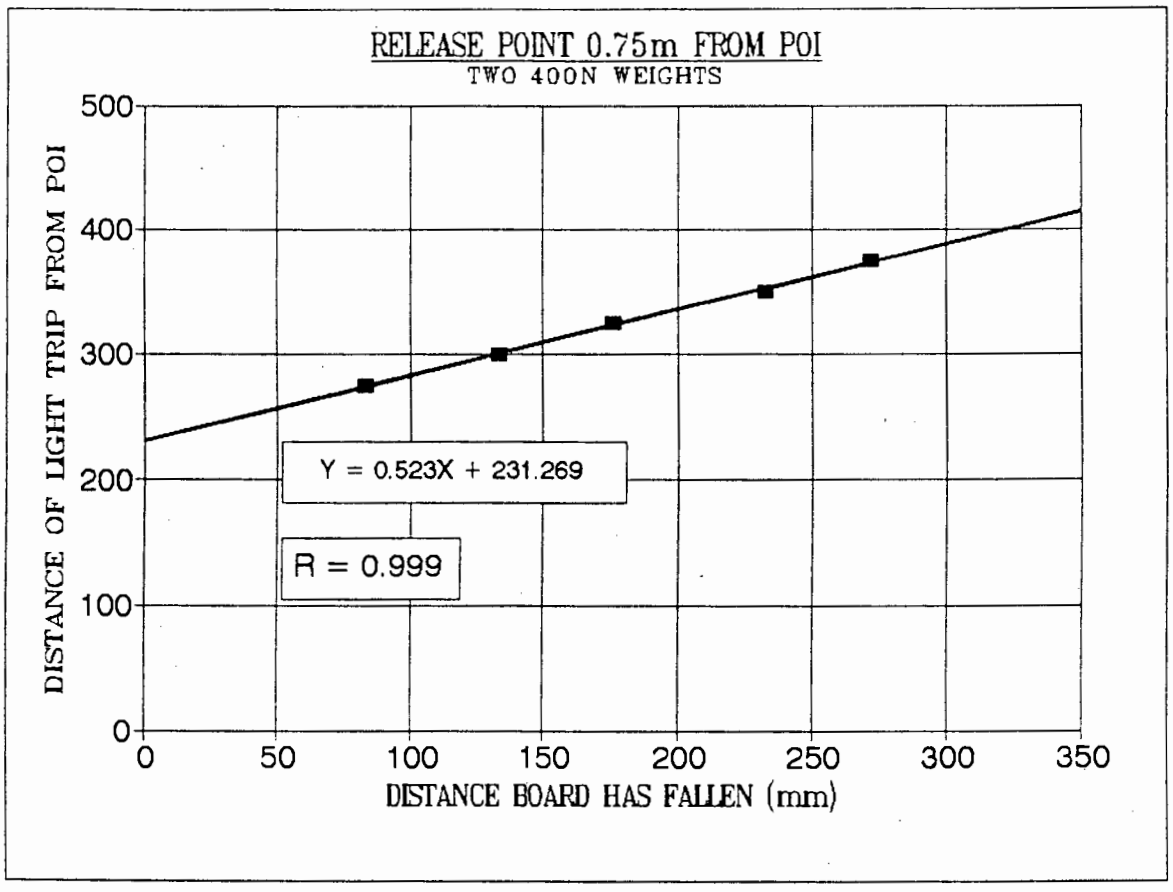
RELEASE POINT 0.75m FROM POI
TWO 400N WEIGHTS
DISTANCE OF LIGHT TRIP FROM POI
500
400
300
200
100
0
0
50
100
150
200
250
300
350
DISTANCE BOARD HAS FALLEN (mm)
Y = 0.523X + 231.269
R = 0.999

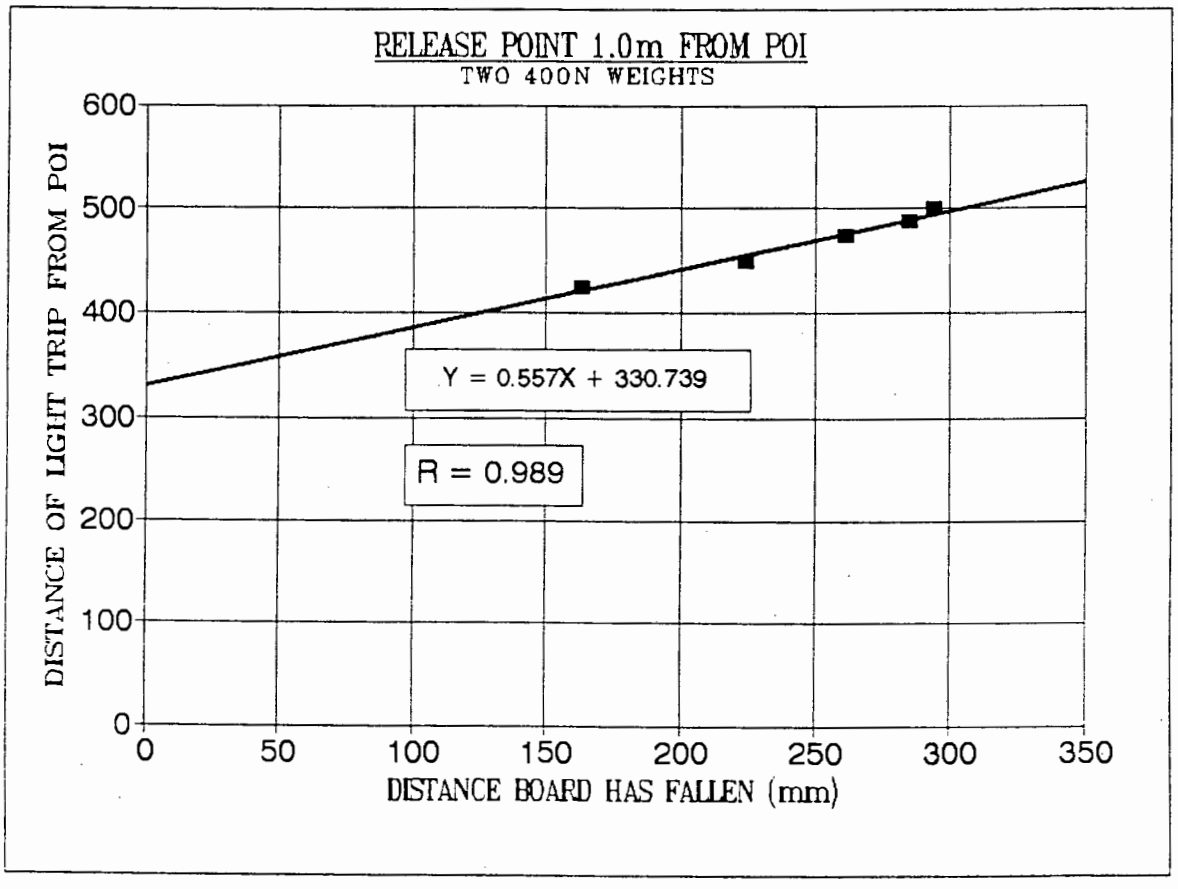
RELEASE POINT 1.0m FROM POI
TWO 400N WEIGHTS
DISTANCE OF LIGHT TRIP FROM POI
600
500
400
300
200
100
0
0
50
100
150
200
250
300
350
DISTANCE BOARD HAS FALLEN (mm)
Y = 0.557X + 330.739
R = 0.989

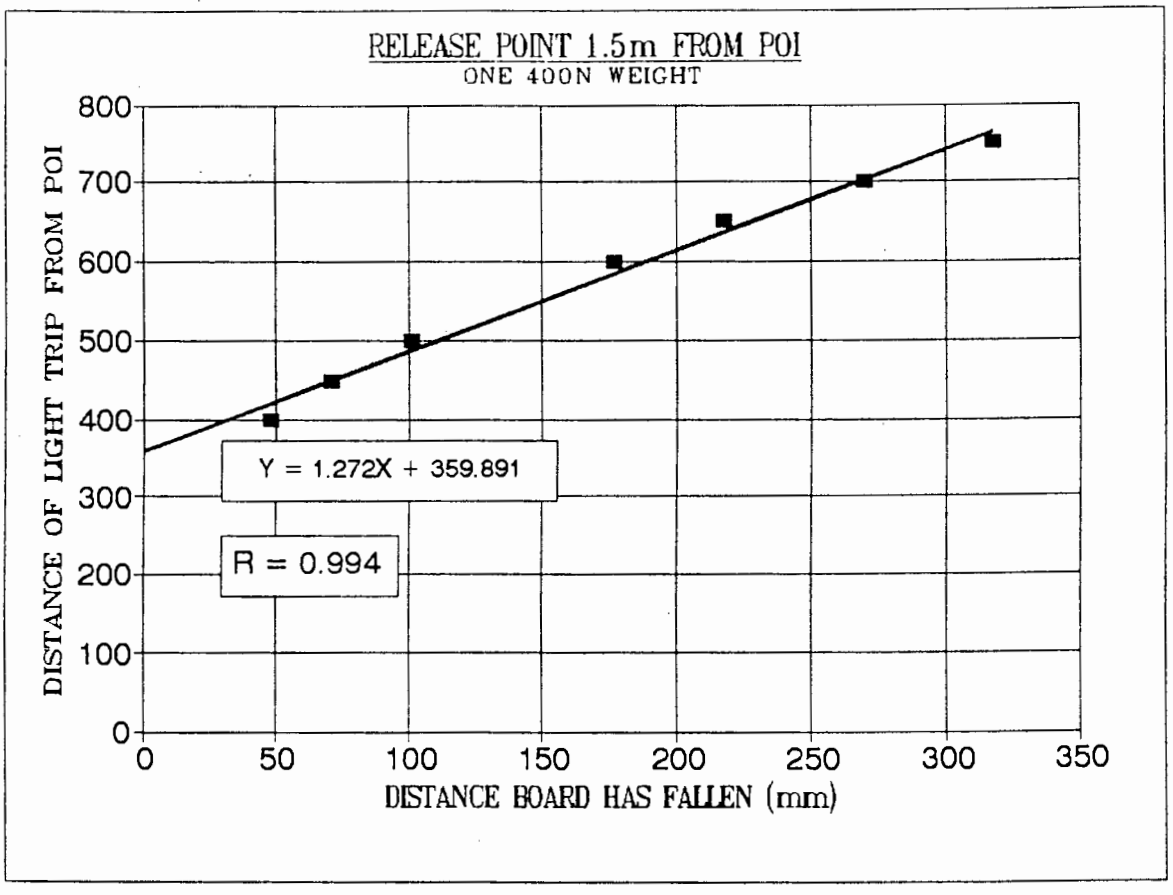
RELEASE POINT 1.5m FROM POI
ONE 400N WEIGHT
DISTANCE OF LIGHT TRIP FROM POI
800
700
600
500
400
300
200
100
0
0
50
100
150
200
250
300
350
DISTANCE BOARD HAS FALLEN (mm)
Y = 1.272X + 359.891
R = 0.994

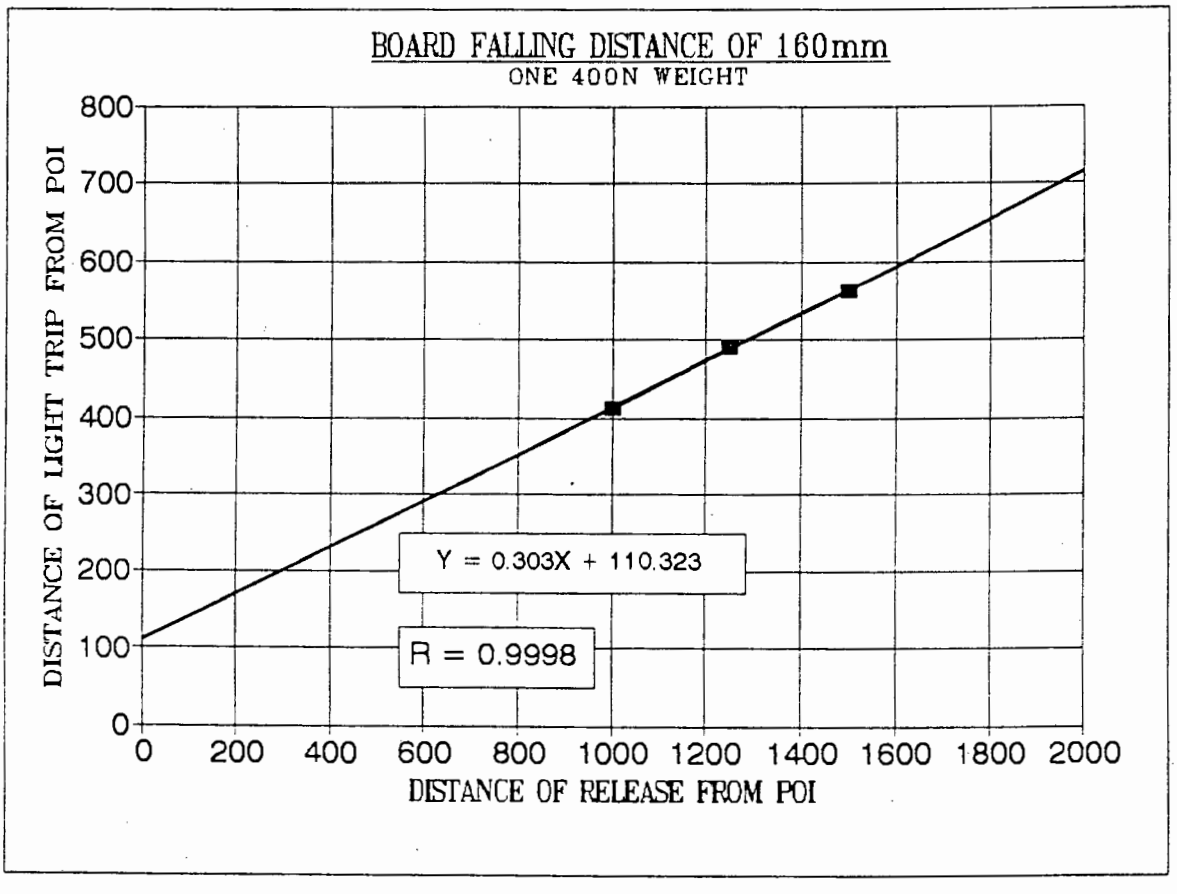
BOARD FALLING DISTANCE OF 160mm
ONE 400N WEIGHT
DISTANCE OF LIGHT TRIP FROM POI
800
700
600
500
400
300
200
100
0
0
200
400
600
800
1000
1200
1400
1600
1800
2000
DISTANCE OF RELEASE FROM POI
Y = 0.303X + 110.323
R = 0.9998

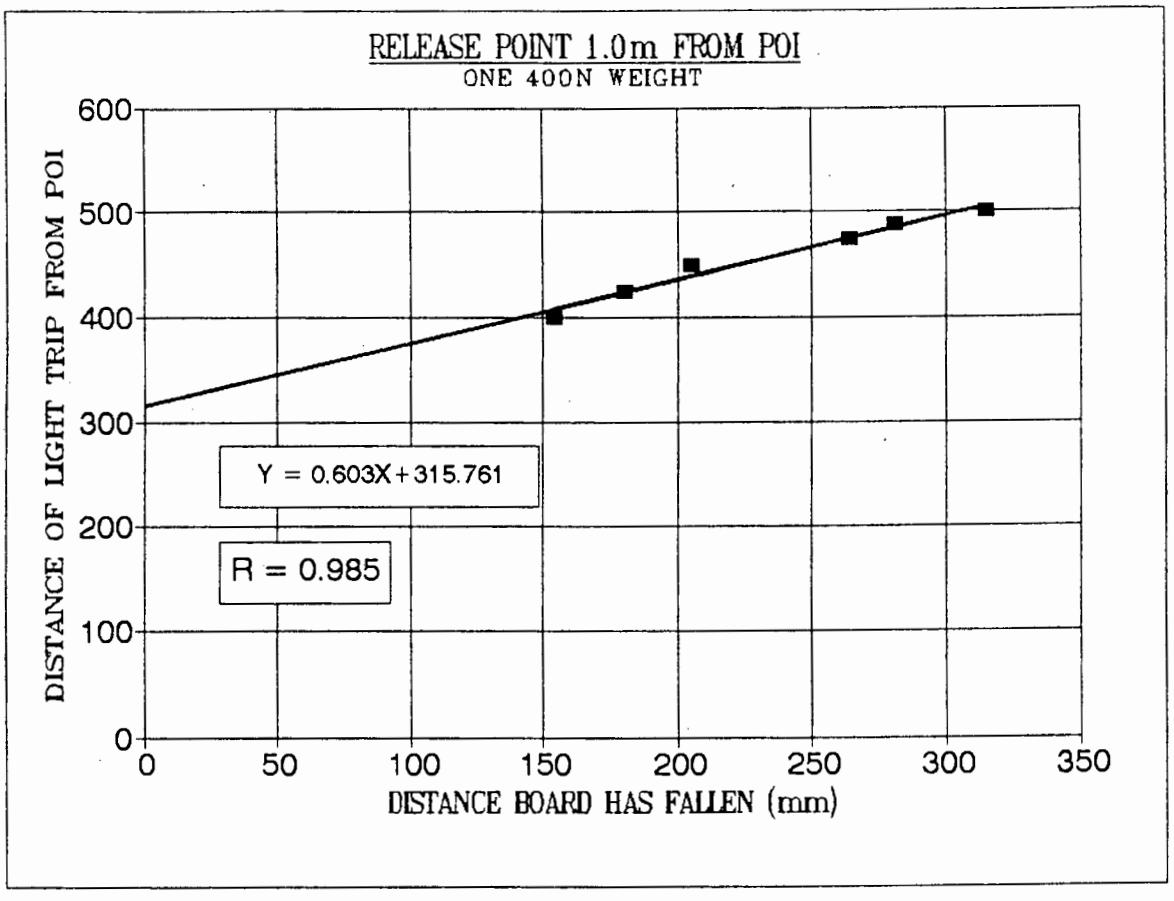
RELEASE POINT 1.0m FROM POI
ONE 400N WEIGHT
DISTANCE OF LIGHT TRIP FROM POI
600
500
400
300
200
100
0
0
50
100
150
200
250
300
350
DISTANCE BOARD HAS FALLEN (mm)
Y = 0.603X+315.761
R = 0.985

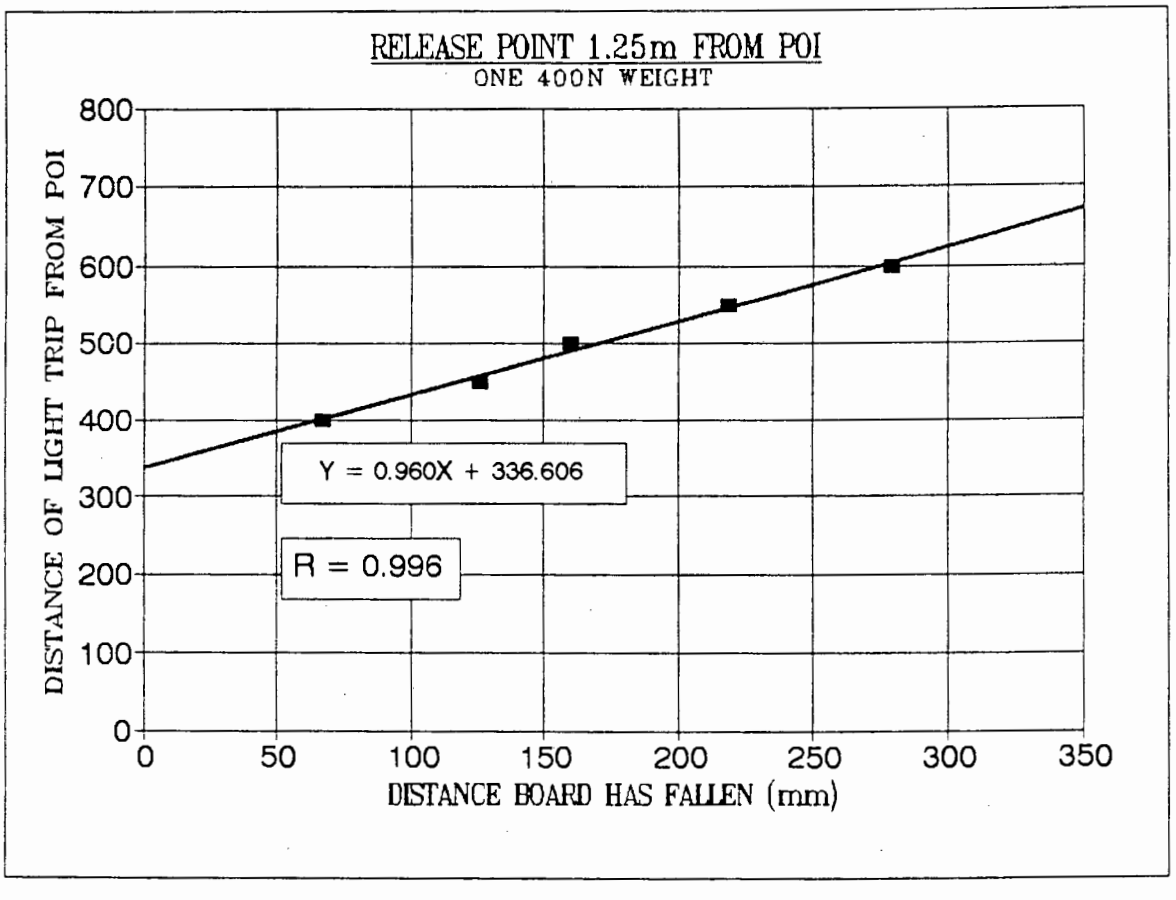
RELEASE POINT 1.25m FROM POI
ONE 400N WEIGHT
DISTANCE OF LIGHT TRIP FROM POI
800
700
600
500
400
300
200
100
0
0
50
100
150
200
250
300
350
DISTANCE BOARD HAS FALLEN (mm)
Y = 0.960X + 336.606
R = 0.996

A P P E N D I X C

STEEL BEAMS

SUMMARY OF 'PLASTIC' IMPACT TESTS ON STEEL BEAMS - SERIES A

NO WEIGHTS

Beam Number	A1	A2	A3
Dist Release From POI (mm)	1.50	2.50	3.00
Max Deflec (mm)	16.5	55.0	83.5
Permanent Deformation	4.5	35	55.5
Original Arc* (mm)	136	245	283
Backswing Arc* (mm)	72	118	110

ONE 400N WEIGHT

Beam Number	A4	A5	A6	A7
Dist Release From POI (mm)	1.00	1.75	1.70	1.90
Max Deflec (mm)	25.0	74.0	71.0	83.3
Permanent Deformation	8.0	51.5	48.0	55.5
Original Arc* (mm)	89	163	165	173
Backswing Arc* (mm)	55	59	59	58

* Arc lengths are those from arc-measuring device

Permanent Deformation representing failure = 55.0mm

SUMMARY OF 'PLASTIC' IMPACT TESTS ON STEEL BEAMS - SERIES B

NO WEIGHTS

Beam Number	B1	B2	B3
Dist Release From POI (mm)	3.25	3.50	3.75
Max Deflec (mm)	68.0	86.0	99.0
Permanent Deformation	41.0	57.0	71.5
Original Arc* (mm)	310	334	353
Backswing Arc* (mm)	137	138	131

ONE 400N WEIGHT

Beam Number	B4	B5	B6	B7
Dist Release From POI (mm)	2.00	2.50	2.35	2.22
Max Deflec (mm)	66.0	118.0	114.5	89.8
Permanent Deformation	38.5	84.5	76.0	60.0
Original Arc* (mm)	188	239	223	210
Backswing Arc* (mm)	77	70	71	74

* Arc lengths are those from arc-measuring device

Permanent Deformation representing failure = 55.0mm

(1)

(2)

STEEL BEAM

WELD

x_E

POI

EAST
NORTH
95 90 85 80 75 70 65 60 55 50 45 40 35 30 25 20 15 10 5 0
EAST

IMPACT CALIBRATION CALCULATIONS ELASTIC ANALYSIS STEEL BEAM A1

DISTANCE BOARD FALLEN BEFORE IMPACT =	0.156	m
ACCELERATION OF FALLING BOARD =	9.72	m/S^2
VALUE OF g AT UCT =	9.80	m/s^2
EFFECTIVE MASS OF PENDULUM =	63.100	kg
EFFECTIVE LENGTH OF PENDULUM =	2.941	m
DISTANCE 'X' =	0.397	m
LENGTH TO IMPACT =	4.267	m
LENGTH TO HAMMER =	3.870	m
PERIOD OF PENDULUM =	3.440	seconds
EFFECTIVE MASS BEAM ETC =	5.957	kg
DIST OF RELEASE FROM POI =	1.000	m

THETA INSWING (RADS) =	0.1896	
THETA BACKSWING (RADS) =	0.0667	
EFF HT OF PENDULUM (m) =	0.053	
EFF VEL OF PENDULUM (m/s) =	1.016	
VEL OF PEND (POI) (m/s) =	1.475	
ACCEL OF BEAM (m/s^2) =	443.7	
FORCE (Be) (N) =	1821.6	

DISTANCE FROM POI (mm)	DEFLECTION X (mm)	TIME BOARD FALLEN (seconds)	VELOCITY OF BOARD (m/s)	CORRECTION FACTOR	CORRECTED DST FROM POI (mm)	VELOCITY OF PENDULUM (m/s)	ACCELERATION OF PENDULUM (m/s^2)	TIME (t) (seconds)
0	0.0	0.1792	1.741	1.0000	0.0	1.475	443.671	0.0000
5	3.6	0.1820	1.769	0.9843	4.9	1.203	43.459	0.0028
10	6.8	0.1848	1.796	0.9694	9.7	1.060	58.795	0.0057
15	9.5	0.1876	1.823	0.9551	14.3	0.820	116.279	0.0084
20	11.3	0.1903	1.850	0.9415	18.8	0.573	65.405	0.0111
25	12.6	0.1930	1.876	0.9284	23.2	0.356	96.661	0.0138
30	13.2	0.1956	1.902	0.9158	27.6	0.171	42.509	0.0165
35	13.5	0.1982	1.927	0.9037	31.6	0.000	89.102	0.0191
40	13.2	0.2008	1.952	0.8921	35.7	-0.137	15.919	0.0217
45	12.8	0.2034	1.977	0.8810	39.6	-0.198	32.228	0.0242
50	12.2	0.2059	2.001	0.8702	43.5	-0.340	81.736	0.0267
55	11.1	0.2084	2.025	0.8598	47.3	-0.425	-14.364	0.0292
60	10.1	0.2108	2.049	0.8498	51.0	-0.471	52.619	0.0317
65	8.8	0.2132	2.073	0.8402	54.6	-0.601	54.369	0.0341
70	7.2	0.2156	2.096	0.8308	58.2	-0.629	-32.228	0.0365
75	5.8	0.2180	2.119	0.8218	61.6	-0.636	38.838	0.0389
80	4.2	0.2204	2.142	0.8130	65.0	-0.621	-52.231	0.0412
85	2.9	0.2227	2.164	0.8046	68.4	-0.498	-53.980	0.0435
90	1.9	0.2250	2.187	0.7963	71.7	-0.415	-17.281	0.0458
95	1.0	0.2273	2.209	0.7884	74.9	-0.420	21.363	0.0481
100	0.0	0.2295	2.231	0.7806	78.1	-0.446	-11.751	0.0503
105	-1.0	0.2317	2.253	0.7731	81.2			

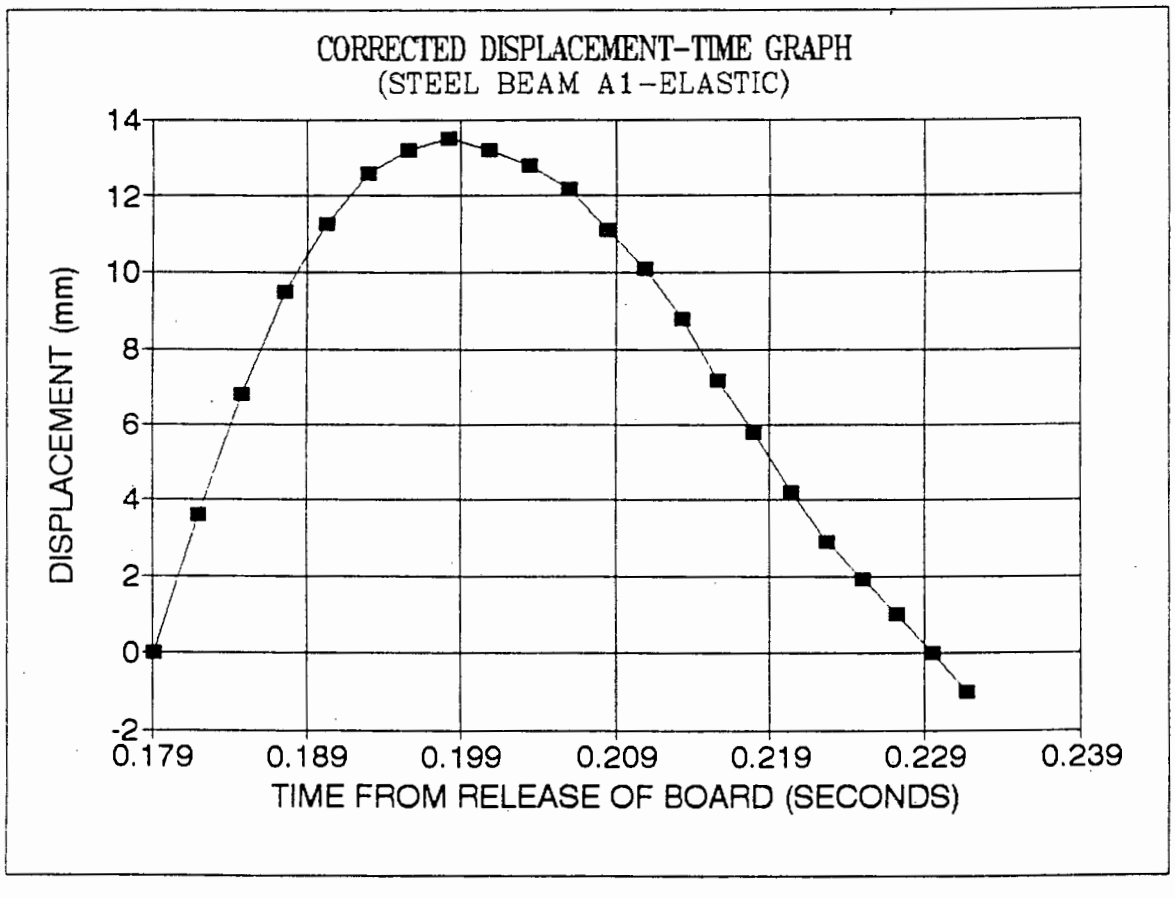

IMPACT CALIBRATION CALCULATIONS — ELASTIC ANALYSIS — STEEL BEAM B2

DISTANCE BOARD FALLEN BEFORE IMPACT =	0.133	m
ACCELERATION OF FALLING BOARD =	9.72	m/S^2
VALUE OF g AT UCT =	9.80	m/s^2
EFFECTIVE MASS OF PENDULUM =	63.100	kg
EFFECTIVE LENGTH OF PENDULUM =	2.941	m
DISTANCE 'X' =	0.397	m
LENGTH TO IMPACT =	4.267	m
LENGTH TO HAMMER =	3.870	m
PERIOD OF PENDULUM =	3.440	seconds
EFFECTIVE MASS BEAM ETC =	6.001	kg
DIST OF RELEASE FROM POI =	1.000	m

THETA INSWING (RADS) =	0.1896
THETA BACKSWING (RADS) =	0.0913
EFF HT OF PENDULUM (m) =	0.053
EFF VEL OF PENDULUM (m/s) =	1.016
VEL OF PEND (POI) (m/s) =	1.475
ACCEL OF BEAM (m/s) =	368.7
FORCE (Be) (N) =	1525.2

DISTANCE FROM POI (mm)	DEFLECTION X (mm)	TIME BOARD FALLEN (seconds)	VELOCITY OF BOARD (m/s)	CORRECTION FACTOR	CORRECTED DST FROM POI (mm)	VELOCITY OF PENDULUM (m/s)	ACCELERATION OF PENDULUM (m/s^2)	TIME (t) (seconds)
0	0.0	0.1654	1.608	1.0000	0.0	1.4747	368.7454	0.0000
5	3.5	0.1685	1.638	0.9817	4.9	1.0153	79.7995	0.0031
10	6.2	0.1715	1.667	0.9644	9.6	0.8669	17.1799	0.0061
15	8.7	0.1745	1.696	0.9480	14.2	0.7801	41.5529	0.0091
20	10.8	0.1774	1.725	0.9324	18.6	0.5863	91.8544	0.0120
25	12.1	0.1803	1.753	0.9175	22.9	0.4030	34.6157	0.0149
30	13.1	0.1831	1.780	0.9033	27.1	0.2136	100.2147	0.0177
35	13.3	0.1859	1.807	0.8898	31.1	0.0000	52.2460	0.0205
40	13.1	0.1887	1.834	0.8768	35.1	-0.1457	54.5791	0.0232
45	12.5	0.1914	1.860	0.8644	38.9	-0.3906	126.5943	0.0260
50	11.0	0.1940	1.886	0.8525	42.6	-0.6035	31.5666	0.0286
55	9.3	0.1967	1.912	0.8411	46.3	-0.6690	18.0189	0.0313
60	7.5	0.1993	1.937	0.8301	49.8	-0.7360	33.7052	0.0329
65	5.5	0.2018	1.962	0.8196	53.3	-0.7847	3.8880	0.0364
70	3.5	0.2044	1.987	0.8094	56.7	-0.7350	-43.7541	0.0389
75	1.8	0.2069	2.011	0.7996	60.0	-0.7037	19.5743	0.0415
80	0.0	0.2093	2.035	0.7902	63.2	-0.6104	-96.4510	0.0439
85	-1.2	0.2118	2.059	0.7811	66.4			

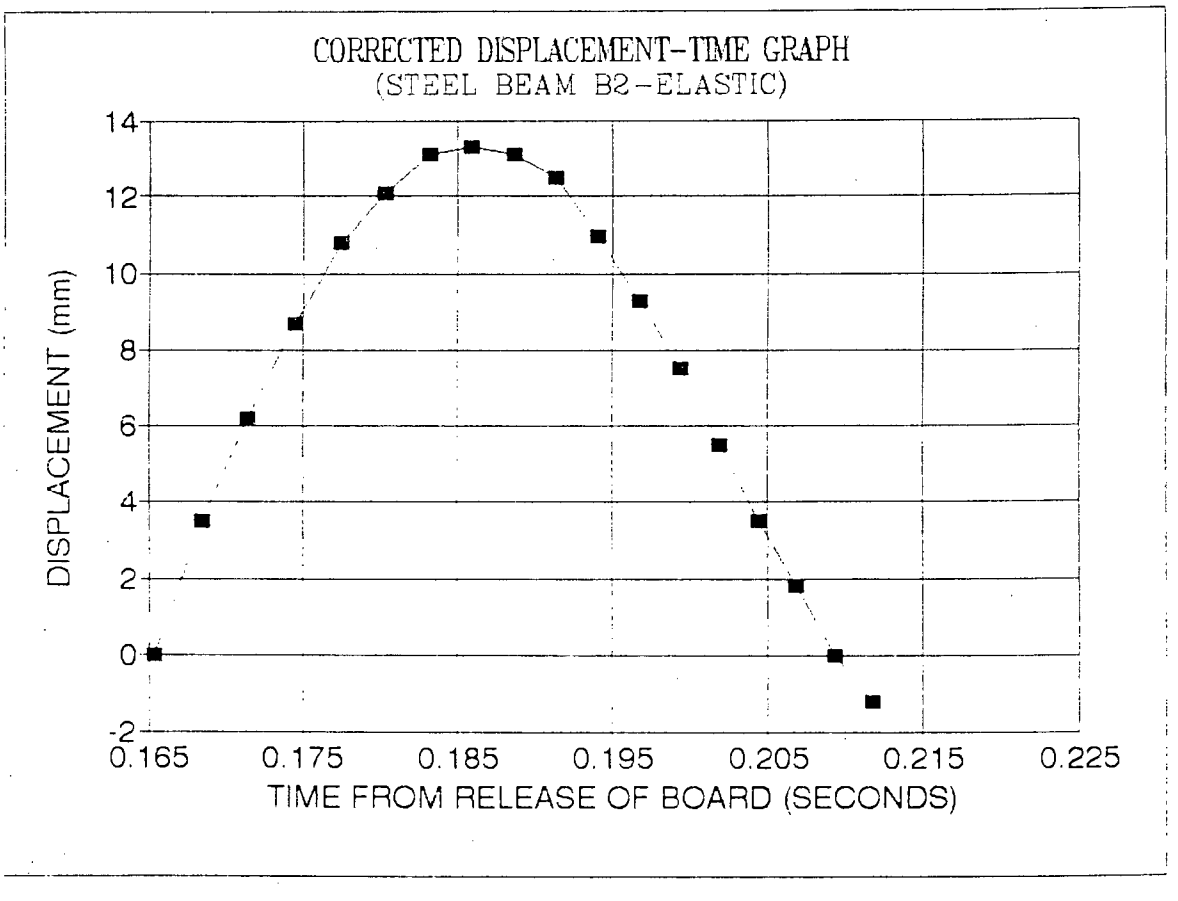

ELASTO-PLASTIC ENERGY METHOD

(Reference 1 Chapter 7)

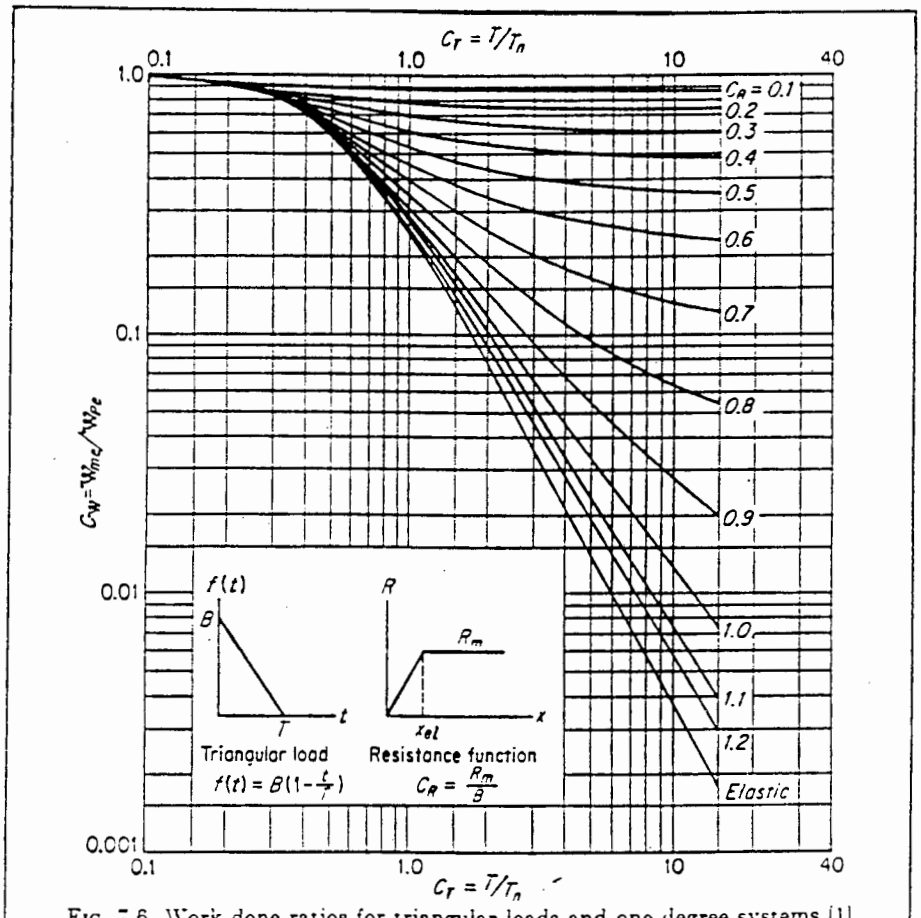

FIG. 7.6. Work-done ratios for triangular loads and one-degree systems [1].

STEEL BEAM ENERGY ANALYSIS - BEAM A1

INPUT	
DIST POI (m) =	1.000
M(e) PEND (kg) =	54.330
L(e) (m) =	2.941
DIST 'X' (m) =	-0.029
L(POI) (m) =	3.841
L(h) (m) =	3.870
'g' UCT (m/s ^ 2) =	9.80
MAX DEFL (m) =	0.0135
BEAM WIDTH (m) =	0.100
BEAM THICK (m) =	0.0059
E STEEL (GPa) =	201.700
ACC POI (m/s ^ 2) =	443.671
STATIC Fy (MPa) =	322.000
DLF Fy =	1.18
Me BEAM(ONLY) (kg) =	5.957
Fr(dyn) ROD 2 (N) =	1.157
Fr(dyn) ROD 3 (N) =	1.067
Fr(dyn) ROD 4 (N) =	1.157
MAX DEFL ROD 2 (m) =	0.0129
MAX DEFL ROD 3 (m) =	0.0135
MAX DEFL ROD 4 (m) =	0.0129

OUTPUT	
THETA(s) (rads) =	0.2091
H(eff)(1) (m) =	0.0641
KE(2) (JOULS) =	34.124
THETA(3) (rads) =	0.0095
H(eff)(3) (m) =	0.00013
PE(3) (JOULS) =	0.071
FrE(TOTAL) (JOULS) =	0.044
NETT E (JOULS) =	34.009
PROP FACT 'fp' =	0.767
E POI (JOULS) =	26.100
Be (N) =	21142.2
I beam (m ^ 4) =	1.711E-09
'k' beam (N/m) =	181837.890
Z(pl) (m ^ 3) =	8.703E-07
M(pl) (Nm) =	330.660
R(m) (N) =	2939.202
X(e) (m) =	0.0162
Xm (max) =	0.0137
Meb (SYSTEM) (kg) =	47.653
IMPULSE (POI)(Ns) =	49.875
IMP DUR 'T' (s) =	0.004718
PERIOD BEAM 'Tn'(s) =	0.101714
TIME 'Tm' (S) =	0.027788

STEEL BEAM ENERGY ANALYSIS - BEAM B2

INPUT	
DIST POI (m) =	1.000
M(e) PEND (kg) =	54.330
L(e) (m) =	2.941
DIST 'X' (m) =	-0.029
L(POI) (m) =	3.841
L(h) (m) =	3.870
'g' UCT (m/s ^ 2) =	9.80
MAX DEFL (m) =	0.0133
BEAM WIDTH (m) =	0.100
BEAM THICK (m) =	0.0061
E STEEL (GPa) =	203.900
ACC POI (m/s ^ 2) =	368.745
STATIC Fy (MPa) =	399.800
DLF Fy =	1.18
Me BEAM(ONLY) (kg) =	6.001
Fr(dyn) ROD 2 (N) =	1.157
Fr(dyn) ROD 3 (N) =	1.067
Fr(dyn) ROD 4 (N) =	1.157
MAX DEFL ROD 2 (m) =	0.0130
MAX DEFL ROD 3 (m) =	0.0133
MAX DEFL ROD 4 (m) =	0.0130

OUTPUT	
THETA(s) (rads) =	0.2091
H(eff)(1) (m) =	0.0641
KE(2) (JOULS) =	34.124
THETA(3) (rads) =	0.0095
H(eff)(3) (m) =	0.00013
PE(3) (JOULS) =	0.070
FrE(TOTAL) (JOULS) =	0.044
NETT E (JOULS) =	34.010
PROP FACT 'fp' =	0.767
E POI (JOULS) =	26.101
Be (N) =	17587.9
I beam (m ^ 4) =	1.892E-09
'k' beam (N/m) =	203155.779
Z(pl) (m ^ 3) =	9.303E-07
M(pl) (Nm) =	438.858
R(m) (N) =	3900.964
X(e) (m) =	0.0192
Xm (max) =	0.0134
Meb (SYSTEM) (kg) =	47.697
IMPULSE (POI)(Ns) =	49.899
IMP DUR 'T' (s) =	0.005674
PERIOD BEAM 'Tn'(s) =	0.096274
TIME 'Tm' (S) =	0.026906

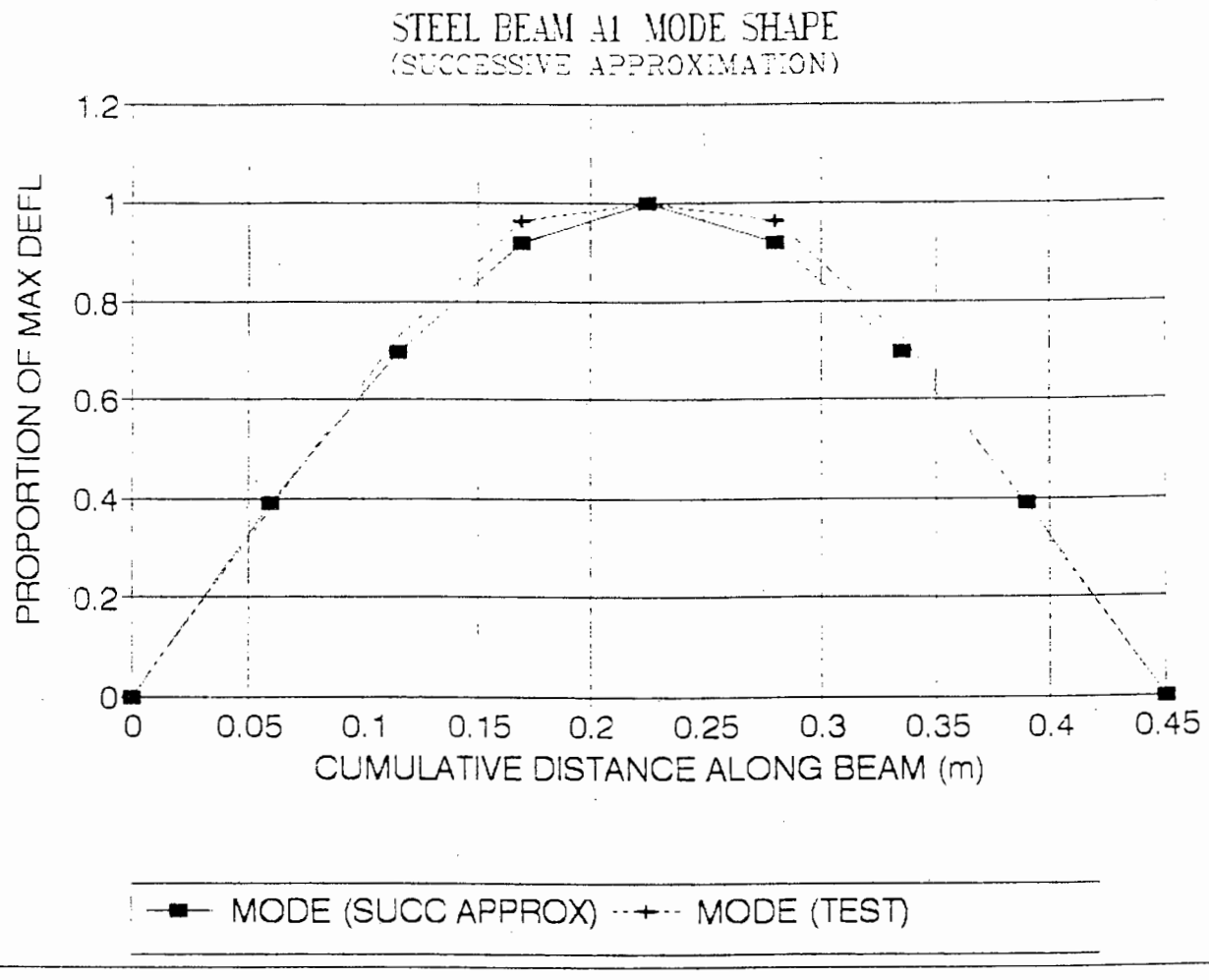
STEEL BEAM A1 MODE SHAPE
(SUCCESSIVE APPROXIMATION)
PROPORTION OF MAX DEFL
1.2
1
0.8
0.6
0.4
0.2
0
0
0.05
0.1
0.15
0.2
0.25
0.3
0.35
0.4
0.45
CUMULATIVE DISTANCE ALONG BEAM (m)
MODE (SUCC APPROX)
MODE (TEST)

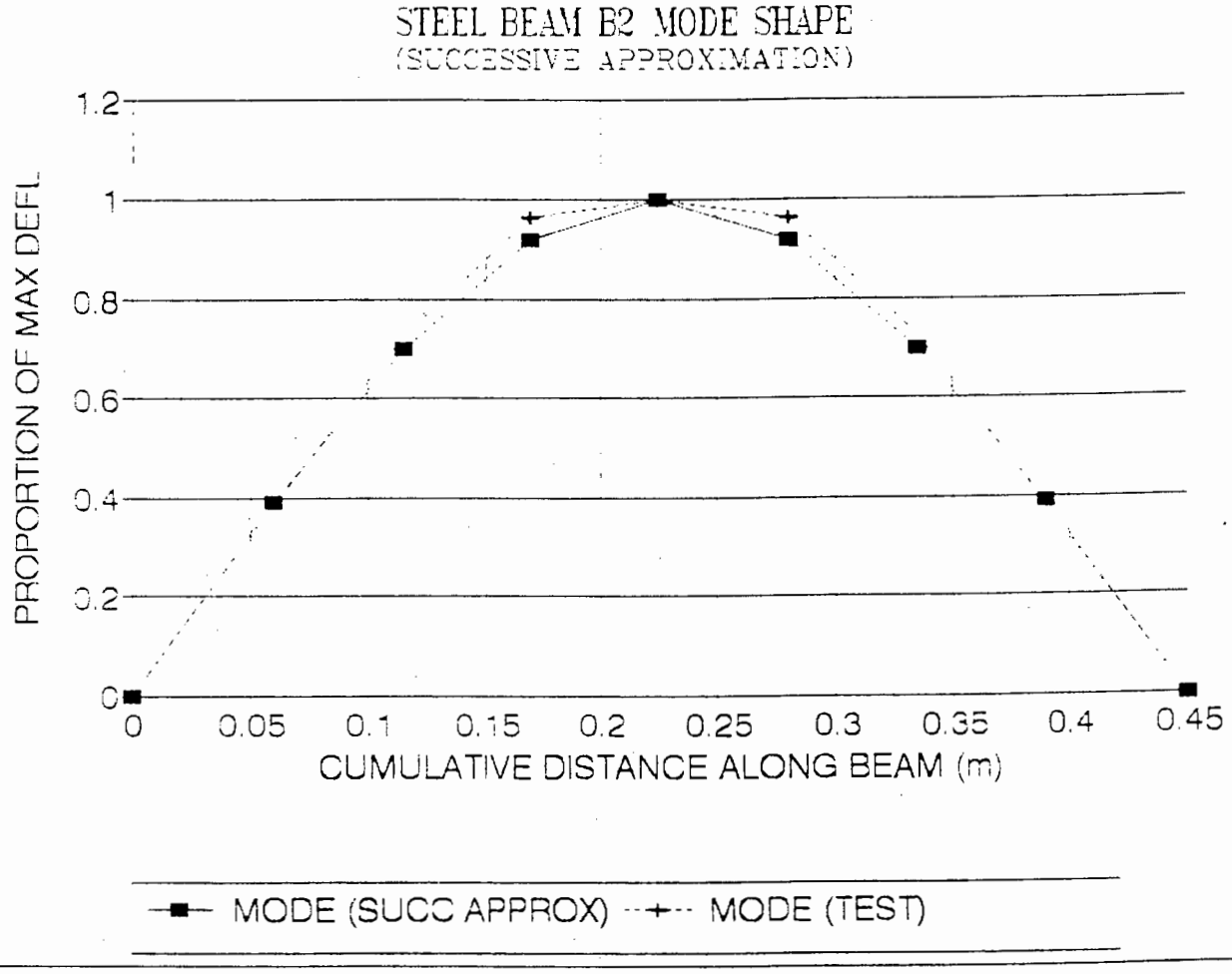
STEEL BEAM B2 MODE SHAPE
(SUCCESSIVE APPROXIMATION)
PROPORTION OF MAX DEFL
1.2
1
0.8
0.6
0.4
0.2
0
0
0.05
0.1
0.15
0.2
0.25
0.3
0.35
0.4
0.45
CUMULATIVE DISTANCE ALONG BEAM (m)
MODE (SUCC APPROX)
MODE (TEST)

SUCCESSIVE APPROXIMATION METHOD STEEL BEAM A1

SPAN (L) = 0 45 m
NUMBER OF SUB-DIVISIONS = 8
MASS OF BEAM 2 693 kg
MASS OF ROD = 1 477 kg
Me(imp) PEND = 41 480 kg
DYNAMIC EI = 345 200 Nm^ 2
Me OF PEND = 63 100 kg

MASS OF BEAM (kg/m) = 4 488
PENDULUM (1 =Y,0=N) 1 000
PENDULUM L(imp) (m) = 4 267
PENDULUM Le (m) = 2 941
DISTANCE 'X' (m) = 0 397

FIRST TRIAL
FREQUENCY = 10 138 cycles/sec
PERIOD = 0 098641 sec/cycle

SECOND TRIAL
FREQUENCY = 10 138 cycles/sec
PERIOD = 0 098642 sec/cycle

POINT No	DIST FROM LHS (m)	MASS (kg)	MODE DISP (mm)	MODE SHAPE Una	FORCE Una*Mn	DISPLACEMENT Unb	MnUna*Unb	Mu*Unb^2	MODE SHAPE Una	FORCE Una*Mn	DISPLACEMENT Unb	MnUna*Unb	Mu*Unb^2
1	0 000	0 269	0 000	0 000	0 000	0 000000	0 000000	0 000000	0 000	0 000	0 000000	0 000000	0 000000
2	0 060	0 247	0 097	0 390	0 096	0 000096	0 000009	0 000000	0 390	0 096	0 000096	0 000009	0 000000
3	0 115	0 247	0 173	0 700	0 173	0 000172	0 000030	0 000000	0 699	0 173	0 000172	0 000030	0 000000
4	0 170	1 724	0 228	0 920	1 586	0 000227	0 000359	0 000000	0 919	1 585	0 000227	0 000359	0 000000
5	0 225	43 204	0 248	1 000	43 204	0 000246	0 010648	0 000003	1 000	43 204	0 000246	0 010648	0 000003
6	0 280	1 724	0 228	0 920	1 586	0 000227	0 000359	0 000000	0 919	1 585	0 000227	0 000359	0 000000
7	0 335	0 247	0 173	0 700	0 173	0 000172	0 000030	0 000000	0 699	0 173	0 000172	0 000030	0 000000
8	0 390	0 247	0 097	0 390	0 096	0 000096	0 000009	0 000000	0 390	0 096	0 000096	0 000009	0 000000
9	0 450	0 269	0 000	0 000	0 000	0 000000	0 000000	0 000000	0 000	0 000	0 000000	0 000000	0 000000
						TOTAL	0 011445	0 000003			TOTAL	0 011445	0 000003

SUCCESSIVE APPROXIMATION METHOD STEEL BEAM B2

SPAN (L) = 0 45 m
NUMBER OF SUB-DIVISIONS = 8
MASS OF BEAM 2 737 kg
MASS OF ROD = 1 477 kg
Me(imp) PEND = 41 480 kg
DYNAMIC EI = 385 700 Nm^ 2
Me OF PEND = 63 100 kg

MASS OF BEAM (kg/m) = 4 612
PENDULUM (1 =Y,0=N) 1 000
PENDULUM L(imp) (m) = 4 267
PENDULUM Le (m) = 2 941
DISTANCE 'X' (m) = 0 397

FIRST TRIAL
FREQUENCY = 10 714 cycles/sec
PERIOD = 0 093336 sec/cycle

SECOND TRIAL
FREQUENCY = 10 714 cycles/sec
PERIOD = 0 093337 sec/cycle

POINT No	DIST FROM LHS (m)	MASS (kg)	MODE DISP (mm)	MODE SHAPE Una	FORCE Una*Mn	DISPLACEMENT Unb	MnUna*Unb	Mu*Unb^2	MODE SHAPE Una	FORCE Una*Mn	DISPLACEMENT Unb	MnUna*Unb	Mu*Unb^2
1	0 000	0 277	0 000	0 000	0 000	0 000000	0 000000	0 000000	0 000	0 000	0 000000	0 000000	0 000000
2	0 060	0 254	0 087	0 390	0 099	0 000086	0 000009	0 000000	0 390	0 099	0 000086	0 000009	0 000000
3	0 115	0 254	0 155	0 700	0 177	0 000154	0 000027	0 000000	0 699	0 177	0 000154	0 000027	0 000000
4	0 170	1 731	0 204	0 920	1 592	0 000203	0 000323	0 000000	0 919	1 591	0 000203	0 000323	0 000000
5	0 225	43 210	0 222	1 000	43 210	0 000221	0 009535	0 000002	1 000	43 210	0 000221	0 009535	0 000002
6	0 280	1 731	0 204	0 920	1 592	0 000203	0 000323	0 000000	0 919	1 591	0 000203	0 000323	0 000000
7	0 335	0 254	0 155	0 700	0 177	0 000154	0 000027	0 000000	0 699	0 177	0 000154	0 000027	0 000000
8	0 390	0 254	0 087	0 390	0 099	0 000086	0 000009	0 000000	0 390	0 099	0 000086	0 000009	0 000000
9	0 450	0 277	0 000	0 000	0 000	0 000000	0 000000	0 000000	0 000	0 000	0 000000	0 000000	0 000000
						TOTAL	0 010253	0 000002			TOTAL	0 010253	0 000002

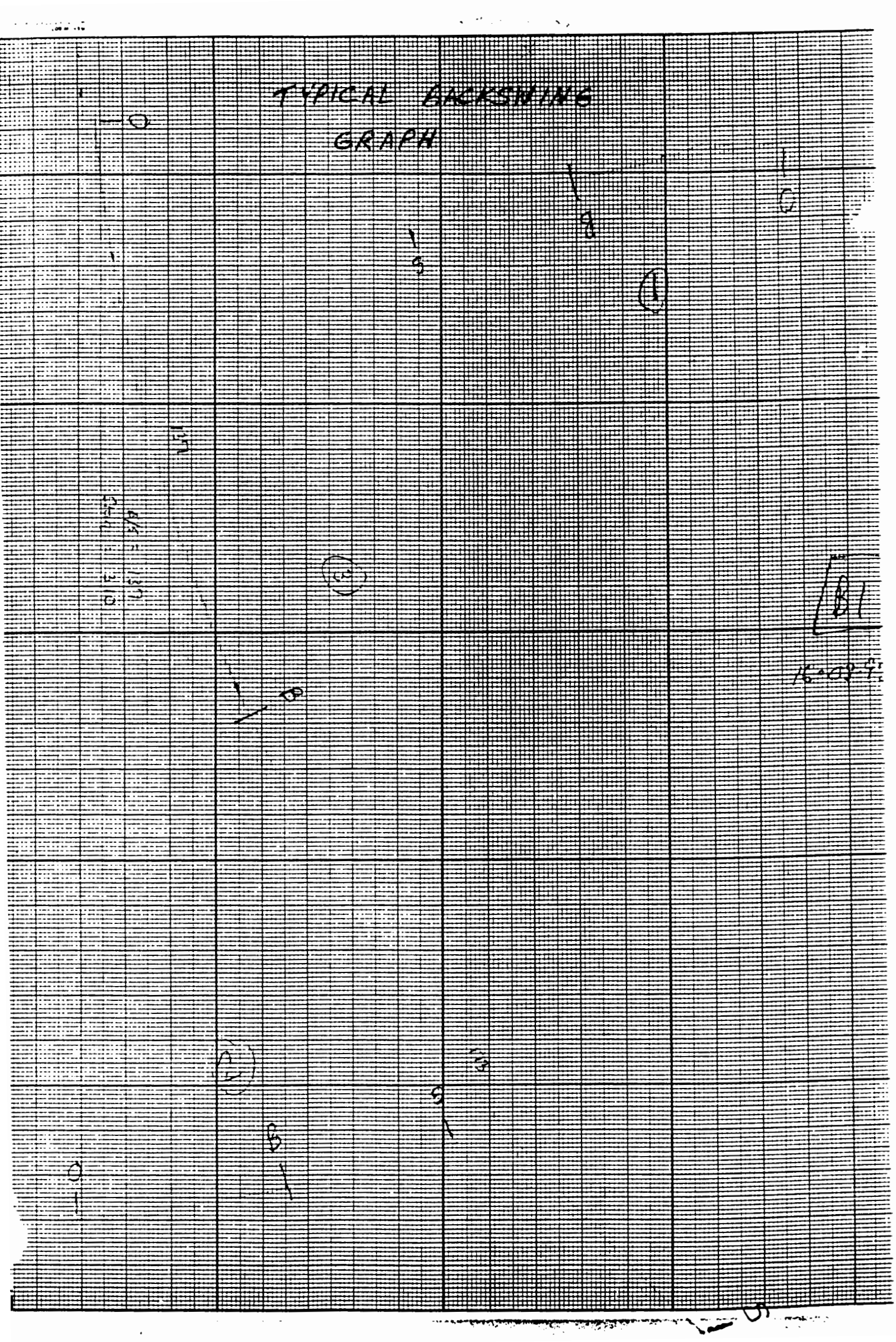
TYPICAL BACKSWING
GRAPH

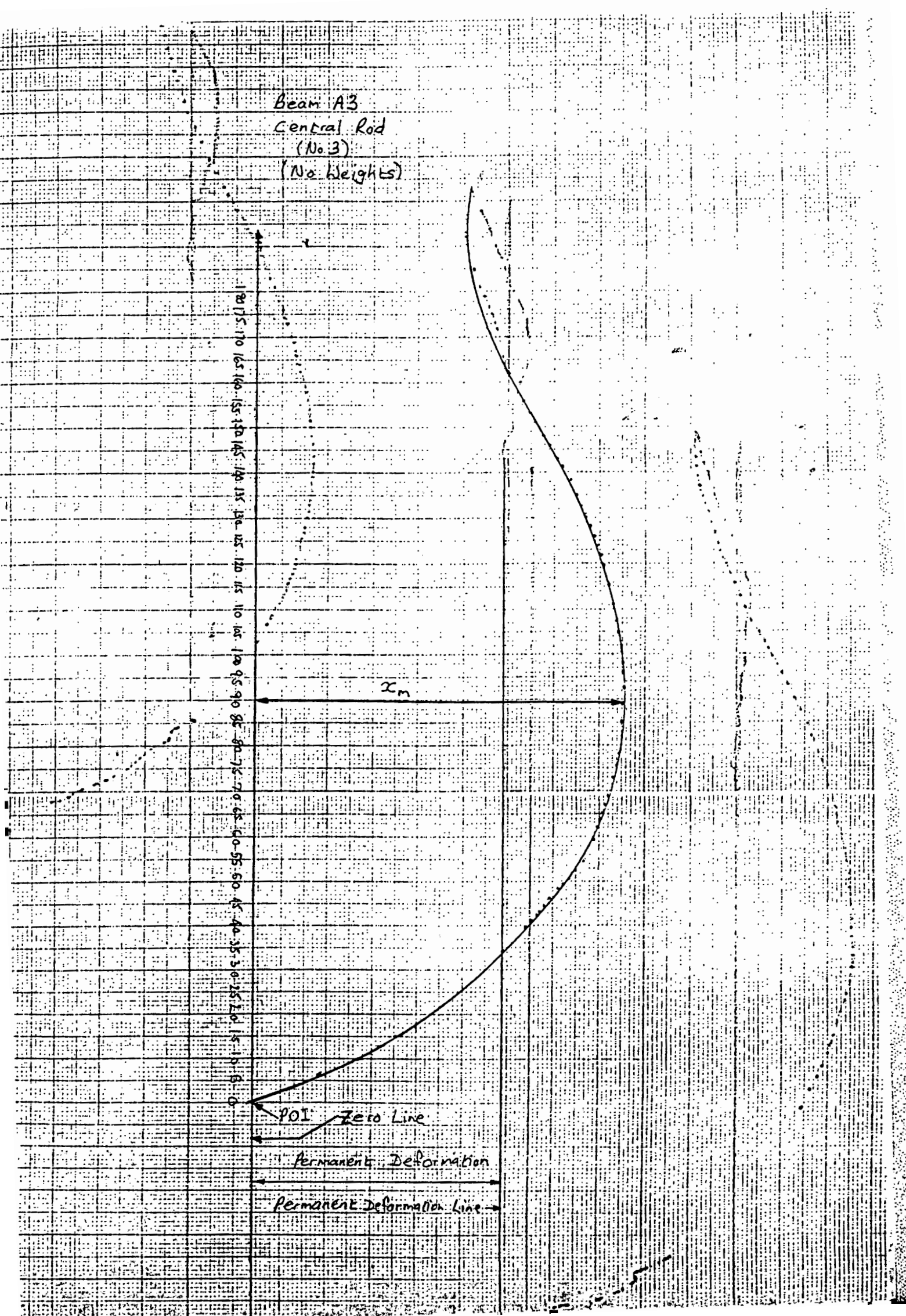
Beam A3
Central Rod
(No. 3)
(No Weights)
x_m
POI
Zero Line
Permanent Deformation
Permanent Deformation Line

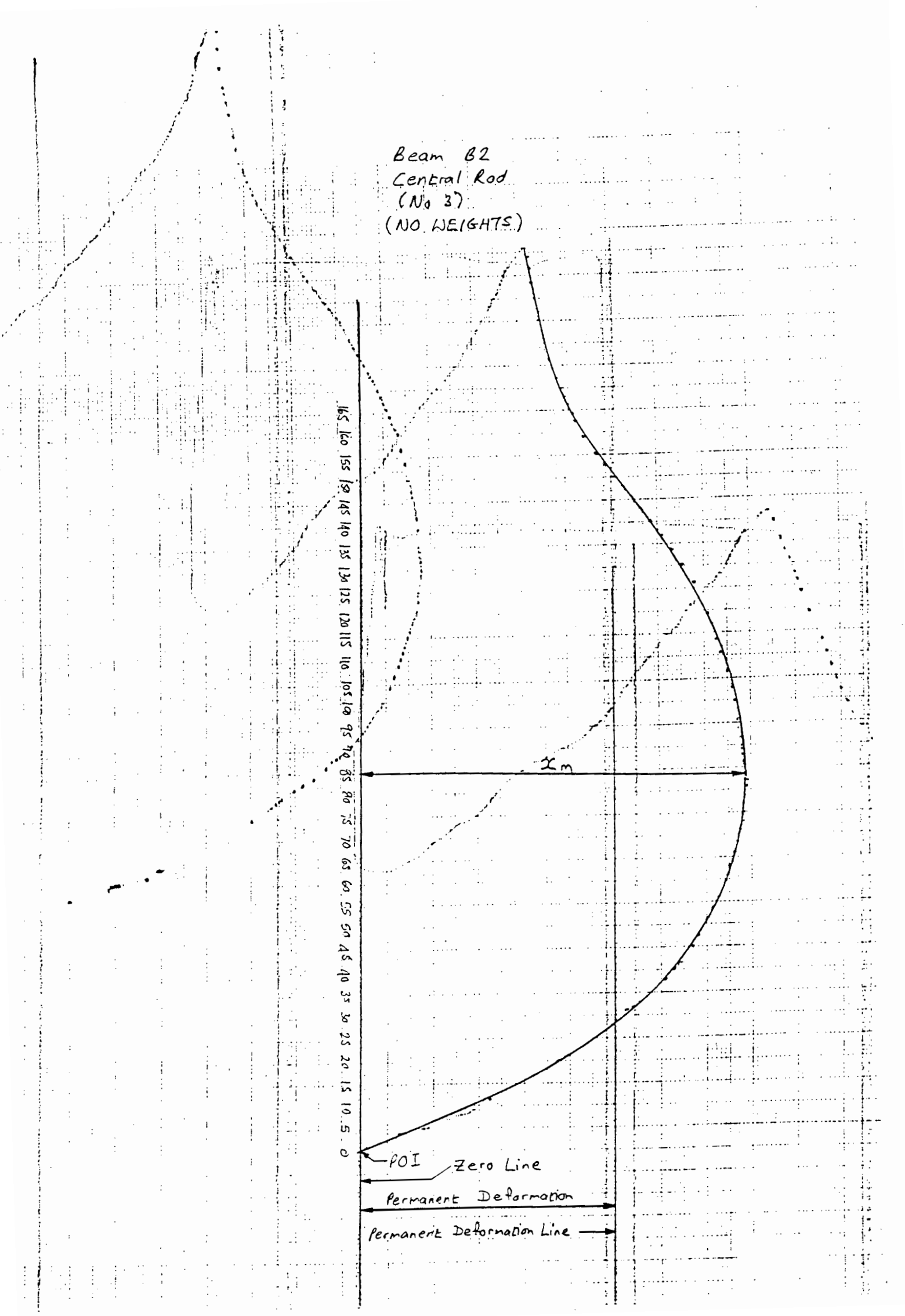
Beam B2
Central Rod
(No 3)
(NO WEIGHTS)
165 160 155 150 145 140 135 130 125 120 115 110 105 100 95 90 85 80 75 70 65 60 55 50 45 40 35 30 25 20 15 10 5 0
x_m
POI
Zero Line
Permanent Deformation
Permanent Deformation Line

STEEL BEAM ENERGY ANALYSIS - BEAM A3 ELASTO-PLASTIC ANALYSIS
(NO WEIGHTS)

INPUT		OUTPUT	
DIST POI (m) =	3.000	THETA(s) (rads) =	0.6927
M(e) PEND (kg) =	54.3	H(eff)(1) (m) =	0.6779
M(e) CHANNEL (kg) =	45.9	KE(2) (JOULS) =	360.931
L(e) (m) =	2.941	THETA(3) (rads) =	0.0277
DIST 'X' (m) =	-0.029	H(eff)(3) (m) =	0.00113
L(POI) (m) =	3.841	PE(3) (JOULS) =	0.602
L(h) (m) =	3.870	FrE(TOTAL) (JOULS) =	0.259
'g' UCT (m/s^2) =	9.80	NETT E (JOULS) =	360.070
MAX DEFL (m) =	0.0835	PROP FACT 'fp' =	0.767
BEAM WIDTH (m) =	0.100	E POI (JOULS) =	276.337
BEAM THICK (m) =	0.0059	Be (N) =	7978.2
E STEEL (GPa) =	201.700	I beam (m^4) =	1.711E-09
ACC POI (m/s^2) =	1339.300	'k' beam (N/m) =	181837.890
STATIC Fy (MPa) =	322.000	Z(pl) (m^3) =	8.703E-07
DLF Fy =	1	M(pl) (Nm) =	403.518
Me BEAM(ONLY) (kg) =	5.957	R(m) (N) =	3586.822
Fr(dyn) ROD 2 (N) =	1.157	X(e) (m) =	0.0197
Fr(dyn) ROD 3 (N) =	1.067	Xm (max) =	0.0869
Fr(dyn) ROD 4 (N) =	1.157	Meb (SYSTEM) (kg) =	49.620
MAX DEFL ROD 2 (m) =	0.0735	IMPULSE (POI)(Ns) =	165.601
MAX DEFL ROD 3 (m) =	0.0835	IMP DUR 'T' (s) =	0.041513
MAX DEFL ROD 4 (m) =	0.0735	PERIOD BEAM 'Tn'(s)=	0.103793
		TIME 'Tm' (S) =	0.046705

STEEL BEAM ENERGY ANALYSIS - BEAM B2 ELASTO-PLASTIC ANALYSIS
(NO WEIGHTS)

INPUT		OUTPUT	
DIST POI (m) =	3.500	THETA(s) (rads) =	0.8136
M(e) PEND (kg) =	54.3	H(eff)(1) (m) =	0.9209
M(e) CHANNEL (kg) =	45.9	KE(2) (JOULS) =	490.334
L(e) (m) =	2.941	THETA(3) (rads) =	0.0284
DIST 'X' (m) =	-0.029	H(eff)(3) (m) =	0.00118
L(POI) (m) =	3.841	PE(3) (JOULS) =	0.630
L(h) (m) =	3.870	FrE(TOTAL) (JOULS) =	0.288
'g' UCT (m/s^2) =	9.80	NETT E (JOULS) =	489.415
MAX DEFL (m) =	0.0860	PROP FACT 'fp' =	0.767
BEAM WIDTH (m) =	0.100	E POI (JOULS) =	375.604
BEAM THICK (m) =	0.0061	Be (N) =	7216.8
E STEEL (GPa) =	203.900	I beam (m^4) =	1.892E-09
ACC POI (m/s^2) =	1202.6	'k' beam (N/m) =	203155.779
STATIC Fy (MPa) =	399.8	Z(pl) (m^3) =	9.303E-07
DLF Fy =	1	M(pl) (Nm) =	537.044
Me BEAM(ONLY) (kg) =	6.001	R(m) (N) =	4773.722
Fr(dyn) ROD 2 (N) =	1.157	X(e) (m) =	0.0235
Fr(dyn) ROD 3 (N) =	1.067	Xm (max) =	0.0904
Fr(dyn) ROD 4 (N) =	1.157	Meb (SYSTEM) (kg) =	49.664
MAX DEFL ROD 2 (m) =	0.0850	IMPULSE (POI)(Ns) =	193.153
MAX DEFL ROD 3 (m) =	0.0860	IMP DUR 'T' (s) =	0.053529
MAX DEFL ROD 4 (m) =	0.0850	PERIOD BEAM 'Tn'(s)=	0.098240
		TIME 'Tm' (S) =	0.051324

Beam A7
Central Rod
(No 3)
(ONE 400N WEIGHT)

215 210 205 200 195 190 185 180 175 170 165 160 155 150 145 140 135 130 125 120 115 110 105 100 95 90 85 80 75 70 65 60 55 50 45 40 35 30 25 20 15 10 5 0

X E

POI

Permanent Deformation

Zero Line

Permanent Deformation Line

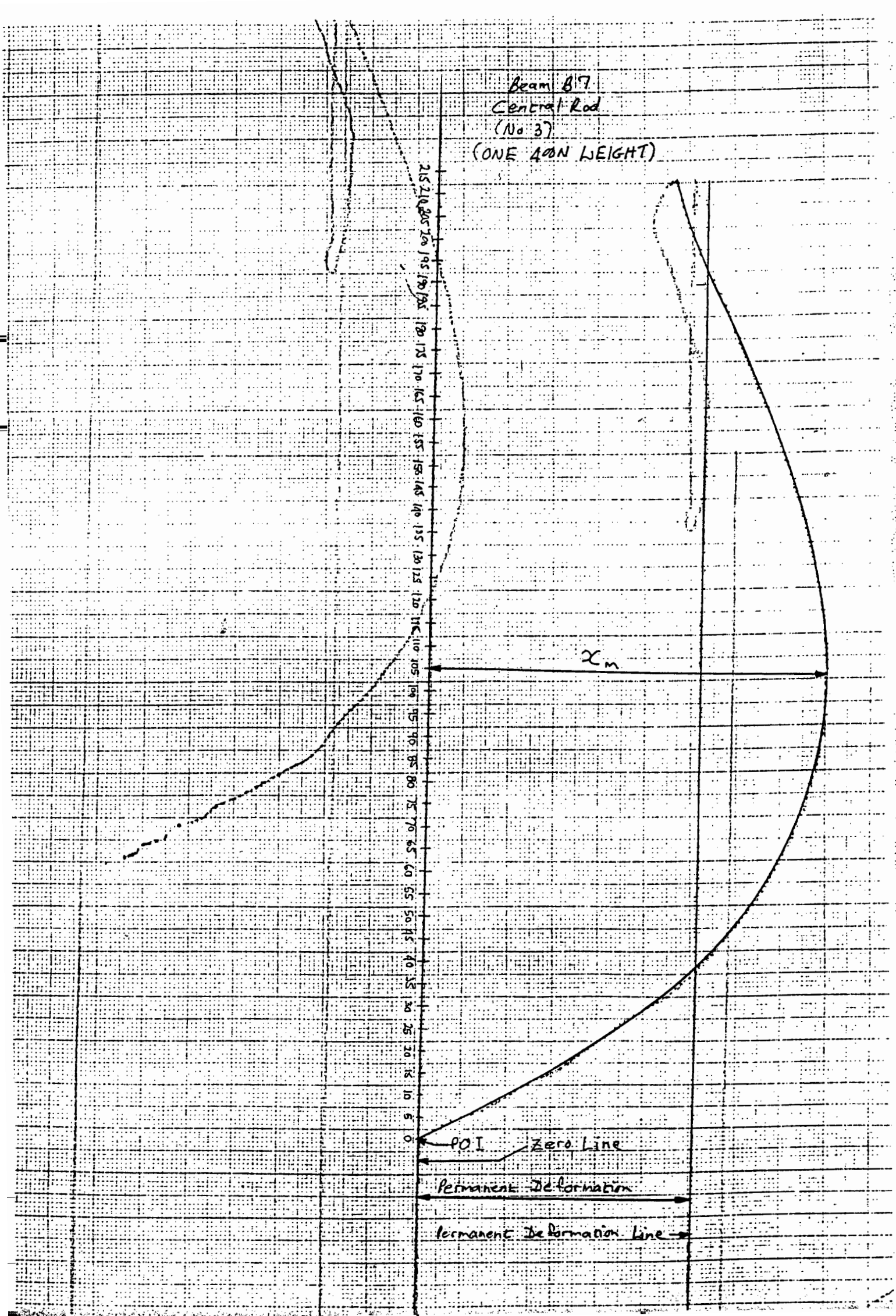
Beam B7
Central Rod
(No 3)
(ONE 400N WEIGHT)
x_m
POI
Zero Line
Permanent Deformation
Permanent Deformation Line

STEEL BEAM ENÉRGY ANALYSIS - BEAM A7 ELASTO-PLASTIC ANALYSIS
(ONE 400N WEIGHT)

INPUT		OUTPUT	
DIST POI (m) =	1.900	THETA(s) (rads) =	0.4231
M(e) PEND (kg) =	98.3	H(eff)(1) (m) =	0.3014
M(e) CHANNEL (kg) =	45.3	KE(2) (JOULS) =	290.446
L(e) (m) =	3.418	THETA(3) (rads) =	0.0274
DIST 'X' (m) =	0.007	H(eff)(3) (m) =	0.00128
L(POI) (m) =	3.877	PE(3) (JOULS) =	1.238
L(h) (m) =	3.870	FrE(TOTAL) (JOULS) =	0.258
'g' UCT (m/s^2) =	9.80	NETT E (JOULS) =	288.950
MAX DEFL (m) =	0.0833	PROP FACT 'fp' =	0.881
BEAM WIDTH (m) =	0.100	E POI (JOULS) =	254.682
BEAM THICK (m) =	0.0059	Be (N) =	6256.3
E STEEL (GPa) =	201.700	I beam (m^4) =	1.711E-09
ACC POI (m/s^2) =	1050.600	'k' beam (N/m) =	181837.890
STATIC Fy (MPa) =	322.000	Z(pl) (m^3) =	8.703E-07
DLF Fy =	1	M(pl) (Nm) =	364.287
Me BEAM(ONLY) (kg) =	5.955	R(m) (N) =	3238.104
Fr(dyn) ROD 2 (N) =	1.157	X(e) (m) =	0.0178
Fr(dyn) ROD 3 (N) =	1.067	Xm (max) =	0.0876
Fr(dyn) ROD 4 (N) =	1.157	Meb (SYSTEM) (kg) =	98.924
MAX DEFL ROD 2 (m) =	0.0730	IMPULSE (POI)(Ns) =	224.473
MAX DEFL ROD 3 (m) =	0.0833	IMP DUR 'T' (s) =	0.071759
MAX DEFL ROD 4 (m) =	0.0730	PERIOD BEAM 'Tn'(s)=	0.146551
		TIME 'Tm' (S) =	0.072517

STEEL BEAM ENERGY ANALYSIS - BEAM B7 ELASTO-PLASTIC ANALYSIS
(ONE 400N WEIGHT)

INPUT		OUTPUT	
DIST POI (m) =	2.220	THETA(s) (rads) =	0.4998
M(e) PEND (kg) =	98.3	H(eff)(1) (m) =	0.4181
M(e) CHANNEL (kg) =	45.3	KE(2) (JOULS) =	402.918
L(e) (m) =	3.418	THETA(3) (rads) =	0.0291
DIST 'X' (m) =	0.007	H(eff)(3) (m) =	0.00145
L(POI) (m) =	3.877	PE(3) (JOULS) =	1.394
L(h) (m) =	3.870	FrE(TOTAL) (JOULS) =	0.289
'g' UCT (m/s^2) =	9.80	NETT E (JOULS) =	401.235
MAX DEFL (m) =	0.0898	PROP FACT 'fp' =	0.881
BEAM WIDTH (m) =	0.100	E POI (JOULS) =	353.650
BEAM THICK (m) =	0.0061	Be (N) =	5758.7
E STEEL (GPa) =	203.900	I beam (m^4) =	1.892E-09
ACC POI (m/s^2) =	959.3	'k' beam (N/m) =	203155.779
STATIC Fy (MPa) =	399.8	Z(pl) (m^3) =	9.303E-07
DLF Fy =	1	M(pl) (Nm) =	483.488
Me BEAM(ONLY) (kg) =	6.003	R(m) (N) =	4297.672
Fr(dyn) ROD 2 (N) =	1.157	X(e) (m) =	0.0212
Fr(dyn) ROD 3 (N) =	1.067	Xm (max) (m) =	0.0929
Fr(dyn) ROD 4 (N) =	1.157	Meb (SYSTEM) (kg) =	98.972
MAX DEFL ROD 2 (m) =	0.0835	IMPULSE (POI)(Ns) =	264.580
MAX DEFL ROD 3 (m) =	0.0898	IMP DUR 'T' (s) =	0.091889
MAX DEFL ROD 4 (m) =	0.0835	PERIOD BEAM 'Tn'(s)=	0.138682
		TIME 'Tm' (S) =	0.080615

STEEL BEAM ENERGY ANALYSIS - BEAM A3 ELASTO-PLASTIC ANALYSIS
(NO WEIGHTS)

INPUT		OUTPUT	
DIST POI (m) =	3.000	THETA(s) (rads) =	0.6927
M(e) PEND (kg) =	54.3	H(eff)(1) (m) =	0.6779
M(e) CHANNEL (kg) =	45.9	KE(2) (JOULS) =	360.931
L(e) (m) =	2.941	THETA(3) (rads) =	0.0277
DIST 'X' (m) =	-0.029	H(eff)(3) (m) =	0.00113
L(POI) (m) =	3.841	PE(3) (JOULS) =	0.602
L(h) (m) =	3.870	FrE(TOTAL) (JOULS) =	0.259
'g' UCT (m/s^2) =	9.80	NETT E (JOULS) =	360.070
MAX DEFL (m) =	0.0835	PROP FACT 'fp' =	0.767
BEAM WIDTH (m) =	0.100	E POI (JOULS) =	276.337
BEAM THICK (m) =	0.0059	Be (N) =	7978.2
E STEEL (GPa) =	201.700	I beam (m^4) =	1.711E-09
ACC POI (m/s^2) =	1339.300	'k' beam (N/m) =	181837.890
STATIC Fy (MPa) =	322.000	Z(pl) (m^3) =	8.703E-07
DLF Fy =	1	M(pl) (Nm) =	403.518
Me BEAM(ONLY) (kg) =	5.957	R(m) (N) =	3586.822
Fr(dyn) ROD 2 (N) =	1.157	X(e) (m) =	0.0197
Fr(dyn) ROD 3 (N) =	1.067	Xm (max) =	0.0869
Fr(dyn) ROD 4 (N) =	1.157	Meb (SYSTEM) (kg) =	49.620
MAX DEFL ROD 2 (m) =	0.0735	IMPULSE (POI)(Ns) =	165.601
MAX DEFL ROD 3 (m) =	0.0835	IMP DUR 'T' (s) =	0.041513
MAX DEFL ROD 4 (m) =	0.0735	PERIOD BEAM 'Tn'(s)=	0.103793
		TIME 'Tm' (S) =	0.046705

STEEL BEAM ENERGY ANALYSIS - BEAM B2 ELASTO-PLASTIC ANALYSIS
(NO WEIGHTS)

INPUT		OUTPUT	
DIST POI (m) =	3.500	THETA(s) (rads) =	0.8136
M(e) PEND (kg) =	54.3	H(eff)(1) (m) =	0.9209
M(e) CHANNEL (kg) =	45.9	KE(2) (JOULS) =	490.334
L(e) (m) =	2.941	THETA(3) (rads) =	0.0284
DIST 'X' (m) =	-0.029	H(eff)(3) (m) =	0.00118
L(POI) (m) =	3.841	PE(3) (JOULS) =	0.630
L(h) (m) =	3.870	FrE(TOTAL) (JOULS) =	0.288
'g' UCT (m/s^2) =	9.80	NETT E (JOULS) =	489.415
MAX DEFL (m) =	0.0860	PROP FACT 'fp' =	0.767
BEAM WIDTH (m) =	0.100	E POI (JOULS) =	375.604
BEAM THICK (m) =	0.0061	Be (N) =	7216.8
E STEEL (GPa) =	203.900	I beam (m^4) =	1.892E-09
ACC POI (m/s^2) =	1202.6	'k' beam (N/m) =	203155.779
STATIC Fy (MPa) =	399.8	Z(pl) (m^3) =	9.303E-07
DLF Fy =	1	M(pl) (Nm) =	537.044
Me BEAM(ONLY) (kg) =	6.001	R(m) (N) =	4773.722
Fr(dyn) ROD 2 (N) =	1.157	X(e) (m) =	0.0235
Fr(dyn) ROD 3 (N) =	1.067	Xm (max) =	0.0904
Fr(dyn) ROD 4 (N) =	1.157	Meb (SYSTEM) (kg) =	49.664
MAX DEFL ROD 2 (m) =	0.0850	IMPULSE (POI)(Ns) =	193.153
MAX DEFL ROD 3 (m) =	0.0860	IMP DUR 'T' (s) =	0.053529
MAX DEFL ROD 4 (m) =	0.0850	PERIOD BEAM 'Tn'(s)=	0.098240
		TIME 'Tm' (S) =	0.051324

IMPACT CALCULATIONS PLASTIC ANALYSIS STEEL BEAM A3

DISTANCE BOARD FALLEN BEFORE IMPACT =	0 130	m	THETA INSWING (RADS) =	0 6280
ACCELERATION OF FALLING BOARD =	9 72	m/S ^ 2	THETA BACKSWING (RADS) =	0 1901
VALUE OF g AT UCT =	9 80	m/s ^ 2	EFF HT OF PENDULUM (m) =	0 561
EFFECTIVE MASS OF PENDULUM =	63 100	kg	EFF VEL OF PENDULUM (m/s) =	3 316
EFFECTIVE LENGTH OF PENDULUM =	2 941	m	VEL OF PEND (POI) (m/s) =	4 812
DISTANCE 'X' =	0 397	m	ACCEL OF BEAM (m/s ^ 2) =	1339 3
LENGTH TO IMPACT =	4 267	m	FORCE 'Be' (N) =	5498 9
LENGTH FROM PIN TO HAMMER =	3 870	m		
PERIOD OF PENDULUM =	3 440	seconds		
EFFECTIVE MASS BEAM ETC =	5 957	kg		
DIST OF RELEASE FROM POI =	3 000	m		

DISTANCE FROM POI (mm)	DEFLECTION X (mm)	TIME BOARD FALLEN (seconds)	VELOCITY OF BOARD (m/s)	CORRECTION FACTOR	CORRECTED DST FROM POI (mm)	VELOCITY OF HAMMER & BEAM (m/s)	ACCELERATION HAMMER & BEAM (m/s ^ 2)	TIME (t) (seconds)
0	0 0	0 1636	1 590	1 0000	0 0	4 812	1339 297	0 0000
5	13 0	0 1667	1 620	0 9813	4 9	3 725	292.491	0 0031
10	23 0	0.1697	1 650	0 9636	9.6	3 216	35 465	0 0062
15	32 5	0 1727	1 679	0 9469	14 2	2.854	208 930	0 0092
20	40 0	0.1757	1 708	0 9309	18 6	2 356	126 525	0 0121
25	46.3	0 1786	1 736	0 9158	22 9	2 117	36 343	0 0150
30	52 2	0.1814	1 764	0 9014	27.0	1 922	101 359	0 0179
35	57.2	0 1843	1 791	0 8876	31 1	1 844	-48 496	0 0207
40	62.5	0.1870	1.818	0 8745	35.0	1 690	162.782	0 0235
45	66 5	0 1898	1 844	0 8619	38 8	1.475	-7 776	0 0262
50	70 5	0.1925	1 871	0 8498	42.5	1 309	133 144	0 0289
55	73 5	0 1951	1 896	0 8383	46 1	1 138	-5 832	0 0316
60	76 5	0 1977	1 922	0 8272	49.6	0 961	142 865	0 0342
65	78 5	0 2003	1 947	0 8165	53 1	0 779	-3 888	0 0368
70	80.5	0 2029	1 972	0 8062	56 4	0 591	152 586	0 0393
75	81 5	0.2054	1 996	0 7963	59.7	0.399	-1 944	0 0418
80	82.6	0 2079	2 020	0 7868	62 9	0 343	47 331	0 0443
85	83 2	0 2103	2 044	0 7776	66 1	0 204	65 895	0 0468
90	83 5	0 2128	2.068	0 7687	69.2	0.000	102 633	0 0492
95	83.2	0 2152	2.091	0 7601	72.2	-0 146	18 175	0 0516
100	82 8	0 2175	2 115	0.7518	75 2	-0 254	72 699	0 0540
105	82.0	0 2199	2.137	0 7438	78 1	-0 385	38 294	0 0563
110	81 0	0 2222	2 160	0 7360	81.0	-0 475	39 460	0 0587
115	79 8	0 2245	2 182	0 7284	83 8	-0 677	136 361	0 0610
120	77 9	0 2268	2.205	0 7211	86.5	-0 794	-35 378	0 0633
125	76 2	0 2291	2 226	0 7140	89 3	-0 801	43 154	0 0655
130	74 3	0 2313	2 248	0 7071	91 9	-0 944	84 947	0 0677
135	72 0	0 2335	2 270	0.7004	94 6	-1 089	45 876	0 0700
140	69 5	0.2357	2 291	0 6939	97.1	-1 260	110 315	0 0722
145	66 5	0 2379	2 312	0 6876	99.7	-1 341	-37 128	0 0743
150	63.7	0.2400	2 333	0 6814	102 2	-1 330	27 312	0 0765
155	60 8	0 2422	2 354	0 6754	104 7	-1 224	-127 908	0 0786
160	58 5	0 2443	2 374	0 6695	107 1	-1 258	162 996	0 0807
165	55 5	0 2464	2.395	0 6638	109 5	-1.269	-155 414	0 0828
170	53 2	0 2485	2.415	0 6583	111 9	-1 106	78 368	0 0849

IMPACT CALCULATIONS PLASTIC ANALYSIS STEEL BEAM B2

DISTANCE BOARD FALLEN BEFORE IMPACT=	0.132	m
ACCELERATION OF FALLING BOARD =	9.72	m/S ^ 2
VALUE OF g AT UCT =	9.80	m/s ^ 2
EFFECTIVE MASS OF PENDULUM =	63.100	kg
EFFECTIVE LENGTH OF PENDULUM =	2.941	m
DISTANCE 'X' =	0.397	m
LENGTH TO IMPACT =	4.267	m
LENGTH FROM PIN TO HAMMER =	3.870	m
PERIOD OF PENDULUM =	3.440	seconds
EFFECTIVE MASS BEAM ETC =	5.957	kg
DIST OF RELEASE FROM POI =	3.500	m

THETA INSWING (RADS) =	0.7376
THETA BACKSWING (RADS) =	0.2943
EFF HT OF PENDULUM (m) =	0.7644
EFF VEL OF PENDULUM (m/s) =	3.871
VEL OF PEND (POI) (m/s) =	5.616
ACCEL OF BEAM (m/s ^ 2) =	1202.6
FORCE 'Be' (N) =	4937.9

DISTANCE FROM POI (mm)	DEFLECTION X (mm)	TIME BOARD FALLEN (seconds)	VELOCITY OF BOARD (m/s)	CORRECTION FACTOR	CORRECTED DST FROM POI (mm)	VELOCITY OF HAMMER & BEAM (m/s)	ACCELERATION HAMMER & BEAM (m/s ^ 2)	TIME (t) (seconds)
0	0.0	0.1648	1.602	1.0000	0.0	5.616	1202.649	0.0000
5	11.5	0.1679	1.632	0.9816	4.9	3.671	31.382	0.0031
10	22.5	0.1709	1.661	0.9641	9.6	3.738	-77.067	0.0061
15	34.0	0.1739	1.690	0.9476	14.2	3.549	208.153	0.0091
20	43.6	0.1768	1.719	0.9319	18.6	2.956	195.990	0.0120
25	51.2	0.1797	1.747	0.9169	22.9	2.446	157.276	0.0149
30	57.5	0.1826	1.775	0.9027	27.1	2.271	-37.631	0.0178
35	64.0	0.1854	1.802	0.8891	31.1	1.982	248.983	0.0206
40	68.5	0.1881	1.829	0.8760	35.0	1.499	99.010	0.0233
45	72.2	0.1908	1.855	0.8636	38.9	1.391	-21.051	0.0260
50	76.0	0.1935	1.881	0.8516	42.6	1.185	177.831	0.0287
55	78.5	0.1962	1.907	0.8402	46.2	0.953	-4.860	0.0314
60	81.0	0.1988	1.932	0.8292	49.7	0.773	145.392	0.0340
65	82.6	0.2013	1.957	0.8186	53.2	0.587	-2.916	0.0365
70	84.0	0.2039	1.982	0.8084	56.6	0.495	76.099	0.0391
75	85.0	0.2064	2.006	0.7985	59.9	0.301	79.015	0.0416
80	85.5	0.2089	2.030	0.7891	63.1	0.203	-0.972	0.0441
85	86.0	0.2113	2.054	0.7799	66.3	0.000	168.722	0.0465
90	85.5	0.2137	2.077	0.7711	69.4	-0.166	-33.745	0.0489
95	85.2	0.2161	2.101	0.7626	72.4	-0.210	71.572	0.0513
100	84.5	0.2185	2.124	0.7543	75.4	-0.425	110.176	0.0537
105	83.2	0.2208	2.146	0.7463	78.4	-0.580	21.052	0.0560
110	81.8	0.2231	2.169	0.7385	81.2	-0.694	78.376	0.0583
115	80.0	0.2254	2.191	0.7310	84.1	-0.855	61.407	0.0606
120	77.9	0.2277	2.213	0.7237	86.8	-1.062	122.230	0.0629
125	75.2	0.2300	2.235	0.7167	89.6	-1.140	-54.992	0.0652
130	72.8	0.2322	2.257	0.7098	92.3	-1.286	188.886	0.0674
135	69.5	0.2344	2.278	0.7031	94.9	-1.481	-14.443	0.0696
140	66.3	0.2366	2.299	0.6966	97.5	-1.610	133.700	0.0718
145	62.5	0.2387	2.321	0.6903	100.1	-1.740	-14.248	0.0739
150	58.8	0.2409	2.341	0.6842	102.6	-1.850	117.314	0.0761
155	54.6	0.2430	2.362	0.6782	105.1	-1.960	-14.248	0.0782
160	50.5	0.2451	2.383	0.6724	107.6	-1.945	7.188	0.0803

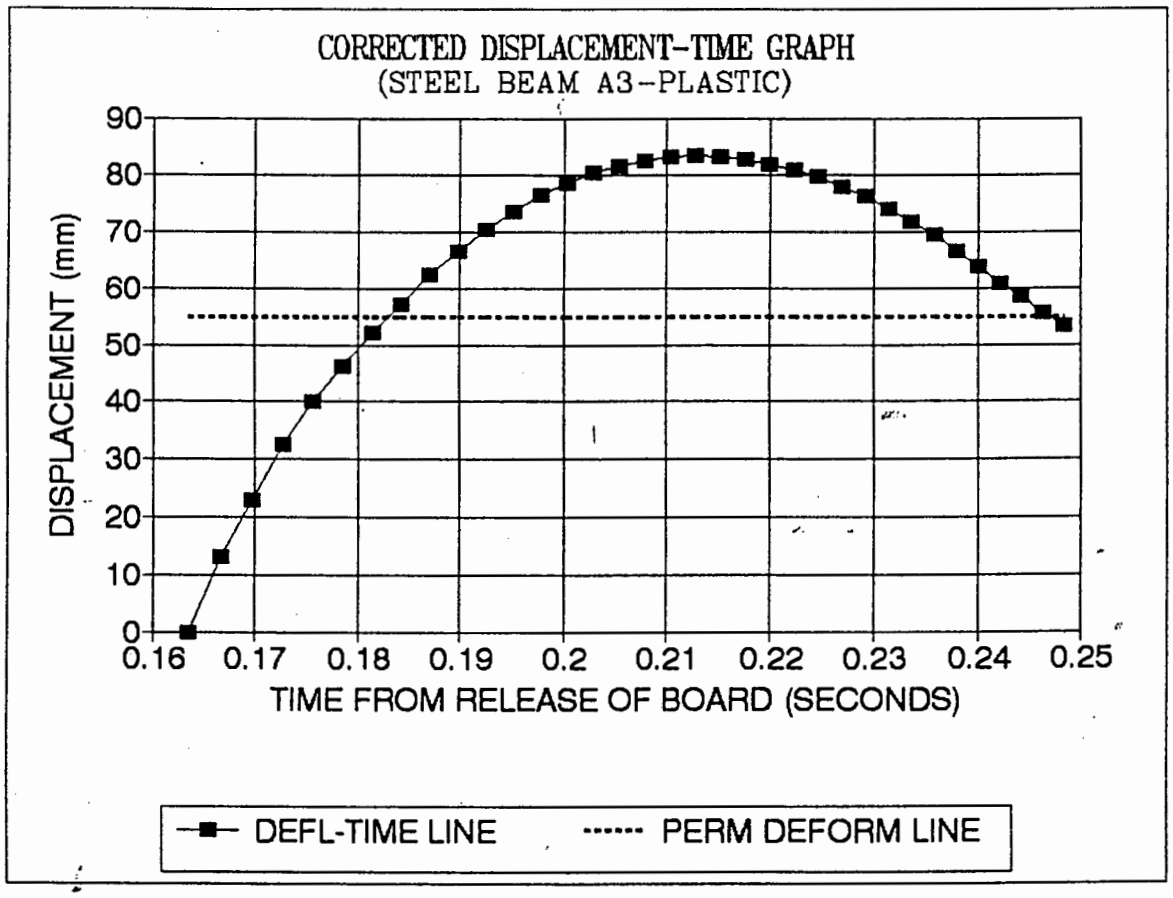
CORRECTED DISPLACEMENT-TIME GRAPH
(STEEL BEAM A3-PLASTIC)
DISPLACEMENT (mm)
90
80
70
60
50
40
30
20
10
0
0.16
0.17
0.18
0.19
0.2
0.21
0.22
0.23
0.24
0.25
TIME FROM RELEASE OF BOARD (SECONDS)
DEFL-TIME LINE
PERM DEFORM LINE

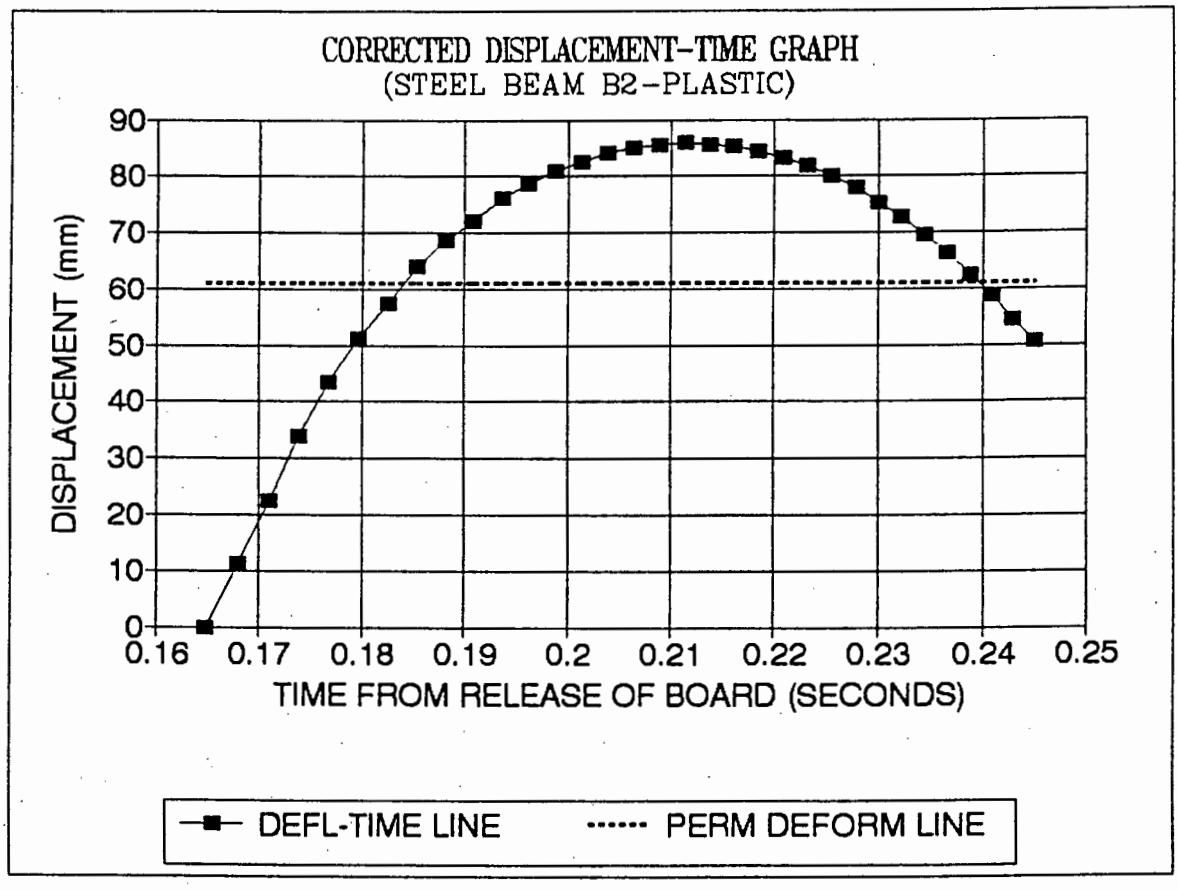
CORRECTED DISPLACEMENT-TIME GRAPH
(STEEL BEAM B2-PLASTIC)
DISPLACEMENT (mm)
90
80
70
60
50
40
30
20
10
0
0.16
0.17
0.18
0.19
0.2
0.21
0.22
0.23
0.24
0.25
TIME FROM RELEASE OF BOARD (SECONDS)
DEFL-TIME LINE
PERM DEFORM LINE

IMPACT CALCULATIONS PLASTIC ANALYSIS STEEL BEAM A7 - ONE 400N WEIGHT

DISTANCE BOARD FALLEN BEFORE IMPACT=	0.115	m	THETA INSWING (RADS) =	0.3819
ACCELERATION OF FALLING BOARD =	9.72	m/S^2	THETA BACKSWING (RADS) =	0.1890
VALUE OF g AT UCT =	9.80	m/s^2	EFF HT OF PENDULUM (m) =	0.2462
EFFECTIVE MASS OF PENDULUM =	102.900	kg	EFF VEL OF PENDULUM (m/s) =	2.1967
EFFECTIVE LENGTH OF PENDULUM =	3.418	m	VEL OF PEND (POI) (m/s) =	2.6968
DISTANCE 'X' =	0.326	m	ACCEL OF BEAM (m/s^2) =	1050.6
LENGTH TO IMPACT =	4.196	m	FORCE 'Be' (N) =	5098.1
LENGTH FROM PIN TO HAMMER =	3.870	m		
PERIOD OF PENDULUM =	3.709	seconds		
EFFECTIVE MASS BEAM ETC =	5.957	kg		
DIST OF RELEASE FROM POI =	1.850	m		

DISTANCE FROM POI (mm)	DEFLECTION X (mm)	TIME BOARD FALLEN (seconds)	VELOCITY OF BOARD (m/s)	CORRECTION FACTOR	CORRECTED DST FROM POI (mm)	VELOCITY OF PENDULUM (m/s)	ACCELERATION OF PENDULUM (m/s^2)	TIME (t) (seconds)
0	0.0	0.1638	1.495	1.0000	0.0	2.697	1050.613	0.0000
5	11.5	0.1571	1.527	0.9789	4.9	3.130	213.278	0.0033
10	20.5	0.1604	1.559	0.9592	9.6	2.494	178.790	0.0065
15	27.5	0.1636	1.590	0.9405	14.1	2.225	-13.608	0.0097
20	34.5	0.1667	1.620	0.9230	18.5	2.025	145.273	0.0128
25	40.0	0.1697	1.650	0.9063	22.7	1.814	-10.692	0.0159
30	45.5	0.1727	1.679	0.8906	26.7	1.763	46.157	0.0189
35	50.5	0.1757	1.708	0.8756	30.6	1.707	-9.720	0.0219
40	55.5	0.1786	1.736	0.8614	34.5	1.562	111.756	0.0248
45	59.5	0.1814	1.764	0.8478	38.2	1.411	-7.776	0.0276
50	63.5	0.1843	1.791	0.8348	41.7	1.343	56.851	0.0304
55	67.0	0.1870	1.818	0.8225	45.2	1.272	-6.804	0.0332
60	70.5	0.1898	1.844	0.8106	48.6	1.107	130.227	0.0359
65	73.0	0.1925	1.871	0.7993	52.0	0.879	37.416	0.0386
70	75.2	0.1951	1.896	0.7884	55.2	0.758	53.647	0.0413
75	77.0	0.1977	1.922	0.7780	58.3	0.692	-3.499	0.0439
80	78.8	0.2003	1.947	0.7679	61.4	0.584	88.052	0.0465
85	80.0	0.2029	1.972	0.7583	64.5	0.434	28.962	0.0490
90	81.0	0.2054	1.996	0.7490	67.4	0.359	30.128	0.0516
95	81.8	0.2079	2.020	0.7400	70.3	0.303	14.870	0.0540
100	82.5	0.2103	2.044	0.7314	73.1	0.245	32.267	0.0565
105	83.0	0.2128	2.068	0.7230	75.9	0.165	33.433	0.0589
110	83.3	0.2152	2.091	0.7149	78.6	0.000	104.966	0.0613
115	83.0	0.2175	2.115	0.7071	81.3	-0.106	-17.397	0.0637
120	82.8	0.2199	2.137	0.6995	83.9	-0.171	73.866	0.0661
125	82.2	0.2222	2.160	0.6922	86.5	-0.281	19.924	0.0684
130	81.5	0.2245	2.182	0.6851	89.1	-0.306	1.361	0.0707
135	80.8	0.2268	2.205	0.6782	91.6	-0.485	157.647	0.0730
140	79.3	0.2291	2.228	0.6716	94.0	-0.445	-198.330	0.0752
145	78.8	0.2313	2.248	0.6651	96.4	-0.472	224.419	0.0775
150	77.2	0.2335	2.270	0.6588	98.8	-0.681	-38.294	0.0797
155	75.8	0.2357	2.291	0.6526	101.2	-0.664	23.813	0.0819
160	74.3	0.2379	2.312	0.6467	103.5	-0.647	-40.044	0.0840
165	73.0	0.2400	2.333	0.6409	105.7	-0.770	155.608	0.0862
170	71.0	0.2422	2.354	0.6352	108.0	-0.824	-107.400	0.0883
175	69.5	0.2443	2.374	0.6297	110.2	-0.760	48.209	0.0904
180	67.8	0.2464	2.396	0.6244	112.4	-0.898	72.410	0.0925
185	65.8	0.2485	2.415	0.6191	114.5	-0.918	-42.960	0.0946
190	64.0	0.2505	2.435	0.6140	116.7	-0.877	3.499	0.0967
195	62.2	0.2526	2.455	0.6091	118.8	-0.908	27.701	0.0987
200	60.3	0.2546	2.475	0.6042	120.8	-0.916	-20.997	0.1008
205	58.5	0.2566	2.494	0.5995	122.9	-1.072	178.354	0.1028
210	56.0	0.2586	2.514	0.5948	124.9	-1.252	-89.876	0.1048

IMPACT CALCULATIONS PLASTIC ANALYSIS STEEL BEAM B7 - ONE 400N WEIGHT

DISTANCE BOARD FALLEN BEFORE IMPACT=	0.115	m	THETA INSWING (RADS) =	0.4643
ACCELERATION OF FALLING BOARD =	9.72	m/S^2	THETA BACKSWING (RADS) =	0.1838
VALUE OF g AT UCT =	9.80	m/s^2	EFF HT OF PENDULUM (m) =	0.382
EFFECTIVE MASS OF PENDULUM =	102.900	kg	EFF VEL OF PENDULUM (m/s) =	2.663
EFFECTIVE LENGTH OF PENDULUM =	3.418	m	VEL OF PEND (POI) (m/s) =	3.269
DISTANCE 'X' =	0.326	m	ACCEL OF BEAM (m/s^2) =	959.3
LENGTH TO IMPACT =	4.198	m	FORCE 'Be' (N) =	4689.2
LENGTH FROM PIN TO HAMMER =	3.870	m		
PERIOD OF PENDULUM =	3.709	seconds		
EFFECTIVE MASS BEAM ETC =	6.001	kg		
DIST OF RELEASE FROM POI =	2.220	m		

DISTANCE FROM POI (mm)	DEFLECTION X (mm)	TIME BOARD FALLEN (seconds)	VELOCITY OF BOARD (m/s)	CORRECTION FACTOR	CORRECTED DST FROM POI (mm)	VELOCITY OF PENDULUM (m/s)	ACCELERATION OF PENDULUM (m/s^2)	TIME (t) (seconds)
0	0.0	0.1538	1.495	1.0000	0.0	3.269	959.255	0.0000
5	10.5	0.1571	1.527	0.9789	4.9	2.749	262.349	0.0033
10	18.0	0.1604	1.559	0.9592	9.6	2.572	-161.794	0.0065
15	27.0	0.1638	1.590	0.9405	14.1	2.702	84.538	0.0097
20	35.0	0.1667	1.620	0.9230	18.6	2.430	90.369	0.0128
25	42.0	0.1697	1.650	0.9063	22.7	2.309	-13.608	0.0159
30	49.0	0.1727	1.679	0.8906	26.7	2.266	43.241	0.0189
35	55.5	0.1757	1.708	0.8758	30.6	2.015	128.469	0.0219
40	60.8	0.1788	1.736	0.8614	34.5	1.736	62.583	0.0248
45	65.5	0.1814	1.764	0.8478	38.2	1.587	41.009	0.0276
50	69.8	0.1843	1.791	0.8348	41.7	1.379	107.969	0.0304
55	73.2	0.1870	1.818	0.8225	45.2	1.254	-19.924	0.0332
60	76.7	0.1898	1.844	0.8106	48.6	1.162	89.118	0.0359
65	79.5	0.1925	1.871	0.7993	52.0	0.954	65.017	0.0386
70	81.8	0.1951	1.896	0.7884	55.2	0.853	10.010	0.0413
75	84.0	0.1977	1.922	0.7780	58.3	0.711	99.811	0.0439
80	85.5	0.2003	1.947	0.7679	61.4	0.623	-33.433	0.0465
85	87.2	0.2029	1.972	0.7583	64.5	0.532	106.227	0.0490
90	88.2	0.2054	1.996	0.7490	67.4	0.359	30.128	0.0516
95	89.0	0.2079	2.020	0.7400	70.3	0.263	47.720	0.0540
100	89.5	0.2103	2.044	0.7314	73.1	0.164	32.656	0.0565
105	89.8	0.2128	2.068	0.7230	75.9	0.000	102.633	0.0589
110	89.5	0.2152	2.091	0.7149	78.6	-0.125	0.583	0.0613
115	89.2	0.2175	2.115	0.7071	81.3	-0.211	72.505	0.0637
120	88.5	0.2199	2.137	0.6995	83.9	-0.299	1.361	0.0661
125	87.8	0.2222	2.160	0.6922	86.5	-0.367	57.635	0.0684
130	86.8	0.2245	2.182	0.6851	89.1	-0.546	97.679	0.0707
135	85.3	0.2268	2.205	0.6782	91.6	-0.617	-36.155	0.0730
140	84.0	0.2291	2.226	0.6716	94.0	-0.623	42.376	0.0752
145	82.5	0.2313	2.248	0.6651	96.4	-0.674	2.916	0.0775
150	81.0	0.2335	2.270	0.6588	98.8	-0.840	147.832	0.0797
155	78.8	0.2357	2.291	0.6526	101.2	-0.916	-80.087	0.0819
160	77.0	0.2379	2.312	0.6467	103.5	-0.879	46.459	0.0840
165	75.0	0.2400	2.333	0.6409	105.7	-0.980	47.625	0.0862
170	72.8	0.2422	2.354	0.6352	108.0	-1.130	93.307	0.0883
175	70.2	0.2443	2.374	0.6297	110.2	-1.092	-130.824	0.0904
180	68.2	0.2464	2.395	0.6244	112.4	-1.054	96.029	0.0925
185	65.8	0.2485	2.415	0.6191	114.5	-1.256	98.362	0.0946
190	63.0	0.2505	2.435	0.6140	116.7	-1.217	-137.434	0.0967
195	60.8	0.2526	2.455	0.6091	118.8	-0.982	-92.530	0.0987
200	59.0	0.2546	2.475	0.6042	120.8	-0.887	46.639	0.1008

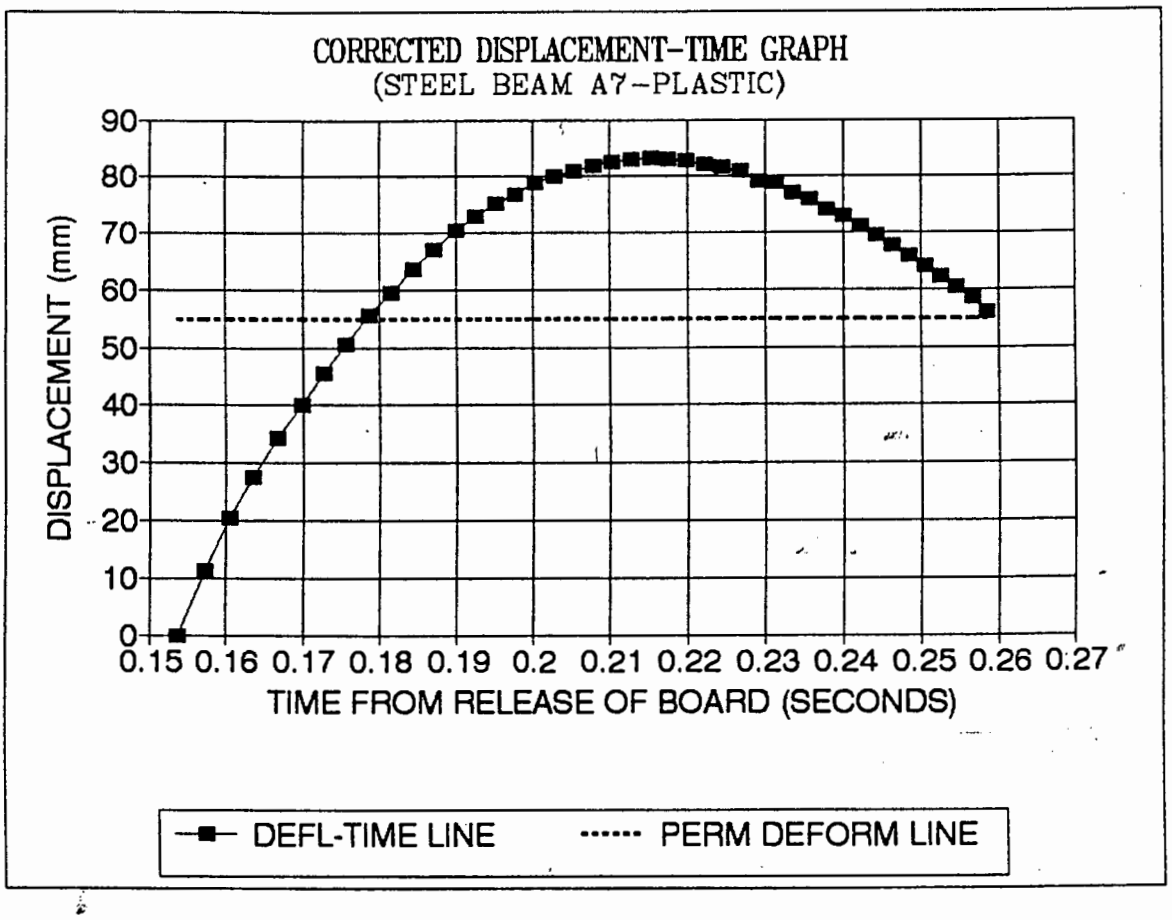
CORRECTED DISPLACEMENT-TIME GRAPH
(STEEL BEAM A7-PLASTIC)
DISPLACEMENT (mm)
0
10
20
30
40
50
60
70
80
90
0.15 0.16 0.17 0.18 0.19 0.2 0.21 0.22 0.23 0.24 0.25 0.26 0.27
TIME FROM RELEASE OF BOARD (SECONDS)
DEFL-TIME LINE
PERM DEFORM LINE

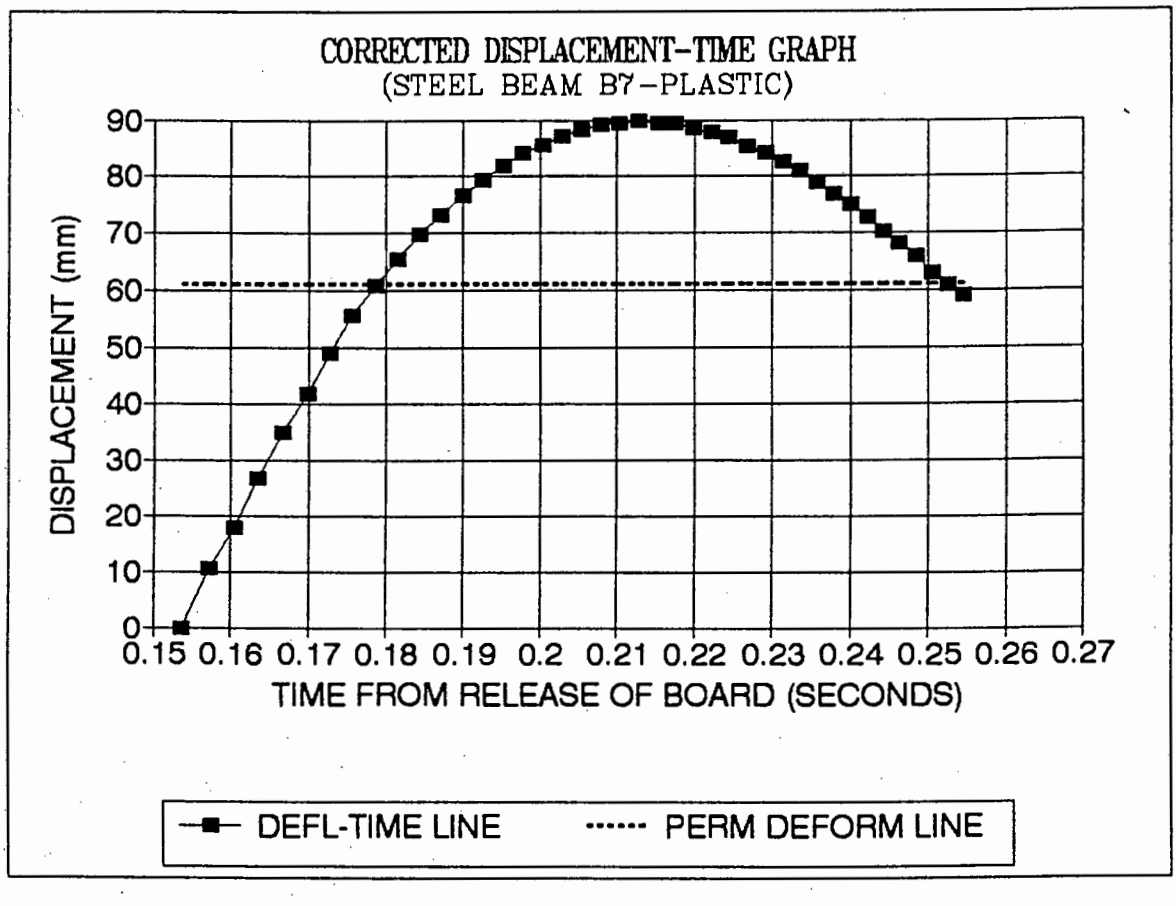
CORRECTED DISPLACEMENT-TIME GRAPH
(STEEL BEAM B7-PLASTIC)
DISPLACEMENT (mm)
0
10
20
30
40
50
60
70
80
90
0.15 0.16 0.17 0.18 0.19 0.2 0.21 0.22 0.23 0.24 0.25 0.26 0.27
TIME FROM RELEASE OF BOARD (SECONDS)
DEFL-TIME LINE
PERM DEFORM LINE

A P P E N D I X D

CONCRETE BEAMS

CB7

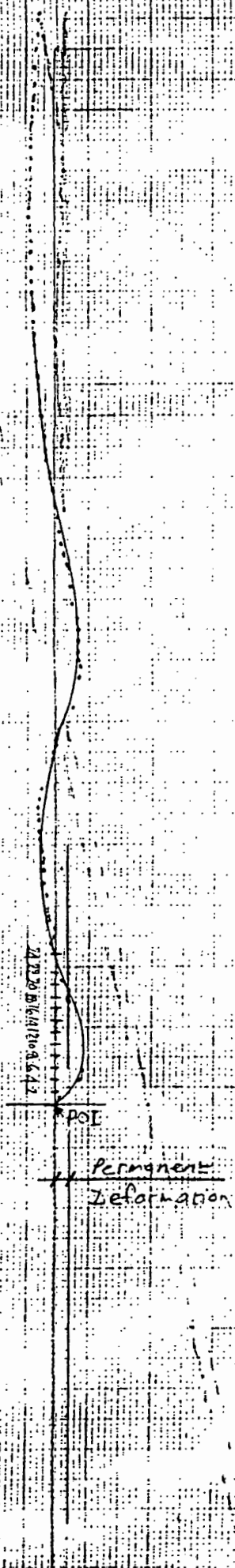

Beam CB7
(Rod 3)
(NO WEIGHTS)

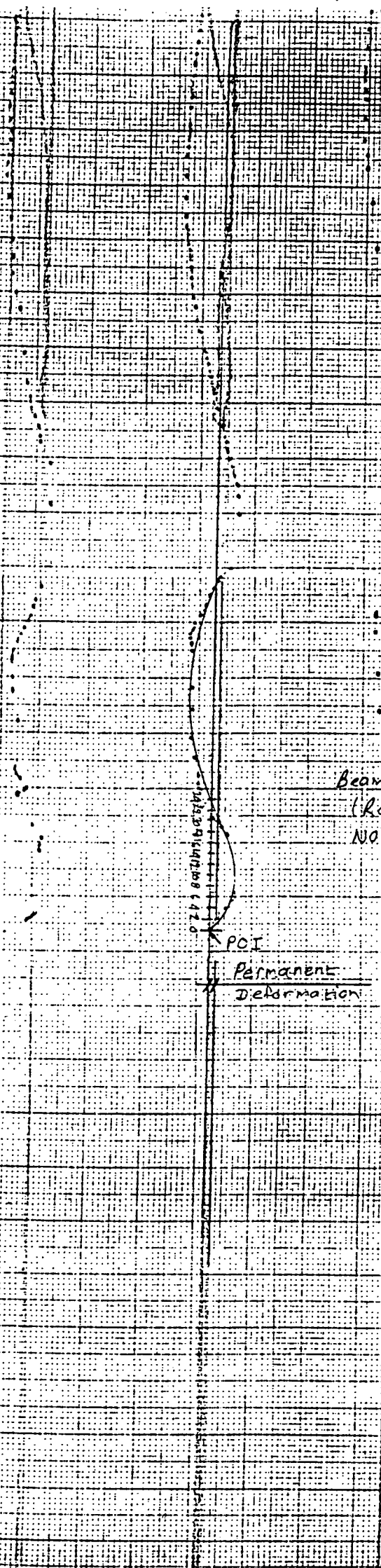
Beam CB9
(Rod 3)
NO WEIGHTS
0.247 Buckling
POI
Permanent
Deformation

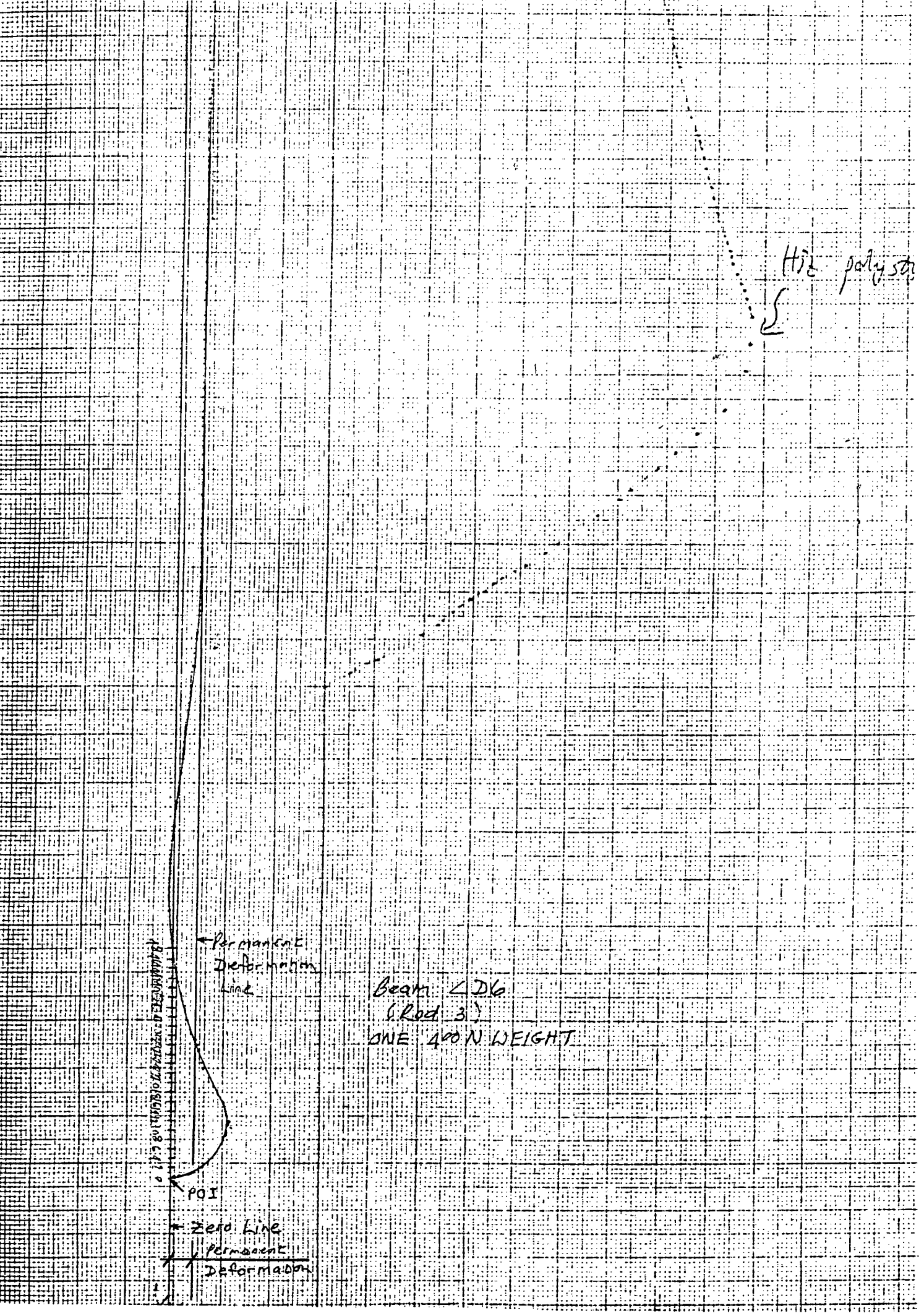
Hit polyst
Permanent Deformation Line
Beam ∠ DG (Rod 3)
ONE 400 N WEIGHT
POI
Zero Line
Permanent Deformation

IMPACT CALCULATIONS PLASTIC ANALYSIS REINFORCED CONCRETE BEAM CB7

DISTANCE BOARD FALLEN BEFORE IMPACT =	0.151	m
ACCELERATION OF FALLING BOARD =	9 72	m/S ^ 2
VALUE OF g AT UCT =	9 80	m/s ^ 2
EFFECTIVE MASS OF PENDULUM =	63.100	kg
EFFECTIVE LENGTH OF PENDULUM =	2.941	m
DISTANCE 'X' =	0.397	m
LENGTH TO IMPACT =	4.267	m
LENGTH FROM PIN TO HAMMER =	3 870	m
PERIOD OF PENDULUM =	3.440	seconds
EFFECTIVE MASS BEAM ETC =	7 521	kg
DIST OF RELEASE FROM POI =	2.600	m

THETA INSWING (RADS) =	0.5403
THETA BACKSWING (RADS) =	0.1835
EFF HT OF PENDULUM (m) =	0.419
EFF VEL OF PENDULUM (m/s) =	2 866
VEL OF PEND (POI) (m/s) =	4.158
ACCEL OF BEAM (m/s ^ 2) =	1699 0
FORCE 'Be' (N) =	83254.0

DISTANCE FROM POI (mm)	DEFLECTION X (mm)	TIME BOARD FALLEN (seconds)	VELOCITY OF BOARD (m/s)	CORRECTION FACTOR	CORRECTED DST FROM POI (mm)	VELOCITY OF HAMMER & BEAM (m/s)	ACCELERATION HAMMER & BEAM (m/s ^ 2)	TIME (t) (seconds)
0	0.0	0.1763	1.713	1 0000	0 0	4.168	1699.038	0 0000
2	2.3	0.1774	1.725	0 9934	2.0	1 552	734.808	0 0012
4	3.6	0.1786	1.736	0.9870	3.9	0 825	522.677	0 0023
6	4.2	0.1797	1.747	0.9807	5 9	0 437	150 169	0 0035
8	4 6	0 1809	1 758	0 9745	7 8	0 264	163.085	0 0046
10	4 8	0.1820	1 769	0 9684	9.7	0.000	312.975	0.0057
12	4.6	0 1831	1.780	0 9625	11.5	-0 312	239.348	0.0069
14	4.1	0.1843	1 791	0.9566	13.4	-0.493	82.861	0 0080
16	3.5	0 1854	1 802	0.9509	15.2	-0.586	84 319	0.0091
18	2 8	0 1865	1 813	0 9452	17 0	-0.725	168.152	0 0102
20	1 9	0.1876	1.823	0.9397	18 8	-0.820	4.374	0.0113
22	1 0	0.1887	1 834	0 9343	20 6	-0.995	421.354	0 0124
23.5	0 0	0.1895	1.842	0.9302	21.9	-1.226	-282.329	0.0132

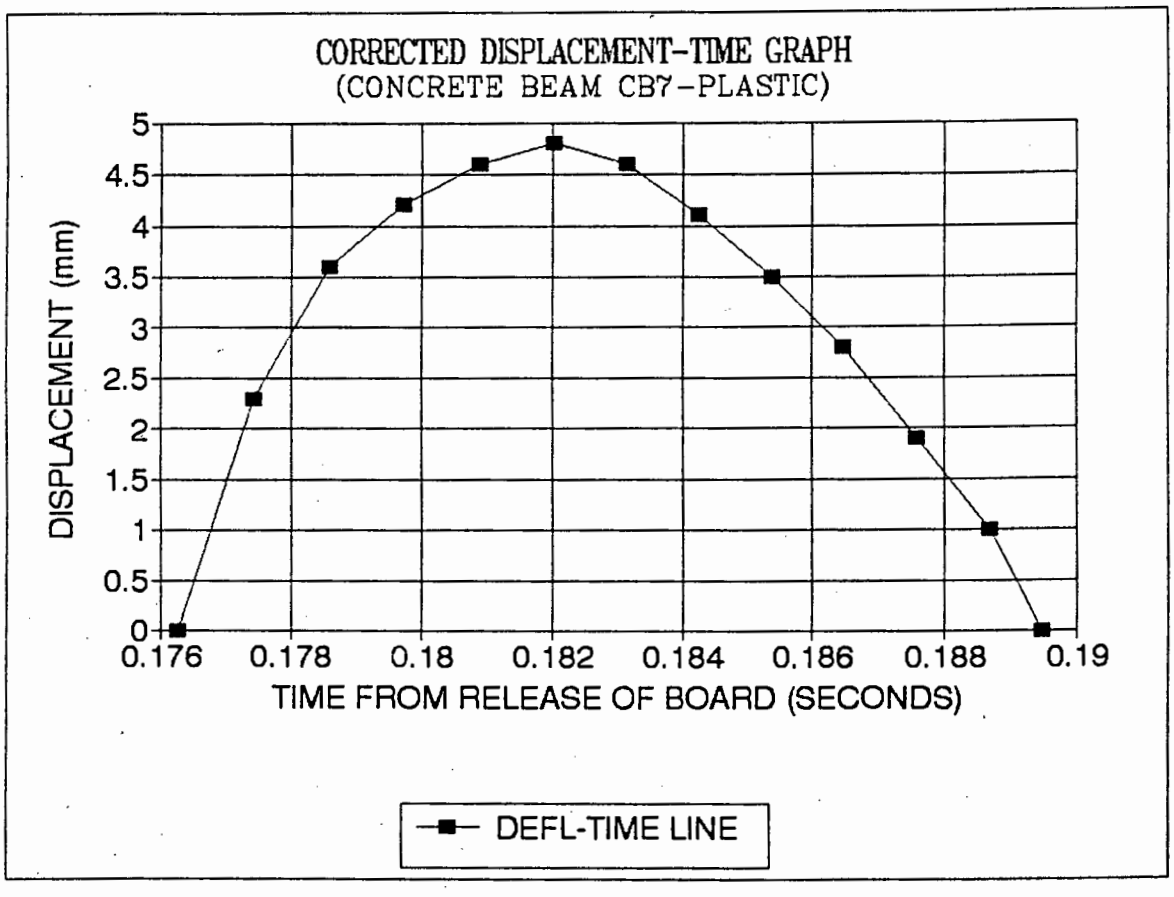

IMPACT CALCULATIONS

PLASTIC ANALYSIS

REINFORCED CONCRETE BEAM CB9
(ONE 400N WEIGHT)

DISTANCE BOARD FALLEN BEFORE IMPACT =	0.156	m
ACCELERATION OF FALLING BOARD =	9.72	m/S ^ 2
VALUE OF g AT UCT =	9.80	m/s ^ 2
EFFECTIVE MASS OF PENDULUM =	102.900	kg
EFFECTIVE LENGTH OF PENDULUM =	3.418	m
DISTANCE 'X' =	0.326	m
LENGTH TO IMPACT =	4.196	m
LENGTH FROM PIN TO HAMMER =	3.870	m
PERIOD OF PENDULUM =	3.709	seconds
EFFECTIVE MASS BEAM ETC =	7.525	kg
DIST OF RELEASE FROM POI =	3.600	m

THETA INSWING (RADS) =	0.7715
THETA BACKSWING (RADS) =	0.1500
EFF HT OF PENDULUM (m) =	0.968
EFF VEL OF PENDULUM (m/s) =	4.355
VEL OF PEND (POI) (m/s) =	5.347
ACCEL OF BEAM (m/s ^ 2) =	1526.0
FORCE 'Be' (N) =	136943.4

DISTANCE FROM POI (mm)	DEFLECTION X (mm)	TIME BOARD FALLEN (seconds)	VELOCITY OF BOARD (m/s)	CORRECTION FACTOR	CORRECTED DST FROM POI (mm)	VELOCITY OF HAMMER & BEAM (m/s)	ACCELERATION HAMMER & BEAM (m/s ^ 2)	TIME (t) (seconds)
0	0.0	0.1792	1.741	1.0000	0.0	5.347	1526.025	0.0000
2	2.0	0.1803	1.753	0.9937	2.0	1.402	606.510	0.0011
4	3.2	0.1814	1.764	0.9874	3.9	0.882	306.171	0.0023
6	4.0	0.1826	1.775	0.9813	5.9	0.577	233.030	0.0034
8	4.5	0.1837	1.786	0.9753	7.8	0.312	237.404	0.0045
10	4.7	0.1848	1.796	0.9694	9.7	0.000	322.695	0.0057
12	4.5	0.1859	1.807	0.9636	11.6	-0.271	164.750	0.0068
14	4.1	0.1870	1.818	0.9579	13.4	-0.500	250.527	0.0079
16	3.4	0.1881	1.829	0.9524	15.2	-0.640	3.402	0.0090
18	2.7	0.1892	1.839	0.9469	17.0	-0.782	257.817	0.0101
20	1.7	0.1903	1.850	0.9415	18.8	-0.879	-80.917	0.0111
22	0.8	0.1914	1.860	0.9362	20.6	-0.903	169.380	0.0122
23.5	0.0	0.1922	1.868	0.9322	21.9	-0.994	-113.477	0.0130

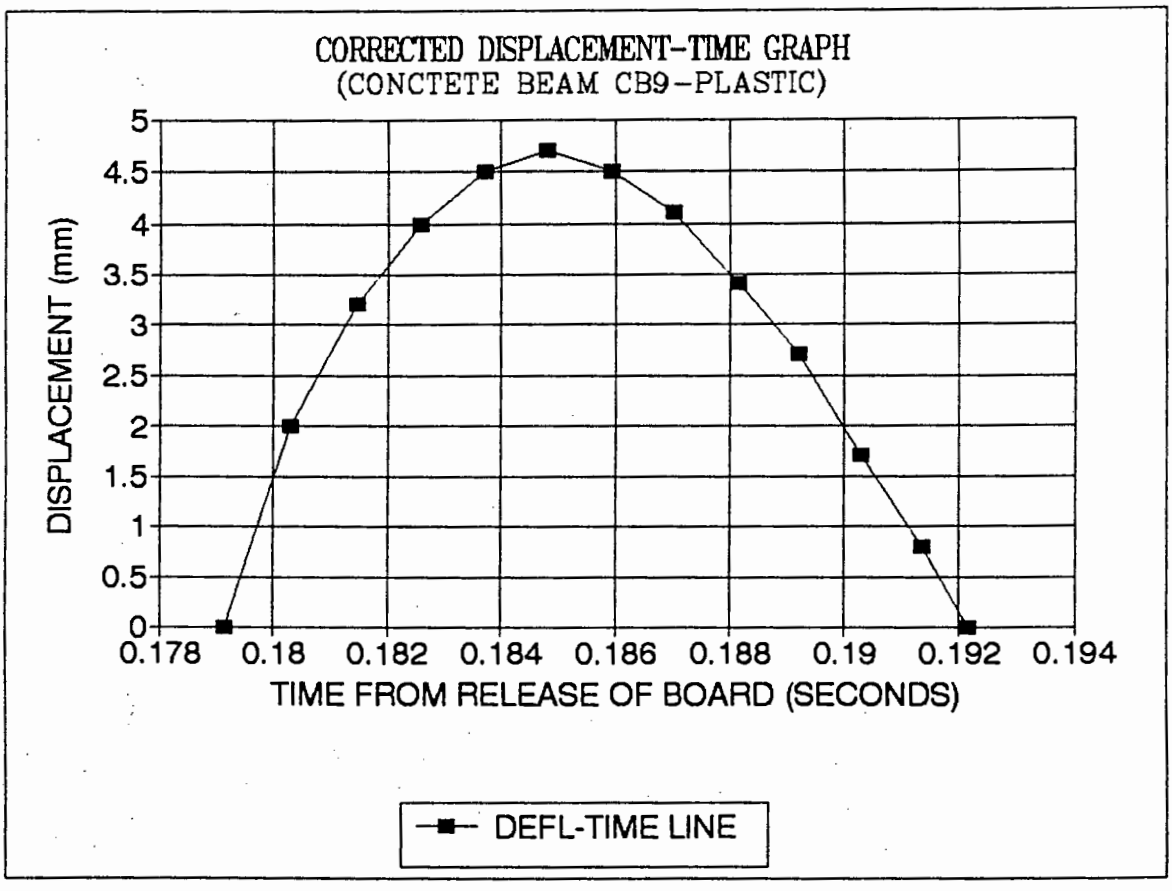

IMPACT CALCULATIONS

PLASTIC ANALYSIS

REINFORCED CONCRETE BEAM CD6
(TWO 400N WEIGHT)

DISTANCE BOARD FALLEN BEFORE IMPACT =	0.500	m	THETA INSWING (RADS) =	0.3135
ACCELERATION OF FALLING BOARD =	9.72	m/S^2	THETA BACKSWING (RADS) =	0.0749
VALUE OF g AT UCT =	9.80	m/s^2	EFF HT OF PENDULUM (m) =	0.171
EFFECTIVE MASS OF PENDULUM =	142.850	kg	EFF VEL OF PENDULUM (m/s) =	1.832
EFFECTIVE LENGTH OF PENDULUM =	3.513	m	VEL OF PEND (POI) (m/s) =	2.188
DISTANCE 'X' =	0.189	m	ACCEL OF BEAM (m/s^2) =	14122.2
LENGTH TO IMPACT =	4.196	m	FORCE 'Be' (kN) =	1779.7
LENGTH FROM PIN TO HAMMER =	3.870	m		
PERIOD OF PENDULUM =	3.764	seconds		
EFFECTIVE MASS BEAM ETC =	7.521	kg		
DIST OF RELEASE FROM POI =	1.500	m		

DISTANCE FROM POI (mm)	DEFLECTION X (mm)	TIME BOARD FALLEN (seconds)	VELOCITY OF BOARD (m/s)	CORRECTION FACTOR	CORRECTED DST FROM POI (mm)	VELOCITY OF HAMMER & BEAM (m/s)	ACCELERATION HAMMER & BEAM (m/s^2)	TIME (t) (seconds)
0	0.0	0.3208	3.118	1.0000	0.0	2.188	14122.174	0.0000
2	5.8	0.3214	3.124	0.9980	2.0	6.248	8763.526	0.0006
4	8.0	0.3220	3.130	0.9960	4.0	3.208	724.867	0.0013
6	9.9	0.3227	3.136	0.9941	6.0	2.431	1713.874	0.0019
8	11.1	0.3233	3.143	0.9921	7.9	1.493	1229.819	0.0026
10	11.8	0.3239	3.149	0.9901	9.9	0.787	989.007	0.0032
12	12.1	0.3246	3.155	0.9882	11.9	0.394	247.616	0.0038
14	12.3	0.3252	3.161	0.9863	13.8	0.000	999.213	0.0045
16	12.1	0.3258	3.167	0.9844	15.7	-0.633	1005.045	0.0051
18	11.5	0.3265	3.173	0.9825	17.7	-1.428	1514.858	0.0057
20	10.3	0.3271	3.179	0.9806	19.6	-1.908	5.832	0.0064
22	9.1	0.3277	3.186	0.9787	21.5	-1.752	-502.037	0.0070
24	8.1	0.3284	3.192	0.9768	23.4	-1.676	259.766	0.0076
26	7.0	0.3290	3.198	0.9750	25.3	-1.759	5.346	0.0082
28	5.9	0.3296	3.204	0.9731	27.2	-1.762	5.346	0.0089
30	4.8	0.3302	3.210	0.9713	29.1	-1.605	-510.299	0.0095
32	3.9	0.3309	3.216	0.9695	31.0	-1.447	4.374	0.0101
34	3.0	0.3315	3.222	0.9676	32.9	-1.128	-1034.691	0.0107
36	2.5	0.3321	3.228	0.9658	34.8	-0.807	2.430	0.0113
38	2.0	0.3327	3.234	0.9640	36.6	-0.726	-259.280	0.0120
40	1.6	0.3333	3.240	0.9623	38.5	-0.810	527.309	0.0126
42	1.0	0.3340	3.246	0.9605	40.3	-0.649	-1051.701	0.0132
44	0.8	0.3346	3.252	0.9587	42.2	-0.569	794.851	0.0138
46	0.3	0.3352	3.258	0.9569	44.0	-0.652	-528.767	0.0144
48	0.0	0.3358	3.264	0.9552	45.8	-0.489	264.868	0.0150

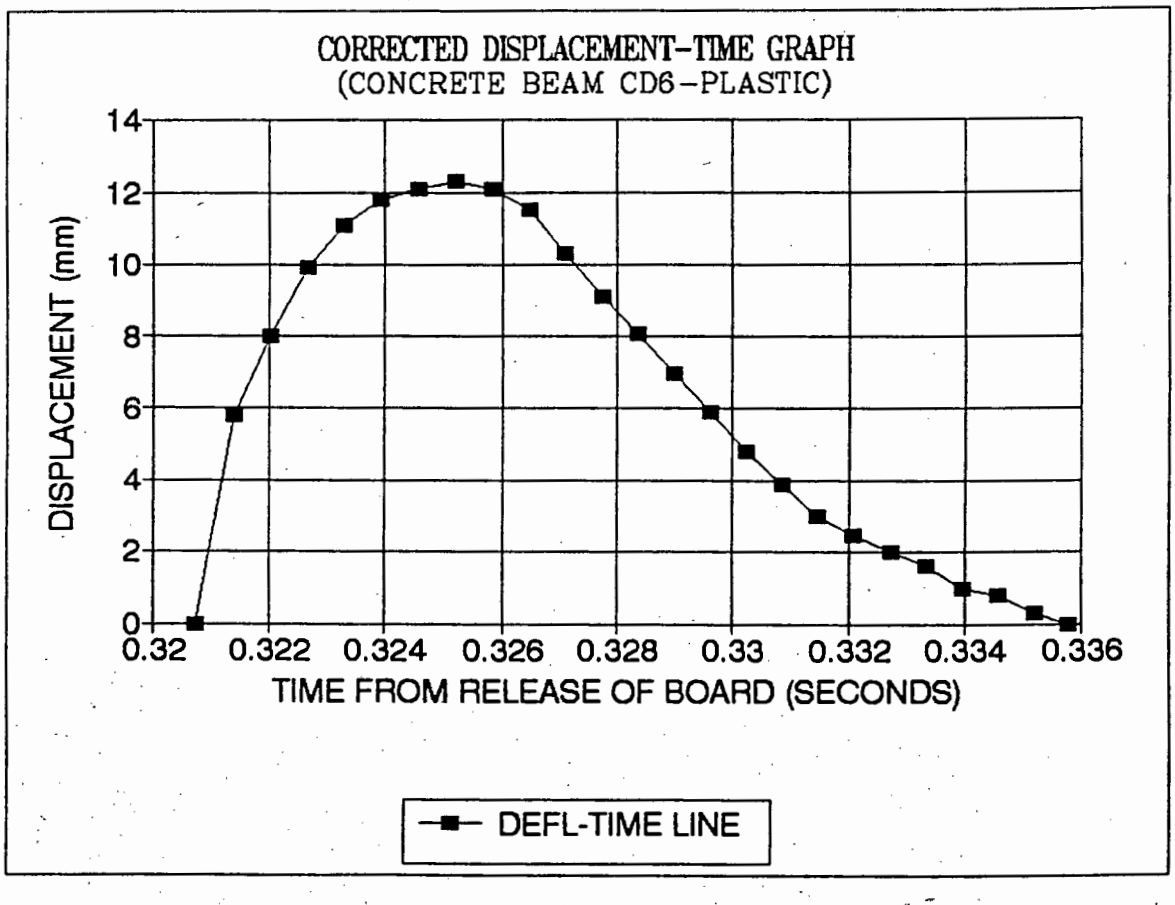

CONCRETE BEAM ENERGY ANALYSIS - BEAM CB7 ELASTO-PLASTIC ENERGY METHOD
(NO WEIGHTS)

INPUT		OUTPUT	
DIST POI (m) =	2.600	THETA(s) (rads) =	0.5960
M(e) PEND (kg) =	54.3	H(eff)(1) (m) =	0.5071
M(e) CHANNEL (kg) =	45.9	KE(2) (JOULS) =	269.992
L(e) (m) =	2.941	THETA(3) (rads) =	0.0072
DIST 'X' (m) =	-0.029	H(eff)(3) (m) =	0.00008
L(POI) (m) =	3.841	PE(3) (JOULS) =	0.041
L(h) (m) =	3.870	FrE(TOTAL) (JOULS) =	0.005
'g' UCT (m/s^2) =	9.80	NETT E (JOULS) =	269.946
MAX DEFL (m) =	0.0048	PROP FACT 'fp' =	0.767
BEAM WIDTH (m) =	0.100	E POI (JOULS) =	207.171
BEAM THICK (m) =	0.100	Be (N) =	12778.2
E STEEL (GPa) =	208.900	I beam (m^4) =	8.333E-06
Fy STEEL (MPa) =	435.600	'k' beam (kN/m) =	171193.416
DLF Fy =	1.2	DEPTH COMP (mm) =	7.0
Edynamic CON (GPa) =	39	M(pl) (kNm) =	1.248
Me BEAM(ONLY) (kg) =	7.521	R(m) (kN) =	11.092
AREA STEEL (mm^2) =	31.2	X(e) (mm) =	0.1
EFFECTIVE d (m) =	0.08	Xm (max) (mm) =	18.7
ACC POI (m/s^2) =	1699.000	Meb (SYSTEM) (kg) =	51.184
Fr(dyn) ROD 3 (N) =	1.067	IMPULSE (POI)(Ns) =	145.629
MAX DEFL ROD 3 (m) =	0.0048	IMP DUR 'T' (s) =	0.022793
		PERIOD BEAM 'Tn'(s) =	0.003436
		TIME 'Tm' (S) =	0.012256

CONCRETE BEAM ANALYSIS - CB7 FORCE BALANCE METHOD
(NO WEIGHTS)

INPUT		OUTPUT	
DIST POI (m) =	2.600	THETA(s) (rads) =	0.5960
M(e) PEND (kg) =	54.3	H(eff)(1) (m) =	0.5071
M(e) CHANNEL (kg) =	45.9	KE(2) (JOULES) =	269.992
L(e) (m) =	2.941	VEL(2) (m/S) =	3.153
DIST 'X' (m) =	-0.029	THETA(3) (rads) =	0.0072
L(POI) (m) =	3.841	H(eff)(3) (m) =	0.00008
L(h) (m) =	3.870	PE(3) (JOULES) =	0.041
'g' UCT (m/s^2) =	9.80	VEL(POI) (m/s) =	4.117
MAX DEFL (m) =	0.0048	PROP FACT 'fp' =	0.767
Me BEAM =	7.521	E POI (JOULES) =	246.651
TIME DELTA 't'(sec) =	0.0002795	V(dt) (m/s) =	3.512
		KE PEND (J) =	100.775
		E GAIN BEAM (JOULES) =	46.392
		KE(lost) POI(J) =	54.383
		MePEND(POI) (kg) =	43.66
		DECCEL PEND (m/s^2) =	2164.604
		ACC BEAM (m/s^2) =	12566.595
		Fo PEND (kN) =	94.513
		Fo BEAM (kN) =	94.513
		IMPULSE (POI)(Ns) =	26.416
		IMP DUR 'T' (s) =	0.000559

CONCRETE BEAM ENERGY ANALYSIS - BEAM CB9 ELASTO-PLASTIC ENERGY METHOD
(ONE 400N WEIGHT)

INPUT		OUTPUT	
DIST POI (m) =	3.600	THETA(s) (rads) =	0.8306
M(e) PEND (kg) =	98.3	H(eff)(1) (m) =	1.1128
M(e) CHANNEL (kg) =	45.3	KE(2) (JOULES) =	1072.402
L(e) (m) =	3.418	THETA(3) (rads) =	0.0072
DIST 'X' (m) =	0.007	H(eff)(3) (m) =	0.00009
L(POI) (m) =	3.877	PE(3) (JOULES) =	0.085
L(h) (m) =	3.870	FrE(TOTAL)(JOULES) =	0.005
'g' UCT (m/s^2) =	9.80	NETT E (JOULES) =	1072.313
MAX DEFL (m) =	0.0048	PROP FACT 'fp' =	0.881
BEAM WIDTH (m) =	0.100	E POI (JOULES) =	945.140
BEAM THICK (m) =	0.100	Be (N) =	153353.5
E STEEL (GPa) =	203.500	I beam (m^4) =	8.333E-06
fy STEEL (MPa) =	396.000	'k' beam (kN/m) =	171193.416
DLF fy =	1.2	DEPTH COMP (mm) =	10.3
Edynamic CON (GPa) =	39	M(pl) (kNm) =	1.797
Me BEAM(ONLY) (kg) =	7.525	R(m) (kN) =	15.971
AREA STEEL (mm^2) =	50.5	X(e) (mm) =	0.1
EFFECTIVE d (m) =	0.08	Xm (max) (mm) =	59.2
ACC POI (m/s^2) =	1526.000	Meb (SYSTEM) (kg) =	100.494
Fr(dyn) ROD 3 (N) =	1.067	IMPULSE (POI)(Ns) =	435.846
MAX DEFL ROD 3 (m) =	0.0047	IMP DUR 'T' (s) =	0.005684
fcu(dynamic) (MPa) =	39	PERIOD BEAM 'Tn'(s)=	0.004814
		TIME 'Tm' (S) =	0.004046

CONCRETE BEAM ANALYSIS - CB9 FORCE BALANCE METHOD
(ONE 400N WEIGHT)

INPUT		OUTPUT	
DIST POI (m) =	3.600	THETA(s) (rads) =	0.8306
M(e) PEND (kg) =	98.3	H(eff)(1) (m) =	1.1128
M(e) CHANNEL (kg) =	45.3	KE(2) (JOULES) =	1072.402
L(e) (m) =	3.418	VEL(2) (m/S) =	4.670
DIST 'X' (m) =	0.007	THETA(3) (rads) =	0.0071
L(POI) (m) =	3.877	H(eff)(3) (m) =	0.00009
L(h) (m) =	3.870	PE(3) (JOULES) =	0.084
'g' UCT (m/s^2) =	9.80	VEL(POI) (m/s) =	5.297
MAX DEFL (m) =	0.0047	PROP FACT 'fp' =	0.881
Me BEAM =	7.525	E POI (JOULES) =	1179.637
TIME DELTA 't'(sec)=	0.0001129	V(dt) (m/s) =	4.901
		KE PEND (J) =	188.034
		E GAIN BEAM (JOULES) =	90.360
		KE(lost) POI(J) =	97.674
		MePEND(POI) (kg) =	92.97
		DECCEL PEND (m/s^2) =	3513.387
		ACC BEAM (m/s^2) =	43406.673
		Fo PEND (kN) =	326.635
		Fo BEAM (kN) =	326.635
		IMPULSE (POI)(Ns) =	36.877
		IMP DUR 'T' (s) =	0.000226

CONCRETE BEAM ENERGY ANALYSIS - BEAM CD6 ELASTO-PLASTIC ENERGY METHOD
(TWO 400N WEIGHTS)

INPUT		OUTPUT	
DIST POI (m) =	1.500	THETA(s) (rads) =	0.3325
M(e) PEND (kg) =	140.7	H(eff)(1) (m) =	0.1924
M(e) CHANNEL (kg) =	46.4	KE(2) (JOULS) =	265.245
L(e) (m) =	3.513	THETA(3) (rads) =	0.0093
DIST 'X' (m) =	-0.060	H(eff)(3) (m) =	0.00015
L(POI) (m) =	3.810	PE(3) (JOULS) =	0.208
L(h) (m) =	3.870	FrE(TOTAL) (JOULS) =	0.013
'g' UCT (m/s^2) =	9.80	NETT E (JOULS) =	265.024
MAX DEFL (m) =	0.0123	PROP FACT 'fp' =	0.923
BEAM WIDTH (m) =	0.100	E POI (JOULS) =	244.685
BEAM THICK (m) =	0.100	Be (N) =	106213.1
E STEEL (GPa) =	207.800	I beam (m^4) =	8.333E-06
Fy STEEL (MPa) =	399.700	'k' beam (kN/m) =	171193.416
DLF Fy =	1	DEPTH COMP (mm) =	9.6
Edynamic CON (GPa) =	39	M(pl) (kNm) =	1.690
Me BEAM(ONLY) (kg) =	7.521	R(m) (kN) =	15.023
AREA STEEL (mm^2) =	39.6	X(e) (mm) =	0.1
EFFECTIVE d (m) =	0.08	Xm (max) (mm) =	16.3
ACC POI (m/s^2) =	14122.200	Meb (SYSTEM) (kg) =	144.612
Fr(dyn) ROD 3 (N) =	1.067	IMPULSE (POI)(Ns) =	266.024
MAX DEFL ROD 3 (m) =	0.0123	IMP DUR 'T' (s) =	0.005009
		PERIOD BEAM 'Tn'(s) =	0.005775
		TIME 'Tm' (S) =	0.003948

CONCRETE BEAM ANALYSIS - CD6 FORCE BALANCE METHOD
(TWO 400N WEIGHTS)

INPUT		OUTPUT	
DIST POI (m) =	1.500	THETA(s) (rads) =	0.3325
M(e) PEND (kg) =	140.7	H(eff)(1) (m) =	0.1924
M(e) CHANNEL (kg) =	46.4	KE(2) (JOULES) =	265.245
L(e) (m) =	3.513	VEL(2) (m/S) =	1.942
DIST 'X' (m) =	-0.060	THETA(3) (rads) =	0.0093
L(POI) (m) =	3.810	H(eff)(3) (m) =	0.00015
L(h) (m) =	3.870	PE(3) (JOULES) =	0.208
'g' UCT (m/s^2) =	9.80	VEL(POI) (m/s) =	2.106
MAX DEFL (m) =	0.0123	PROP FACT 'fp' =	0.923
Me BEAM =	7.521	E POI (JOULES) =	289.863
TIME DELTA 't'(sec) =	0.000686	V(dt) (m/s) =	1.997
		KE PEND (J) =	30.808
		E GAIN BEAM (JOULES) =	14.993
		KE(lost) POI(J) =	15.815
		MePEND(POI) (kg) =	137.09
		DECCEL PEND (m/s^2) =	159.685
		ACC BEAM (m/s^2) =	2910.691
		Fo PEND (kN) =	21.891
		Fo BEAM (kN) =	21.891
		IMPULSE (POI)(Ns) =	15.017
		IMP DUR 'T' (s) =	0.001372

RIGID PLASTIC ANALYSIS — CONCRETE BEAM CB7

INPUT			OUTPUT			
MASS OF BEAM/m =	24.67	kg/m	AT t=0 :	yo" = fo =	16115.071	m/s^2
MASS OF ROD 2 =	0	kg		yo' = vel =	0.000	m/s
MASS OF ROD 3 =	1.476	kg		yo = displ =	0.000	m
SPAN 'L' =	0.45	m	AT t=T :	yT" = fT =	-2143.018	m/s^2
IMP FORCE 'Fo' =	94513	N		yT' = vT =	3.905	m/s
Mpl =	1248	Nm		yT = dT =	0.0016	m
DURATION IMP 'T' =	0.000559	sec	FOR t>T:	T2 =	0.0018	sec
Me(PEND)(POI) =	43.66	kg		y2 = d2 =	0.0004	m
				y(total) =	0.0019	m
				tm =	0.0024	sec

RIGID PLASTIC ANALYSIS — CONCRETE BEAM CB9

INPUT			OUTPUT			
MASS OF BEAM/m =	24.67	kg/m	AT t=0 :	yo" = fo =	60013.845	m/s^2
MASS OF ROD 2 =	0	kg		yo' = vel =	0.000	m/s
MASS OF ROD 3 =	1.476	kg		yo = displ =	0.000	m
SPAN 'L' =	0.45	m	AT t=T :	yT" = fT =	-3085.740	m/s^2
IMP FORCE 'Fo' =	326635	N		yT' = vT =	6.433	m/s
Mpl =	1797	Nm		yT = dT =	0.0010	m
DURATION IMP 'T' =	0.000226	sec	FOR t>T:	T2 =	0.0021	sec
Me(PEND)(POI) =	92.97	kg		y2 = d2 =	0.0004	m
				y(total) =	0.0013	m
				tm =	0.0023	sec

RIGID PLASTIC ANALYSIS — CONCRETE BEAM CD6

INPUT			OUTPUT			
MASS OF BEAM/m =	24.67	kg/m	AT t=0 :	yo" = fo =	1752.772	m/s^2
MASS OF ROD 2 =	0	kg		yo' = vel =	0.000	m/s
MASS OF ROD 3 =	1.476	kg		yo = displ =	0.000	m
SPAN 'L' =	0.45	m	AT t=T :	yT" = fT =	-2476.148	m/s^2
IMP FORCE 'Fo' =	21891	N		yT' = vT =	-0.496	m/s
Mpl =	1442	Nm		yT = dT =	0.0003	m
DURATION IMP 'T' =	0.00137	sec	FOR t>T:	T2 =	-0.0002	sec
Me(PEND)(POI) =	137.09	kg		y2 = d2 =	0.0000	m
				y(total) =	0.0003	m
				tm =	0.0012	sec

APPENDIX E

REINFORCED CONCRETE SLABS

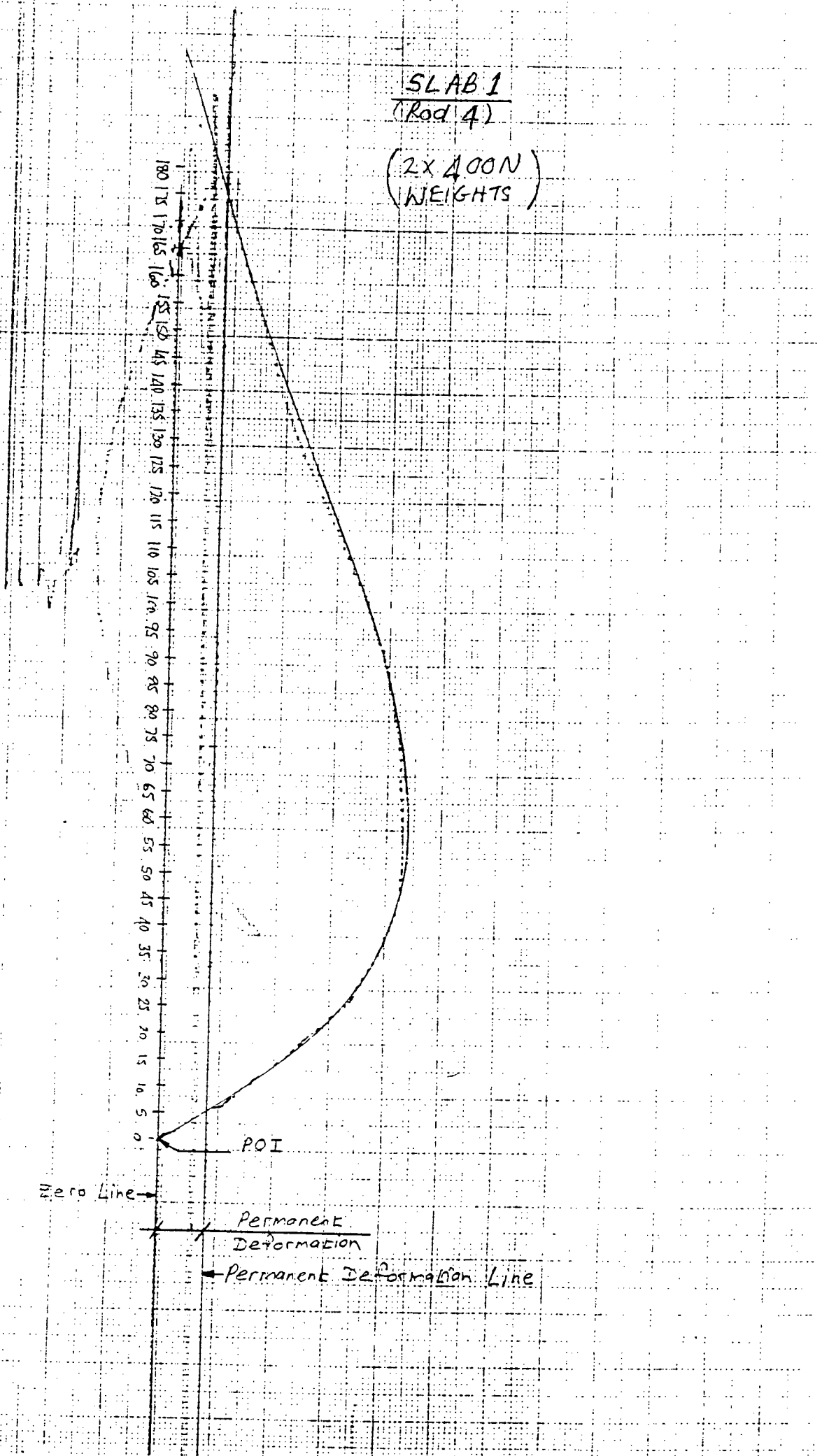
SLAB 1
(Rod 4)
(2x 400N WEIGHTS)
180 175 170 165 160 155 150 145 140 135 130 125 120 115 110 105 100 95 90 85 80 75 70 65 60 55 50 45 40 35 30 25 20 15 10 5 0
POI
Zero Line
Permanent Deformation
Permanent Deformation Line

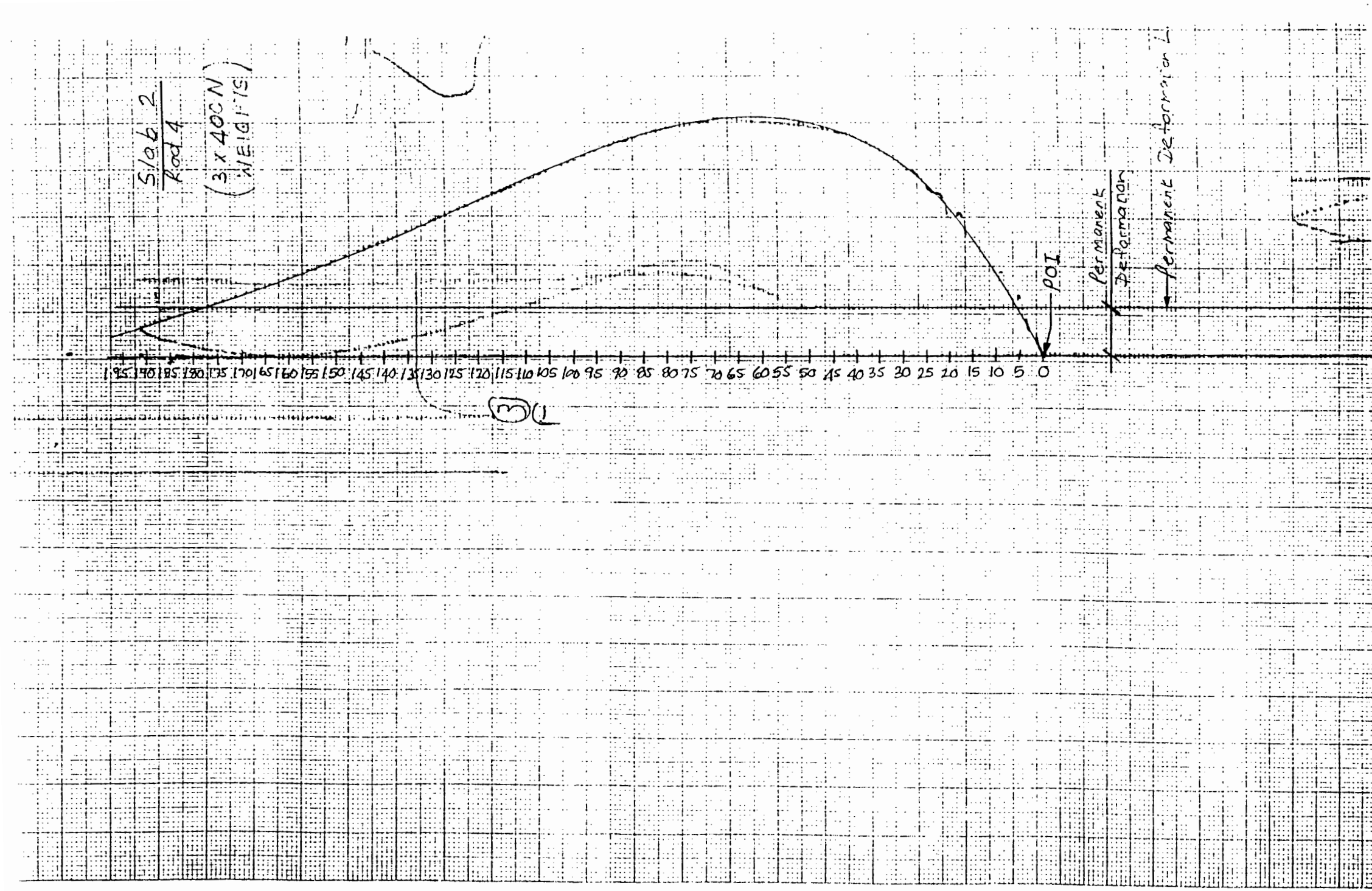
Slab 2
Rod 4
(3 x 400 N
WEIGHTS)
POI
Permanent
Deformation
Permanent Deformation
195 190 185 180 175 170 165 160 155 150 145 140 135 130 125 120 115 110 105 100 95 90 85 80 75 70 65 60 55 50 45 40 35 30 25 20 15 10 5 0

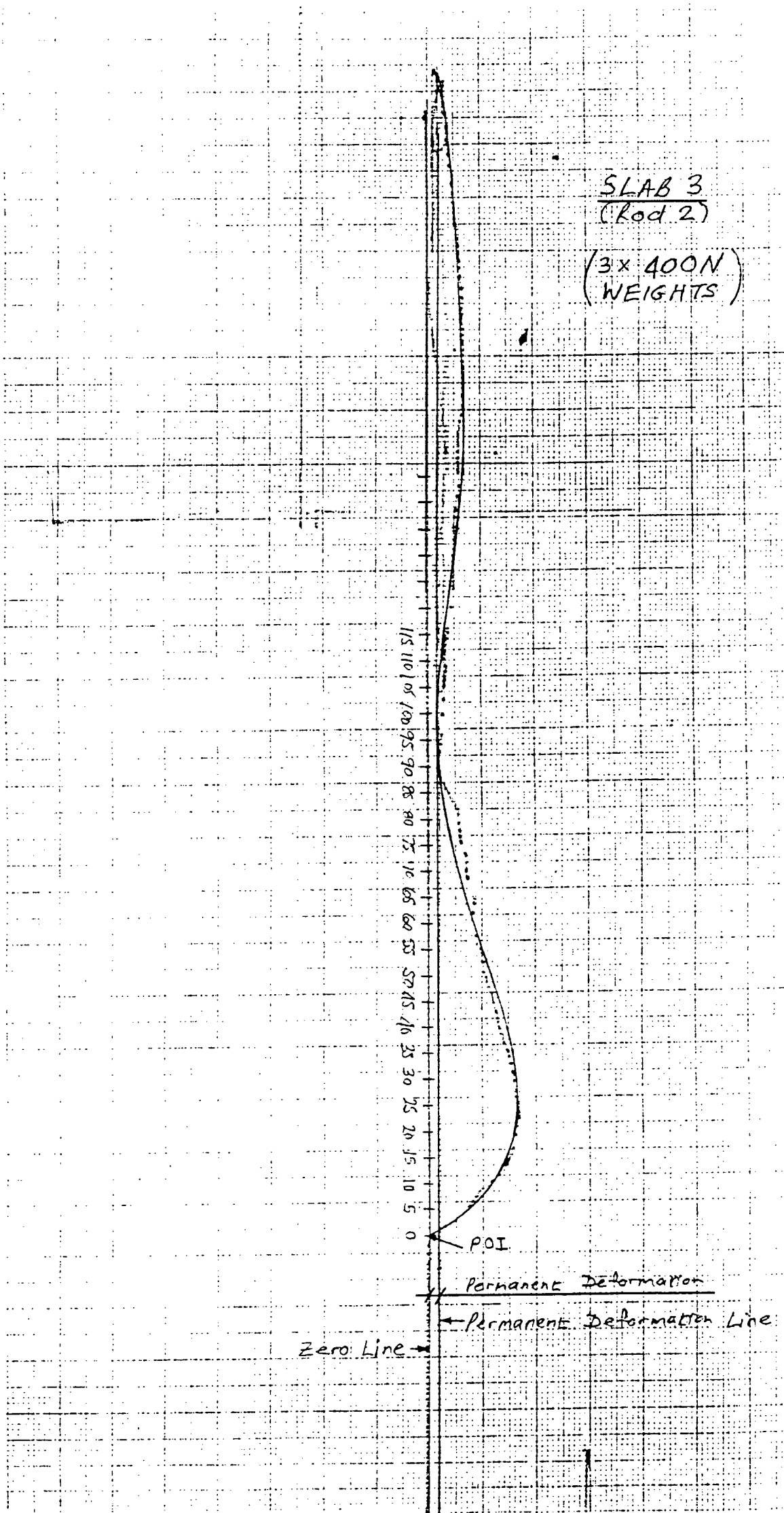
SLAB 3
(Rod 2)
(3 x 400N
WEIGHTS)
0
5
10
15
20
25
30
35
40
45
50
55
60
65
70
75
80
85
90
95
100
105
110
115
POI
Permanent Deformation
Permanent Deformation Line
Zero Line

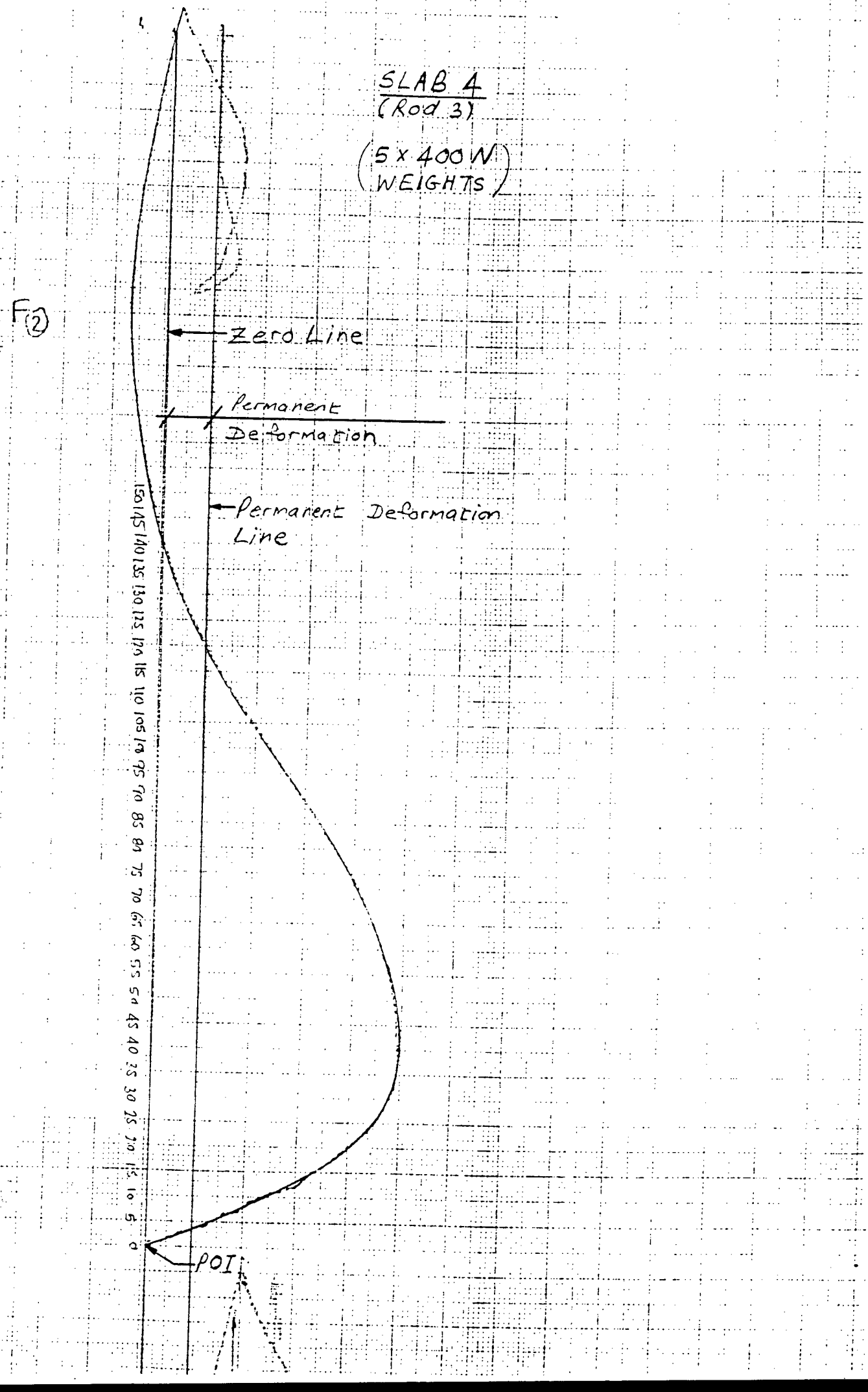
SLAB 4
(Rod 3)
(5 x 400W
WEIGHTS)
F(2)
Zero Line
Permanent
Deformation
Permanent Deformation
Line
150 145 140 135 130 125 120 115 110 105 100 95 90 85 80 75 70 65 60 55 50 45 40 35 30 25 20 15 10 5 0
POI

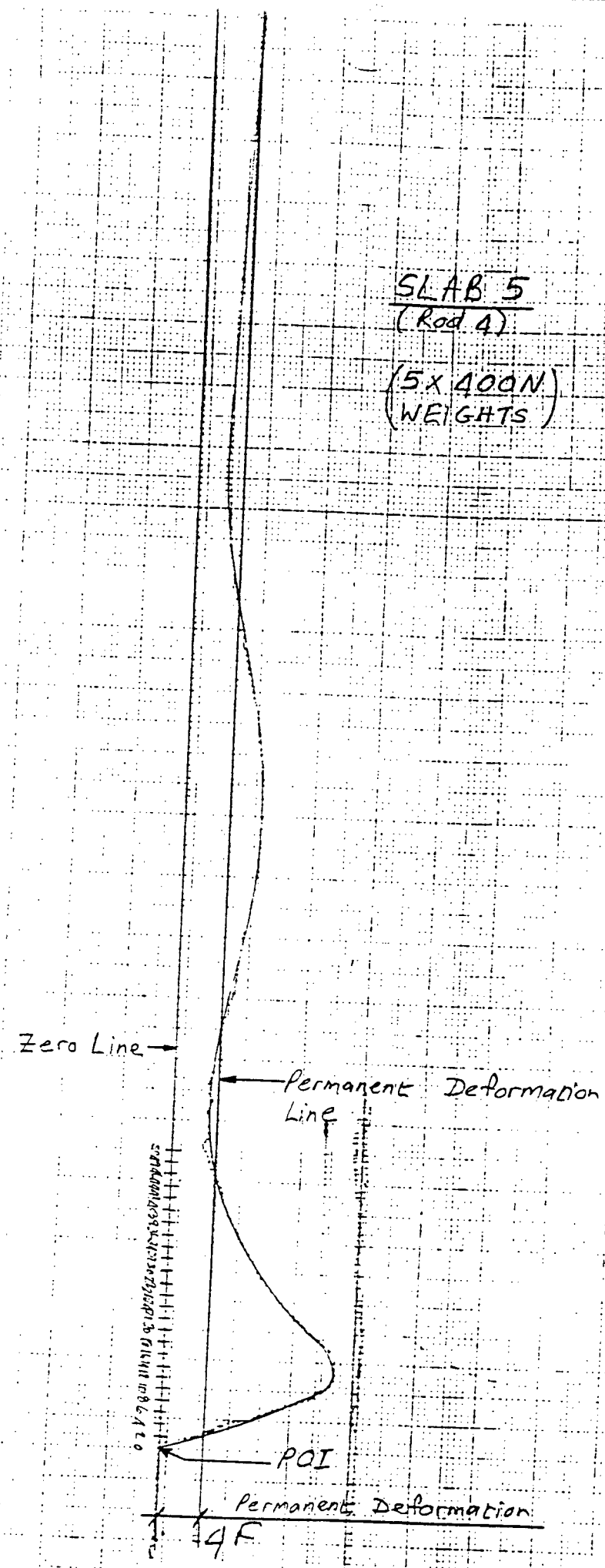
SLAB 5
(Rod 4)
(5 x 400N
WEIGHTS)
Zero Line
Permanent Deformation
Line
POI
Permanent Deformation
14F

IMPACT CALCULATIONS — ELASTIC ANALYSIS — REINFORCED CONCRETE SLAB 1 (SERIES A) (2x400N WEIGHTS)

DISTANCE BOARD FALLEN BEFORE IMPACT =	0.151	m	THETA INSWING (RADS) =	0.9852
ACCELERATION OF FALLING BOARD =	9.72	m/s^2	THETA BACKSWING (RADS) =	0.1320
VALUE OF g AT UCT =	9.80	m/s^2	EFF HT OF PENDULUM (m) =	1.323
EFFECTIVE MASS OF PENDULUM =	144.000	kg	EFF VEL OF PENDULUM (m/s) =	5.093
EFFECTIVE LENGTH OF PENDULUM =	2.958	m	VEL OF PEND (POI) (m/s) =	5.550
DISTANCE 'X' =	0.164	m	ACCEL OF SLAB (m/s^2) =	931.0
LENGTH TO IMPACT =	3.224	m	FORCE 'Be' (kN) =	148.2
LENGTH FROM PIN TO HAMMER =	3.060	m		
PERIOD OF PENDULUM =	3.450	seconds		
EFFECTIVE MASS SLAB ETC =	159.2	kg		
DIST OF RELEASE FROM POI =	4.400	m		
DEFL CORR FACTOR 'CF' =	1.23			

DISTANCE FROM POI (mm)	DEFLECTION X (mm)	ADJ DEFL X(adj) (mm)	TIME BOARD FALLEN (seconds)	VELOCITY OF BOARD (m/s)	CORRECTION FACTOR	CORRECTED DST FROM POI (mm)	VELOCITY OF HAMMER & BEAM (m/s)	ACCELERATION HAMMER & BEAM (m/s^2)	TIME (t) (seconds)
0	0.0	0	0.1763	1.713	1.0000	0.0	5.550	930.959	0.0000
5	7.8	9.594	0.1792	1.741	0.9838	4.9	2.612	58.189	0.0029
10	15.0	18.45	0.1820	1.769	0.9684	9.7	2.530	-1.383	0.0057
15	22.1	27.183	0.1848	1.796	0.9537	14.3	2.299	168.242	0.0085
20	27.8	34.194	0.1876	1.823	0.9397	18.8	1.969	69.271	0.0113
25	32.9	40.467	0.1903	1.850	0.9263	23.2	1.665	155.456	0.0140
30	36.8	45.264	0.1930	1.876	0.9134	27.4	1.313	105.776	0.0167
35	39.9	49.077	0.1956	1.902	0.9010	31.5	0.951	168.677	0.0194
40	41.8	51.414	0.1982	1.927	0.8891	35.6	0.771	-33.589	0.0220
45	43.9	53.997	0.2008	1.952	0.8777	39.5	0.605	164.617	0.0246
50	44.9	55.227	0.2034	1.977	0.8667	43.3	0.316	60.957	0.0271
55	45.5	55.965	0.2059	2.001	0.8562	47.1	0.200	31.062	0.0296
60	45.9	56.457	0.2084	2.025	0.8460	50.8	0.000	131.245	0.0321
65	45.5	55.965	0.2108	2.049	0.8361	54.3	-0.143	-16.114	0.0346
70	45.2	55.596	0.2132	2.073	0.8266	57.9	-0.269	121.547	0.0370
75	44.2	54.366	0.2156	2.096	0.8174	61.3	-0.398	-15.725	0.0394
80	43.3	53.259	0.2180	2.119	0.8085	64.7	-0.445	55.924	0.0417
85	42.1	51.783	0.2204	2.142	0.7999	68.0	-0.514	2.333	0.0441
90	40.9	50.307	0.2227	2.164	0.7916	71.2	-0.563	40.004	0.0464
95	39.5	48.585	0.2250	2.187	0.7835	74.4	-0.678	60.396	0.0487
100	37.8	46.494	0.2273	2.209	0.7756	77.6	-0.795	42.532	0.0510
105	35.9	44.157	0.2295	2.231	0.7680	80.6	-0.892	43.698	0.0532
110	33.8	41.574	0.2317	2.253	0.7606	83.7	-0.901	-36.700	0.0555
115	31.9	39.237	0.2339	2.274	0.7534	86.6	-0.910	45.254	0.0577
120	29.8	36.654	0.2361	2.295	0.7465	89.6	-1.010	46.420	0.0599
125	27.5	33.825	0.2383	2.316	0.7397	92.5	-0.996	-60.202	0.0620
130	25.5	31.365	0.2405	2.337	0.7331	95.3	-0.935	2.888	0.0642
135	23.5	28.905	0.2426	2.358	0.7266	98.1	-0.990	48.559	0.0663
140	21.3	26.199	0.2447	2.378	0.7203	100.8	-0.999	-41.171	0.0684
145	19.3	23.739	0.2468	2.399	0.7142	103.6	-0.912	-42.338	0.0705
150	17.5	21.525	0.2489	2.419	0.7083	106.2	-0.847	-20.003	0.0726
155	15.8	19.434	0.2509	2.439	0.7025	108.9	-0.878	51.086	0.0747
160	13.9	17.097	0.2530	2.459	0.6968	111.5	-0.885	-44.865	0.0767
165	12.2	15.006	0.2550	2.479	0.6913	114.1	-0.843	3.305	0.0787
170	10.5	12.915	0.2570	2.498	0.6859	116.6	-0.799	-46.809	0.0807
175	9	11.07	0.2590	2.517	0.6806	119.1	-0.806	53.808	0.0827
180	7.2	8.979	0.2610	2.537	0.6754	121.6	-0.859	-27.111	0.0847

IMPACT CALCULATIONS — PLASTIC ANALYSIS — REINFORCED CONCRETE SLAB 2 (SERIES A) (3x400N WEIGHTS)

DISTANCE BOARD FALLEN BEFORE IMPACT =	0.138	m	THETA INSWING (RADS) =	0.9260
ACCELERATION OF FALLING BOARD =	9.72	m/S^2	THETA BACKSWING (RADS) =	0.1785
VALUE OF g AT UCT =	9.80	m/s^2	EFF HT OF PENDULUM (m) =	1.217
EFFECTIVE MASS OF PENDULUM =	184.600	kg	EFF VEL OF PENDULUM (m/s) =	4.883
EFFECTIVE LENGTH OF PENDULUM =	2.989	m	VEL OF PEND (POI) (m/s) =	5.220
DISTANCE 'X' =	0.135	m	ACCEL OF SLAB (m/s^2) =	961.3
LENGTH TO IMPACT =	3.195	m	FORCE 'Be' (kN) =	153.0
LENGTH FROM PIN TO HAMMER =	3.060	m		
PERIOD OF PENDULUM =	3.468	seconds		
EFFECTIVE MASS SLAB ETC =	159.2	kg		
DIST OF RELEASE FROM POI =	4.160	m		
DEFL CORR FACTOR 'CF' =	1.23			

DISTANCE FROM POI (mm)	DEFLECTION X (mm)	ADJ DEFL X(adj) (mm)	TIME BOARD FALLEN (seconds)	VELOCITY OF BOARD (m/s)	CORRECTION FACTOR	CORRECTED DST FROM POI (mm)	VELOCITY OF HAMMER & BEAM (m/s)	ACCELERATION HAMMER & BEAM (m/s^2)	TIME (t) (seconds)
0	0.0	0	0.1685	1.638	1.0000	0.0	5.220	961.349	0.0000
5	8.8	10.824	0.1715	1.667	0.9824	4.9	2.834	50.179	0.0030
10	17.0	20.91	0.1745	1.696	0.9656	9.7	2.612	100.091	0.0060
15	24.2	29.766	0.1774	1.725	0.9497	14.2	2.380	57.956	0.0089
20	30.8	37.884	0.1803	1.753	0.9346	18.7	2.050	172.884	0.0118
25	35.9	44.157	0.1831	1.780	0.9201	23.0	1.691	79.475	0.0146
30	40.3	49.569	0.1859	1.807	0.9063	27.2	1.464	83.557	0.0174
35	44.0	54.12	0.1887	1.834	0.8931	31.3	1.082	196.021	0.0202
40	46.2	56.826	0.1914	1.860	0.8805	35.2	0.781	23.596	0.0229
45	48.2	59.286	0.1940	1.886	0.8684	39.1	0.698	39.088	0.0255
50	49.9	61.377	0.1967	1.912	0.8568	42.8	0.516	99.694	0.0282
55	50.9	62.607	0.1993	1.937	0.8456	46.5	0.232	118.880	0.0308
60	51.1	62.853	0.2018	1.962	0.8348	50.1	0.078	-0.389	0.0333
65	51.3	63.099	0.2044	1.987	0.8245	53.6	0.000	63.134	0.0359
70	51.1	62.853	0.2069	2.011	0.8145	57.0	-0.221	114.275	0.0384
75	50.2	61.746	0.2093	2.035	0.8049	60.4	-0.407	35.066	0.0408
80	49.1	60.393	0.2118	2.059	0.7956	63.7	-0.473	19.186	0.0433
85	47.9	58.917	0.2142	2.082	0.7867	66.9	-0.604	89.513	0.0457
90	46.2	56.826	0.2166	2.105	0.7780	70.0	-0.758	38.955	0.0481
95	44.3	54.489	0.2190	2.128	0.7696	73.1	-0.787	-14.520	0.0504
100	42.5	52.275	0.2213	2.151	0.7615	76.1	-0.882	96.512	0.0528
105	40.2	49.446	0.2236	2.173	0.7536	79.1	-0.978	-14.520	0.0551
110	38.0	46.74	0.2259	2.196	0.7460	82.1	-0.944	-15.103	0.0574
115	35.9	44.157	0.2282	2.218	0.7385	84.9	-0.998	63.390	0.0597
120	33.5	41.205	0.2304	2.240	0.7314	87.8	-1.053	-15.492	0.0619
125	31.2	38.376	0.2326	2.261	0.7244	90.5	-0.995	-36.622	0.0641
130	29.1	35.793	0.2348	2.283	0.7176	93.3	-0.959	4.082	0.0663
135	27.0	33.21	0.2370	2.304	0.7110	96.0	-0.968	4.082	0.0685
140	24.9	30.627	0.2392	2.325	0.7046	98.6	-0.930	-39.344	0.0707
145	23.0	28.29	0.2413	2.346	0.6983	101.3	-0.938	47.898	0.0728
150	20.9	25.707	0.2434	2.366	0.6922	103.8	-0.923	-63.390	0.0749
155	19.1	23.493	0.2455	2.387	0.6863	106.4	-0.931	72.138	0.0770
160	17.0	20.91	0.2476	2.407	0.6805	108.9	-0.939	-65.723	0.0791
165	15.2	18.696	0.2497	2.427	0.6749	111.4	-0.777	-91.130	0.0812
170	13.8	16.974	0.2517	2.447	0.6694	113.8	-0.783	98.906	0.0832
175	12	14.76	0.2538	2.467	0.6640	116.2	-0.888	3.499	0.0853
180	10.2	12.546	0.2558	2.486	0.6588	118.6	-0.870	-21.325	0.0873
185	8.5	10.455	0.2578	2.506	0.6536	120.9	-1.002	154.580	0.0893
190	6.2	7.626	0.2598	2.525	0.6486	123.2	-1.157	-77.891	0.0913

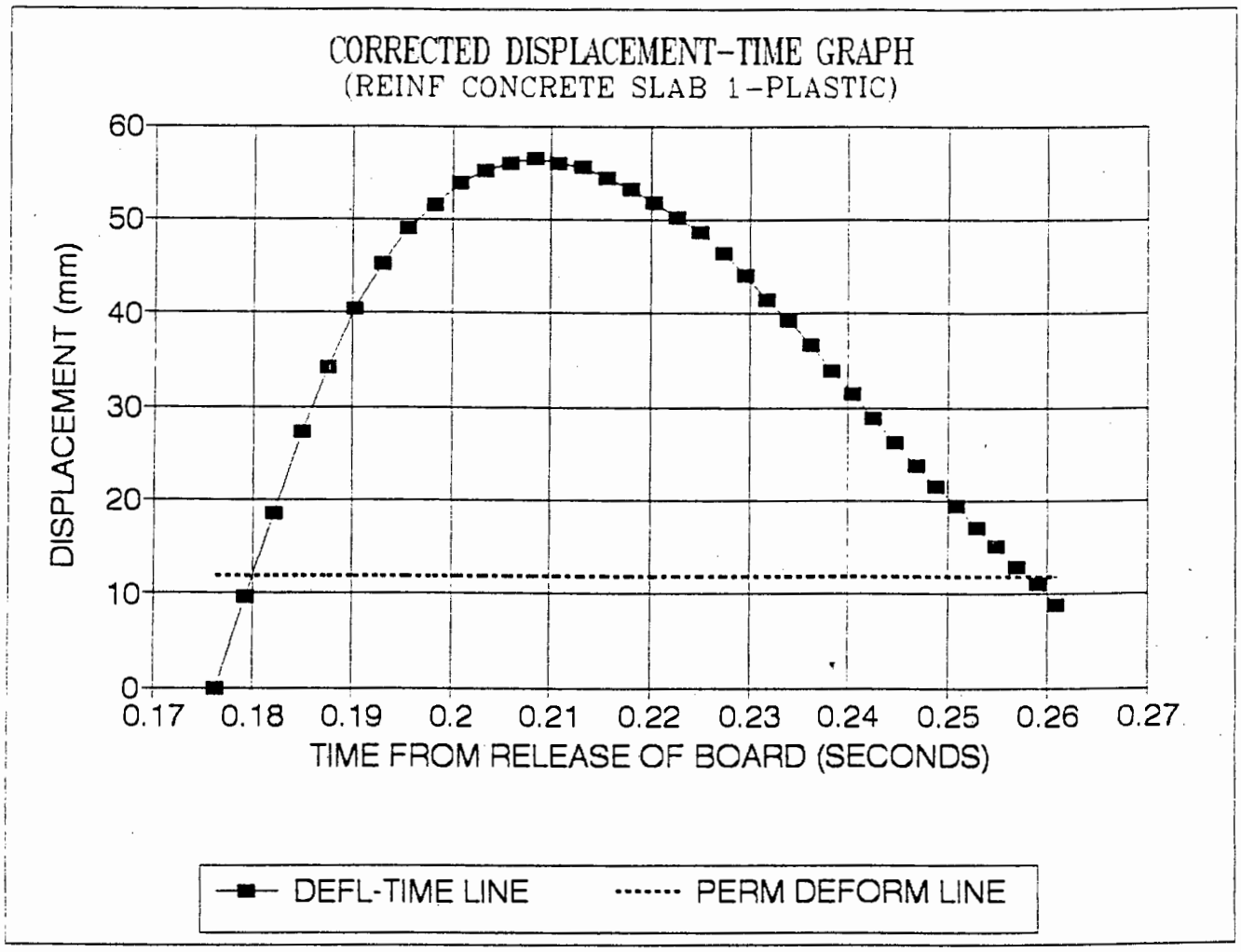
CORRECTED DISPLACEMENT-TIME GRAPH
(REINF CONCRETE SLAB 1-PLASTIC)
DISPLACEMENT (mm)
60
50
40
30
20
10
0
0.17
0.18
0.19
0.2
0.21
0.22
0.23
0.24
0.25
0.26
0.27
TIME FROM RELEASE OF BOARD (SECONDS)
DEFL-TIME LINE
PERM DEFORM LINE

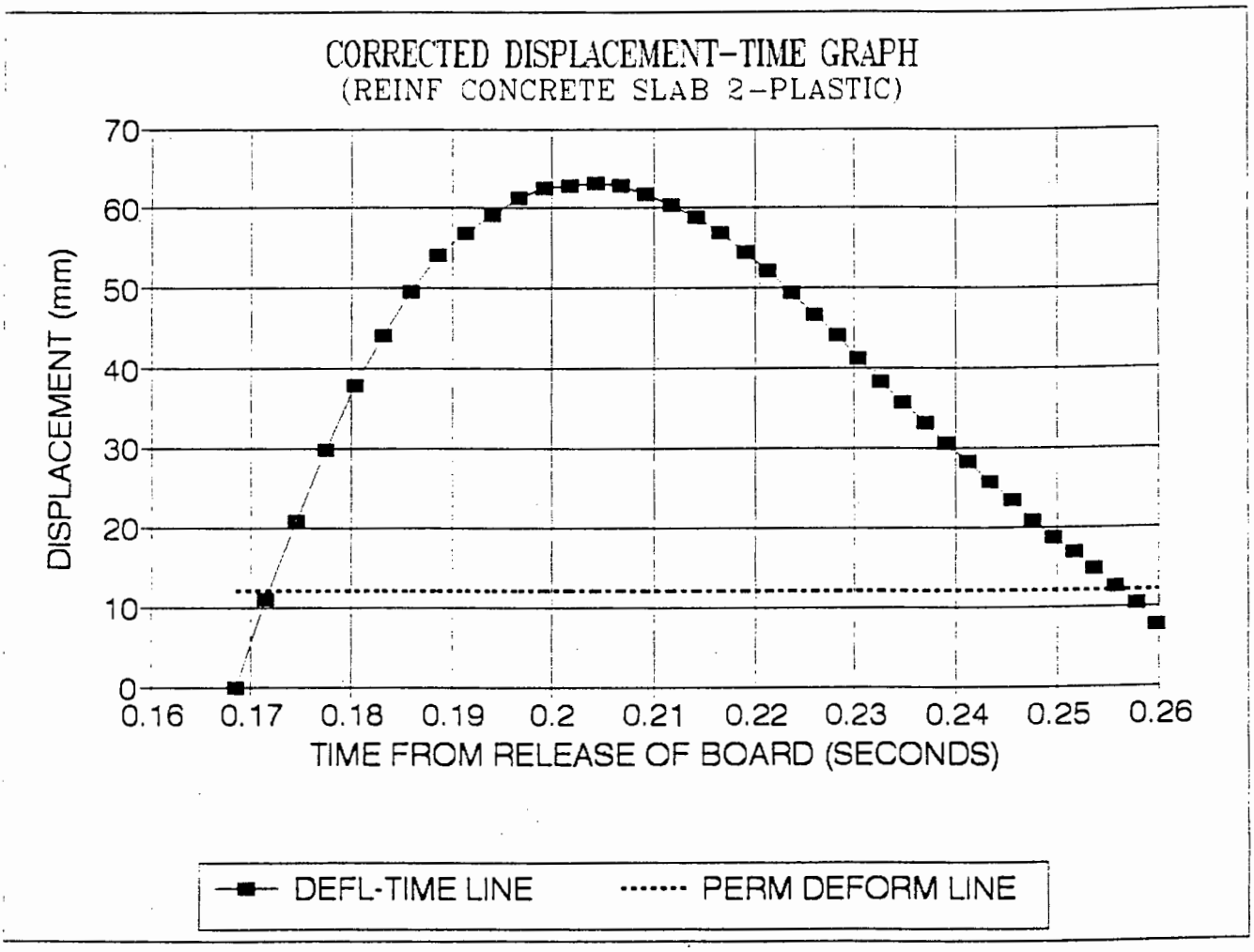
CORRECTED DISPLACEMENT-TIME GRAPH
(REINF CONCRETE SLAB 2-PLASTIC)
DISPLACEMENT (mm)
70
60
50
40
30
20
10
0
0.16
0.17
0.18
0.19
0.2
0.21
0.22
0.23
0.24
0.25
0.26
TIME FROM RELEASE OF BOARD (SECONDS)
DEFL-TIME LINE
PERM DEFORM LINE

IMPACT CALCULATIONS — PLASTIC ANALYSIS — REINFORCED CONCRETE SLAB 3 (SERIES A) (3x400N WEIGHTS)

DISTANCE BOARD FALLEN BEFORE IMPACT =	0.109	m	THETA INSWING (RADS) =	0.9616
ACCELERATION OF FALLING BOARD =	9.72	m/s^2	THETA BACKSWING (RADS) =	0.0384
VALUE OF g AT UCT =	9.80	m/s^2	EFF HT OF PENDULUM (m) =	1.279
EFFECTIVE MASS OF PENDULUM =	184.600	kg	EFF VEL OF PENDULUM (m/s) =	5.006
EFFECTIVE LENGTH OF PENDULUM =	2.989	m	VEL OF PEND (POI) (m/s) =	5.351
DISTANCE 'X' =	0.135	m	ACCEL OF SLAB (m/s^2) =	606.8
LENGTH TO IMPACT =	3.195	m	FORCE 'Be' (kN) =	96.6
LENGTH FROM PIN TO HAMMER =	3.060	m		
PERIOD OF PENDULUM =	3.468	seconds		
EFFECTIVE MASS SLAB ETC =	159.2	kg		
DIST OF RELEASE FROM POI =	4.270	m		
DEFL CORR FACTOR 'CF' =	1.23			

DISTANCE FROM POI (mm)	DEFLECTION X (mm)	ADJ DEFL X(adj) (mm)	TIME BOARD FALLEN (seconds)	VELOCITY OF BOARD (m/s)	CORRECTION FACTOR	CORRECTED DST FROM POI (mm)	VELOCITY OF HAMMER & BEAM (m/s)	ACCELERATION HAMMER & BEAM (m/s^2)	TIME (t) (seconds)
0	0.0	0	0.1498	1.456	1.0000	0.0	5.351	606.841	0.0000
5	7.0	8.61	0.1532	1.489	0.9778	4.9	1.771	174.523	0.0034
10	11.9	14.637	0.1565	1.521	0.9571	9.6	1.110	224.164	0.0067
15	14.3	17.589	0.1597	1.553	0.9376	14.1	0.667	44.017	0.0100
20	16.2	19.926	0.1629	1.584	0.9192	18.4	0.427	107.686	0.0132
25	17.0	20.91	0.1660	1.614	0.9019	22.5	0.097	103.588	0.0163
30	16.8	20.664	0.1691	1.644	0.8855	26.6	-0.131	44.002	0.0194
35	16.2	19.926	0.1721	1.673	0.8700	30.5	-0.284	57.627	0.0224
40	15.1	18.573	0.1751	1.702	0.8553	34.2	-0.391	13.819	0.0253
45	13.9	17.097	0.1780	1.730	0.8413	37.9	-0.502	62.682	0.0282
50	12.2	15.006	0.1809	1.758	0.8280	41.4	-0.598	3.305	0.0311
55	10.5	12.915	0.1837	1.786	0.8153	44.8	-0.589	-9.543	0.0339
60	8.9	10.947	0.1865	1.813	0.8031	48.2	-0.598	16.347	0.0367
65	7.2	8.856	0.1892	1.839	0.7915	51.4	-0.552	-51.197	0.0395
70	5.9	7.257	0.1919	1.866	0.7803	54.6	-0.448	-25.501	0.0422
75	4.8	5.904	0.1946	1.891	0.7697	57.7	-0.378	-26.668	0.0448
80	3.9	4.797	0.1972	1.917	0.7594	60.8	-0.383	31.333	0.0474
85	2.8	3.444	0.1998	1.942	0.7496	63.7	-0.330	-73.765	0.0500
90	2.2	2.706	0.2024	1.967	0.7401	66.6	-0.157	-61.112	0.0526
95	2.0	2.46	0.2049	1.991	0.7310	69.4	0.000	-63.445	0.0551
100	2.2	2.706	0.2074	2.016	0.7222	72.2	0.060	15.958	0.0576
105	2.3	2.829	0.2098	2.040	0.7137	74.9	0.061	-16.931	0.0601
110	2.5	3.075	0.2123	2.063	0.7055	77.6	0.165	-68.889	0.0625
115	3.1	3.813	0.2147	2.087	0.6976	80.2	0.249	34.840	0.0649

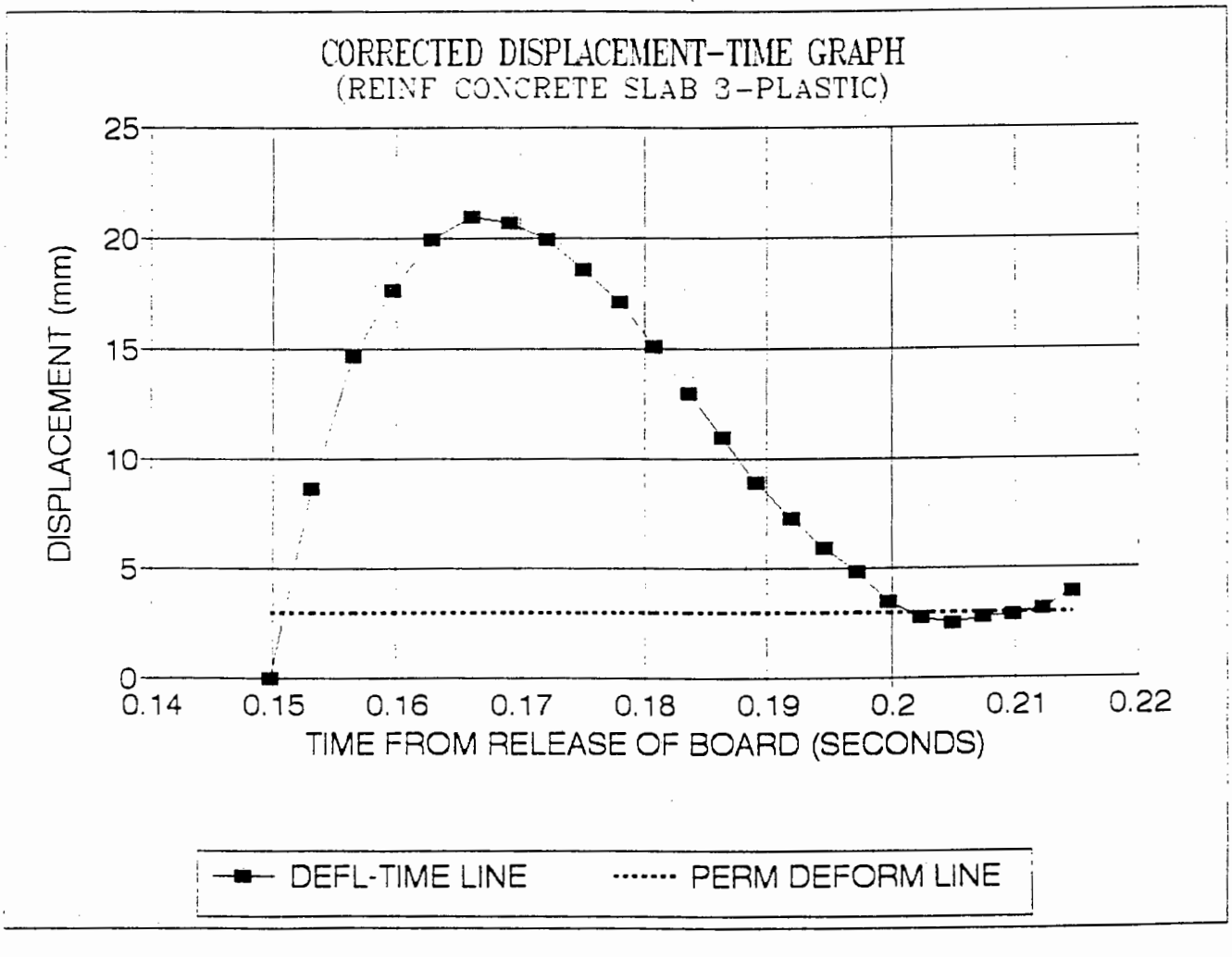

IMPACT CALCULATIONS — PLASTIC ANALYSIS — REINFORCED CONCRETE SLAB 4 (SERIES B)
(5x400N WEIGHTS)

DISTANCE BOARD FALLEN BEFORE IMPACT =	0 083	m	THETA INSWING (RADS) =	0 6716
ACCELERATION OF FALLING BOARD =	9 72	m/s^2	THETA BACKSWING (RADS) =	0 1410
VALUE OF g AT UCT =	9 80	m/s^2	EFF HT OF PENDULUM (m) =	0 655
EFFECTIVE MASS OF PENDULUM =	266 100	kg	EFF VEL OF PENDULUM (m/s) =	3 584
EFFECTIVE LENGTH OF PENDULUM =	3 018	m	VEL OF PEND (POI) (m/s) =	3 754
DISTANCE 'X' =	0 101	m	ACCEL OF SLAB (m/s^2) =	797 6
LENGTH TO IMPACT =	3 161	m	FORCE 'Be' (kN) =	127 0
LENGTH FROM PIN TO HAMMER =	3 060	m		
PERIOD OF PENDULUM =	3 485	seconds		
EFFECTIVE MASS SLAB ETC =	159 2	kg		
DIST OF RELEASE FROM POI =	3 000	m		
CORRECTION FACTOR (CF) =	1 00			

DISTANCE FROM POI (mm)	DEFLECTION X (mm)	ADJ DEFL X(adj) (mm)	TIME BOARD FALLEN (seconds)	VELOCITY OF BOARD (m/s)	CORRECTION FACTOR	COPRECTED DST FROM POI (mm)	VELOCITY OF HAMMER & BEAM (m/s)	ACCELERATIO HAMMER & BE (m/s^2)	TIME (t) (seconds)
0	0 0	-1	0 1307	1 270	1 0000	0 0	3 754	797 647	0 0000
5	12 0	11	0 1346	1 308	0 9712	4 9	2 942	80 711	0 0039
10	22 5	21 5	0 1383	1 345	0 9447	9 4	2 715	38 188	0 0076
15	32 2	31 2	0 1420	1 380	0 9203	13 8	2 277	204 848	0 0113
20	39 0	38	0 1456	1 415	0 8977	18 0	1 740	92 119	0 0149
25	44 5	43 5	0 1491	1 449	0 8767	21 9	1 231	201 606	0 0184
30	47 5	46 5	0 1525	1 482	0 8570	25 7	0 696	109 619	0 0218
35	49 2	48 2	0 1558	1 515	0 8387	29 4	0 379	80 123	0 0251
40	50 0	49	0 1591	1 546	0 8215	32 9	0 062	114 349	0 0284
45	49 6	48 6	0 1623	1 577	0 8053	36 2	-0 126	0 778	0 0316
50	49 2	48 2	0 1654	1 608	0 7900	39 5	-0 289	105 143	0 0347
55	47 8	46 8	0 1685	1 638	0 7755	42 7	-0 491	24 372	0 0378
60	46 2	45 2	0 1715	1 667	0 7619	45 7	-0 583	36 753	0 0409
65	44 3	43 3	0 1745	1 696	0 7489	48 7	-0 729	61 710	0 0438
70	41 9	40 9	0 1774	1 725	0 7366	51 6	-0 879	40 642	0 0467
75	39 2	38 2	0 1803	1 753	0 7248	54 4	-0 946	5 249	0 0496
80	35 5	35 5	0 1831	1 780	0 7136	57 1	-1 050	69 098	0 0525
85	33 3	32 3	0 1859	1 807	0 7029	59 7	-1 193	32 538	0 0552
90	29 9	28 9	0 1887	1 834	0 6927	62 3	-1 302	47 252	0 0580
95	26 2	25 2	0 1914	1 860	0 6829	64 9	-1 302	-48 553	0 0607
100	22 9	21 9	0 1940	1 886	0 6735	67 3	-1 339	78 042	0 0634
105	19 1	18 1	0 1967	1 912	0 6644	69 8	-1 357	-66 184	0 0660
110	15 8	14 8	0 1993	1 937	0 6558	72 1	-1 278	6 415	0 0686
115	12 5	11 5	0 2018	1 962	0 6475	74 5	-1 295	6 415	0 0712
120	9 2	8 2	0 2044	1 987	0 6394	76 7	-1 232	-57 108	0 0737
125	6 3	5 3	0 2069	2 011	0 6317	79 0	-1 005	-124 519	0 0762
130	4 2	3 2	0 2093	2 035	0 6242	81 2	-0 834	-12 576	0 0787
135	2 2	1 2	0 2118	2 059	0 6170	83 3	-0 865	37 982	0 0811
140	0 0	-1	0 2142	2 082	0 6101	85 4	-0 911	-19 210	0 0835

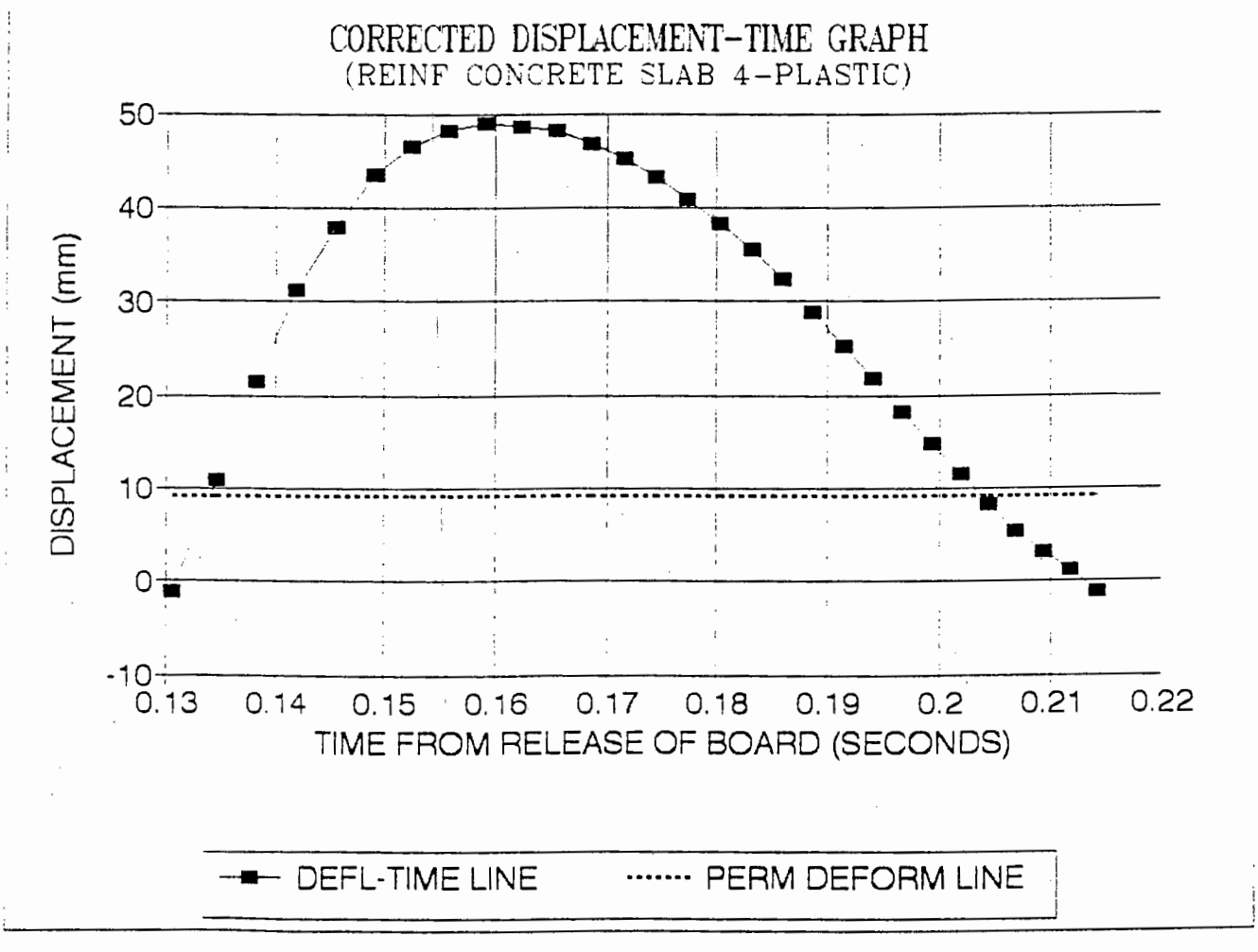

IMPACT CALCULATIONS — PLASTIC ANALYSIS — REINFORCED CONCRETE SLAB 5 (SERIES B)
(px400N WEIGHTS)

DISTANCE BOARD FALLEN BEFORE IMPACT =	0.019	m	THETA INSWING (RADS) =	0.9060
ACCELERATION OF FALLING BOARD =	9.72	m/s^2	THETA BACKSWING (RADS) =	0.0178
VALUE OF g AT UCT =	9.80	m/s^2	EFF HT OF PENDULUM (m) =	1.156
EFFECTIVE MASS OF PENDULUM =	266.100	kg	EFF VEL OF PENDULUM (m/s) =	4.760
EFFECTIVE LENGTH OF PENDULUM =	3.018	m	VEL OF PEND (POI) (m/s) =	1.986
DISTANCE 'X' =	0.101	m	ACCEL OF SLAB (m/s^2) =	486.7
LENGTH TO IMPACT =	3.161	m	FORCE 'P' (KN) =	77.3
LENGTH FROM PIN TO HAMMER =	3.060	m		
PERIOD OF PENDULUM =	3.485	seconds		
EFFECTIVE MASS SLAB ETC =	159.2	kg		
DIST OF RELEASE FROM POI =	4.000	m		
DEFL CORR FACTOR 'CF' =	1.23			

DISTANCE FROM POI (mm)	DEFLECTION X (mm)	ADJ DEFL X(adj) (mm)	TIME BOARD FALLEN (seconds)	VELOCITY OF BOARD (m/s)	CORRECTION FACTOR	CORRECTED DST FROM POI (mm)	VELOCITY OF HAMMER & BEAM (m/s)	ACCELERATION HAMMER & BEAM (m/s^2)	TIME (t) (seconds)
0	0.0	0	0.0625	0.608	1.0000	0.0	4.986	-485.696	0.0000
2	5.0	6.15	0.0657	0.639	0.9512	1.9	1.835	180.774	0.0032
4	11.5	14.145	0.0688	0.669	0.9089	3.6	1.887	162.297	0.0063
6	16.3	20.049	0.0717	0.697	0.8718	5.2	1.672	-23.328	0.0092
8	21.1	25.953	0.0745	0.724	0.8389	6.7	1.611	70.132	0.0120
10	25.2	30.996	0.0772	0.751	0.8094	8.1	1.294	166.291	0.0147
12	28.0	34.44	0.0799	0.776	0.7829	9.4	0.698	292.337	0.0173
14	28.8	35.424	0.0824	0.801	0.7588	10.6	0.000	256.431	0.0199
16	28.0	34.44	0.0849	0.825	0.7368	11.8	-0.309	-13.355	0.0223
18	27.3	33.579	0.0873	0.848	0.7166	12.9	-0.615	276.629	0.0247
20	25.1	30.873	0.0896	0.871	0.6980	14.0	-0.936	-8.496	0.0271
22	23.0	28.29	0.0918	0.893	0.6807	15.0	-0.959	30.366	0.0293
24	20.8	25.584	0.0941	0.914	0.6647	16.0	-0.868	116.103	0.0315
26	18.2	23.616	0.0962	0.935	0.6498	16.9	-0.771	39.881	0.0337
28	17.5	21.525	0.0983	0.956	0.6358	17.8	0.812	8.262	0.0358
30	15.8	19.434	0.1004	0.976	0.6227	18.7	-0.781	-39.837	0.0379
32	14.3	17.589	0.1024	0.996	0.6104	19.5	-0.647	92.797	0.0399
34	13.3	16.236	0.1044	1.015	0.5987	20.4	-0.584	31.340	0.0419
36	12.0	14.76	0.1064	1.034	0.5878	21.2	-0.594	-21.134	0.0439
38	10.9	13.407	0.1083	1.053	0.5774	21.9	-0.579	5.346	0.0458
40	9.8	12.054	0.1102	1.071	0.5675	22.7	-0.535	-52.476	0.0477
42	8.9	10.947	0.1120	1.089	0.5581	23.4	-0.490	4.374	0.0495
44	8.0	9.84	0.1139	1.107	0.5492	24.2	-0.387	119.047	0.0513
46	7.5	9.225	0.1156	1.124	0.5407	24.9	-0.281	2.430	0.0531
48	7.0	8.61	0.1174	1.141	0.5326	25.6	-0.200	-95.969	0.0549
50	6.8	8.364	0.1192	1.158	0.5247	26.2	-0.115	48.706	0.0566

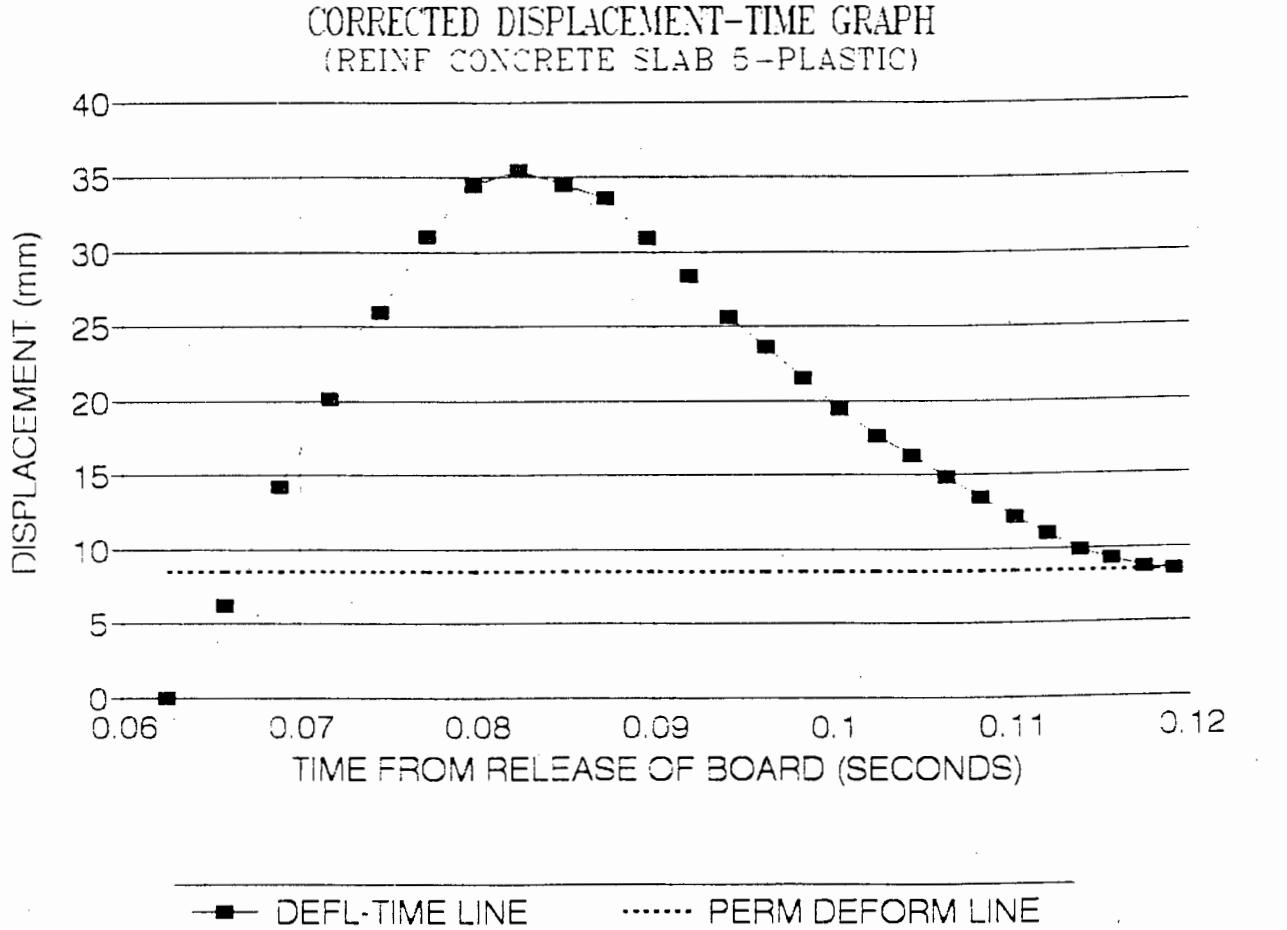

CONCRETE SLAB ENERGY ANALYSIS - SLAB 1

ELASTO-PLASTIC ANALYSIS
(TWO 400N WEIGHTS)

INPUT

DIST POI (m) =	4.400
M(e) PEND (kg) =	147.6
M(e) CHANNEL (kg) =	57.6
L(e) (m) =	2.958
DIST 'X' (m) =	-0.007
L(POI) (m) =	3.067
L(h) (m) =	3.060
'g' UCT (m/s ^ 2) =	9.80
MAX DEFL (m) =	0.0459
SLAB 'k' (kN/m) =	2570.800
Rme (kN) =	49.600
E STEEL (GPa) =	207.800
Fy STEEL (MPa) =	399.700
DLF fy =	1.2
Edynamic CON (GPa) =	39
Me SLAB (ONLY)(kg) =	159.200
ACC POI (m/s ^ 2) =	930.960

OUTPUT

THETA(s) (rads) =	1.0257
H(eff)(1) (m) =	1.4244
KE(2) (JOULS) =	2060.363
THETA(3) (rads) =	0.0225
H(eff)(3) (m) =	0.00075
PE(3) (JOULS) =	1.080
NETT E (JOULS) =	2059.283
PROP FACT 'fp' =	0.965
E POI (JOULS) =	1986.265
Be (N) =	148208.8
R(m) (kN) =	49.600
X(e) (mm) =	19.3
Xm (max) (mm) =	49.7
Meb (SYSTEM) (kg) =	304.759
IMPULSE (POI)(Ns) =	1100.302
IMP DUR 'T' (s) =	0.014848
PERIOD SLAB 'Tn'(s) =	0.068411
TIME 'Tm' (S) =	0.024527

CONCRETE SLAB ENERGY ANALYSIS - SLAB 2

ELASTO-PLASTIC ANALYSIS
(THREE 400N WEIGHTS)

INPUT

DIST POI (m) =	4.160
M(e) PEND (kg) =	188.5
M(e) CHANNEL (kg) =	57.4
L(e) (m) =	2.989
DIST 'X' (m) =	0.002
L(POI) (m) =	3.062
L(h) (m) =	3.060
'g' UCT (m/s ^ 2) =	9.80
MAX DEFL (m) =	0.0578
SLAB 'k' (kN/m) =	2570.800
Rme (kN) =	49.600
E STEEL (GPa) =	207.800
Fy STEEL (MPa) =	399.700
DLF fy =	1.2
Edynamic CON (GPa) =	39
Me SLAB (ONLY)(kg) =	159.200
ACC POI (m/s ^ 2) =	961.350

OUTPUT

THETA(s) (rads) =	0.9658
H(eff)(1) (m) =	1.2891
KE(2) (JOULS) =	2381.310
THETA(3) (rads) =	0.0264
H(eff)(3) (m) =	0.00104
PE(3) (JOULS) =	1.922
NETT E (JOULS) =	2379.387
PROP FACT 'fp' =	0.976
E POI (JOULS) =	2322.618
Be (kN) =	153.047
R(m) (kN) =	49.600
X(e) (mm) =	19.3
Xm (max) (mm) =	56.5
Meb (SYSTEM) (kg) =	346.331
IMPULSE (POI)(Ns) =	1268.381
IMP DUR 'T' (s) =	0.016575
PERIOD SLAB 'Tn'(s) =	0.072928
TIME 'Tm' (S) =	0.026519

CONCRETE SLAB ENERGY ANALYSIS - SLAB 3

ELASTO-PLASTIC ANALYSIS
(THREE 400N WEIGHTS)

INPUT

DIST POI (m) =	4.270
M(e) PEND (kg) =	188.5
M(e) CHANNEL (kg) =	57.4
L(e) (m) =	2.989
DIST 'X' (m) =	0.002
L(POI) (m) =	3.062
L(h) (m) =	3.060
'g' UCT (m/s^2) =	9.80
MAX DEFL (m) =	0.0162
SLAB 'k' (kN/m) =	2570.800
Rme (kN) =	49.600
E STEEL (GPa) =	207.800
Fy STEEL (MPa) =	399.700
DLF fy =	1.2
Edynamic CON (GPa) =	39
Me SLAB (ONLY)(kg) =	159.200
ACC POI (m/s^2) =	606.840

OUTPUT

THETA(s) (rads) =	0.9922
H(eff)(1) (m) =	1.3546
KE(2) (JOULS) =	2502.269
THETA(3) (rads) =	0.0128
H(eff)(3) (m) =	0.00024
PE(3) (JOULS) =	0.452
NETT E (JOULS) =	2501.817
PROP FACT 'fp' =	0.976
E POI (JOULS) =	2442.126
Be (N) =	96608.9
R(m) (kN) =	49.600
X(e) (mm) =	19.3
Xm (max) (mm) =	58.9
Meb (SYSTEM) (kg) =	346.331
IMPULSE (POI)(Ns) =	1300.603
IMP DUR 'T' (s) =	0.026925
PERIOD SLAB 'Tn'(s)=	0.072928
TIME 'Tm' (S) =	0.031694

CONCRETE SLAB ENERGY ANALYSIS - SLAB 4

ELASTO-PLASTIC ANALYSIS
(FIVE 400N WEIGHTS)

INPUT

DIST POI (m) =	3.000
M(e) PEND (kg) =	270.2
M(e) CHANNEL (kg) =	57.3
L(e) (m) =	3.018
DIST 'X' (m) =	0.008
L(POI) (m) =	3.068
L(h) (m) =	3.060
'g' UCT (m/s^2) =	9.80
MAX DEFL (m) =	0.0381
SLAB 'k' (kN/m) =	2570.800
Rme (kN) =	107.100
E STEEL (GPa) =	207.800
Fy STEEL (MPa) =	399.700
DLF fy =	1.2
Edynamic CON (GPa) =	39
Me SLAB (ONLY)(kg) =	159.200
ACC POI (m/s^2) =	797.647

OUTPUT

THETA(s) (rads) =	0.6865
H(eff)(1) (m) =	0.6837
KE(2) (JOULS) =	1810.458
THETA(3) (rads) =	0.0199
H(eff)(3) (m) =	0.00060
PE(3) (JOULS) =	1.585
NETT E (JOULS) =	1808.874
PROP FACT 'fp' =	0.984
E POI (JOULS) =	1779.315
Be (N) =	126985.4
R(m) (kN) =	107.100
X(e) (mm) =	41.7
Xm (max) (mm) =	37.4
Meb (SYSTEM) (kg) =	428.464
IMPULSE (POI)(Ns) =	1234.806
IMP DUR 'T' (s) =	0.019448
PERIOD SLAB 'Tn'(s)=	0.081115
TIME 'Tm' (S) =	0.030003

CONCRETE SLAB ENERGY ANALYSIS - SLAB 5 ELASTO-PLASTIC ANALYSIS
(FIVE 400N WEIGHTS)

INPUT		OUTPUT	
DIST POI (m) =	4.000	THETA(s) (rads) =	0.9262
M(e) PEND (kg) =	270.2	H(eff)(1) (m) =	1.2044
M(e) CHANNEL (kg) =	57.3	KE(2) (JOULS) =	3189.299
L(e) (m) =	3.018	THETA(3) (rads) =	0.0169
DIST 'X' (m) =	0.008	H(eff)(3) (m) =	0.00043
L(POI) (m) =	3.068	PE(3) (JOULS) =	1.148
L(h) (m) =	3.060	NETT E (JOULS) =	3188.151
'g' UCT (m/s ^ 2) =	9.80	PROP FACT 'fp' =	0.984
MAX DEFL (m) =	0.0290	E POI (JOULS) =	3136.054
SLAB 'k' (kN/m) =	2570.800	Be (N) =	77323.4
Rme (kN) =	107.100	R(m) (kN) =	107.100
E STEEL (GPa) =	207.800	X(e) (mm) =	41.7
Fy STEEL (MPa) =	399.700	Xm (max) (mm) =	50.1
DLF fy =	1.2	Meb (SYSTEM) (kg) =	428.464
Edynamic CON (GPa) =	39	IMPULSE (POI)(Ns) =	1639.322
Me SLAB (ONLY)(kg) =	159.200	IMP DUR 'T' (s) =	0.042402
ACC POI (m/s ^ 2) =	485.700	PERIOD SLAB 'Tn'(s) =	0.081115
		TIME 'Tm' (S) =	0.041480

SLAB ANALYSIS

ELASTO-PLASTIC DESIGN METHOD
(SLABS 1 TO 3-SERIES A)

INPUT

As (mm^2/m) =	99
Ave fcu (MPa) =	33.5
EFFEC d (mm) =	31.5
fy (MPa) =	538.7
Esteel (GPa) =	208.9
Econc (MPa) =	39
Mcr (kNm) =	2.674
Xcr (mm) =	3.6
Xy (mm) =	46.7
LENGTH SLAB (m) =	2
POINT LOAD P (kN)=	49.6
CRACK FORCE (kN)	31.2
DLF (conc) =	1.27
DLF (steel) =	1.2

OUTPUT

Fs (kN) =	64.0
Xyield (mm) =	3.8
STRAIN(yield) =	0.0025
PHI(yield) (rads)=	0.0893
STRAIN CONCyield	0.0003
PHIcr =	0.0066
Xu (mm) =	2.5097
Mpl (kNm/m) =	1.9356
CURVAT AREA ABC	0.1994
PHIy(eff) (rads) =	0.0275
EI(eff) (kNm^2) =	70.470
PHIu (rads) =	1.3946
PHIp (rads) =	1.4221
THETAp (rads) =	0.0448
DEFLp (mm) =	31.7
LOAD AREA ABCD =	1797.4
DEFLy(eff) (mm) =	20.9
DEFLmax (mm) =	52.6
DUCTILITY INDEX =	2.51
TOUGHNESS INDEX	4.03

SLAB ANALYSIS

ELASTO-PLASTIC DESIGN METHOD
(SLABS 4&5-SERIES B)

INPUT

As (mm^2/m) =	255
Ave fcu (MPa) =	36.9
EFFEC d (mm) =	29.3
fy (MPa) =	517.4
Esteel (GPa) =	208.3
Econc (MPa) =	39
Mcr (kNm) =	2.674
Xcr (mm) =	3.6
Xy (mm) =	46.7
LENGTH SLAB (m) =	2
POINT LOAD P (kN)=	107.1
CRACK FORCE (kN)	31.2
DLF (conc) =	1.24
DLF (steel) =	1.2

OUTPUT

Fs (kN) =	158.3
Xyield (mm) =	8.6
STRAIN(yield) =	0.0024
PHI(yield) (rads)=	0.1153
STRAIN CONCyield	0.0010
PHIcr =	0.0066
Xu (mm) =	5.7489
Mpl (kNm/m) =	4.1838
CURVAT AREA ABC	0.3817
PHIy(eff) (rads) =	0.0482
EI(eff) (kNm^2) =	86.801
PHIu (rads) =	0.6088
PHIp (rads) =	0.5606
THETAp (rads) =	0.0164
DEFLp (mm) =	11.6
LOAD AREA ABCD =	3036.525
DEFLy(eff) (mm) =	36.7
DEFLmax (mm) =	48.3
DUCTILITY INDEX =	1.32
TOUGHNESS INDEX	1.63

CONCRETE SLAB ANALYSIS - SLAB 1 FORCE BALANCE METHOD
(TWO 400N WEIGHTS)

INPUT

DIST POI (m) =	4.400
M(e) PEND (kg) =	147.6
M(e) CHANNEL (kg) =	57.6
L(e) (m) =	2.958
DIST 'X' (m) =	-0.007
L(POI) (m) =	3.067
L(h) (m) =	3.060
'g' UCT (m/s ^ 2) =	9.80
MAX DEFL (m) =	0.0423
Me SLAB =	159.200
TIME DELTA 't'(sec)=	0.00367

OUTPUT

THETA(s) (rads) =	1.0257
H(eff)(1) (m) =	1.4244
KE(2) (JOULES) =	2060.363
VEL(2) (m/S) =	5.284
THETA(3) (rads) =	0.0213
H(eff)(3) (m) =	0.00067
PE(3) (JOULES) =	0.970
VEL(POI) (m/s) =	5.478
PROP FACT 'fp' =	0.965
E POI (JOULES) =	2126.210
V(dt) (m/s) =	2.617
KE PEND (J) =	1686.076
E GAIN SLAB (JOULES) =	545.000
KE(lost) POI(J) =	1141.075
MePEND(POI) (kg) =	145.56
DECCEL PEND (m/s ^ 2) =	779.794
ACC SLAB (m/s ^ 2) =	712.977
Fo PEND (kN) =	113.506
Fo SLAB (kN) =	113.506
IMPULSE (POI)(Ns) =	416.567
IMP DUR 'T' (s) =	0.007340

CONCRETE SLAB ANALYSIS - SLAB 2 FORCE BALANCE METHOD
(THREE 400N WEIGHTS)

INPUT

DIST POI (m) =	4.160
M(e) PEND (kg) =	188.5
M(e) CHANNEL (kg) =	57.4
L(e) (m) =	2.989
DIST 'X' (m) =	0.002
L(POI) (m) =	3.062
L(h) (m) =	3.060
'g' UCT (m/s ^ 2) =	9.80
MAX DEFL (m) =	0.0423
Me SLAB =	159.200
TIME DELTA 't'(sec)=	0.00374

OUTPUT

THETA(s) (rads) =	0.9658
H(eff)(1) (m) =	1.2891
KE(2) (JOULES) =	2381.310
VEL(2) (m/S) =	5.027
THETA(3) (rads) =	0.0213
H(eff)(3) (m) =	0.00068
PE(3) (JOULES) =	1.256
VEL(POI) (m/s) =	5.149
PROP FACT 'fp' =	0.976
E POI (JOULES) =	2445.922
V(dt) (m/s) =	2.782
KE PEND (J) =	1756.600
E GAIN SLAB (JOULES) =	616.191
KE(lost) POI(J) =	1140.409
MePEND(POI) (kg) =	187.13
DECCEL PEND (m/s ^ 2) =	632.887
ACC SLAB (m/s ^ 2) =	743.926
Fo PEND (kN) =	118.433
Fo SLAB (kN) =	118.433
IMPULSE (POI)(Ns) =	442.939
IMP DUR 'T' (s) =	0.007480

CONCRETE SLAB ANALYSIS - SLAB 3 FORCE BALANCE METHOD
(THREE 400N WEIGHTS)

INPUT		OUTPUT	
DIST POI (m) =	4.270	THETA(s) (rads) =	0.9922
M(e) PEND (kg) =	188.5	H(eff)(1) (m) =	1.3546
M(e) CHANNEL (kg) =	57.4	KE(2) (JOULES) =	2502.269
L(e) (m) =	2.989	VEL(2) (m/S) =	5.153
DIST 'X' (m) =	0.002	THETA(3) (rads) =	0.0213
L(POI) (m) =	3.062	H(eff)(3) (m) =	0.00068
L(h) (m) =	3.060	PE(3) (JOULES) =	1.256
'g' UCT (m/s ^ 2) =	9.80	VEL(POI) (m/s) =	5.278
MAX DEFL (m) =	0.0423	PROP FACT 'fp' =	0.976
Me SLAB =	159.200	E POI (JOULES) =	2570.163
TIME DELTA 't'(sec)=	0.00238	V(dt) (m/s) =	2.852
		KE PEND (J) =	1845.827
		E GAIN SLAB (JOULES) =	647.491
		KE(lost) POI(J) =	1198.337
		MePEND(POI) (kg) =	187.13
		DECCEL PEND (m/s ^ 2) =	1019.483
		ACC SLAB (m/s ^ 2) =	1198.349
		Fo PEND (kN) =	190.777
		Fo SLAB (kN) =	190.777
		IMPULSE (POI)(Ns) =	454.050
		IMP DUR 'T' (s) =	0.004760

CONCRETE SLAB ANALYSIS - SLAB 4 FORCE BALANCE METHOD
(FIVE 400N WEIGHTS)

INPUT		OUTPUT	
DIST POI (m) =	3.000	THETA(s) (rads) =	0.6865
M(e) PEND (kg) =	270.2	H(eff)(1) (m) =	0.6837
M(e) CHANNEL (kg) =	57.3	KE(2) (JOULES) =	1810.458
L(e) (m) =	3.018	VEL(2) (m/S) =	3.661
DIST 'X' (m) =	0.008	THETA(3) (rads) =	0.0199
L(POI) (m) =	3.068	H(eff)(3) (m) =	0.00060
L(h) (m) =	3.060	PE(3) (JOULES) =	1.585
'g' UCT (m/s ^ 2) =	9.80	VEL(POI) (m/s) =	3.721
MAX DEFL (m) =	0.0381	PROP FACT 'fp' =	0.984
Me SLAB =	159.200	E POI (JOULES) =	1851.860
TIME DELTA 't'(sec)=	0.0108	V(dt) (m/s) =	2.339
		KE PEND (J) =	1128.118
		E GAIN SLAB (JOULES) =	435.358
		KE(lost) POI(J) =	692.760
		MePEND(POI) (kg) =	269.26
		DECCEL PEND (m/s ^ 2) =	128.029
		ACC SLAB (m/s ^ 2) =	216.543
		Fo PEND (kN) =	34.474
		Fo SLAB (kN) =	34.474
		IMPULSE (POI)(Ns) =	372.315
		IMP DUR 'T' (s) =	0.021600

CONCRETE SLAB ANALYSIS - SLAB 5 FORCE BALANCE METHOD
(FIVE 400N WEIGHTS)

INPUT		OUTPUT	
DIST POI (m) =	4.000	THETA(s) (rads) =	0.9262
M(e) PEND (kg) =	270.2	H(eff)(1) (m) =	1.2044
M(e) CHANNEL (kg) =	57.3	KE(2) (JOULES) =	3189.299
L(e) (m) =	3.018	VEL(2) (m/S) =	4.859
DIST 'X' (m) =	0.008	THETA(3) (rads) =	0.0169
L(POI) (m) =	3.068	H(eff)(3) (m) =	0.00043
L(h) (m) =	3.060	PE(3) (JOULES) =	1.148
'g' UCT (m/s ^ 2) =	9.80	VEL(POI) (m/s) =	4.939
MAX DEFL (m) =	0.0290	PROP FACT 'fp' =	0.984
Me SLAB =	159.200	E POI (JOULES) =	3262.232
TIME DELTA 't'(sec)=	0.00382	V(dt) (m/s) =	3.104
		KE PEND (J) =	1987.291
		E GAIN SLAB (JOULES) =	766.926
		KE(lost) POI(J) =	1220.364
		MePEND(POI) (kg) =	269.26
		DECCEL PEND (m/s ^ 2) =	480.420
		ACC SLAB (m/s ^ 2) =	812.563
		Fo PEND (kN) =	129.360
		Fo SLAB (kN) =	129.360
		IMPULSE (POI)(Ns) =	494.155
		IMP DUR 'T' (s) =	0.007640

RIGID PLASTIC ANALYSIS

REINFORCED CONCRETE SLAB 1
(SERIES A)

INPUT			OUTPUT			
MASS OF SLAB/m ^ 2 =	122.5	kg/m ^ 2	AT t=0 :	yo" = fo =	1800.331	m/s ^ 2
SPAN 'L' =	2	m		yo' = vel =	0.000	m/s
IMP FORCE 'Fo' =	113506	N		yo = displ =	0.000	m
Mpl =	3872	Nm	AT t=T :	yT" = fT =	-284.473	m/s ^ 2
DURATION IMP 'T' =	0.00734	sec		yT' = vT =	5.563	m/s
Me PENDULUM =	147.6	kg		yT = dT =	0.0298	m
			FOR t>T:	T2 =	0.0196	sec
				y2 = d2 =	0.0106	m
				y(total) =	0.0404	m
				tm =	0.0269	sec

RIGID PLASTIC ANALYSIS

REINFORCED CONCRETE SLAB 2
(SERIES A)

INPUT			OUTPUT			
MASS OF SLAB/m ^ 2 =	122.5	kg/m ^ 2	AT t=0 :	yo" = fo =	1890.827	m/s ^ 2
SPAN 'L' =	2	m		yo' = vel =	0.000	m/s
IMP FORCE 'Fo' =	118433	N		yo = displ =	0.000	m
Mpl =	3872	Nm	AT t=T :	yT" = fT =	-284.473	m/s ^ 2
DURATION IMP 'T' =	0.00748	sec		yT' = vT =	6.008	m/s
Me PENDULUM =	188.5	kg		yT = dT =	0.0326	m
			FOR t>T:	T2 =	0.0211	sec
				y2 = d2 =	0.0132	m
				y(total) =	0.0458	m
				tm =	0.0286	sec

RIGID PLASTIC ANALYSIS

REINFORCED CONCRETE SLAB 3
(SERIES A)

INPUT			OUTPUT			
MASS OF SLAB/m ^ 2 =	122.5	kg/m ^ 2	AT t=0 :	yo" = fo =	3219.594	m/s ^ 2
SPAN 'L' =	2	m		yo' = vel =	0.000	m/s
IMP FORCE 'Fo' =	190777	N		yo = displ =	0.000	m
Mpl =	3872	Nm	AT t=T :	yT" = fT =	-284.473	m/s ^ 2
DURATION IMP 'T' =	0.00476	sec		yT' = vT =	6.986	m/s
Me PENDULUM =	188.5	kg		yT = dT =	0.0232	m
			FOR t>T:	T2 =	0.0246	sec
				y2 = d2 =	0.0279	m
				y(total) =	0.0511	m
				tm =	0.0293	sec

RIGID PLASTIC ANALYSIS

REINFORCED CONCRETE SLAB 4
(SERIES B)

INPUT			OUTPUT			
MASS OF SLAB/m^2 =	122.5	kg/m^2	AT t=0 :	yo" = fo =	18.827	m/s^2
SPAN 'L' =	2	m		yo' = vel =	0.000	m/s
IMP FORCE 'Fo' =	34497	N		yo = displ =	0.000	m
Mpl =	8368	Nm	AT t=T :	yT" = fT =	-614.792	m/s^2
DURATION IMP 'T' =	0.0216	sec		yT' = vT =	-6.436	m/s
Me PENDULUM =	270.2	kg		yT = dT =	-0.0449	m
			FOR t>T:	T2 =	-0.0105	sec
				y2 = d2 =	0.0337	m
				y(total) =	-0.0112	m
				tm =	0.0111	sec

RIGID PLASTIC ANALYSIS

REINFORCED CONCRETE SLAB 5
(SERIES B)

INPUT			OUTPUT			
MASS OF SLAB/m^2 =	122.5	kg/m^2	AT t=0 :	yo" = fo =	1761.208	m/s^2
SPAN 'L' =	2	m		yo' = vel =	0.000	m/s
IMP FORCE 'Fo' =	129360	N		yo = displ =	0.000	m
Mpl =	8368	Nm	AT t=T :	yT" = fT =	-614.792	m/s^2
DURATION IMP 'T' =	0.00764	sec		yT' = vT =	4.379	m/s
Me PENDULUM =	270.2	kg		yT = dT =	0.0283	m
			FOR t>T:	T2 =	0.0071	sec
				y2 = d2 =	0.0156	m
				y(total) =	0.0439	m
				tm =	0.0148	sec

A P P E N D I X F

Successive Approximation Method

This method is an extension of Rayleigh's method. The following section is a direct quote from notes of Reference 3 Chapter 7 which in turn gave the reference (given as Reference 4 Chapter 7 here.) The author has substituted his equation numbers (ie from Equation (1) to (10)).

"Consider a system with a number of masses "lumped" at particular points, letting m_n represent the nth mass of the system and assume that the system is vibrating in the jth mode. If the system is vibrating in a steady-state condition, without damping, the displacement at the nth mass can be written in the form

$$\omega_{nj} \sin \omega_j t \qquad (1)$$

The acceleration experienced by the mass during its oscillatory motion is given by the second derivative with respect to time of the expression (equation 1) and is as follows:

$$-\omega_j^2 u_{nj} \sin \omega_j t \qquad (2)$$

The negative value of this acceleration, multiplied by the mass m_n, is considered a reversed effective force or inertial force, applied at the point n. The inertial forces $Q_{nj} \sin \omega_j t$ are considered as being applied to the structure at each mass point, where the coefficient of the sine term in the inertial force expression has the form

$$Q_{nj} = m_n \omega_j^2 u_{nj} \qquad (3)$$

Since the inertial forces were considered to take account of the mass effects, the displacements of the structure due to the forces Q_{nj} must be precisely equal to quantities u_{nj}. Consequently, in order to find a square of the circular frequency for the jth mode, ω_j^2, it is necessary merely to find a set of displacements u_{nj} at each mass point n of such a magnitude that forces corresponding to this displacement multiplied by the local mass m_n, and by the square of circular frequency for the jth mode, ω_j^2, give rise to the displacement u_{nj}. Any procedure that will establish this condition will give both the modal frequencies and the modal deflection shapes. It is clear from

the discussion that multiplying the magnitudes of the modal deflections by a constant does not change the situation since all the forces, and consequently all of the deflections consistent with those forces, will be multiplied by the same constant.

However, it is not possible without other knowledge of the situation to write down directly a correct set of displacements for the jth mode. Therefore the calculations must be made by a process that makes it possible to arrive at these deflections as a result of systematic method of computation. The most useful procedures, at least for the determination of the fundamental mode, are Rayleigh's method or modifications thereof, or methods based on a procedure of successive approximations developed originally by Stodola. A description of the successive approximations procedure follows:

1. Assume a set of deflections at each mass point of magnitude u_{na}. Compute for these deflections an inertial force Q_{na} given by the expression:

$$Q_{na} = m_n u_{na} \omega^2 \qquad (4)$$

where the quantity ω^2 is an unknown circular frequency. It may be carried in the calculations as an unknown.

2. Apply these forces to the system and compute the deflections corresponding to them. Let these deflections be designated by the symbol u_{nb}.

$$u_{nb} = u_{nb}\omega^2 \qquad (5)$$

3. The problem is to make u_{nb} and u_{na} as nearly equal as possible. To do this ω may be varied. The value of $\hat{\omega}$ that gives the best fit is a good approximation to the circular frequency for the mode that corresponds to the deflection u_{nn} which in general will be an approximation to the fundamental mode. In general, u_{nb} will be a better approximation to the fundamental mode shape than was u_{na}.

4. Consequently, a repetition of the calculations using u_{nb} as the starting point will lead to a new derived deflection

that will be an even better approximation.

In most cases, even with a very poor first assumption for the fundamental mode deflection, the process will converge with negligible errors to ω_1 in at most two or three cycles. However, one can obtain a good approximation in only one cycle. The mode shape will not be as accurately determined unless the calculation is repeated several times.

If the quantity shown in equation (5) is made a minimum, in effect minimizing the square of the error between the derived deflection and the assumed deflection, the "best value of ω" consistent with the assumed deflection curve can be determined. The quantity it is desired to minimize is

$$\sum_n m_n (u_{nb} - u_{na})^2 = \text{minimum} \qquad (6)$$

When equation (5) is substituted into equation (6) one obtains

$$\sum m_n (\omega^2 u_{nb} - u_{na})^2 = \text{minimum} \qquad (7)$$

Now if the derivative of equation (7) is taken with respect to ω^2, the result obtained is

$$2\sum m_n (\omega^2 u_{nb} - u_{na}) u_{nb} = 0 \qquad (8)$$

This is equivalent to the following relationship for the best value of ω :

$$\omega^2 = \frac{\sum m_n u_{na} u_{nb}}{\sum m_n u_{nb}^2} \qquad (9)$$

The value of ω given by equation (9) exceeds, generally only slightly, the true value for the fundamental mode." [1] The first or lowest natural frequency (f_n) of the beam can be calculated as follows:

A P P E N D I X G

Rigid Plastic Method of Analysis of Concrerte Beams

This method assumes that the material is rigid-perfectly plastic. If the load is not large enough to cause a plastic hinge then the method does not apply. The method is based on the following assumptions from Reference 3 (Chapter 7).

"i) Nearly all the analyses are restricted to consideration of bending stress only; plastic failure or yielding which includes shear and/or direct stress is usually neglected.

ii) The material is taken to be rigid-perfectly plastic and all elastic strains are omitted.

iii) Local effects, ie. the local deformation surrounding the region where a striker impinges on a structure, are neglected.

iv) All analyses proceed on the assumption that the initial or given configuration is unchanged throughout the period of impact.

v) Strain-rate effects and strain-hardening do not enter into the analyses directly."

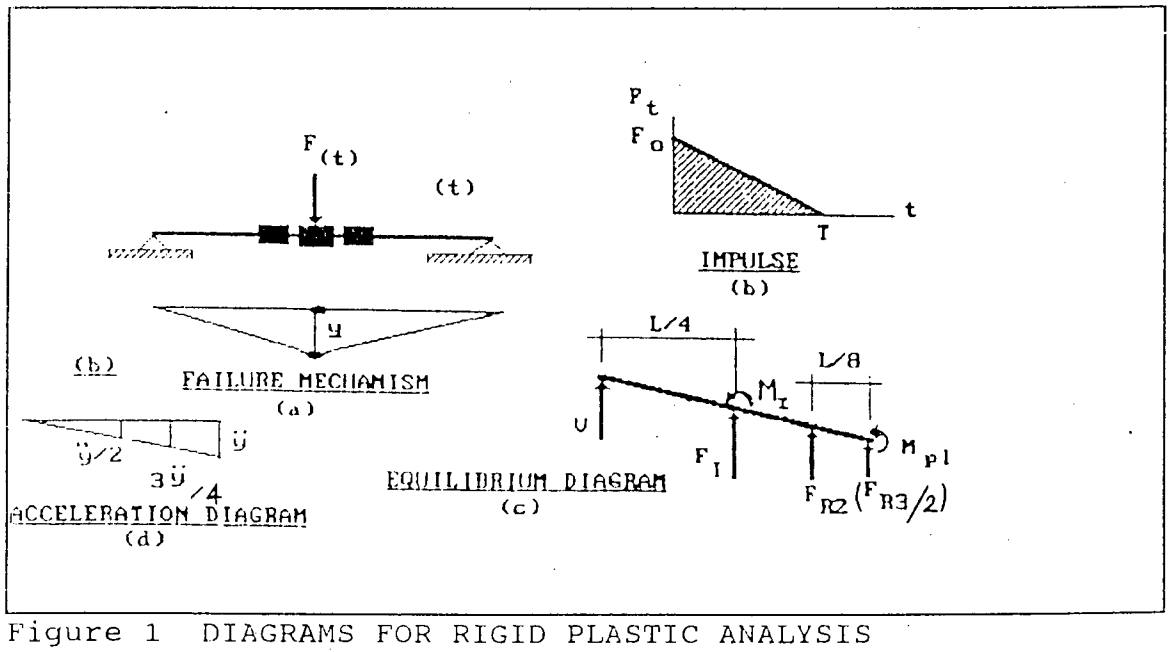

Figure 1 DIAGRAMS FOR RIGID PLASTIC ANALYSIS

The idealized structure is shown in Figure 1(a) together with the mode of failure. The triangular shaped impulse is shown in Figure 1(b). For any time (t) $\leq$ Duration of Impulse (T): The

impulsive force (F_o) must be given by the following equation for a plastic hinge to form: (for a simply supported beam):

$$F_o = \frac{4M_{pl}}{L} \qquad (1)$$

where M_{pl} = Plastic moment capacity of beam

L = Span of beam

For $t \leq T$:

At $t = o$: $\ddot{y}_o = f_o$

At $t = T$: $\ddot{y}_r = f_T$

where $\ddot{y}_o$ and f_o are acceleration of beam at time $t = 0$

where $\ddot{y}_T$ and f_T are acceleration at time $t = T$

However the acceleration drops off due to the triangular load. The acceleration at any time (t) is given by the following equation:

$$\ddot{y}(t) = f_o - (f_o - f_T)\ \frac{t}{T} \qquad (2)$$

By integrating Equation (2) the velocity ($\dot{y}(t)$) is obtained. By integrating once more, the displacement ($y(t)$) is obtained

$$\dot{y}(t) = f_o t - \frac{1}{2}(f_o - f_T)\frac{t^2}{T} \qquad (3)$$

$$y(t) = \frac{1}{2}f_o t^2 - \frac{1}{6}(f_o - f_T)\ \frac{t^3}{T} \qquad (4)$$

The relevant kinematics during the duration of the impulse (ie accelerations, velocities and displacements) can now be calculated. The evaluation procedure can be based on equilibrium or energy principles. The equilibrium approach will be used here.

By referring to Figure 1(c) and taking vertical equilibrium:

$$\frac{F(t)}{2} = V + F_I + F_{R2} + \frac{F_{R3}}{2} \qquad (5)$$

$$\frac{F_o(1-\frac{t}{T})}{2} = V + F_I + F_{R2} + \frac{F_{R3}}{2} \qquad (6)$$

Taking moments about the support point:

$$(\frac{F_{(t)}}{2})(\frac{L}{2}) = M_{PL} + F_I(\frac{L}{4}) + M_I + F_{R2}(\frac{L}{2} - \frac{L}{8}) + \frac{F_{R3}}{2}(\frac{L}{2}) \qquad (7)$$

$$\frac{F_{(t)}L}{4} = M_{PL} + \frac{F_IL}{4} + M_I + \frac{3F_{R2}L}{8} + \frac{F_RL}{4} \qquad (8)$$

where $F_I = (m\ddot{y}L)\ /4$

$F_{R2} = (3M_{R2}\ddot{y})\ /\ 4$

$F_{R3} = M_{R3}\ddot{y}$

$M_I = (mL^2\ddot{y})\ /\ 48$

m = mass of beam/m length

M_{R2} = mass of deflection rod 2

M_{R3} = mass of deflection rod 3

$\ddot{y}$ = acceleration of beam at centre of beam

From Eqation (8):

$$\frac{F_oL}{4}(1-\frac{t}{T}) = M_{PL} + \frac{m\ddot{y}L^2}{16} + \frac{m\ddot{y}L^2}{48} + \frac{9M_{R2}\ddot{y}L}{32} + \frac{M_{R3}\ddot{y}L}{4}$$
$$= M_{pl} + \frac{m\ddot{y}L^2}{12} + \frac{9M_{R2}\ddot{y}L}{32} + \frac{M_{R3}\ddot{y}L}{4} \qquad (9)$$

Solving Equation 9 for $\ddot{y}$

$$\ddot{y} = \frac{96(\frac{F_oL}{4}(1 - \frac{t}{T}) - M_{pl})}{(8mL^2 + 27M_{R2}L + 24M_{R3}L)} \qquad (10)$$

$$\text{At } t = o : \ddot{y} = f_o = \frac{96(\frac{F_oL}{4} - M_{pl})}{(8mL^2 + 27M_{R2}L + 24M_{R3}L)} \qquad (11)$$

$$\text{At } t = T : \ddot{y}_T = f_T = \frac{-96M_{pl}}{(8mL^2 + 27M_{R2}L + 24M_{R3}L)} \qquad (12)$$

By integrating Equation (10) with respect to time, the velocity ($\dot{y}$) and displacement (y) can be determined.

Taking moment equilibrium about V:

$$\left(\frac{F_{(t)}}{4}\right)\left(\frac{L}{2}\right) = m_{pl}L + F_I\left(\frac{L}{6}\right) \tag{7}$$

$$\therefore \frac{F_{(t)}L}{8} = m_{pl}L + \frac{F_IL}{6} \tag{8}$$

where $F_I = (m\ddot{y}L^2) / 12$

m = mass of slab/m^2

$\ddot{y}$ = acceleration of slab at centre of slab

Note: The masses of the deflection rods have been ommitted as they are very small relative to the mass of the slab.

From Equation (8)

$$\frac{F_oL}{8}\left(1-\frac{t}{T}\right) = m_{pl}L + \frac{m\ddot{y}L^2}{12} * \frac{L}{6} = m_{pl}L + \frac{m\ddot{y}L^3}{72} \tag{9}$$

Solving Equation 9 for $\ddot{y}$

$$\ddot{y} = \frac{72\left(\frac{F_oL}{8}\left(1 - \frac{t}{T}\right) - m_{pl}L\right)}{mL^3} \tag{10}$$

$$\text{At } t = o : \ddot{y} = f_o = \frac{72\left(\frac{F_oL}{8} - m_{pl}L\right)}{mL^3} \tag{11}$$

$$\text{At } t = T : \ddot{y}_T = f_T = \frac{-72m_{pl}L}{mL^3} \tag{12}$$

By integrating Equation (10) with respect to time, the velocity ($\acute{y}$) and displacement (y) can be determined.

$$\acute{y} = \frac{\left(72\,\frac{F_oL}{8}\left(t - \frac{t^2}{2T}\right) - m_{pl}Lt\right)}{mL^3}$$

$$y = \frac{72\left(\frac{F_oL}{8}\left(\frac{t^2}{2} - \frac{t^3}{6T}\right) - m_{pl}Lt^2\right)}{mL^3} \tag{13}$$

$$\dot{y} = \frac{96\left(\frac{F_o L}{4}\left(t - \frac{t^2}{2T}\right) - M_{p1}t\right)}{(8mL^2 + 27M_{R2}L + 24M_{R3}L)}$$

$$y = \frac{48\left(\frac{F_o L}{2}\left(\frac{t^2}{2} - \frac{t^3}{6T}\right) - M_{p1}t^2\right)}{(8mL^2 + 27M_{R2}L + 24M_{R3}L)} \qquad (13)$$

At t = T

$$\ddot{y}_T = f_T = \frac{-96\ M_{p1}}{(8mL^2 + 27M_{R2}L + 24M_{R3}L)}$$

$$\dot{y}_T = v_T = \frac{96\left(\frac{F_o L}{8} - M_{p1}t\right)}{(8mL^2 + 27M_{R2}L + 24M_{R3}L)} \qquad (14)$$

$$y_T = \delta_T = \frac{48\left(\frac{F_o L T^2}{6} - M_{p1}T^2\right)}{(8mL^2 + 27M_{R2}L + 24M_{R3}L)}$$

for t > T

This will only occur if time to maximum displacement (t_m) is greater than the duration of the impulse (T)

ie if $t_m > T$ and $F_o > (8M_{pl}) / L$

"The forcing function has expired. The driving force is now the inertia. Use the energy balance approach to convert KE to SE. From t = T we can use f_T (which now remains constant) and V_T"[(3)Ch7]

(See Figure 2)

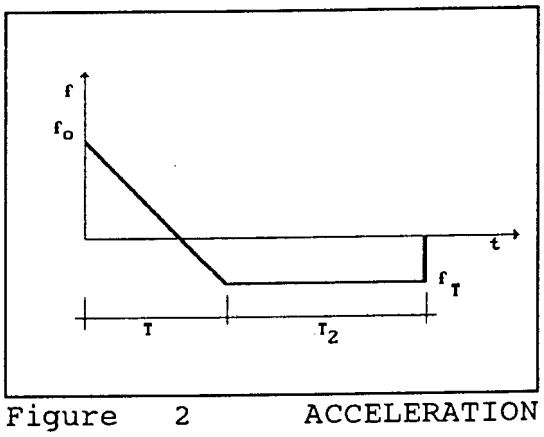

Figure 2 ACCELERATION DIAGRAM

The time taken to standstill (T_2) can be calculated from the following equation:

$$o = V_T + f_T T_2 \qquad (15)$$

Rearranging Equation(15):

$$T_2 = \frac{-V_T}{f_T} = T\left(\frac{F_o L}{8M_{pl}} - 1\right) \tag{16}$$

Since $\delta_2 = V_T\ (T_2 / 2)$ the displacement for this interval can be calculated as follows:

$$\delta_2 = \frac{6T(F_o L - 8M_{pl})\left(\frac{F_o LT}{8} - M_{pl}T\right)}{M_{pl}(8mL^2 + 27M_{R2}L + 24M_{R3}^{T}L)} \tag{17}$$

Where M_{R3}^{T} = Mass of deflection rod 3 + M_{ep} at t > T
Total Deflection (δ_m) is calculated as follows:

$$\delta_m = \delta_T + \delta_2 = \frac{48\left(\frac{F_o LT^2}{6} - M_{pl}T^2\right)}{(8mL^2 + 27M_{R2}L + 24M_{R3}L)} + \frac{6T(F_o L - 8M_{pl})\ \left(\frac{F_o LT}{8} - M_{pl}T\right)}{M_{pl}(8mL^2 + 27M_{R2}L + 24M_{R3}^{T}L)} \tag{18}$$

The time to maximum deflection (t_m) is given by the following equation:

$$t_m = T + T_2 = T + T\left(\frac{F_o L}{8M_{pl}} - 1\right) = \frac{F_o LT}{8M_{pl}} \tag{19}$$

A P P E N D I X H

Yield Line Analysis for Slabs

The first mode of failure (Mode 1) is shown in Figure 1. Using the principle of Virtual Work, the internal energy was found by means of the following equation:

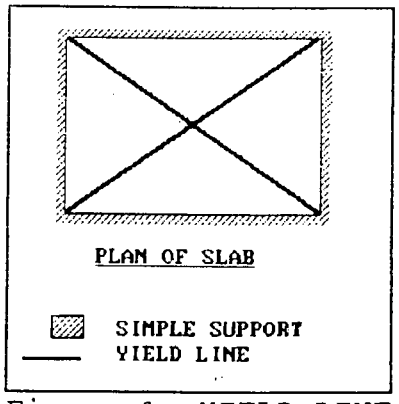

Figure 1 YIELD LINE FAILURE MODE 1

$$\sum(M\theta) = 2\left(m\left(\left(\frac{2L}{\sqrt{2}}\left(\frac{2}{L/\sqrt{2}}\right)\right)\right)\right) \qquad (1)$$
$$= 8m$$

where $\sum(M\theta)$ = sum of internal work

m = ultimate moment per unit length along the yield line

L = side length of the slab

Total External Work:

$$\sum(W\delta) = F * 1 = F \qquad (2)$$

Equating Internal and External work, the force (F) that would cause the yield lines, was calculated.

$$F = 8m \qquad (3)$$

The alternative yield line pattern (Mode 2) is shown in Figure 2 and is more commonly known as a 'fan' failure and could occur due to a concentrated point load on the slab.

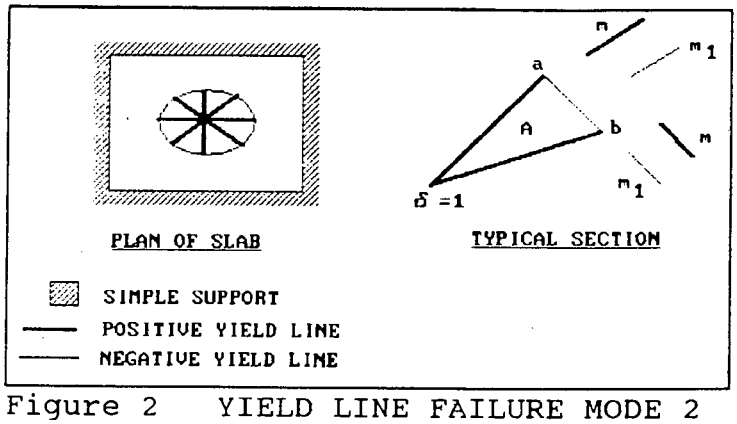

Figure 2 YIELD LINE FAILURE MODE 2

If the deflection at the centre of the slab is given a magnitude of unity (ie $\delta = 1$) and the radius of the fan is denoted by 'r', then the external work ($\sum(W\delta)$) is given by the following formula: (ignoring self-weight of the slab)

$$\sum (W\delta) = P\delta \tag{4}$$

where P = Point load

For internal work done, in a typical rigid zone A (See Figure 2):

$$(M\theta) = \frac{m + m_1}{r}(ab) \tag{5}$$

where m = ultimate moment per unit length along the positive yield line

m_1 = ultimate moment per unit length along negative yield line

∴ Total internal work done is given by the following equation:

$$\begin{aligned} \sum (M\theta) &= \frac{m + m_1}{r} \sum ab \\ &= \frac{m + m_1}{r} * 2\pi r \\ &= 2\pi (m + m_1) \end{aligned} \tag{6}$$

By equating the external and internal work, P is given by the following equation:

$$P = 2\pi (m + m_1) \tag{7}$$

The magnitude of P is therefore independent of the radius (r) of the fan.

A P P E N D I X I

Rigid Plastic Method of Analysis for Concrete Slabs

This method assumes that the material is rigid-perfectly plastic. If the load is not large enough to cause a plastic hinge then the method does not apply. The method is based on the following assumptions from Reference 3 (Chapter 7).

"i) Nearly all the analyses are restricted to consideration of bending stress only; plastic failure or yielding which includes shear and/or direct stress is usually neglected.

ii) The material is taken to be rigid-perfectly plastic and all elastic strains are omitted.

iii) Local effects, ie. the local deformation surrounding the region where a striker impinges on a structure, are neglected.

iv) All analyses proceed on the assumption that the initial or given configuration is unchanged throughout the period of impact.

v) Strain-rate effects and strain-hardening do not enter into the analyses directly."

For any time (t) $\leq$ Duration of Impulse (T): The impulsive force (F_o) must be given by the following equation for a plastic hinge to form: (for a yield line failure mode shape shown in Figure 1)

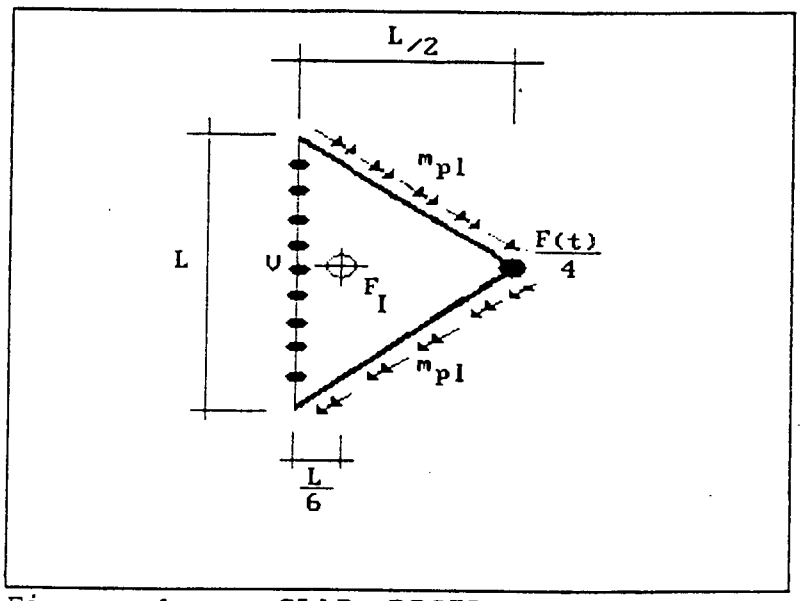

Figure 1 SLAB RIGID PLASTIC FORCE EQUILIBRIUM

$$F_o > 8m_{pl} \qquad (1)$$

where m_{pl} = Plastic moment capacity of slab per m

For $t \leq T$:

At $t = o$: $\ddot{y}_o = f_o$

At $t = T$: $\ddot{y}_T = f_T$

where $\ddot{y}_o$ and f_o are acceleration of slab at time $t = 0$

where $\ddot{y}_T$ and f_T are acceleration at time $t = T$

However the acceleration drops off due to the triangular load. The acceleration at any time (t) is given by the following equation:

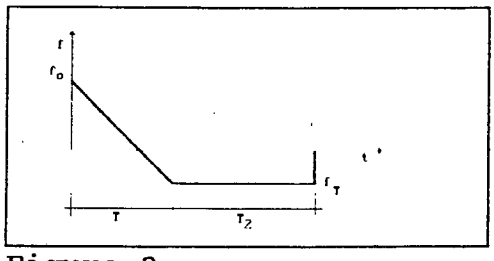

Figure 2

$$\ddot{y}(t) = f_o - (f_o - f_T)\frac{t}{T} \qquad (2)$$

By integrating Equation (2) the velocity ($\dot{y}(t)$)is obtained. By integrating once more, the displacement (y(t)) is obtained

$$\dot{y}(t) = f_o t - \frac{1}{2}(f_o - f_T)\frac{t^2}{T} \qquad (3)$$

$$y(t) = \frac{1}{2}f_o t^2 - \frac{1}{6}(f_o - f_T)\frac{t^3}{T} \qquad (4)$$

The relevant kinematics during the duration of the impulse (ie accelerations, velocities and displacements) can now be calculated. The evaluation procedure can be based on equilibrium or energy principles. The equilibrium approach will be used here.

By referring to Figure (1) and taking vertical equilibrium:

$$\frac{F(t)}{4} = V + F_I \qquad (5)$$

$$\therefore \frac{F_o(1-\frac{t}{T})}{4} = V + F_I \qquad (6)$$

At t = T

$$\ddot{y}_T = f_T = \frac{-72\, m_{pl} L}{mL^3}$$

$$\dot{y}_T = v_T = \frac{72\left(\frac{F_o LT}{16} - m_{pl} LT\right)}{mL^3} \qquad (14)$$

$$y_T = \delta_T = \frac{36\left(\frac{F_o LT^2}{12} - m_{pl} LT^2\right)}{mL^3}$$

for t > T

This will only occur if time to maximum displacement (t_m) is greater than the duration of the impulse (T)

"The forcing function has expired. The driving force is now the inertia. Use the energy balance approach to convert KE to SE. From t = T we can use f_T (which now remains constant) and V_T"[3]Ch7

The time taken to standstill (T_2) can be calculated from the following equation:

$$o = V_T + f_T T_2 \qquad (15)$$

Rearranging Equation(15):

$$T_2 = \frac{-V_T}{f_T} = T\left(\frac{F_o L}{16 m_{pl} L} - 1\right) \qquad (16)$$

Since $\delta_2 = V_T\ (T_2 / 2)$ the displacement for this interval can be calculated as follows:

$$\delta_2 = \frac{36T^2\left(\frac{F_o L}{16} - m_{pl} L\right)^2}{(m_{pl} mL^4 + M_{ep})} \qquad (17)$$

Total Deflection (δ_m) is calculated as follows:

$$\begin{aligned}\delta_m &= \delta_T + \delta_2 \\ &= \frac{36T^2\left(\frac{F_oL}{12} - m_{pl}L\right)}{mL^3} + \\ &\quad \frac{36T^2\left(\frac{F_oL}{16} - m_{pl}L\right)^2}{m_{pl}mL^4} \\ &= \frac{F_oLT^2\left(\frac{9F_oL}{64} - 1.5m_{pl}L\right)}{(m_{pl}mL^4 + M_{ep})}\end{aligned} \tag{18}$$

The time to maximum deflection (t_m) is given by the following equation:

$$\begin{aligned}t_m &= T + T_2 \\ &= T + T\left(\frac{F_oL}{16m_{pl}L} - 1\right) \\ &= \frac{F_oLT}{16m_{pl}L}\end{aligned} \tag{19}$$